

Syracuse University

SURFACE

Dissertations - ALL

SURFACE

December 2020

Natural and Synthetic Ligand-Binding Induce Different Pilin Assemblies in vitro and Control *P. aeruginosa* Bioactivities in vivo, and Development of Bacterial-Motility Enabled Binding Assays

Arizza Chiara Siwa Ibañez
Syracuse University

Follow this and additional works at: <https://surface.syr.edu/etd>



Part of the [Physical Sciences and Mathematics Commons](#)

Recommended Citation

Ibañez, Arizza Chiara Siwa, "Natural and Synthetic Ligand-Binding Induce Different Pilin Assemblies in vitro and Control *P. aeruginosa* Bioactivities in vivo, and Development of Bacterial-Motility Enabled Binding Assays" (2020). *Dissertations - ALL*. 1222.

<https://surface.syr.edu/etd/1222>

This Dissertation is brought to you for free and open access by the SURFACE at SURFACE. It has been accepted for inclusion in Dissertations - ALL by an authorized administrator of SURFACE. For more information, please contact surface@syr.edu.

Abstract

Proteins found on bacterial cells surfaces are capable of sensing and transducing signals from the environment to elicit a biological response. Fibrous appendages formed by assembly of pilin proteins on *P. aeruginosa* are surface proteins that are necessary for host colonization, adhesion on abiotic surfaces, controlling motilities, formation of biofilm, horizontal gene transfer and virulence production of the bacterium. Upon contact with stimuli, pili appendages extend and retract on the cell surface, driven by the assembly and disassembly of pili at inner membrane of the bacteria cells. The dynamic response of this protein assembly is likely caused by a conformational change in the pilin monomers at the tip of the pili appendage upon making contact with a ligand or surface, as well as caused by chemical signals within the bacterium. Despite all the functions of pili identified, the natural and synthetic ligands specific for pilin proteins remain elusive. In this research, we report natural and synthetic ligands of pilin that control *P. aeruginosa* bioactivities.

For biochemical and structural studies on pilin protein, we used a common technique of recombinantly expressing truncated pilin in *E. coli*. The truncation of pilin from the N'-terminal α -helix retains the perceived binding region within the disulfide loop and yields a soluble pilin. Our approach of expressing truncated variants of the *P. aeruginosa* PA1244N3(pPAC46) and single amino acid mutants have demonstrated that pilin binds to the natural and synthetic ligands and that the disulfide loops plays an important role for this function.

Using a novel bacterial motility-enabled binding assay, we demonstrated that spreading expressed pilin monomers on the hydrated gel surface can inhibit the swarming motilities of the wild-type *P. aeruginosa* by binding and sequestering rhamnolipids secreted by the bacterium, or reactivate the swarming motility of the bacteria by sequestering the synthetic inhibitor added in the hydrated gel. Separating the components of rhamnolipids reveal that monorhamnolipid is more active than dirhamnolipid at controlling the swarming motility of *P. aeruginosa*.

Ligand-induced changes to pilin structures were detected by circular dichroism, nuclear magnetic resonance (NMR) and fluorescence spectroscopy. Pilin monomers bind to the rhamnolipids at picomolar ranges and induce pilin proteins to form linear nano-assemblies. About one pico-molar of the ligands causes the transition of fluorescence signal to plateau for 100 nM of pilin monomers. This 10^{-5} equivalence effect is likely due to tight ligand-receptor binding rather than a catalytic effect based on titration studies. The mechanism of the assembly appears to be isodesmic and does not require a critical aggregation concentration to form linear assemblies. A class of synthetic ligands consists of saturated farnesol tethered with disaccharide also binds directly to pilin proteins at picomolar range by intrinsic fluorescence, and to dominate rhamnolipids resulting in complete inhibition of swarming motilities, and to induce the pilin proteins to form an amorphous assembly.

The nonamphiphilic chromonic salt, disodium cromoglycate (5'DSCG) was used to conduct preliminary crystallization studies on pilin from *P. aeruginosa*. We demonstrated that the 5'DSCG molecules demix in the presence of peptides and form isodesmic assemblies. This

demixing phenomenon was then further explored to precipitate and crystallize pilin proteins. The resulting precipitates include radial precipitates for the native 1244 pilin and needle-like crystals for the truncated pilin. These results, along with past findings, suggest that 5'DSCG isodesmic assemblies has the potential to assist in protein purification and crystallization.

This work presents the use of a label-free bacterial motility enabled assay, together with biophysical techniques to provide a mechanistic understanding of the ligand binding between natural and synthetic ligands to pilin. The findings and methods in this study have potential use for the development and screening of therapeutics targeting the protein receptor that control the bioactivities of *P. aeruginosa*.

Natural and Synthetic Ligand-Binding Induce Different Pilin Assemblies *in vitro* and Control
P. aeruginosa Bioactivities *in vivo*, and Development of Bacterial-Motility Enabled Binding
Assays

by

Arizza Chiara S. Ibañez

B.S., University of the Philippines-Diliman, 2009

M. Phil., Syracuse University, 2017

Dissertation

Submitted in partial fulfillment of the requirements for the degree of

Doctor of Philosophy in Chemistry

Syracuse University

December 2020

Copyright © Arizza Chiara S. Ibañez 2020
All Rights Reserved

Acknowledgements

To my PhD advisor, Dr. Yan-Yeung Luk, thank you for allowing me to join your research group and providing me with the opportunity to do research in a field that I am passionate about. I grateful for the intellectual freedom that you gave me, the constant discussions of ideas and being open to listening to my thoughts and opinions. You have inspired and motivated me to always be critical, think outside of the box, strive to keep learning and deliver high quality of work. All these have contributed to my development as a person and a scientist. Thank you for believing in me. I would not be where I am right now without your guidance.

To my co-advisor, Dr. Olga V. Makhlynets, thank you for the constant guidance, unwavering support and the time you spent to train me. You have taught me a lot of biochemistry concepts and skills that were new to me, and I will never forget those. For the times that I have served as your TA, I appreciate that you allowed me to work on projects outside my research that expanded my proficiency in Biochemistry; and also for encouraging me to sit-in your lectures as I have learned a lot from them.

To my committee members, Dr. Carlos Castañeda and Dr. Michael Sponsler, thank you for all the guidance, reading my annual reports, providing meaningful insights and feedback that helped me to move forward with my research and improve the quality of my work. Thank you also for taking time off from your schedules to be a part of my PhD defense committee.

To Dr. Wei Wei Zheng, thank you for agreeing to be a part of my PhD defense committee. I am also grateful allowing me to use your fluorometer for my experiments. To Dr. Anthony Garza, thank you for taking time to serve as my PhD defense chair. To Dr. Ivan

Korendovych, thank you for your generosity in allowing me to use the resources and instruments in your lab.

To the Chemistry department at SU, thank you for all the help and support throughout these years especially whenever I needed help in teaching and in research.

Thank you LifeUnit, Inc. for providing me with an opportunity to work in your facility during summers. I have gained more experience in research because of this.

To my family, I dedicate this PhD degree to all of you- my parents, Fred and Josylina, and my siblings, Bodgie and Ana. You have been very supportive of me throughout my journey these past years. Thank you for checking up on me constantly and for all the words of encouragement during the difficult times. I am blessed with a family who always taught me to be strong and independent, and to always pursue whatever I want to do, as long as it made me happy. You always reminded me that no dream is too big, and that I can achieve anything if I work hard for it.

To my friends at SU and fellow Luk lab members- Felicia, Yuchen, Pankaj, Aimee, Elaine and Dr. Hewen Zheng, I enjoyed the time spent, friendships and working with you during these past years. Felicia, thank you for always being there for me, I will cherish the moments we shared from collaborative work in lab, to walking down to the office to get coffee, to being your personal exterminator, and our trips to the gym, mall, Ulta and Bath and Body. Yuchen and Pankaj, thank you for always bringing us to different restaurants all over Syracuse and introducing us to good food. Elaine, thank you for allowing me to share my knowledge and train you during your stay in Luk lab. Wish you all the best in Pharmacy school! I know you will do well. Liz, thanks for reminding me about the time we first had an actual conversation about my

fear of frostbite. I am glad that you remain as one of my closest friends at SU and I will definitely miss our lunch and dinner dates! To all of you, I am grateful for all the laughter and fun times that we have shared in and out of lab. Most importantly, thank you for your patience with me. I will miss all of you and I hope our paths will cross again soon.

To Nick, thank you for being my rock. For all the times I panicked, freaked out and overreacted, you were always willing to listen and calm me down. Thank you for being very patient even when I am being difficult. I hope you know that I really appreciate everything you do for me.

To my Filipino friends here in the US, Beki Maes- Herdeline, Maxx, Kiall, Jennifer, Marco and Daben – thank you for the friendship and being my support system throughout these years. There are too many good memories for me to mention here, but I hope you know that I will always keep them close to my heart. I always looked forward to our mini-trips and Thanksgiving parties to sing karaoke and eat good food and have a break from our PhD life. I can't wait until our next get-together! For now, I'll settle with our weekly Zoom meetings, they're still as fun! Dennis, although you graduated from SU years ago, I am glad that our paths crossed and now you are one of my good friends. You never fail to check up on me and ask me if I was okay, I really appreciate it. "Sir" Gino, I still remember the day I met you as my lab instructor in UP Diliman, and the day you stole my orange from the limonene extraction experiment. Now, you are one of my closest friends here in the US. Thanks for all the times you listened to me when I would just randomly call you about nonsense. All of you have inspired me to go on with my PhD and never give up on this dream. And to my other Filipino friends, you know who you are, I'm glad that you have all been part of my journey. Maraming Salamat!

To my closest friends in the Philippines, Jenny, Irene, Kat, Gia, thank you for being my best friends since high school. It seemed like it was only yesterday...Char! To Zye, thanks for the couple of times you visited me in Syracuse because you had no choice (and to Char who keeps asking me to buy stuff for Zye to bring home to her). Just kidding! I'm glad that I was able to share the beauty of Upstate NY with you. To the Kiffy girls- Monch and RJ, my two ancient dinosaur friends. I can't remember how our friendship started but I am glad that we're still close to this day. I appreciate all the efforts to keep in touch with me, checking if I'm okay and updating me with what's happening back home. I miss all of you and I hope to see you soon!

To Mrs. Gloria Naypes, this dream all started when I took that high school chemistry class with you. You taught chemistry in such an enjoyable way that it sparked my interest in the subject matter and led me to take this course in college. Now, here I am pursuing an advance degree and a career in chemistry.

Arizza

“The brick walls are there for a reason. The brick walls are not there to keep us out. The brick walls are there to give us a chance to show how badly we want something.”

-Randy Pausch, The Last Lecture

Table of Contents

Chapter 1. Introduction: Ligands for controlling pili assembly dynamics and functions are important but remain elusive.	1
1.1 Pili are surface proteins in multiple bacterial activities leading to infections.....	1
1.2 The pili assembly is comprised of individual pilin monomers that assemble and disassemble.....	2
1.3 Pili is the major adhesin of <i>P. aeruginosa</i> leading to host colonization and infections.....	4
1.4 Pili is important in bacterial motility.....	4
1.5 Pili facilitates DNA uptake between bacterial cells	7
1.6 Pilin as an antigen for vaccine development	8
1.7 Open question and Our hypothesis: Pilin proteins are protein receptors to small molecules that control swarming bioactivities of <i>P. aeruginosa</i>	10
1.8 Summary of chapters	11
 Chapter 2. Cloning, Expression and Purification of Pilin Mutants for Structural Characterization and Ligand-Binding Studies	14
2.1 Background and Significance.....	14
2.1.1 Pilin protein general structure; status of literatures.....	14
2.1.2 <i>P. aeruginosa</i> PA1244N3(pPAC46) and PyMOL modelling of pilin protein.	17
2.1.3 Disulfide loop of pilin contains the host cell receptor binding epitope.....	19
2.1.4 Chapter Aim: Cloning, expression and purification of minimum structured and single amino acid mutants.....	20
2.2 Results and Discussion.....	22
2.2.1 Expression of native pilin in <i>P. aeruginosa</i> PA1244N3(pPAC46).....	22
2.2.2 Recombinant expression and purification of truncated pilin structures	23
2.2.3 Recombinant expression and purification of single amino acid pilin mutants.....	30
2.3 Conclusion.....	36
2.4 Experimental Section	36
2.4.1 Expression and purification of native pilin from <i>P. aeruginosa</i> PA1244N3(pPAC46).....	36
2.4.2 Cloning and recombinant expression of truncated pilin proteins.	38
2.4.3 Purification of pilin $\Delta(1-31)$, pilin $\Delta(1-28)$ and pilin $\Delta(1-23)$ from the lysate	39
2.4.4 Purification of pilin $\Delta(1-28)$ from the inclusion bodies	40
2.4.5 Expression and purification of truncated native pilin mutants.....	41
2.4.6 MALDI-TOF analysis of truncated pilin molecular weight.	41
 Chapter 3. Interactions of Truncated Pilin with Small Molecules Control the Swarming Motility of <i>P. aeruginosa</i>	43
3.1 Background and Significance.....	43
3.1.1 Swarming motility of <i>P. aeruginosa</i> is influenced by different factors	43
3.1.2 Rhamnolipids and synthetic disaccharides control the swarming motility of <i>P. aeruginosa</i>	45
3.1.3 Chapter aim: To test the hypothesis that pilin is the protein receptor of rhamnolipids and synthetic molecules.....	49

3.2 Results and Discussion.....	50
3.2.1 The design of the swarming competition assay to identify protein receptors of rhamnolipids: Bacterial motility binding-enabled motility assay	50
3.2.2 Individual rhamnolipids components control <i>P. aeruginosa</i> swarming motility	54
3.2.3 Truncated pilin inhibits the rhamnolipids- induced swarming of <i>P. aeruginosa</i>	56
3.2.4 Pilin-rhamnolipids interactions modulate the swarming motility of <i>P. aeruginosa</i>	64
3.3 Conclusion.....	66
3.4 Experimental Section	67
3.4.1 Bacteria strains used in this study	67
3.4.2 Rhamnolipids and synthetic ligands stocks preparation.....	67
3.4.3 Proteins used in this study	68
3.4.4 General swarming motility assay	68
3.4.5 Binding enabled motility (modified swarming) assay.....	69
3.4.6 Separation of rhamnolipids.....	70
Chapter 4. Rhamnolipids and Synthetic Disaccharides Induce Structural Changes in Pilin Upon Ligand-Binding Characterized by Circular Dichroism, Nuclear Magnetic Resonance and Dynamic Light Scattering	73
4.1 Background and Significance.....	73
4.1.1 Tools to characterize protein structures and their interactions with ligands	73
4.1.2 Ligand binding between pilin protein and rhamnolipids and SF-disaccharides	77
4.1.3 Chapter aim: To characterize the secondary structure of recombinant truncated pilin proteins and effects of interactions with small molecules on the pilin structure.....	78
4.2 Results and Discussion.....	78
4.2.1 The secondary structure of truncated pilin $\Delta(1-31)$ is mainly comprised of coiled structures and β -sheets.....	78
4.2.2 Rhamnolipids and synthetic disaccharides induces a change in the secondary structure of pilin $\Delta(1-31)$	82
4.2.3 ^1H NMR of spectrum of native pilin from <i>P. aeruginosa</i> 1244N3 (pPAC46) shows interference of polyethylene glycol 8000 and arotein assembly formation	88
4.2.4 Ligand-binding studies by ^{15}N HSQC show additional peaks after adding ligands to pilin $\Delta(1-31)$	89
4.2.5 Truncated native pilin structure with coiled and β -sheet structures.	92
4.2.6 Ligand-binding studies by ^{15}N HSQC show additional peaks after adding ligands to pilin $\Delta(1-31)$	94
4.2.7 Dynamic light scattering shows an increase in particle size upon addition of ligands.	96
4.3 Conclusion.....	99
4.4 Experimental Section	100
4.4.1 ^{15}N -labelled native pilin expression, purification and SDS-PAGE analysis.	100
4.4.2 ^{15}N -labelled truncated pilin expression, purification and SDS-PAGE analysis.....	101
4.4.3 Circular dichroism of pilin proteins	101
4.4.4 ^{15}N HSQC studies on pilin protein.	102
4.4.5 Dynamic light scattering.....	103

Chapter 5. Rhamnolipids and Synthetic Disaccharides Bind to Pilin at Low Picomolar Concentrations and Induce Different Assembly Structures	104
5.1 Background and Significance	104
5.1.1 Importance of hydrophobic groups to protein-ligand binding	104
5.1.2 Fluorescence spectroscopy as a method to determine ligand-binding of pilin and ligands.....	105
5.1.3 Molecules induce the assembly of truncated pilin protein.	106
5.1.4 Chapter aim: To characterize Binding of Truncated Pilin with Rhamnolipids and Synthetic Disaccharides.	108
5.2 Results and Discussion	109
5.2.1 Rhamnolipids and synthetic disaccharides bind to pilin protein at low picomolar concentrations.....	109
5.2.2 Tight-binding between ligand binding between pilin and SF-compounds and rhamnolipids induces pilin assembly.....	117
5.2.3 Ligand-binding to pilin induces pilin assembly formation in vivo via the isodesmic process.	119
5.2.4 Transmission electron microscopy shows linear and amorphous assemblies of pilin induced by rhamnolipids and synthetic disaccharides.	123
5.3 Conclusion.....	129
5.4 Experimental Section	130
5.4.1 Cloning, recombinant expression and purification of truncated native pilin protein and mutants.	130
5.4.2 Fluorescence spectroscopy	130
5.4.3 Transmission electron microscopy of the pilin assemblies	131
Chapter 6. Cromoglycate Mesogen Forms Isodesmic Assembly Promoted by Peptides and Induce Aggregation of a Range of Proteins	132
6.1 Background and Significance.....	132
6.1.1 Disodium Cromoglycate (5'DSCG) is a biocompatible nonamphiphilic mesogen	132
6.1.2 Disodium Cromoglycate (5'DSCG) is a crystallizing agent for proteins.....	133
6.1.3 Limited available crystal structure of pilin proteins.....	134
6.1.4 Chapter Aim: Crystallization of pilin protein from <i>P. aeruginosa</i> by utilizing the isodesmic assemblies of 5'DSCG.	135
6.2 Results and Discussion.....	135
6.2.1 Components of Luria Bertani media promote isodesmic assembly of 5'DSCG	135
6.2.2 Peptides promote the isodesmic assembly of 5'DSCG.	146
6.2.3 Non-ionic polymers do not promote 5'DSCG to form isolated isodesmic assemblies	150
6.2.4 Protein aggregation is induced by 5'DSCG.	153
6.3 Conclusion.....	158
6.4 Experimental Section	159
6.4.1 Chemicals	159
6.4.2 Preparation of Isodesmic assemblies of disodium cromoglycate (5'DSCG).	160
6.4.3 ¹ H NMR Spectroscopy Measurements	160
6.4.4 Pilin Expression.....	161

6.4.5 Hanging drops precipitation of proteins	161
Chapter 7. Exploring Filamentous Bacteria as Hosts for Protein Expression	162
7.1 Background and Significance.....	162
7.1.1 Antibiotics induce surface-mediated bacterial growth.	162
7.1.2 Chapter Aim: Explore filamentous bacteria for potential as protein expression host.	163
7.2 Results and Discussion.....	164
7.2.1 Carbenicillin induces filament formation of <i>E. coli</i> BL21(DE3).	164
7.2.2 Filament growth of <i>E. coli</i> BL21(DE3) is promoted by stationary growth and containers with a large surface area.....	165
7.2.3 Filament formation of <i>E. coli</i> BL21(DE3) favors plastic vs. glass substrates.	167
7.2.4 Filamentous bacteria produce red cell pellets when proteorhodopsin expression is induced.	168
7.3 Conclusion.....	175
7.4 Experimental Section	176
7.4.1 Aerobic filament growth and protein expression.	176
7.4.2 Stationary filament growth and protein expression.	177
Chapter 8. Conclusions and Future Directions	178
8.1 Conclusions	178
8.2 Future Directions and Thoughts	180
References	186
Appendix	213
Curriculum Vitae	222

List of Figures

- Figure 1.1 Schematic representation of *P. aeruginosa* protein appendages with multiple pili and a single flagellum.2
- Figure 1.2 The pili assembly and retraction of the pili assembly. The protein machinery involved in the assembly/retraction and their localization on the bacterium are shown. Pilin monomers (purple), secretin pilQ (blue), alignment proteins pilMNOP (green), platform protein pilC (yellow), prepilin peptidase pilD (yellow), assembly ATPase pilB (red) and retraction ATPase pilT (gray).3
- Figure 1.3 Different motilities by the bacterium *P. aeruginosa*.5
- Figure 1.4 Models of DNA binding (top) and DNA uptake in the cell (bottom) by pili. [Piepenbrink KH (2019) DNA Uptake by Type IV Filaments. *Front. Mol. Biosci.* 6:1. doi: 10.3389/fmolb.2019.00001; Image Credit: K.H. Piepenbrink; Copyright © 2019 Piepenbrink. This is an open-access article distributed under the terms of the Creative Commons Attribution License, which permits unrestricted use, distribution and reproduction in any medium, provided the original author and source are credited.]8
- Figure 1.5 The amino acid sequences of four pilin peptides from the C-terminal regions of the four strains of *P. aeruginosa* for which NMR solution structures have been determined. The PAK, PAO and KB7 pilin peptides are each 17 residues long with a disulfide-bridged loop of 14 residues between Cys129 and Cys142. The P1 pilin peptide is 23 residues long with a disulfide-bridged loop of 19 residues between Cys127 and Cys145. Cysteine residues are circled in the sequences, and residues in bold face are those conserved in the PAK, PAO and KB7 strains. The location of the β -turns in the PAK, PAO, KB7 and P1 peptides are designated by the boxes. The PAK, PAO and KB7 peptides all display a type I β -turn in the conserved sequence Asp134-X-X-Phe137 and a type II β -turn in the conserved sequence Pro139-X-Gly-Cys142. The P1 peptide displays a type I β -turn in the region spanned by residues Thr134-Ala135-Trp136-Lys137, followed by another turn (boxed in by the broken line) of undefined conformation in the region spanned by Pro138-Asn139-Tyr140-Ala141. Figure is reprinted with permission from Ref 68 Copyright © 1997 Academic Press. All rights reserved.9
- Figure 2.1 Crystal structure of pilin proteins from different bacterial species. *P. aeruginosa* PAK PilA (PDB code: 1dzo), PA11059 (PDB code: 3JZZ) and K122-4 PilA (PDB code: 1qve) and *N. gonorrhoeae* MS11 PilE (PDB code: 1ay2), while the three structures at the bottom are previously solved T4b pilins *S. typhi* PilS (PDB code: 1q5f) and *V. cholerae* TcpA (PDB code: 1oqv). Crystal structures were generated using PyMOL software. Color representation: α -helices in blue, β -sheet in gray and coiled structures in red.15
- Figure 2.2 Pilin modification and assembly systems in *P. aeruginosa*. Group I pilins are glycosylated by TfpO on the C-terminal Ser with an O antigen unit synthesized by the LPS machinery. Group II pilins have no accessory proteins. Group III and V pilins each have a specific accessory protein that promotes their assembly: TfpY for group III and TfpZ for group V. Group IV pilins are glycosylated at several positions by TfpW with mono-, di-, and trisaccharides of d-arabinofuranose synthesized by the ArfO/R proteins (Harvey and Burrows, unpublished data). Group IV pilins have a TfpX accessory protein that is similar to TfpY and TfpZ. Figure is reprinted with permission from Ref. 81. Copyright © 2009 Elsevier Ltd. All rights reserved.16

Figure 2.3 Structures of PA1244N3(pPAC46) native pilin (top) generated by Phyre2 and visualized by PyMOL. The pilin was rotated at different angles to show the predicted structural features of the protein. The α -helix is in blue, β -sheet in gray and coils in red. The amino acid sequence of the native pilin (bottom) with leader peptide in black, α -helices in blue, β -sheet in gray and loops in red.19

Figure 2.4 Amino acid sequences of the full-length pilin (top) and the truncated pilin proteins (middle). The predicted secondary structures of the full, native pilin from PA1244N3 (pPAC46) and truncated pilin mutants pilin Δ (1-31), pilin Δ (1-28) and pilin Δ (1-23) were generated by Phyre2 and visualized by PyMOL (bottom).21

Figure 2.5 SDS-PAGE gel of native pilin expressed and purified from *P. aeruginosa* PA1244N3(pPAC46). Lane (1) ladder and (2) purified native pilin.22

Figure 2.6 Agarose gel of the PCR products of the pulled-out genes for the truncated pilin proteins. (A) lane 1 – 100 bp ladder, lane 2 – PCR product for pilin Δ (1-31) and (B) lane 1 – 100 bp ladder, lane 2- PCR product for pilin Δ (1-28), lane 3- PCR product for pilin Δ (1-23).....23

Figure 2.7 PCR Colony screening results for pilin Δ (1-31) (A) lane 1 – ladder, lanes 2-7 – PCR products ; pilin Δ (1-28), and pilin Δ (1-23) (B) lane1 – ladder, lanes 2-6 PCR product for pilin Δ (1-28), lane 8-11- PCR product for pilin Δ (1-23). Successful colony screens are bright bands around 800 bp.25

Figure 2.8 SDS-PAGE gel of pilin Δ (1-31) purification. Lanes (1) ladder, (2) pre-induction, (3) induced sample, (4) cell debris, (5) cell lysate, (6) flow through, (7) wash flow through, (8) pre-SUMO cleavage, (9) final pilin Δ (1-31), (10) final pilin Δ (1-31)+ β -mercaptoethanol (Left) and the MALDI-TOF results of the pilin Δ (1-31) (Right).26

Figure 2.9 SDS-PAGE gel of pilin Δ (1-28) purification from the lysate. Lanes (1) ladder, (2) pre-induction, (3) induced sample, (4) cell debris, (5) cell lysate, (6) flow through, (7) wash flow through, (8,9) pre-SUMO cleavage, (10) post-cleavage final pilin Δ (1-28), (11) final pilin Δ (1-28).26

Figure 2.10 SDS-PAGE gel of pilin Δ (1-28) purification from the lysate. Lanes (1) ladder, (2) pre-induction, (3) induced sample, (4) cell debris, (5) cell lysate, (6) flow through, (7) wash flow through, (8,9) pre-SUMO cleavage, (10) post-cleavage final pilin Δ (1-28), (11) final pilin Δ (1-28).28

Figure 2.11 SDS-PAGE gel of pilin Δ (1-28) purification from the inclusion bodies. Lanes (1) post-sonication lysate, (2) post-sonication cell debris, (3) supernatant after recovering inclusion bodied from the cell debris, (4) inclusion bodies, (5) post-refolding from inclusion bodies, (6) flow through from Ni-NTA, (7) wash flow through, (10) post-cleavage final pilin Δ (1-28), (11) final pilin Δ (1-28) passed through Ni-NTA column second time.28

Figure 2.12 SDS-PAGE gel of the final pilin Δ (1-28) purification. Lanes (1) ladder, (2,3) final pilin Δ (1-28) from first attempts of purification showing contamination. These proteins were not used in this study. (4) final pilin Δ (1-28) from Fig. 2.10, (5) re-purified pilin Δ (1-28) from Fig. 2.10 by passing through Ni-NTA then buffer exchanged in storage buffer, (6) final pilin Δ (1-28) purified pilin from supernatant in Fig 2.11, lane (7) re-purified pilin Δ (1-28) from supernatant in Fig 2.11 by passing through Ni-NTA then buffer exchanged in storage buffer (Left) and the MALDI-TOF results of the combined pilin Δ (1-28) fractions (Right).29

Figure 2.13 Amino acid sequences of the single amino acid mutants of pilin Δ (1-31) (top). The predicted secondary structure of the single amino acid mutant proteins generated by Phyre2 and visualized by PyMOL	31
Figure 2.14 W105K and I98D mutations of pET-SUMO- pilin Δ (1-31) vector (A). Successful mutations are lanes with a band at ~6 kilobase pairs. Lane (1) 1 kilobase pair ladder, (2) W105K and (3) I98D and P111G mutations of pET-SUMO- pilin Δ (1-31) (B). Successful mutations are lanes with a band at ~6 kilobase pairs. Lane (1) 1 kilobase pair ladder, (2) pET-SUMO- pilin Δ (1-31) vector template and (3) P111G.	32
Figure 2.15 SDS-PAGE gel of P111G mutant of pilin Δ (1-31). Lanes (1) ladder, (2) pre-induction, (3) induced sample, (4) cell lysate, (5) cell debris, (6) flow through, (7) wash flow through, (8) pre-SUMO cleavage, (9) post-cleavage and (10) final P111G protein.	33
Figure 2.16 SDS-PAGE gel of I98D mutant of pilin Δ (1-31). Lanes (1) ladder, (2) pre-induction, (3) induced sample, (4) cell lysate, (5) cell debris, (6) flow through, (7) wash flow through, (8) pre-SUMO cleavage, (9) post-cleavage and (10) final I98D protein.	34
Figure 2.17 SDS-PAGE gel of W105K mutant of pilin Δ (1-31) and I98D final pilin Δ (1-31) vector purified protein. Lanes (1) ladder, (2) pre-induction, (3) induced sample, (4) cell lysate, (5) cell debris, (6) flow through, (7) wash flow through, (8) pre-SUMO cleavage, (9) post-cleavage and (10) final W105K protein (11) final I98D protein.	35
Figure 3.1 Different swarming patterns of two <i>P. aeruginosa</i> strains PAO1 (left) and PA14 (right) on M8 soft agar gel (0.5 wt% agar). The swarming assays were performed by Dr. Hewen Zheng (Luk lab).	45
Figure 3.2 Structures of the individual components of rhamnolipids produced by <i>P. aeruginosa</i>	46
Figure 3.3 The swarming motility of <i>P. aeruginosa</i> strain <i>rhlA</i> and PAO1 on soft agar plates with SDS.	47
Figure 3.4 Synthetic disaccharides that inhibit swarming of <i>P. aeruginosa</i> : SF β M, SF β C and SF-EG ₄ OH. These molecules are synthesized by Luk lab.	48
Figure 3.5 Swarm gel prepared by dissolving increasing concentrations of D β M. Droplets (3 μ L) of water or PAO1. The droplet assay was performed by Yuchen Jin (Luk lab member).....	51
Figure 3.6 Design of the bacterial motility enabled binding assay. The surface of soft gels containing ligand molecules that either inhibit swarming of PAO1 or promote swarming of <i>rhlA</i> are introduced with a receptor protein candidate by either (A) spreading a solution of protein (10.5 nmol; 150 μ L of 70 μ M), or (B) placing droplets of protein (250 pmol; 2.5 μ L of 100 μ M). Bacteria (3 μ L, OD ₆₀₀ ~ 0.6) is inoculated on the center of gel surface and incubated to monitor the swarming motility.	53
Figure 3.7 Modified swarming binding enabled assay scheme describing case 1: proteins on the gel do not bind ligands and case 2: proteins bind ligands.	54
Figure 3.8 Swarming motility of <i>rhlA</i> on soft gel mixed with increasing concentrations of monorhamnolipid or dirhamnolipid.	56
Figure 3.9 Swarming motilities of wild-type PAO1 with and without pilin proteins. Proteins spread on the gel: 1 mL of 0.5 mg/mL native pilin (35 nmol), pilin Δ (1-31) (41 nmol), pilin Δ (1-28): (40 nmol) and Δ pilin (1-23) (38 nmol). Protein solutions were prepared in 25 mM Tris, 100 mM	

NaCl buffer, pH= 7.5, and 40 mM sodium phosphate buffer, pH= 7.2 Images were taken 24 hours after inoculation.	58
Figure 3.10 Bacterial motility enabled binding assay. The effect of protein droplets on the swarming motility of <i>P. aeruginosa</i> PAO1 on soft agar gel (top). Scheme of the swarming motility-based ligand-binding assay (bottom). The amount of protein in each drop on the surface of the gel is 250 pmol (●) 2.5 μ L of native pilin (1.6 mg/mL; 100 μ M) or BSA (6.6 mg/mL; 100 μ M) spot and (x) 3 μ L PAO1 (OD~ 0.7) inoculation spot on soft agar gel. Protein solutions were prepared in 40 mM sodium phosphate buffer, pH= 7.2	59
Figure 3.11 Swarming motilities of wild-type PAO1 with increasing amount of native pilin protein spread on the gel; Volume spread: 150 μ L. Protein solutions was prepared in 40 mM sodium phosphate buffer, pH= 7.2 Images were taken 24 hours after inoculation.	60
Figure 3.12 Swarming motilities of wild-type PAO1 with increasing amount of pilin Δ (1-31); Volume spread: 150 μ L Protein solutions were prepared in 25 mM Tris, 100 mM NaCl buffer, pH= 7.5. Images were taken 24 hours after inoculation.	61
Figure 3.13 Swarming motility of <i>rhlA</i> on soft gels with 5 μ M rhamnolipids mixture with increasing amounts of pilin proteins. Proteins spread on the gel: 150 μ L native pilin (top) and pilin Δ (1-31) (bottom). Native pilin was prepared in 40 mM sodium phosphate buffer, pH= 7.2. Solution of pilin Δ (1-31) was prepared in 25 mM Tris, 100 mM NaCl buffer, pH= 7.5. Images were taken 24 hours after inoculation.	62
Figure 3.14 Swarming motility of <i>rhlA</i> on soft gels with 20 μ M rhamnolipids mixture with increasing amounts of pilin proteins. Proteins spread on the gel: 150 μ L native pilin (top) and BSA (bottom). Protein solutions were prepared in 25 mM Tris, 100 mM NaCl buffer, pH= 7.5, and 40 mM sodium phosphate buffer, pH= 7.2 Images were taken 24 hours after inoculation.	63
Figure 3.15 The swarming motility of <i>P. aeruginosa</i> strain PAO1 on soft gel without and with (25 or 30 μ M) rhamnolipids. Proteins spread on the gel surface: 10.5 nmol of native pilin (150 μ L of 1.1 mg/ mL) and 10.5 nmol pilin Δ (1-31) (150 μ L of 0.84 mg/ mL). Native pilin was prepared in 4 mM sodium phosphate buffer, pH=7.2 and pilin Δ (1-31) pilin was prepared in 50 mM Tris, 100 mM NaCl, pH=7.5. Swarmn plates were inoculated overnight at 37 $^{\circ}$ C.....	65
Figure 3.16 The swarming motility of <i>P. aeruginosa</i> strain PAO1 on soft gel with pilin Δ (1-31) mutants- 17.7 nmol (150 μ L of 1.41 mg/mL) I98D, 13.8 nmol (150 μ L of 1.11 mg/mL) P111G, 12 nmol W105K (150 μ L of 0.96 mg/mL) spread on the gel surface. Proteins were prepared in 50 mM Tris, 100 mM NaCl buffer, pH=7.5.	66
Figure 4.1 Circular dichroism spectra of secondary structures of proteins.	75
Figure 4.2 Circular dichroism spectrum of 25 μ M native 1244 pilin expressed in <i>P. aeruginosa</i> (left). Model of the native pilin generated by Phyre2 (right). Protein was prepared in 4 mM sodium phosphate buffer, pH= 7.2.	79
Figure 4.3 Circular dichroism spectrum of 25 μ M pilin Δ (1-31) heterologously expressed in <i>E. coli</i> (left). Model of the native pilin generated by Phyre2 (right) Protein was prepared in 2 mM Tris and 7 mM NaCl, pH= 7.5.	80
Figure 4.4 Circular dichroism (CD) spectra of 25 μ M pilin Δ (1-31) (black) and single amino acid mutants: 25 μ M pilin Δ (1-31) W105K (green), 25 μ M pilin Δ (1-31) I98D (blue), and 20 μ M pilin	

$\Delta(1-31)$ P111G (red). Proteins were prepared to a final volume of 300 μ L in 2 mM Tris and 7 mM NaCl, pH= 7.5.	81
Figure 4.5 CD spectra of 22 μ M pilin $\Delta(1-31)$ only (blue) and with 200 μ M rhamnolipids mixture (black). Both proteins and ligands are dissolved in 2 mM Tris and 7 mM NaCl, pH= 7.5.	82
Figure 4.6 CD spectra of 25 μ M pilin $\Delta(1-31)$ with increasing amounts of rhamnolipids mixture. Both proteins and ligands are dissolved in 2 mM Tris and 7 mM NaCl, pH= 7.5.	83
Figure 4.7 CD spectra of 30 μ M pilin $\Delta(1-31)$ with increasing amounts of monorhamnolipid (top) and dirhamnolipid (bottom). Both proteins and ligands are dissolved in 2 mM Tris and 7 mM NaCl, pH= 7.5.	85
Figure 4.8 CD spectra of 22 μ M pilin $\Delta(1-31)$ with 220 μ M rhamnolipids (blue), SF β M (green), (SF β M & rhamnolipids) (competitive assay) (red). Spectrum of pilin $\Delta(1-31)$ only (black). Proteins and ligands were dissolved in 2 mM Tris and 7 mM NaCl, pH= 7.5.	86
Figure 4.9 CD spectra of 25 μ M native 1244 pilin without(black) and with 250 μ M rhamnolipids (blue), SF β M (green), (SF β M & rhamnolipids) (competitive assay) (red). Spectrum of pilin $\Delta(1-31)$ only (black). Proteins and ligands were dissolved in 4 mM sodium phosphate buffer, pH= 7.2.	87
Figure 4.10 1 H NMR of native 1244 pilin expressed from <i>P. aeruginosa</i> PA1244N3(pPAC46). Original spectra (inset). Protein was prepared in 90%/10% H ₂ O/D ₂ O containing 50 mM sodium phosphate buffer, 2.6 mM NaN ₃ and 2.6 mM DSS, pH=5.55. The spectrum was taken on a 800 MHz Bruker NMR.	89
Figure 4.11 15 N HSQC of full pilin from PA1244 overlay spectra. 350 μ M native pilin in black, 120 μ M native pilin in red. The sample solution was prepared in 90%/10% H ₂ O/D ₂ O containing 50 mM sodium phosphate buffer, 2.6 mM NaN ₃ and 2.6 mM DSS, pH=5.55. The spectra were taken on a 800 MHz Bruker NMR.	90
Figure 4.12 15 N HSQC of native pilin from PA1244 overlay spectra. 120 μ M native pilin in black, w/ 50 μ M SF β C in blue. The samples were prepared in 90%/10% H ₂ O/D ₂ O containing 50 mM sodium phosphate buffer, 2.6 mM NaN ₃ and 2.6 mM DSS, pH=5.55. The spectra were taken on a 800 MHz Bruker NMR.	91
Figure 4.13 15 N HSQC of native pilin from PA1244 overlay spectra with 50 μ M SF β C in blue and 120 μ M in pink. The samples were prepared in 90%/10% H ₂ O/D ₂ O containing 50 mM sodium phosphate buffer, 2.6 mM NaN ₃ and 2.6 mM DSS, pH=5.55	92
Figure 4.14 1 H NMR of 120 μ M pilin $\Delta(1-31)$. Protein was prepared in 50 mM 90%/10% H ₂ O/D ₂ O containing 50 mM NaPB buffer, pH= 7.5. The spectrum was taken on a 400 MHz Bruker NMR.	93
Figure 4.15 15 N- Heteronuclear quantum coherence (HSQC) NMR spectra of pilin $\Delta(1-31)$. Proteins were prepared in 90%/10% H ₂ O/D ₂ O, 25 mM Tris, 100 NaCl, 2.6 mM NaN ₃ and 2.6 mM DSS, pH=7.5. The spectrum was taken on a 400 MHz Bruker NMR.	94
Figure 4.16 15 N- Heteronuclear quantum coherence (HSQC) NMR spectra of pilin $\Delta(1-31)$ with ligands added (A) SF β M overlay spectra: pilin $\Delta(1-31)$ control (black), pilin $\Delta(1-31)$ + SF β M (red), (B) rhamnolipids overlay spectra. pilin $\Delta(1-31)$ control (black), pilin $\Delta(1-31)$ + rhamnolipids (blue). Proteins were prepared in 90%/10% H ₂ O/D ₂ O, 25 mM Tris, 100 NaCl, 2.6 mM NaN ₃ and 2.6 mM DSS, pH=7.5. The spectra were taken on a 400 MHz Bruker NMR.	95

Figure 4.17 The number distribution measured by dynamic light scattering of (A) 25 μ M pilin Δ (1-31), (B) w/ 200 μ M rhamnolipids, (C) w/ 200 μ M SF β M. Measurements were done on 50 μ L solutions in 25 mM Tris and 100 mM NaCl, pH= 7.5.	97
Figure 4.18 The number distribution measured by dynamic light scattering of (A) 200 μ M rhamnolipids, (B) 200 μ M SF β M. Measurements were done on 50 μ L solutions in 25 mM Tris and 100 mM NaCl, pH= 7.5.	98
Figure 4.19 The number distribution measured by dynamic light scattering of (A) 25 μ M pilin Δ (1-31), (B) w/ 10 nM monorhamnolipid, (C) w/ 1 nM monorhamnolipid and (D) 10 nm monorhamnolipid . Measurements were done on 50 μ L solutions in 25 mM Tris and 100 mM NaCl, pH= 7.5.	99
Figure 5.1 Scheme of protein assembly models by cooperative (left) and isodesmic (right) assembly.	108
Figure 5.2 Fluoresce emission of native 1244 pilin (black) and Δ (1-31) (blue) excited at 260 nm. Proteins were prepared as 1 mL solutions of 100 nM proteins in 50 mM Tris, 100 mM NaCl, pH=7.5.	110
Figure 5.3 Fluorescence emission of native 1244 pilin (top) and pilin Δ (1-31) (bottom) with ligands 1 μ M rhamnolipids and 1 μ M SDS. Proteins with and without ligands were prepared in 50 mM Tris, 100 mM NaCl, pH=7.5 with a total final volume of 1 mL.	111
Figure 5.4 Fluorescence emission spectra of 100 nM pilin Δ (1-31) single amino acid mutants I98D, W105K and P111G (bottom) with ligands 1 μ M rhamnolipids. Proteins with and without ligands were prepared in 50 mM Tris, 100 mM NaCl, pH=7.5 with a total final volume of 1 mL.	112
Figure 5.5 Fluorescence emission spectra of 100 nM of pilin Δ (1-31) with (A)SF-EG ₄ OH, (B) SF β C, (C) dirhamnolipid, (D) monorhamnolipid and (E) SDS. Proteins and ligands were dissolved in 50 mM Tris and 100 mM NaCl, pH= 7.5. Samples were equilibrated for 16 hours prior to fluorescence measurements.	114
Figure 5.6 Plot of intrinsic fluorescence vs. ligand concentration for individual solutions of 100 nM pilin Δ (1-31) with different ligands: (A) SF-EG ₄ OH, (B) SF β C, (C) dirhamnolipid and (D) monorhamnolipid and (E) SDS. Proteins and ligands were dissolved in 50 mM Tris and 100 mM NaCl, pH= 7.5. Fluorescence measurements were taken after 16 h of incubation. n=3.....	116
Figure 5.7 (A) Fluorescence emission spectra of 100 nM monorhamnolipid titrated with increasing concentrations of pilin Δ (1-31). (B) Plot of intrinsic fluorescence vs. pilin conc. titrated into monorhamnolipid solution. Proteins and ligands were dissolved in 50 mM Tris and 100 mM NaCl, pH= 7.5. Measurements were made ~12h after adding 10 μ L aliquots of 10 nM, 1 μ M and 9 μ M of truncated pilin into 1 mL of 100 nM of monorhamnolipid.	119
Figure 5.8 Plot of intrinsic fluorescence vs. time (hr) of 500 nM mono-rhamnolipid and varying concentrations of pilin Δ (1-31) (360, 100 and 75 nM). Proteins and ligands were dissolved in 50 mM Tris and 100 mM NaCl, pH= 7.5.	121
Figure 5.9 Plot of intrinsic fluorescence vs. time (hr) of 1 nM mono-rhamnolipid and varying concentrations of pilin Δ (1-31) (100 and 50 nM). Proteins and ligands were dissolved in 50 mM Tris and 100 mM NaCl, pH= 7.5.	122

Figure 5.10 TEM images of 80 μM pilin $\Delta(1-31)$ (A), + 8 nM monorhamnolipid (B), and + 8 nM SF β C (C). Micrographs were taken on a FEI Tecnai 12 BioTwin TEM. (Cornell Center for Materials Research, NY, USA) operating at 120 kV.	124
Figure 5.11 Transmission electron micrographs of negatively stained assemblies from a solution of 80 μM pilin $\Delta(1-31)$ with 8 nM monorhamnolipid (A) and 8 nM SF β C (B). Micrographs were taken on a FEI Tecnai 12 BioTwin TEM. (Cornell Center for Materials Research, NY, USA) operating at 120 kV.	125
Figure 5.12 TEM images of 80 μM pilin $\Delta(1-31)$ with 8 nM SF β C from three different aggregates on the grid. Micrographs were taken on a FEI Tecnai 12 BioTwin TEM. (Cornell Center for Materials Research, NY, USA) operating at 120 kV.	126
Figure 5.13 TEM images of 266 μM pilin $\Delta(1-31)$ (A), + 400 μM monorhamnolipid (B), and + 400 μM SF β C (C). Micrographs were taken on a FEI Tecnai 12 BioTwin TEM. (Cornell Center for Materials Research, NY, USA) operating at 120 kV.	127
Figure 5.14 Transmission electron micrographs of negatively stained assemblies from a solution of 266 μM pilin $\Delta(1-31)$ and 400 μM monorhamnolipid. Scale bar: 10 nm. Images were taken at SUNY-ESF using the JEOL JSM-2000EX microscope.	128
Figure 5.15 Proposed scheme of ligand-induced protein assembly for rhamnolipids.	129
Figure 6.1 Chemical structure of disodium cromoglycate (5'DSCG).	133
Figure 6.2 Schematic representation of formation of isodesmic assembly of 5'DSCG induced by chemical additives.	136
Figure 6.3 Images of 5'DSCG solutions at different concentrations in (A) Millipore water (B) Luria Bertani (LB) media (1 wt% sodium chloride, 1 wt% tryptone and 0.5 wt% yeast extract) viewed under cross polars. Scale bar = 760 μm	137
Figure 6.4 Optical density (OD_{600}) measurements versus the concentrations 5'DSCG in deionized water and in LB medium. Arrows indicate the concentrations at which the liquid crystal (LC) phase forms.	138
Figure 6.5 ^1H NMR spectra of 1.5 wt% of 5'DSCG without (A) and with (B) LB components, 2.5 wt% 5'DSCG without (C) and with (D) LB components, and (E) LB components in D_2O . The protons of 5'DSCG and peak assignments are labelled in red.	140
Figure 6.6 ^1H NMR spectra of 5 wt% 5'DSCG (A), 4 wt% 5'DSCG (B), 2 wt% 5'DSCG without (C) and with LB components (D) in D_2O . The protons of 5'DSCG and peak assignments are labelled in red.	142
Figure 6.7 NOESY spectra of 2 wt% 5'DSCG with LB components (1 wt% sodium chloride, 1 wt% tryptone and 0.5 wt% yeast extract).	143
Figure 6.8 NOESY spectra of 2 wt% 5'DSCG with (A) and without (B) LB components in D_2O . With LB, cross peaks 1, 2, 5 are intermolecular NOEs; 3 and 4 are a mixture of inter- and intramolecular NOEs. Without LB, cross peaks 3 and 4 are intramolecular NOEs.	144
Figure 6.9 NOESY spectra of 2 wt% 5'DSCG with LB components at different temperatures: 221°C (A), 27°C (B), 29°C (C), 31°C (D) , and 33°C (E). Plot of NOE intensity of peak 2 vs. temperature (F).	145

Figure 6.10 Plot of intensity of NOE cross peaks vs. temperature for 2 wt% 5'DSCG with LB components.	146
Figure 6.11 Optical density (OD ₆₀₀) measurements of solutions containing 7 wt% 5'DSCG mixed with individual LB media components: yeast extract, tryptone and sodium chloride at different concentrations. (7 wt% 5'DSCG with yeast extract at concentration higher than 2.5 wt% caused precipitation).	147
Figure 6.12 Optical density (OD ₆₀₀) measurements of the solutions containing 1 wt% peptide mixtures (peptone, casitone, and tryptone) mixed with different concentrations of 5'DSCG. The arrow indicates 5'DSCG concentration at which the liquid crystal (LC) droplets appear.	148
Figure 6.13 Optical density (OD ₆₀₀) measurements of solutions containing 3 wt% 5'DSCG mixed with different concentrations of peptides: casitone, peptone, and tryptone.	149
Figure 6.14 Optical density (OD ₆₀₀) measurements of solutions containing additives: 4.6 wt% NaCl, 1 wt% casamino acids, 31.5 wt% urea, 8.53 wt% L- glutamic acid, 2.35 wt% L-alanine and 2.94 wt% L-arginine mixed with different concentrations of 5'DSCG.	150
Figure 6.15 Optical density (OD ₆₀₀) measurements of solutions containing 7 wt% 5'DSCG mixed with different concentrations of non-ionic polymers: poly-vinylalcohol (PVA, mw ~ 9,000-10,000), poly-vinylpyrrolidone (PVP, mw ~40,000), and poly-acrylamide (PAAm, mw~ 9,000-10,000). Arrows indicate the polymer concentration mixed with 7 wt% 5'DSCG at which the the liquid crystal (LC) droplets appear.	151
Figure 6.16 Optical density (OD ₆₀₀) measurements of solutions containing 3 wt% 5'DSCG mixed with different concentrations of non-ionic polymers: poly-vinylalcohol (PVA, mw ~ 9,000-10,000), poly-vinylpyrrolidone (PVP, mw ~40,000), and poly-acrylamide (PAAm, mw~ 9,000-10,000)	152
Figure 6.17 Different protein aggregates induced by 5'DSCG in hanging droplets. The droplets (5 μL) contained (A) 0.625 wt% 5'DSCG and 25 mg/mL pilin, (B) 0.625 wt% 5'DSCG and 1 mg/mL lectin A, (C) 0.625 wt% 5'DSCG and 20.5 mg/mL esterase, (D) 0.625 wt% 5'DSCG and 20.5 mg/mL bovine serum albumin, and (E) 0.14 wt% 5'DSCG + 37.5 mg/mL lipase. The reservoir solution contained 350 μL of (A, B, C, D) 1.25 wt% 5'DSCG, and (E) 0.28 wt% 5'DSCG. Hanging drops kept at ambient temperature were observed over 5-15 days. All solutions were prepared using 25 mM Tris buffer, pH = 7.5; except for (D) where pH = 6.5. Scale bar = 380μm.	155
Figure 6.18 Native pilin aggregates induced by different precipitants in hanging droplets. The droplets (5 μL) contained (A) 0.15 wt% 5'DSCG and 50 mg/mL pilin, (B) 0.375 wt% 5'DSCG and 5 mg/mL pilin, (C) 0.625 wt% 5'DSCG and 25 mg/mL pilin, (D) 0.5 wt% NaCl and 10 mg/mL pilin, and (E) 1.5 wt% PEG8000 and 5 mg/mL pilin. The reservoir solution contained 350 μL of (A) 0.30 wt% 5'DSCG, (B) 0.75 wt% 5'DSCG, (C) 1.25 wt% 5'DSCG, (D) 1 wt% NaCl, and (E) 3 wt% PEG8000. Hanging drops kept at ambient temperature were observed over 5-15 days. All solutions were prepared using 25 mM Tris buffer, pH = 7.5. Scale bar = 380μm.	156
Figure 6.19 Truncated pilin (pilin Δ(1-31)), aggregates induced by different precipitants in hanging droplet. The droplets (5 μL) contained 0.375 wt% 5'DSCG & 5 mg/mL truncated pilin, without polarizer (A), and under cross polars (B); 0.625 wt% 5'DSCG & 1 mg/mL truncated pilin, without polarizer (C), and under cross polars (D); 1.25 wt% 5'DSCG & 5 mg/mL truncated pilin, without polarizer (E), and under cross polars (F); 0.15 wt% 5'DSCG & 0.375 wt% NaCl & 2.5 mg/mL truncated pilin without polarizer (G) and under cross polars (H) and 25 wt% PEG4000 &	

1 mg/mL truncated pilin without polarizer (I). The reservoir solution contained 350 μ L of (A, B) 0.75 wt% 5'DSCG, (C, D) 1.25 wt% 5'DSCG, (E, F) 2.5 wt% 5'DSCG and (G,H) 0.3 wt% 5'DSCG & 0.75 wt% NaCl, and (I) 50 wt% PEG4000. Hanging drops kept at ambient temperature were observed over 5-15 days. All solutions were prepared using 25 mM Tris buffer, pH = 7.5. Scale bar = 76 μ m.158

Figure 7.1 Cell cultures of *E. coli* BL21(DE3) with pET-26b plasmid expressing proteorhodopsin grown with shaking at 250 rpm, 37 °C (top) and microscope images of the cell culture (bottom).165

Figure 7.2 Cell culture of *E. coli* BL21(DE3) with pET-26b plasmid expressing proteorhodopsin grown under stationary conditions (top) and microscope images of the cell culture (bottom). ..166

Figure 7.3 Images of *E. coli* BL21(DE3) with pET-26b plasmid expressing proteorhodopsin grown under stationary conditions at two different carbenicillin concentrations: 20 and 100 μ g/mL. ..167

Figure 7.4 Images of *E. coli* BL21(DE3) with pET-26b plasmid expressing proteorhodopsin grown under stationary conditions with 100 μ g/mL.168

Figure 7.5 Cell pellets of *E. coli* BL21(DE3) with pET-26b plasmid expressing proteorhodopsin grown under shaking conditions. The growth conditions are indicated for each tube, chemicals were added at $A_{600} \sim 0.2$ for all tubes.170

Figure 7.6 Absorbance spectra of resuspended filaments *E. coli* BL21(DE3) with pET-26b plasmid expressing proteorhodopsin in 0.9 % NaCl solution.171

Figure 7.7 Absorbance measurements of the resuspended filaments from 300 -700 nm (left). Cell pellets of induced filaments of *E. coli* BL21(DE3) with pET-26b plasmid expressing proteorhodopsin grown under shaking conditions with different carbenicillin concentrations. The growth conditions are indicated for each tube. All tubes have 0.5 mM IPTG and 21 μ M retinal (right).172

Figure 7.8 Cell pellets of induced filaments of *E. coli* BL21(DE3) with pET-26b plasmid expressing proteorhodopsin grown under shaking conditions with different carbenicillin concentrations (top). Post-sonication solutions (bottom). Filaments were resuspended in 50 mM HEPES, 150 mM KCl, 2% D β M and 0.5 mM PMSF, pH = 7. All tubes have 0.5 mM IPTG and 21 μ M retinal.173

Figure 7.9 Absorbance measurements of the sonicated *E. coli* BL21(DE3) with pET-26b plasmid expressing proteorhodopsin grown under shaking conditions filaments from 300 -600 nm174

Figure 7.10 Absorbance measurements of the resuspended filaments from 300 -700 nm (left). Cell pellets of induced filaments of *E. coli* BL21(DE3) with pET-26b plasmid expressing proteorhodopsin grown under stationary conditions with different carbenicillin concentrations. The growth conditions are indicated for each tube. All tubes have 0.5 mM IPTG and 21 μ M retinal (right).175

Figure 8.1 (A) Cryoelectron micrograph of *P. aeruginosa* pilin. Red rectangles indicate boxed pilus filaments. Reprinted with permission from reference 1. Copyright © 2017 Elsevier Ltd. (B) Axial view of a single turn of the type IV pilus. The α -helix in blue, β -sheet in green, and loops in purple are shown. Reprinted with permission from reference 2. Copyright © 2004, American Chemical Society . (C) *P. aeruginosa* PAK pilin fiber model based on the assembly parameters

described by Parge *et al.* (1995). The α -helix (blue) and major β -sheet (green) are shown. The minor β -sheet region (yellow coils), the C-terminal disulphide-bonded loop (red coils) and the remainder of the residues (purple coils) are also shown. The graphical elements of the second monomer from the bottom are enclosed in bold lines to highlight the boundary of a pilin monomer. The receptor analogue β -d-GalNAc(1 \rightarrow 4)- β -d-Gal, represented as a ball-and-stick model, is shown in a position suggested by molecular docking studies. It has been included to illustrate the location of the binding site and the size of the disaccharide relative to the pilus. However, the depicted binding mode is not expected to be correct in its details. Adopted from reference 3. Copyright © 2000 Academic Press. All rights reserved. (D) Predicted full *P. aeruginosa* 1244 pilin (left) and truncated pilin Δ (1-31) using Phyre2 and visualized by PyMOL.182

List of Tables

Table 2.1 Primers used for recombinant expression of pilin in <i>E.coli</i>	38
Table 3.1 Composition of salts in M8 agar gel.	51
Table 6.1 Correlation between the effect of polymers on 5'DSCG assembly and the types of liquid crystal droplets promoted by the polymers.....	153
Table 6.2 Native pilin protein precipitation with NaCl and 5'DSCG as precipitants.....	157

List of Equations

Equation 4.1 Stokes-Einstein equation77

Equation 5.1 Equation to describe ligand-induced protein binding.123

Chapter 1. Introduction: Ligands for controlling pili assembly dynamics and functions are important but remain elusive.

1.1 Pili are surface proteins in multiple bacterial activities leading to infections.

Pseudomonas aeruginosa is a gram-negative, rod-shaped bacteria linked to a wide array of diseases. This bacterium is an opportunistic human pathogen that can cause nosocomial infections in immunocompromised patients with cystic fibrosis, cancer, diabetes and burn wounds.¹ *P. aeruginosa* has developed resistance to a multitude of antibiotics including β -lactams, aminoglycosides and quinolones, posing a challenge to treating infections related to this bacterium.² *P. aeruginosa* infections are primarily mediated by adhesion of their surface appendages, pili, to the sialic acid moieties on mammalian cells that further develops into proliferation on host cells.³⁻¹³ Pili or type IV pili are long, thin filamentous surface protein appendages (Fig. 1.1), that are responsible for a range of *P. aeruginosa* biological activities including recognition of a variety of surfaces and adhere to host cells and abiotic surfaces,³⁻¹⁷ initiating biofilm formation,¹⁸⁻²³ mediating horizontal gene transfer,²⁴⁻²⁶ , swarming^{27, 28} and twitching motility.²⁹⁻³² The surface sensing mechanism of pili is one major determinant for the global signalling of the cyclic di-GMP (cdG) levels that controls multiple bacterial activities.³³⁻³⁶ The surface sensing by pili is critical for initiating a wide range of virulence factors³³ and for the formation of biofilm,³⁴ which is associated with the increase of the cdG levels.³⁵ Pili are also responsible for the motility of bacteria dispersed from a biofilm,³⁶ and the increase of associated virulence factors, which are associated with decreases of the cdG level.³⁶ While pili are implicated for multiple biological activities, additional studies are still underway to understand how a single protein could display versatility in function.

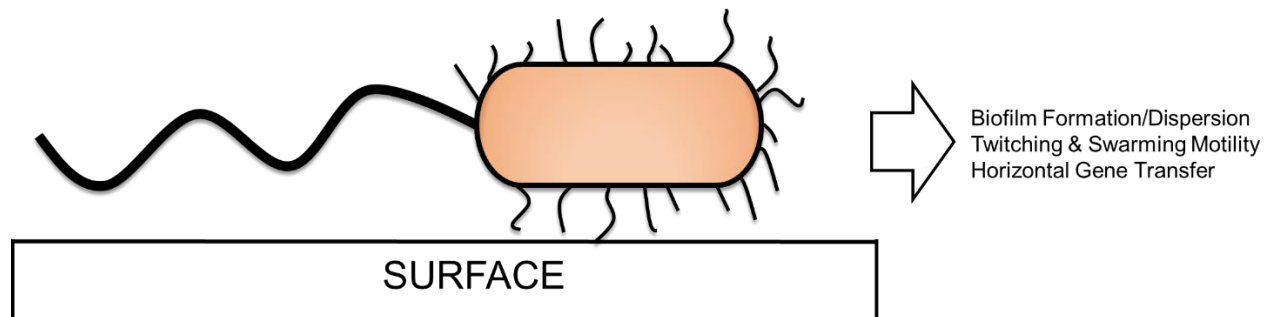


Figure 1.1 Schematic representation of *P. aeruginosa* protein appendages with multiple pili and a single flagellum.

1.2 The pili assembly is comprised of individual pilin monomers that assemble and disassemble

Pili are long, thin filamentous protein appendages that are found on the surface of *P. aeruginosa*. The expression of the pili assembly involves a complex, large number of genes that include both structural and regulatory genes.³⁷⁻⁴⁰ Within the chromosomal DNA of the *P. aeruginosa* species, there is only one copy of the structural pilin gene, *pilA*.⁴¹ The *pilA* gene encodes for the pilin monomer that are assembled circularly (4-5 monomers) and stack to form the pili appendage. The pilin monomer is a general class of protein consisting of an exposed N^o terminal α -helix and a variable C' terminal globular head comprised of β -sheets and terminal disulfide loop (Fig 1.2). The α -helices at the N-terminus assemble in the core of the linear fibrous structure with the D-loop and the β -sheet exposed to the aqueous environment.

Transcription of this gene requires the *rpoN* σ -factor that RNA polymerase recognizes to express pilin in *P. aeruginosa*.^{42,43} Pilin monomers are prematurely expressed as pre-pilins containing a 6-7 amino acid leader peptide sequence that is recognized and cleaved by the

prepilin peptidase pilD enzyme prior to the assembly into pili (Fig 1.2).⁴⁴⁻⁴⁶ A cytoplasmic ATPase, pilB, powers the assembly of the mature pilin monomers that assembles as a filament that passes through the inner membrane, peptidoglycan and out the secretin embedded in the outer membrane as the polymerized pili assemble. The assembly reverses its course as the pili retracts into the bacterium by the aid of the retraction ATPase, pilT, as the ATP is hydrolyzed, and the pili assembly retracts into the bacterium from the outer membrane into the cytoplasm. In response to external stimuli, pili are capable of extension and retraction (assemble and disassemble) at a rate of ~ 1000 subunits/s generating ~ 100 pN of force.⁴⁷⁻⁴⁹ (Fig. 1.2).

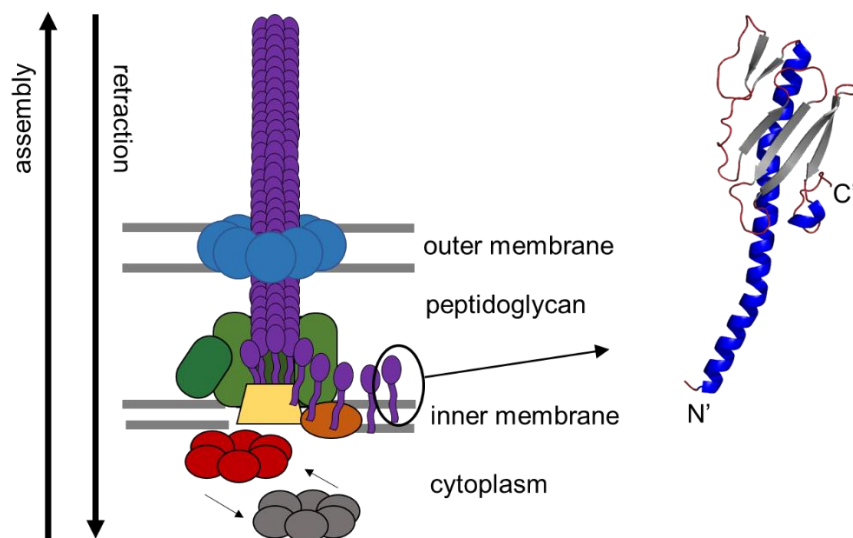


Figure 1.2 The pili assembly and retraction of the pili assembly. The protein machinery involved in the assembly/retraction and their localization on the bacterium are shown. Pilin monomers (purple), secretin pilQ (blue), alignment proteins pilMNOP (green), platform protein pilC (yellow), prepilin peptidase pilD (orange), assembly ATPase pilB (red) and retraction ATPase pilT (gray).

1.3 Pili is the major adhesin of P. aeruginosa leading to host colonization and infections.

The primary step of bacterial colonization and infections is mediated by adhesion.⁵⁰ Several studies have demonstrated that pili is required for the attachment of bacteria to mammalian cells including tracheal cells^{3, 4, 13} human buccal epithelial cells,^{7, 10} and pneumocyte cells¹¹ as pili binds to the glycolipid Asialo-GM₁ found on the mammalian cell surface.¹² Further studies by Irvin and co-workers demonstrated that pili recognizes and binds to the GalNAc(1→4)β-DGal structure found in Asialo-GM₁.^{8, 9, 51} Pili also binds abiotic surfaces such as stainless steel and hydrophobic surfaces such as polystyrene.¹⁴⁻¹⁶ These binding events are tip-associated, and the adhesinotope is located within disulfide loop (D-loop) of the pilin monomer at the C-terminus that is exposed when the pilin monomers assemble into pili. Competitive binding studies demonstrated that the disulfide loop of the pilin can inhibit binding of pilin to host cells and surfaces.^{12, 16} Collectively, these findings suggest that the pilin protein contains a binding pocket that has a dual function of binding both hydrophilic and hydrophobic moieties on surfaces.

1.4 Pili is important in bacterial motility.

P. aeruginosa are capable of different types of motility such as twitching, swarming, swimming, gliding and sliding (Fig. 1.3).^{52, 53} Upon attachment of *P. aeruginosa* on surfaces, bacterial motility plays a significant role by allowing the mobilization of the cells leading to effective colonization on both biotic and abiotic surfaces. Pili is also involved in bacterial motility, particularly in twitching motility of *P. aeruginosa*. Twitching motility is the most common pili-mediated motility that arise as a consequence of the dynamic behavior of the pili assembly, powered by the extension and retraction of the pili assembly.^{29, 54, 55} The retraction

force of pilin is so strong that the pull of a single fiber generates 100 pN of force (*N. gonorrhoea*).^{47, 48} Twitching motility is implicated for *P. aeruginosa* bioactivities such as the traversal of the cells in corneal epithelium infections³² and the development of biofilm architecture.^{30, 31} Previous reports have shown that *P. aeruginosa* mutants deficient for pilus biogenesis did not form microcolonies that are essential for biofilms,³¹ while pili-retraction deficient mutants form larger and more irregular biofilms than the strains fully functional for twitching.³⁰ These results demonstrate that fully functional pili assembly is needed for biofilm development.

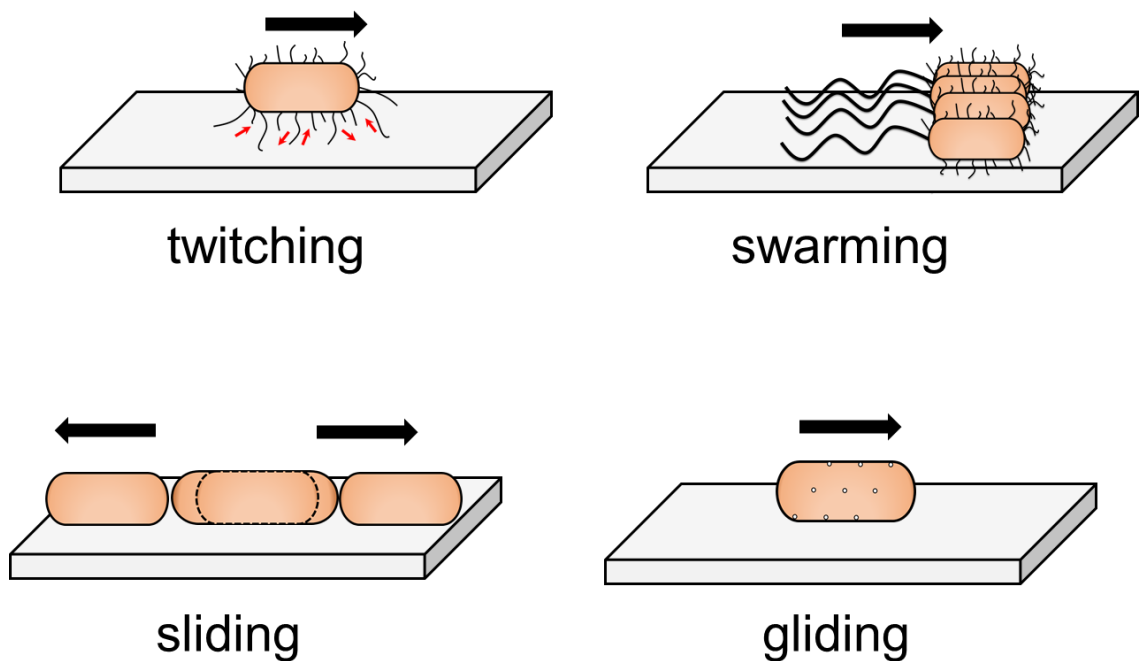


Figure 1.3 Different motilities by the bacterium *P. aeruginosa*.

Another mode of motility by *P. aeruginosa* that involves pili is swarming.^{27, 28} Swarming motility is the flagellum-mediated collective motion of cells inoculated on soft agar gel (0.4- 0.7

% agar). It was previously reported that swarming is influenced by different factors such as bacterial cell density/quorum sensing, surface wetness, nutrient medium, the presence of flagella and pili, and complex phenotypic adaptation.^{27, 28, 56-58} The presence of pili on *P. aeruginosa* is known to influence swarming, but the exact role of pili is unclear. In a previous study, the deletion of the *pilA* gene abolishes swarming motility of *P. aeruginosa*,²⁸ while other studies have shown that deleting the *pilA* gene results in hyper swarming of *P. aeruginosa*.²⁷ Pili has been reported to facilitate cell-to-cell interactions between swarming cells that results in bacteria clustering together instead of swarming.²⁷ Quorum sensing regulates swarming of bacteria, as well as the production of rhamnolipids by *P. aeruginosa*. The production of rhamnolipids is essential for the swarming of *P. aeruginosa*. Structurally characterized as surfactants, rhamnolipids are believed to lower the surface tension of the soft agar gel surface.²⁸ However, rhamnolipids have also been reported to function as signaling molecules in controlling swarming motilities.^{23, 59} For example, *P. aeruginosa* transposon mutant strain, *rhlA*, is unable to produce rhamnolipids and does not swarm on the agar plate.^{23, 28, 59, 60} When rhamnolipids are externally added in the swarming gel, *rhlA* swarming is re-activated. Reversal of activity from initiating to inhibiting swarming motility is observed when the rhamnolipids concentration in the soft gel is increased.²³ Such reversal of bioactivity as a result molecule concentration increases has been observed for quorum sensing molecules⁶¹ and is a classical sign of cell signaling controlled by chemicals. These results suggest that swarming arises from a biological effect, rather than a physical effect, in which rhamnolipids bind to one or more protein receptors, triggering a cascade of signaling events leading to observed regulation of bioactivities. To-date, no protein receptors of rhamnolipids have been identified although previous reports have shown that pili are important for rhamnolipids-induced swarming. Because pili has been reported to recognize

disaccharide groups and hydrophobic chains, we hypothesize that the pilin recognizes rhamnolipids, both the sugar and the aliphatic chain moiety. Here, we investigate pilin protein as a receptor of rhamnolipids in controlling pilin-mediated swarming of *P. aeruginosa*.

1.5 Pili facilitates DNA uptake between bacterial cells.

Horizontal gene transfer involves the acquisition of new genetic material by bacteria and one of the known mechanisms by which a bacterial species increase their antibiotic resistance, develop antigenic variation and other virulence factors.^{26, 62-64} The binding of pili to double-stranded DNA (dsDNA) were visually observed by confocal and electron microscopy, showing that DNA is brought into the cell by retraction forces.^{26, 64, 65} Different proposed methods of where the DNA binds to the pilin include binding to the major pilin, binding to a tip complex or minor pilin. The most prevalent model for the DNA uptake is by retraction of the pili assembly, but other possible models have also been proposed (Fig. 1.4). Pili has been reported to be involved in the horizontal gene transfer of a number of gram-negative bacteria such as *Vibrio cholerae*,⁶⁴ *Nisseria gonorrhoeae*,⁶⁶ *Thermus thermophilus*,⁶⁷ and *Pseudomonas stutzeri*.⁶⁷ For *P. aeruginosa*, the binding between pilin and DNA have been reported, however, it is only recently that evidence of horizontal gene transfer was demonstrated in both biofilm and shaking conditions.⁶³ The binding of pilin to DNA occurs at ~micromolar (μM) Kd ranges and is a tip-associated binding event via the disulfide loop.^{24, 26}

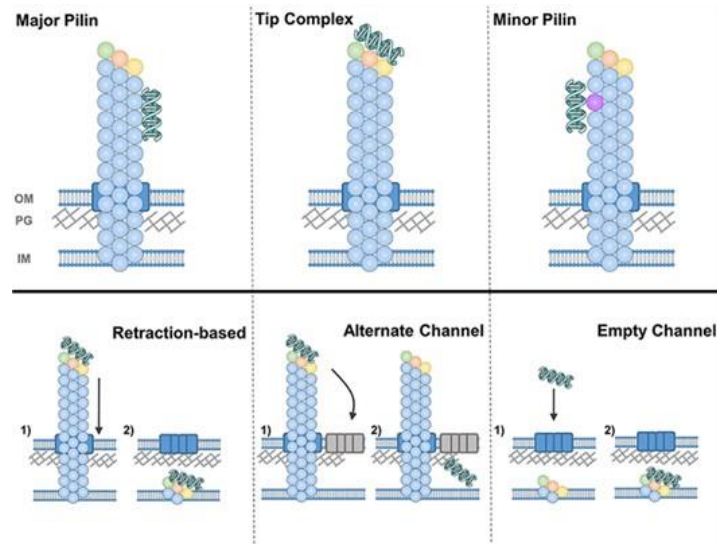


Figure 1.4 Models of DNA binding (top) and DNA uptake in the cell (bottom) by pili.

[Piepenbrink KH (2019) DNA Uptake by Type IV Filaments. *Front. Mol. Biosci.* 6:1. doi:

10.3389/fmolb.2019.00001; Image Credit: K.H. Piepenbrink; **Copyright** © 2019 Piepenbrink.

This is an open-access article distributed under the terms of the Creative Commons Attribution License, which permits unrestricted use, distribution and reproduction in any medium, provided the original author and source are credited.]

1.6 Pilin as an antigen for vaccine development.

Because the disulfide loop has been identified to contain the binding region of the pilin proteins, this region became the central focus of vaccine development for pilin.^{13, 68-70}

Antibodies raised against the peptides corresponding to the disulfide loop of PAO and PAK pilin were able to block pilin binding to buccal epithelial cells (BECs).^{69, 70} Based on these findings, synthetic peptides corresponding to the disulfide loop of pilin proteins from different *P.*

aeruginosa strains (PAK 128-144, PAO 128-144, KB7 128-144 and P1 126-148) were used to study the molecular interactions by NMR showing that despite the limited amino acid sequence

conservation of the disulfide loops, the secondary structure for all peptides were found to contain two β -turns (Fig 1.5).⁶⁸ The β -turn is a significant structural motif for antibody recognition and binding as most antigenic peptides adopt this conformation with the β -turn embedded in the combining site of the antigen.⁷¹⁻⁷³ The binding of a cross-reactive monoclonal antibody to all four peptides were monitored by NMR and showed that conformational changes induced by antibody binding are mostly confined in the hydrophobic pocket of peptides. Furthermore, the same conformational changes were also observed when the ligand was β GalNAc(1 \rightarrow 4) β Gal, suggesting that the antigenic epitope and adhesion epitope are the same for pilin. Despite these efforts to develop vaccines for pilin, there is still no available vaccines for pilin in the market.

Strain	126	127	128	129	130	131	132	133	134	135	136	137	138	139	140	141	142	143	144	145	146	147	148
PAK			K	Ⓢ	T	S	D	Q	D	E	Q	F	I	P	K	G	Ⓢ	S	K				
KB7			S	Ⓢ	A	T	T	V	D	A	K	F	R	P	N	G	Ⓢ	T	D				
PAO			A	Ⓢ	K	S	T	Q	D	P	M	F	T	P	K	G	Ⓢ	D	N				
P1	N	Ⓢ	K	I	T	K	T	P	T	A	W	K	P	N	Y	A	P	A	N	Ⓢ	P	K	S

Figure 1.5 The amino acid sequences of four pilin peptides from the C-terminal regions of the four strains of *P. aeruginosa* for which NMR solution structures have been determined. The PAK, PAO and KB7 pilin peptides are each 17 residues long with a disulfide-bridged loop of 14 residues between Cys129 and Cys142. The P1 pilin peptide is 23 residues long with a disulfide-bridged loop of 19 residues between Cys127 and Cys145. Cysteine residues are circled in the sequences, and residues in bold face are those conserved in the PAK, PAO and KB7 strains. The location of the β -turns in the PAK, PAO, KB7 and P1 peptides are designated by the boxes. The PAK, PAO and KB7 peptides all display a type I β -turn in the conserved sequence Asp134-X-X-Phe137 and a type II β -turn in the conserved sequence Pro139-X-Gly-Cys142. The P1 peptide

displays a type I β -turn in the region spanned by residues Thr134-Ala135-Trp136-Lys137, followed by another turn (boxed in by the broken line) of undefined conformation in the region spanned by Pro138-Asn139-Tyr140-Ala141. Figure is reprinted with permission from Ref. 68 Copyright © 1997 Academic Press. All rights reserved.

1.7: Open question and Our hypothesis: Pilin proteins are protein receptors to small molecules that control swarming bioactivities of P. aeruginosa.

The pili proteins sense and transduce chemical and environmental signals that result in multiple biological activities of *P. aeruginosa*. However, the natural and synthetic ligands for pili that help regulate these activities have been elusive. To understand the mechanism of action by pilin, it is important to identify the ligands for pilin -both natural and synthetic. Prompted by previous studies suggesting that rhamnolipids act as signaling molecules rather than a surfactant in controlling the swarming of *P. aeruginosa*,^{22, 23, 28, 59, 60} we believe that there must be a protein receptor for these molecules that exist. Luk lab has synthesized surfactant-like molecules, disaccharides tethered with a saturated farnesol (SF) group, that inhibit the swarming motility of *P. aeruginosa* swarming motility,^{22, 23} while general surfactants such as tetra(ethyleneglycol)monododecyl ether (C₁₂EG₄OH) and SDS exhibited no swarming modulation on *P. aeruginosa*.^{23, 74} Because pilin has been shown to be important for swarming motility,^{27, 28} we hypothesize that the pilin is the protein receptor of rhamnolipids and the SF-disaccharide analogs. This hypothesis is corroborated by a previous study by Dr. Hewen Zheng (Luk lab) demonstrating that externally added pilin on hydrated soft gel sequesters the rhamnolipids produced by PAO1 and inhibits the swarming, suggesting that rhamnolipids bind to pilin.⁷⁵ We conduct further studies to characterize the binding between pilin and the ligand

candidates at a molecular level to gain understanding of the molecular details for potential development of therapeutics targeting the pilin protein of *P. aeruginosa*.

1.8 This dissertation is organized in the following 8 chapters:

In Chapter 2, the design, cloning, recombinant expression and purification of truncated pilin from *P. aeruginosa* are discussed. We employ the common approach for studying the pilin protein by truncating the pilin from the N'-terminus to yield proteins that retain the putative binding region while improving the solubility. The *pilA* gene encoding the pilin from PA1244N3(pPAC46) was used as the DNA template for the truncations. Three different truncations of the *pilA* gene were prepared by removing 23, 28 and 31 amino acid from the N-terminus and recombinantly expressed in *E. coli*. Here, we study minimum structures of pilin that will bind to the natural and synthetic ligands. Furthermore, three single amino acid mutants of truncated pilin were also expressed to determine the importance of the C-terminal D-loop for binding pocket of the pilin protein.

In Chapter 3, we demonstrated the direct binding and sequestering of pilin to ligands on hydrated gel surfaces using a novel bacterial motility-enabled binding assay. Separating the components of rhamnolipids reveal that monorhamnolipid is more active than dirhamnolipid at controlling the swarming motility of *P. aeruginosa*. Using the bacterial motility-enabled binding assay, we identified that among the three truncated pilin mutants, only the pilin $\Delta(1-31)$ binds rhamnolipids with similar activity as the full, native pilin from *P. aeruginosa* PA1244N3(pPAC46). We also show that three single amino acid mutants of the pilin $\Delta(1-31)$, where the mutation occurs in the disulfide region (D-loop) of C-terminus, are inactive for

controlling swarming motility of PAO1, indicating that this region is important for binding of pilin to rhamnolipids.

In Chapter 4, biophysical techniques such as circular dichroism, nuclear magnetic resonance and dynamic light scattering were used to gain structural insight on the truncated pilin mutants and how they compare to the native 1244 pilin. Using these methods, we were able to determine that the natural and synthetic ligands induced structural changes to the truncated pilin protein. Circular dichroism spectroscopy showed that rhamnolipids, particularly monorhamnolipid, induces a different structural change than the SF-disaccharide analog. The NMR studies on both native pilin and truncated pilin were challenging because of the lack of dispersion of the spectra. However, adding ligands to the both the native pilin and truncated pilin results in the appearance of additional peaks in the pilin spectra indicating ligand interactions with the proteins. Dynamic light scattering showed that addition of ligands to the pilin induced the formation of larger aggregates in the solution.

In Chapter 5, the intrinsic fluorescence of the truncated pilin was used to probe binding to rhamnolipids and saturated farnesol (SF)- disaccharide analogues. Our fluorescence spectroscopy results show that about 1 pM of ligands (monorhamnolipid, dirhamnolipid, SF β C and SF-EG₄OH) is enough to saturate the fluorescence signal of 100 nM of truncated pilin. We determined that the ligands induce the assembly of pilin *in vitro* via tight-binding mechanism rather than a catalytic effect by the ligand. Kinetic studies show that pilin assembly induced by monorhamnolipid occurs via the isodesmic process. Transmission electron microscopy (TEM) show that rhamnolipids and SF β C induce two different assemblies, linear and amorphous, respectively.

In Chapter 6, the presence of peptides can promote the isodesmic assembly of 5'DSCG over a broad range of concentrations before reaching the liquid crystal phase indicative of demixing between 5'DSCG and peptides in aqueous solution. This demixing mechanism was explored to precipitate a wide range of proteins, including lectin A, esterase, lipase, bovine serum albumin, trypsin, and the pilin proteins. We found that 5'DSCG caused the aggregation of all these proteins except trypsin. These results, along with past findings, suggest that 5'DSCG isodesmic assemblies has the potential to assist in protein purification and crystallization.

In Chapter 7, the exploratory work on using filamentous bacteria to express proteins were discussed. Because filament growth is rapid, we would like to explore if protein expression can be maximized over a short time scale. Luk lab has previously discovered that antibiotics induce surface-mediated filament formation of bacteria and have identified optimum conditions that produce these filamentous bacteria. We show that the strain *E. coli* BL21 (DE3) carrying the plasmid encoding for proteorhodopsin can form filaments and express proteorhodopsin under the conditions for filament formation. Furthermore, attempts to express, purify and quantify of proteorhodopsin from filamentous bacteria will also be discussed in this chapter.

In Chapter 8, the conclusions and summary of our finding in this thesis are discussed. We also present the existing open questions and future directions of this research.

Chapter 2. Cloning, Expression and Purification of Pilin Mutants for Structural Characterization and Ligand-Binding Studies

2.1 Background and Significance

2.1.1 *Pilin protein general structure; status of literatures.*

Pilin proteins are a class of proteins that possess a general folded structure with a long, N-terminal α -helix and a C-terminal globular domain with coiled structures and β -sheets (Fig. 2.1). The long α -helix has an exposed region comprised of the first 28 amino acid residues from the N'-terminus, which is relatively hydrophobic and form surfaces for assembly and disassembly of the pili appendages. The α -helix connects to an $\alpha\beta$ -loop followed by a 4 to 7 stranded β -sheet then a C'-terminal disulfide loop (D-loop). Alignment of the amino acid sequence show that the both the N' terminal helix and the presence of a D-loop is highly conserved among pilin from different species. While the D-loop may vary in the amino acid sequence conserved across *P. aeruginosa* strains, the secondary structure of this loop is conserved, consisting of coils and two β -turns.^{68, 76-81} There are two main subclasses of pilin that exist – type 4a and type 4b pilin that differ in their amino acid sequence, size and origin. Pilin protein from species *Neisseria gonorrhoeae* and *Pseudomonas aeruginosa* are classified as type 4a; while *Salmonella typhimurium*, *Vibrio cholerae* and *E. coli* express type 4b pilin. Structures of pilin from both subclasses have been solved and reveal that the general scaffold with the α -helix, β -sheets and D-loop are observed for both subclasses, but each would have a distinct fold due to the differences in the number of α -helices and β -sheets at the C'-terminus. (Fig 2.1).

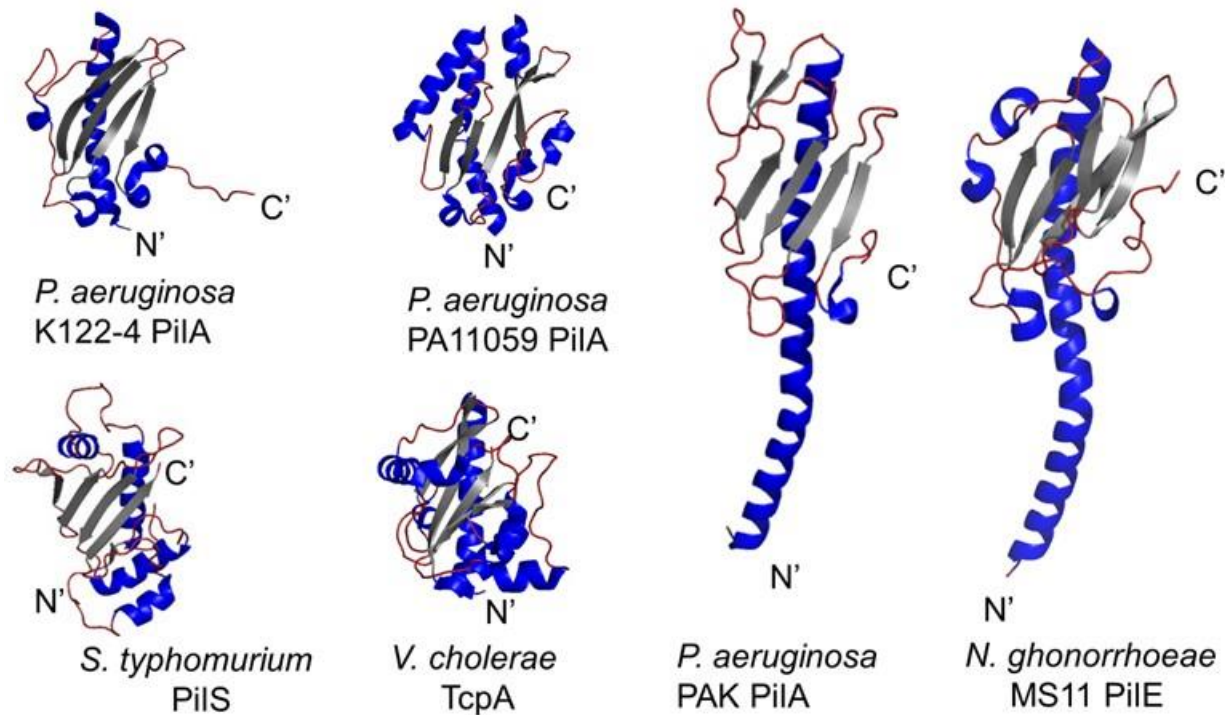


Figure 2.1 Crystal structure of pilin proteins from different bacterial species. *P. aeruginosa* PAK PilA (PDB code: 1dzo), PA11059 (PDB code: 3JZZ) and K122-4 PilA (PDB code: 1qve) and *N. gonorrhoeae* MS11 PilE (PDB code: 1ay2), while the three structures at the bottom are previously solved T4b pilins *S. typhi* PilS (PDB code: 1q5f) and *V. cholerae* TcpA (PDB code: 1oqv). Crystal structures were generated using PyMOL software. Color representation: α -helices in blue, β -sheet in gray and coiled structures in red.

Within the *P. aeruginosa* species, there are five distinct allele groups of type 4a pilin that have been identified.⁸¹⁻⁸³ Each of these groups are distinguished by the amino acid sequence length, size of the D-loop, and pilin accessory proteins involved in pilin expression (Fig. 2.2). The pilin expressed by PA1244 belongs to the group I pilin, with a TfpO (pilO) accessory gene involved in the glycosylation of the pilin at Ser 148. Pilin from common laboratory strains

PAO1, PAK, and PA103 are classified as group II pilins which are smaller than group I and do not have accessory genes. Three other groups, groups III, IV and V have been found to possess distinct accessory genes that is believed to express and inner membrane protein that aid in the pili assembly.⁸² Isolates belonging to these groups include PA14 (group III) alleles (including the well-characterized PA14 strain), and PA5196 (group IV) and PA110594 and PA281457 (group V).

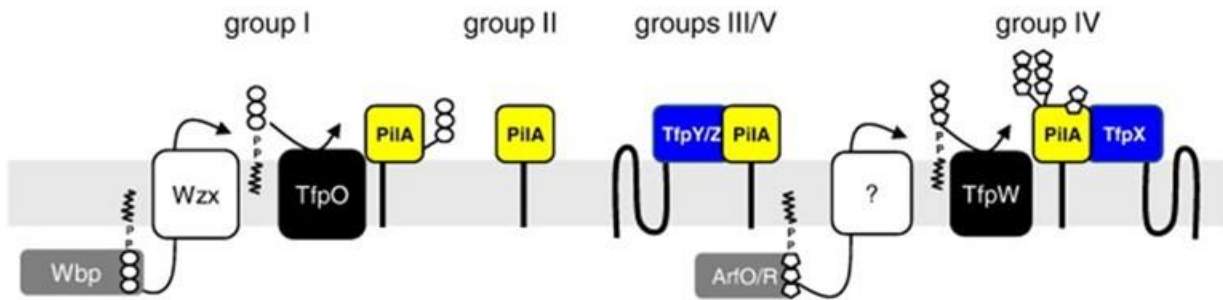


Figure 2.2 Pilin modification and assembly systems in *P. aeruginosa*. Group I pilins are glycosylated by TfpO on the C-terminal Ser with an O antigen unit synthesized by the LPS machinery. Group II pilins have no accessory proteins. Group III and V pilins each have a specific accessory protein that promotes their assembly: TfpY for group III and TfpZ for group V. Group IV pilins are glycosylated at several positions by TfpW with mono-, di-, and trisaccharides of d-arabinofuranose synthesized by the ArfO/R proteins (Harvey and Burrows, unpublished data). Group IV pilins have a TfpX accessory protein that is similar to TfpY and TfpZ. Figure is reprinted with permission from Ref. 81. Copyright © 2009 Elsevier Ltd. All rights reserved.

Structural studies on pilin proteins are limited by its secondary structure. There are several crystal structures of pilin that have also been solved by x-ray crystallography,^{77, 78, 81, 84} most of

which are of the truncated versions of pilin and only a few full-length pilin.^{76-79, 81, 84} Currently, crystal structures only exist for *P. aeruginosa* PAK^{78, 79, 84} K122-4 proteins.⁷⁷ and PA11059 proteins.⁸¹ The difficulty of crystallizing pilin is reportedly due to the presence of the N-terminal α -helix that is highly hydrophobic and insoluble, further, the full-length pilin monomers have the propensity to self-aggregate.⁷⁸ By removing 28 amino acids starting from the N'-terminus, a truncated protein retaining the C'-terminus becomes suitable for structural studies by NMR and X-ray crystallography and are also functional as evaluated by pilin binding to DNA and asialo-GM1.^{77, 78, 81, 84} Truncating pilin proteins is a commonly used method for structural characterization of pilin proteins. Despite some available pilin structures, pilin proteins from other groups still need to be solved and characterized.

2.1.2 *P. aeruginosa* PA1244N3(pPAC46) and PyMOL modelling of pilin protein.

P. aeruginosa PA1244 is clinically isolated strain from human blood characterized as a hyperpiliated strain.^{4, 85} An engineered strain, PA1244N3, is a mutant of PA1244 with an inactive *rpoN* gene and therefore, cannot produce pili and flagella.⁸⁵⁻⁸⁷ Castric and co-workers constructed the pPAC46 plasmid by cloning the pilin structural gene, *pilA*, and the adjacent DNA(*pilO*) by ligation into the pMMB66EH vector and expression is under the control of the tac promoter. The strain PA1244N3(pPAC46) which was introduced into *P. aeruginosa* PA1244N3 by triparental mating. When PA1244N3 carries the pPAC46 plasmid PA1244N3(pPAC46), a glycosylated pilin protein is expressed by IPTG induction.^{85, 87, 88} The pilin protein expressed is able to assembly into the pilus fiber which protrudes out of the bacterial surface. The pilin monomer, belonging to the group I, is glycosylated with an aminoglycan trisaccharide bound covalently to the β -carbon of the Ser-148 at the C-terminus.^{87, 89, 90} The role of glycosylation is

unclear but has been found not to interfere with the pilus biogenesis and basic pilin functions such as twitching, biofilm and phage attachment.⁹⁰

The pilin protein from *P. aeruginosa* PA1244 has not yet been structurally solved.⁸⁵ We therefore used tools to model the predicted structure of native pilin protein (Fig. 2.3). The predicted structure of the native pilin contains the general conserved general domains with the long N-terminal α -helix, $\alpha\beta$ -loop and a 4 stranded β -sheet and the C-terminal loop. The first 6 amino acids are the leader peptide which gets cleaved by prepilin peptidase D (pilD) as the mature pilin forms.^{40, 85} Consequently, Phe7 gets methylated in the mature pilin.^{40, 85} Amino acid residues 9-59 are predicted to form the α -helix. This region is followed by the $\alpha\beta$ -loop from residues 60-89 which also have two small β -sheets within the loop. From residues 90-135, there are 4 β -sheets predicted to be anti-parallel. A loop region forms to the C-terminus from residues 135-154. There are two cysteine residues that would form a disulfide loop (not shown in the model) in between Cys133 and Cys151. The predicted structure was used for further design of truncated pilin.

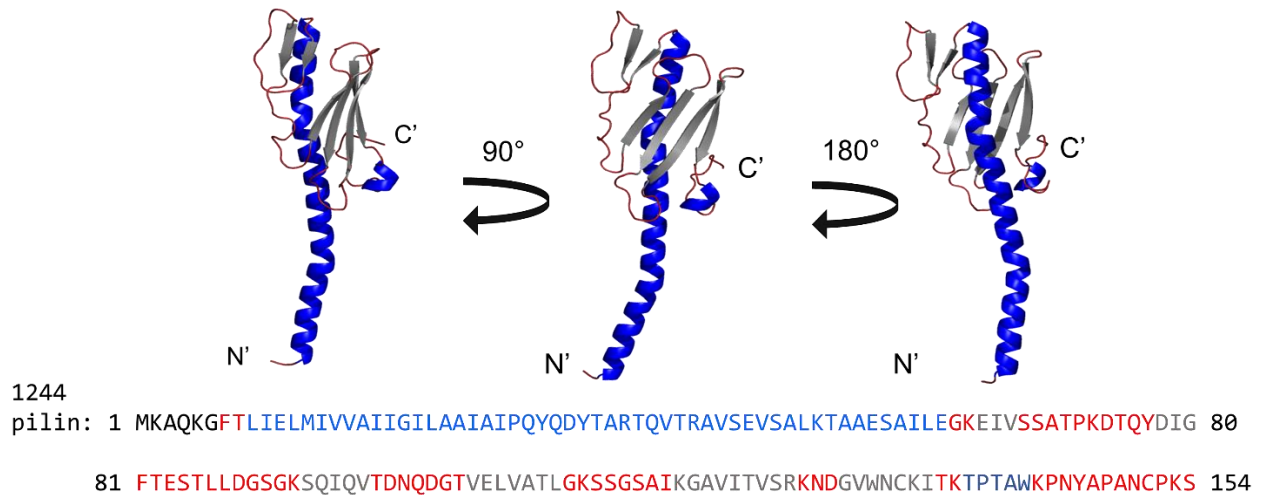


Figure 2.3 Structures of PA1244N3(pPAC46) native pilin (top) generated by Phyre2 and visualized by PyMOL. The amino acid sequence of the native pilin (bottom) with leader peptide in black, α -helices in blue, β -sheet in grey and loops in red. The pilin was rotated at different angles to show the predicted structural features of the protein. The α -helix is in blue, β -sheet in gray and coils in red.

2.1.3 Disulfide loop of pilin contains the host cell receptor binding epitope.

Pilin proteins contain a C-terminal disulfide loop (D-loop) recognized as the host cell receptor binding site. Paranchych and co-workers introduced a chloramphenicol acetyltransferase into the pilin gene resulting in the alteration of the D-loop, which then was expressed in *P. aeruginosa* PAO1. The alteration in the D-loop did not affect the pili assembly biogenesis, but significantly decreased the binding to lung epithelial cells suggesting that the D-loop is not essential for pilus biogenesis but is important for binding to host cell receptors.⁹¹ These results were corroborated by Irvin and co-workers who demonstrated that the natural and synthetic peptides corresponding to the D-loop bind to mammalian cells,¹³ and would only need to recognize the β -D-GalNAc(1 \rightarrow 4) β -DGal moiety of the host cell Asialo-GM₁.^{8, 12} The D-loop of

different pilin strains, despite having limited sequence homology, surprisingly binds to the same receptor.⁹² Based on NMR studies on synthetic peptides, these different D-loops share a common structural feature containing two β -turns,^{68, 77, 80, 93} and the binding of the D-loop to β -D-GalNAc(1 \rightarrow 4) β -DGal is observed to induce a conformational change in the inner hydrophobic pocket of the D-loop. Collectively, these findings implicate the D-loop as the receptor binding epitope of the pilin protein.

2.1.4 Chapter Aim: Cloning, expression and purification of minimum structured and single amino acid mutants.

The aim of this chapter is to design and express minimum structures of the pilin from *P. aeruginosa* PA1244N3(pPAC46) suitable for ligand-binding and structural studies. Because the native pilin expressed by PA1244N3(pPAC46) has no affinity tags, purification of pilin requires manually shearing off the protein from the bacteria cell followed by the use of PEG-8000 and NaCl to precipitate the protein from the cell culture.^{46, 88} Unfortunately, PEG8000 cannot be easily removed after the pilin is precipitated from the supernatant which further complicates our structural studies. The purified protein by this method is mostly in aggregate/assembly form will need the use of high concentrations of detergents to dissociate the proteins into monomers – these two conditions could potentially interfere with our ligand-binding studies.

We based our experimental design on the common approach of deleting amino acids from the N-terminal α -helix to improve solubility while still retaining binding properties of the pilin. Our approach is to express truncated pilin proteins with different lengths by cutting off a part of the α -helix, by a difference of 1 helical turn so three different truncated pilin proteins

were designed by removing 23, 28 and 31 amino acids from the pilin N'-terminus of the mature pili (excluding the leader peptide) (Fig. 2.4). We present the heterologous expression of the truncated pilin in *E. coli* BL21(DE3) with an affinity tag to eliminate the use PEG-8000 for purification. We aim to explore the minimum structure that will be bioactive as well as be soluble for potential structural studies. Furthermore, removing a part of the α -helix would minimize any possible hydrophobic self-association of the individual pilin monomers in solution. Lastly, single amino acid mutants of the bioactive truncated pilin were expressed to determine the importance of the disulfide loop for ligand recognition.

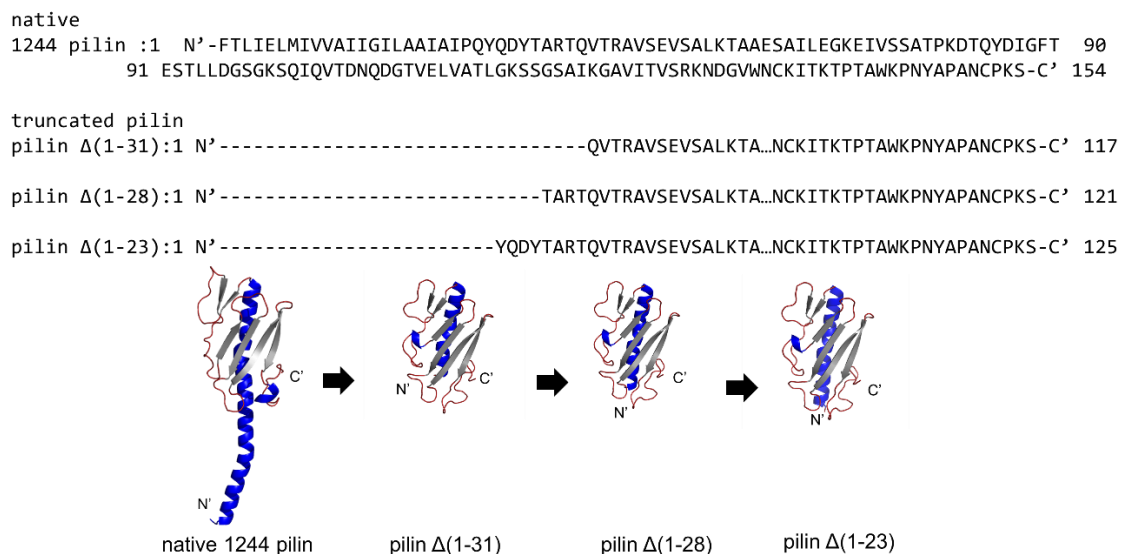


Figure 2.4 Amino acid sequences of the full-length pilin (top) and the truncated pilin proteins (middle). The predicted secondary structures of the full, native pilin from PA1244N3 (pPAC46) and truncated pilin mutants- pilin Δ (1-31), pilin Δ (1-28) and pilin Δ (1-23) were generated by Phyre2 and visualized by PyMOL (bottom).

2.2 Results and Discussion

2.2.1 Expression of native pilin in *P. aeruginosa* PA1244N3(pPAC46)

Expression and the purification of the full-length, native pilin from *P. aeruginosa* PA1244N3(pPAC46) was done by standard methods provided by Dr. Peter Castric.^{75, 90} The final, purified pilin protein was evaluated by SDS-PAGE gel, showing a single band corresponding to a molecular weight of approximately higher than 15 kDa (Fig. 2.5), and previous MALDI-TOF measurements on the pilin by Dr. Hewen Zheng show a molecular weight of 16,326.9189 Da,⁷⁵ which are both consistent with the reported m.w. of 16,307 (± 25) Da for this protein.⁹⁴ For the purification method, the typical yield is ~2-3 mg native pilin/ L culture.

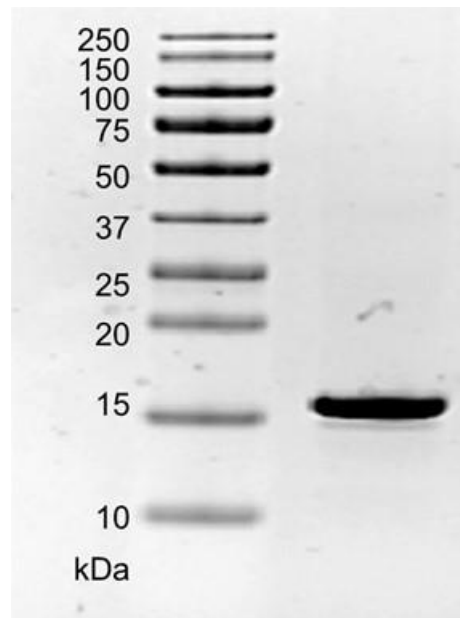


Figure 2.5 SDS-PAGE gel of native pilin expressed and purified from *P. aeruginosa* PA1244N3(pPAC46). Lane (1) ladder and (2) purified native pilin.

2.2.2 Recombinant expression and purification of truncated pilin structures.

Three truncated pilin proteins by removing 31, 28 and 23 amino acids from the N^o-terminus. (Fig. 2.4). The proteins will be referred to as pilin Δ (1-31), pilin Δ (1-28) and pilin Δ (1-23) corresponding to the 31, 28 and 23 amino acid deletion, respectively.

First, the pPAC46 plasmid was isolated and purified from PA1244N3(pPAC46). The genes corresponding to the targeted truncations of *pilA* was pulled out from the plasmid by polymerase chain reaction (PCR) using the primers listed in Table 2.1, Experimental Section. The PCR product of each truncation was analyzed by DNA gel electrophoresis to confirm the number of base pairs (bp) for each product. (Fig. 2.6) The bands of the PCR products on the agarose gel are in between 300-400 bp size which matches the expected bp size for the truncations. The expected bp size for each truncation corresponds to 354 bp (31 amino acids deletion), 366 bp (28 amino acids deletion), and 378 bp (23 amino acid deletion).

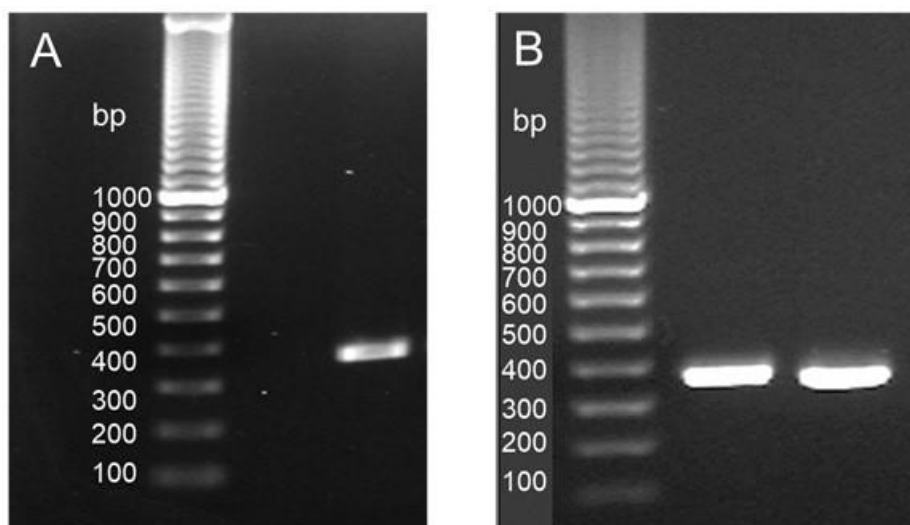


Figure 2.6 Agarose gel of the PCR products of the pulled-out genes for the truncated pilin proteins. (A) lane 1 – 100 bp ladder, lane 2 – PCR product for pilin Δ (1-31) and (B) lane 1 – 100 bp ladder, lane 2- PCR product for pilin Δ (1-28), lane 3- PCR product for pilin Δ (1-23).

The three different genes were then ligated into the Champion™ pET-SUMO vector (Thermo Fisher Scientific) using T4 DNA ligase to generate 3 different plasmid constructs. Ligating into the pET-SUMO yields a fusion protein with a SUMO (small ubiquitin-like modifier) protein (~11 kDa) attached to the N-terminal end of the insert. The three different plasmid constructs after the ligation will the fusion proteins SUMO-pilin $\Delta(1-31)$, SUMO-pilin $\Delta(1-28)$, and SUMO-pilin $\Delta(1-23)$. The successful ligations were confirmed by colony screen PCR using the T7 forward primer and the corresponding reverse primer for each insert. Colony screening was done for 8-16 colonies for each construct and the bp size was confirmed by DNA gel electrophoresis (Fig. 2.7). For all the PCR products, the band appears at approximately ~800 bp, consistent with the estimated or calculated bp for the PCR colony screen products: SUMO-pilin $\Delta(1-31)$ – 799 bp, SUMO-pilin $\Delta(1-28)$ - 811 bp, and SUMO-pilin $\Delta(1-23)$ – 823 bp, encompassing the region from the T7 promoter, SUMO priming site and the gene insert. These results confirm the successful ligation of the gene inserts corresponding to truncated pilin proteins into the pET-SUMO vector. The successful colony screens were sent for protein sequencing and confirmed no errors in the protein sequence.

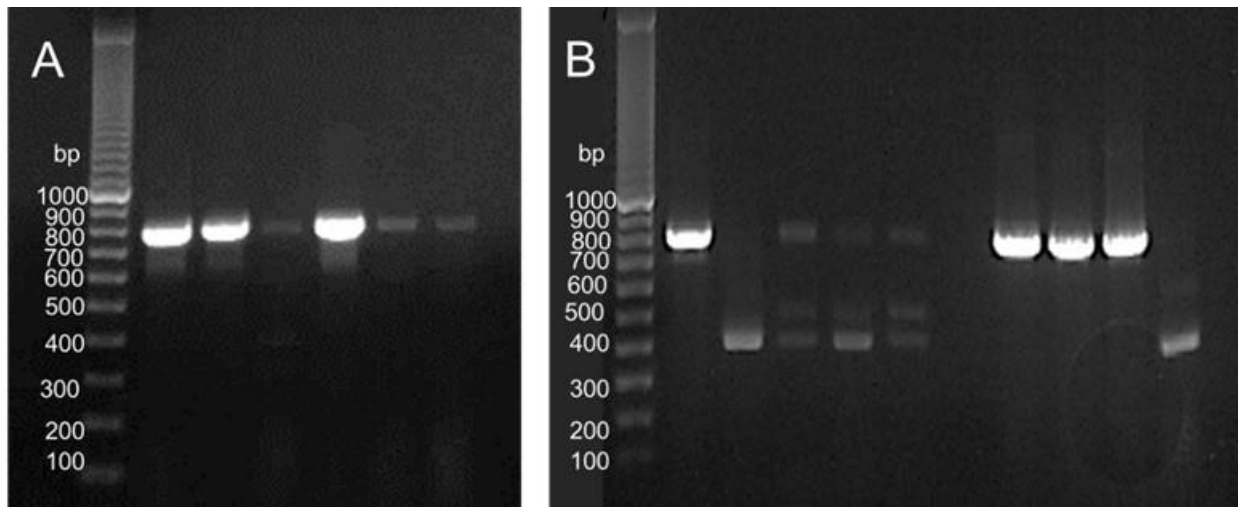


Figure 2.7 PCR Colony screening results for pilin $\Delta(1-31)$ (A) lane 1 – ladder, lanes 2-7 – PCR products; pilin $\Delta(1-28)$, and pilin $\Delta(1-23)$; (B) lane 1 – ladder, lanes 2-6 PCR product for pilin $\Delta(1-28)$, lane 8-11- PCR product for pilin $\Delta(1-23)$. Successful colony screens are bright bands around 800 bp.

We proceeded with the transformation by heat-shock and expression in *E. coli* BL21(DE3) cells by IPTG induction of the proteins. Preliminary evaluation of the expression of the protein showed that the expressed proteins were not soluble and most of the expressed proteins were found in the cell debris rather than the lysate when the protein was induced at 30 °C. We changed the expression temperature to 18 °C for all the truncated pilin mutants to improve the solubility where more proteins were found in the lysate and not in the debris, except for pilin $\Delta(1-28)$. The purification method was same for pilin $\Delta(1-23)$ and pilin $\Delta(1-31)$ where the bacteria cells were then lysed by sonication, and the SUMO-pilin proteins were purified from the lysate by a Nickel affinity column (Fig. 2.8, 2.9). The SUMO tag was cleaved using SUMO protease (OD₂₈₀ of protein: OD₂₈₀ of protease = 200:1), then removed by Ni-NTA column. The

final proteins, pilin $\Delta(1-23)$ and pilin $\Delta(1-31)$, were buffer exchanged in storage buffer. This procedure yielded $\sim 2-3$ mg/mL of the proteins.

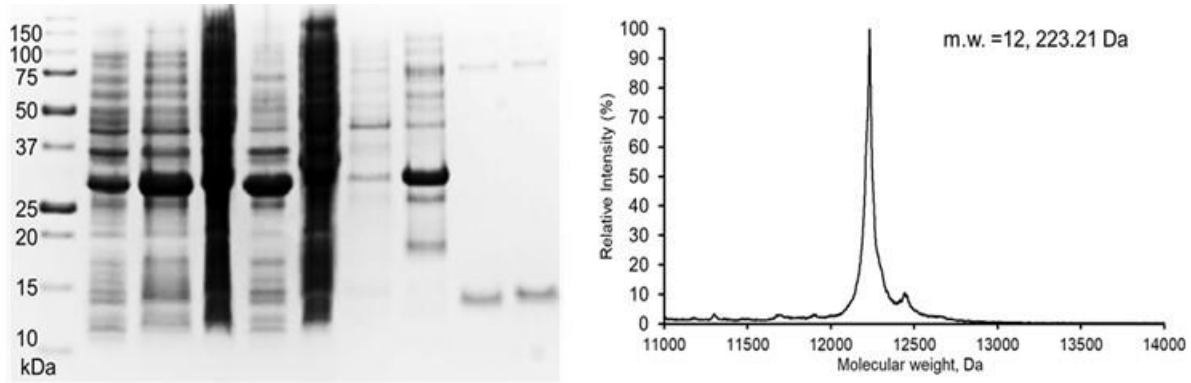


Figure 2.8 SDS-PAGE gel of pilin $\Delta(1-31)$ purification. Lanes (1) ladder, (2) pre-induction, (3) induced sample, (4) cell debris, (5) cell lysate, (6) flow through, (7) wash flow through, (8) pre-SUMO cleavage, (9) final pilin $\Delta(1-31)$, (10) final pilin $\Delta(1-31)$ + β -mercaptoethanol (Left) and the MALDI-TOF results of the pilin $\Delta(1-31)$ (Right).

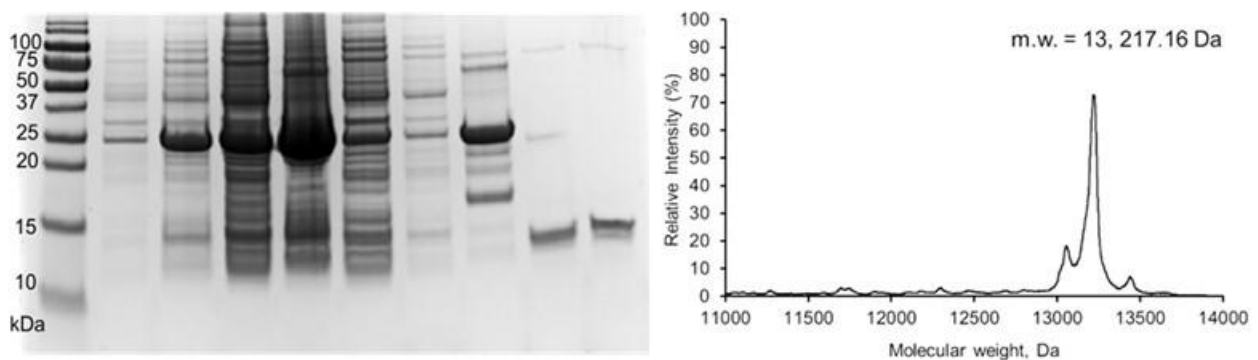


Figure 2.9 SDS-PAGE gel of pilin $\Delta(1-28)$ purification from the lysate. Lanes (1) ladder, (2) pre-induction, (3) induced sample, (4) cell debris, (5) cell lysate, (6) flow through, (7) wash flow

through, (8,9) pre-SUMO cleavage, (10) post-cleavage final pilin $\Delta(1-28)$, (11) final pilin $\Delta(1-28)$).

However, for SUMO- pilin $\Delta(1-28)$, the protein expressed at 18 °C was localized in the debris (Fig. 2.10, lane 4), which required recovering the protein from inclusion bodies. First, the standard purification of the protein from the lysate was carried out (Fig. 2.10), but the SDS-PAGE analysis shows that the final protein is not pure, with a band that matches the SUMO tag. We then further purified the protein by passing through a Ni-NTA column to remove the suspected SUMO tag (Fig. 2.12, lanes 4 & 5). The final protein yield was 0.5 mg/ L culture. Next, the cell debris were resuspended in 50 mM Tris, 100 mM NaCl, 4% (v/v) Triton-X and 1 M urea (pH=8.0) to resolubilize the inclusion bodies. The inclusion bodies were spun down by centrifugation and judging the SDS-PAGE, the supernatant and the cell debris both have the SUMO-pilin $\Delta(1-28)$. The supernatant was kept for further purification using the same method as the lysate (Fig 2.11, 2.12). We obtained 0.5 mg of inclusion bodies which were resolubilized in 50 mM Tris, 100 mM NaCl, 8M urea, pH= 7.5 followed by refolding the protein. The solution containing the refolded protein was passed thru a Ni-NTA column to obtain the protein. The protein was eluted, cleaved and buffer exchanged with the standard procedures. (Fig 2.11). The yield of proteins recovered from inclusion bodies was ~ 2 mg per L of culture. The protein from the supernatant was purified using the standard SUMO cleavage, removal of tag and buffer final exchange in storage buffer which yielded ~1 mg of protein per L of culture (Fig. 2.12, lanes 4 and 5). The total amount of pilin $\Delta(1-28)$ is ~3.5 mg per L of culture from combining from the lysate, supernatant from re-solubilization of the inclusion bodies and refolding from inclusion bodies (Fig. 2.12).

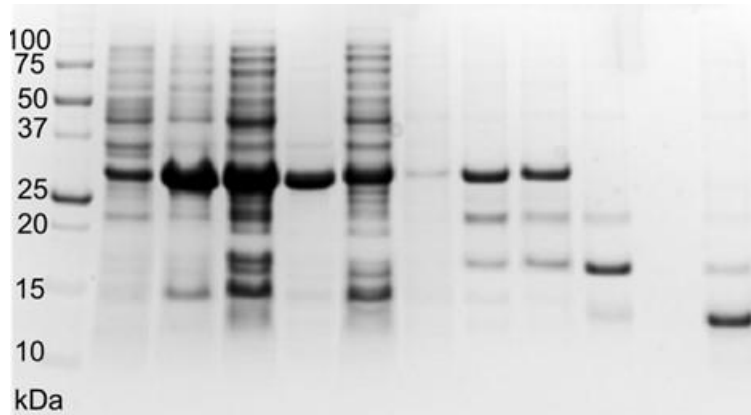


Figure 2.10 SDS-PAGE gel of pilin $\Delta(1-28)$ purification from the lysate. Lanes (1) ladder, (2) pre-induction, (3) induced sample, (4) cell debris, (5) cell lysate, (6) flow through, (7) wash flow through, (8,9) pre-SUMO cleavage, (10) post-cleavage final pilin $\Delta(1-28)$, (11) final pilin $\Delta(1-28)$.

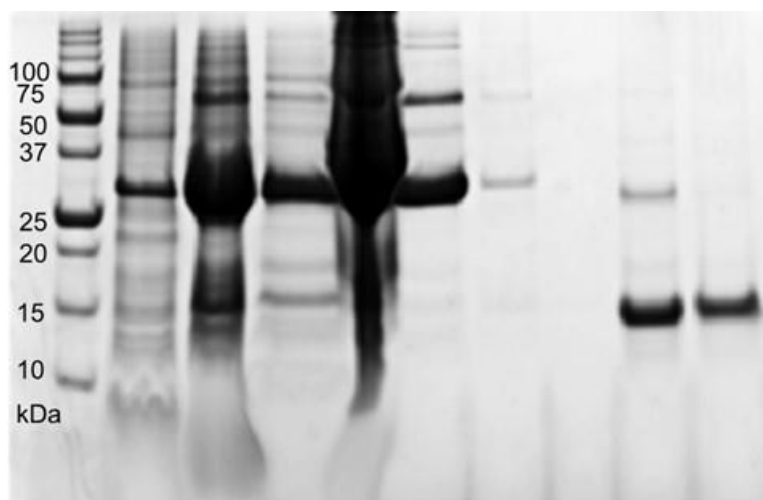


Figure 2.11 SDS-PAGE gel of pilin $\Delta(1-28)$ purification from the inclusion bodies. Lanes (1) post-sonication lysate, (2) post-sonication cell debris, (3) supernatant after recovering inclusion bodies from the cell debris, (4) inclusion bodies, (5) post-refolding from inclusion bodies, (6) flow through from Ni-NTA, (7) wash flow through, (10) post-cleavage final pilin $\Delta(1-28)$, (11) final pilin $\Delta(1-28)$ passed through Ni-NTA column second time.

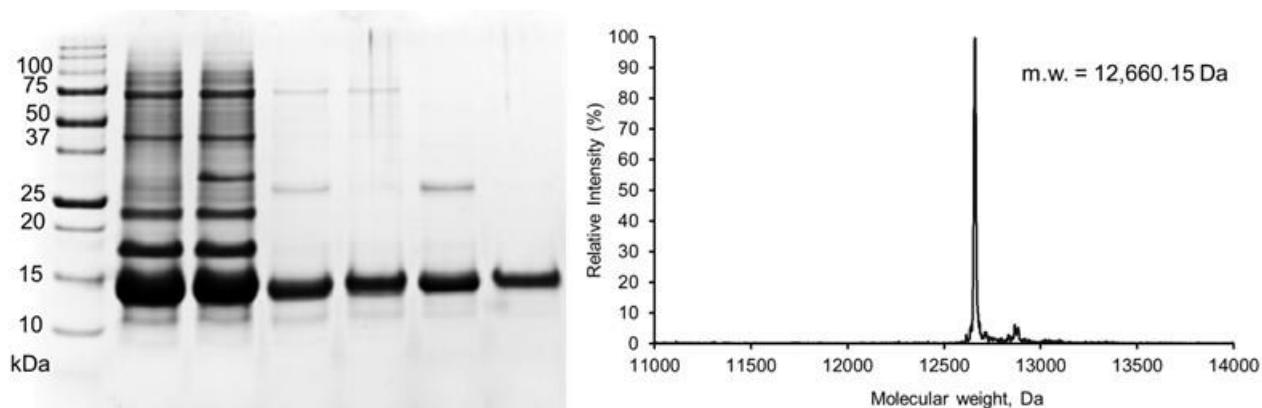


Figure 2.12 SDS-PAGE gel of the final pilin $\Delta(1-28)$ purification. Lanes (1) ladder, (2,3) final pilin $\Delta(1-28)$ from first attempts of purification showing contamination. These proteins were not used in this study. (4) final pilin $\Delta(1-28)$ from Fig. 2.10, (5) re-purified pilin $\Delta(1-28)$ from Fig. 2.10 by passing through Ni-NTA then buffer exchanged in storage buffer, (6) final pilin $\Delta(1-28)$ purified pilin from supernatant in Fig 2.11, lane (7) re-purified pilin $\Delta(1-28)$ from supernatant in Fig 2.11.

The progress of the purification was monitored by protein gel (Fig 2.8-2.12). Using the molecular weight of ~ 13.4 kDa for SUMO tag, the expression of the SUMO-pilin proteins were confirmed by the appearance of the peak at ~ 25.6 , ~ 26 and ~ 26.6 kDa for pilin $\Delta(1-23)$, pilin $\Delta(1-28)$ and pilin $\Delta(1-31)$, respectively (Fig. 2.8, 2.10, 2.11). The SUMO fusion tag was then cleaved using the SUMO protease (from Korendovych lab, Syracuse University) with 3 hours of incubation to yield the final truncated proteins. On the gel, the bands of the final proteins are found in between 10-15 kDa, which would match the calculated molecular weight of the protein (Fig. 2.8 – 2.12). Furthermore, the exact mass of the protein was then determined by MALDI-TOF. For pilin $\Delta(1-31)$ the m.w. = 12,223.21 Da (Fig. 2.8), pilin $\Delta(1-28)$ m.w. = 12,660.15 Da (Fig. 2.12) and pilin $\Delta(1-23)$ m.w. = 13,217.16 Da (Fig. 2.9). We also note that due to the

purification method of the SUMO-pilin, we sometimes observed dimers in the protein gel, but they only contribute to a small population in the whole protein hence, some samples we have a lane for the protein + (β -mercaptoethanol) β ME.

2.2.3 Recombinant expression and purification of single amino acid pilin mutants.

Single amino acid mutants of the pilin $\Delta(1-31)$ were designed and expressed to determine the importance of the D-loop of pilin for binding to natural and synthetic ligands (Fig. X). Based on NMR studies by Irvin and co-workers, important structural features of this D-loop binding epitope were identified as β -turns, a hydrophobic pocket and the disulfide bond. Included in this study is a D-loop peptide from *P. aeruginosa* P1 strain that has the same sequence as the PA1244 pilin D-loop allowing us to choose which amino acids to mutate.^{68, 93, 95, 96} The following mutations of amino acids were selected based on their positions in the binding epitope of the truncated pilin $\Delta(1-31)$ - I98D, W105K, and P111G (Fig. 2.13). We decided to study hydrophobic effects and structural effects by changing hydrophobic amino acids to charged amino acids and changing proline to glycine, respectively. The isoleucine at position 98 (I98) is part of the hydrophobic core and hidden from the solvent, mutated to a charged aspartic acid (D) residue. The tryptophan at position 105 (W105) is part of the β -turn and hydrophobic and mutated to a charged lysine (K) residue. The proline at position 111 (P111) is part of the hydrophobic core but fairly solvent exposed, mutated to a smaller glycine (G) residue.

pilin $\Delta(1-31):1$ N'-----QVTRAVSEVSALKTA...NCKITKTPTAWKPNYAPANCPKS-C' 117
 single amino acid mutants
 pilin $\Delta(1-31)I98D:1$ N'-----QVTRAVSEVSALKTA...NCK**D**TKTPTAWKPNYAPANCPKS-C' 117
 pilin $\Delta(1-31)P111G:1$ N'-----QVTRAVSEVSALKTA...NCKITKTPTAWKPNY**A**PANCPKS-C' 117
 pilin $\Delta(1-31)W105K:1$ N'-----QVTRAVSEVSALKTA...NCKITKTPTA**K**KPNYAPANCPKS-C' 117

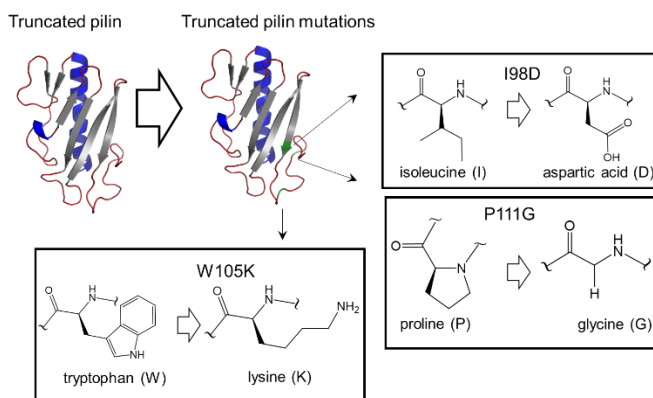


Figure 2.13 Amino acid sequences of the single amino acid mutants of pilin $\Delta(1-31)$ (top). The predicted secondary structure of the single amino acid mutant proteins generated by Phyre2 and visualized by PyMOL.

Single amino acid mutants were constructed by site-directed mutagenesis directly on the on isolated and purified plasmid containing the pET-SUMO-pilin $\Delta(1-31)$ construct with Phusion polymerase. The primers used for each mutation are indicated in Table 2.1, Experimental Section. Upon performing site-directed mutagenesis, successful mutations were checked by PCR to see if there are any bands appearing at ~ 6000 bp corresponding to the pET-SUMO plasmid (5634 bp) with the pilin $\Delta(1-31)$ insert (54 bp) (Fig. 2.14). Since the site -directed mutagenesis is done on the pET-SUMO plasmid directly, the base pairs of the single amino acids will be the same as the wild-type pET-SUMO-pilin $\Delta(1-31)$ vector. The PCR products were purified and subjected to DpnI digestion to remove parent plasmids present.

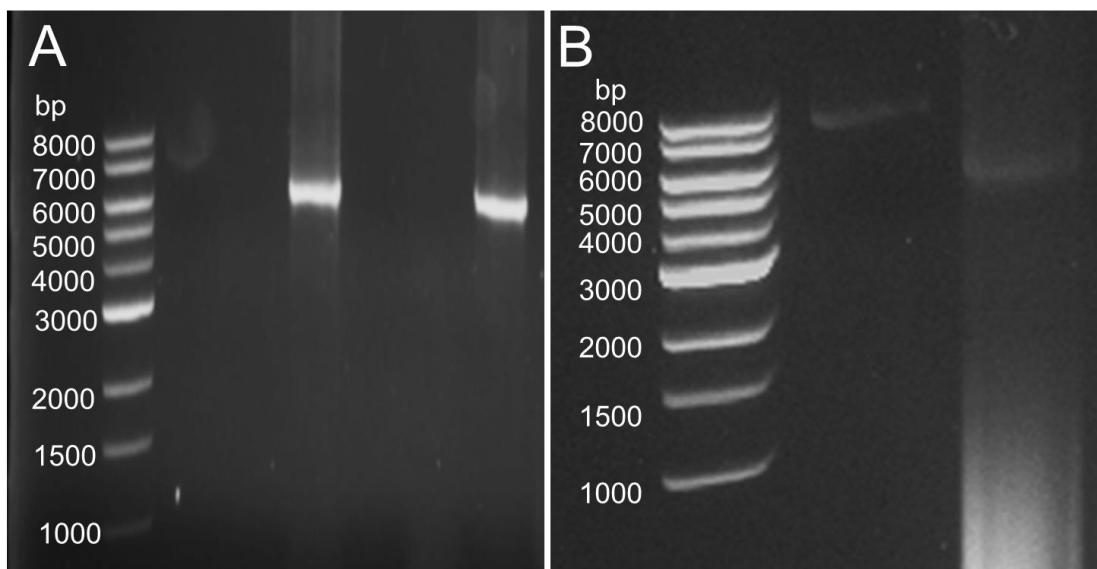


Figure 2.14 W105K and I98D mutations of pET-SUMO- pilin $\Delta(1-31)$ vector (A). Successful mutations are lanes with a band at ~6 kilobase pairs. Lane (1) 1 kilobase pair ladder, (2) W105K and (3) I98D and P111G mutations of pET-SUMO- pilin $\Delta(1-31)$ (B). Successful mutations are lanes with a band at ~6 kilobase pairs. Lane (1) 1 kilobase pair ladder, (2) pET-SUMO- pilin $\Delta(1-31)$ vector template and (3) P111G.

Once the plasmids were confirmed to have no errors, the single amino acid mutants were expressed and purified by the same method as the truncated pilin mutants. The progression and purity of the purification were monitored by SDS-PAGE gel (Fig. 2.16, 2.16, 2.17). Similar to the truncated pilin mutants, the proteins are soluble judged by the presence in the lysate, post sonication. For I98D, the initial purification yielded a mixture of the protein and the SUMO-I98D, a second purification step was performed by Ni-NTA to remove the SUMO-I98D (Fig. 2.17). The procedure yield was 1 g/ L culture and ~0.5 mL of ~92 μ M pilin protein per L of

culture for P111G, 1.5 g/ L culture and ~0.75 mL of ~118 μ M pilin protein per L of culture for I98D and 0.5 g/L culture and ~ 0.3 mL of 90 μ M of W105K.

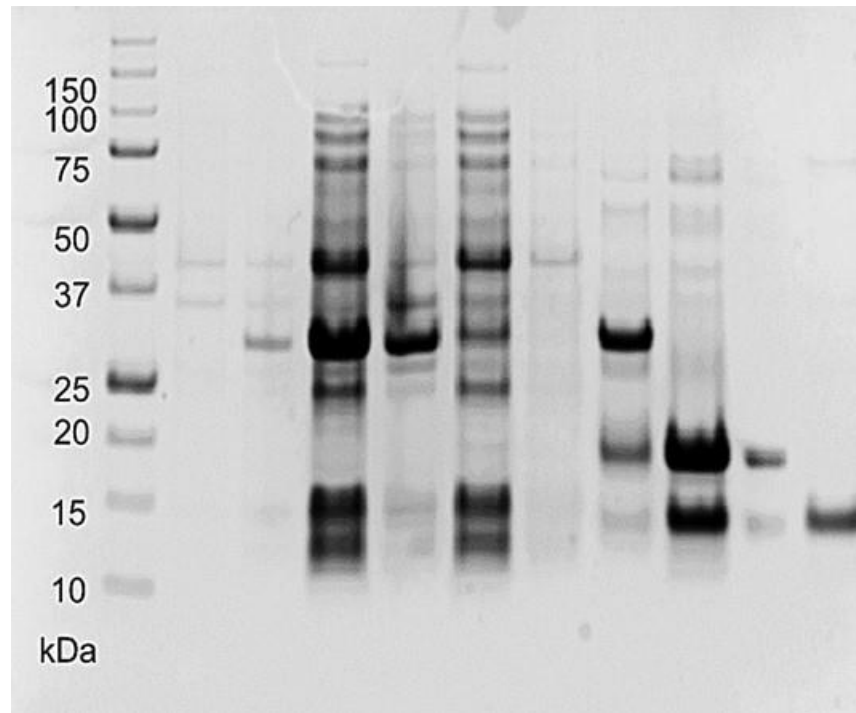


Figure 2.15 SDS-PAGE gel of P111G mutant of pilin $\Delta(1-31)$. Lanes (1) ladder, (2) pre-induction, (3) induced sample, (4) cell lysate, (5) cell debris, (6) flow through, (7) wash flow through, (8) pre-SUMO cleavage, (9) post-cleavage and (10) final P111G protein.

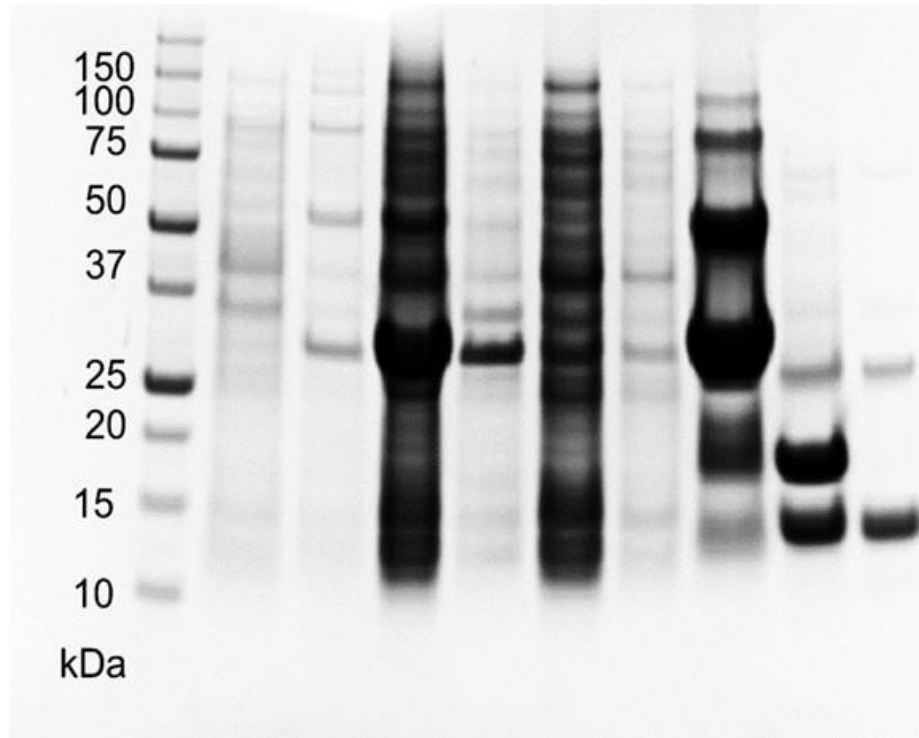


Figure 2.16 SDS-PAGE gel of I98D mutant of pilin $\Delta(1-31)$. Lanes (1) ladder, (2) pre-induction, (3) induced sample, (4) cell lysate, (5) cell debris, (6) flow through, (7) wash flow through, (8) pre-SUMO cleavage, (9) post-cleavage and (10) final I98D protein.



Figure 2.17 SDS-PAGE gel of W105K mutant of pilin $\Delta(1-31)$ and I98D final pilin $\Delta(1-31)$ vector purified protein. Lanes (1) ladder, (2) pre-induction, (3) induced sample, (4) cell lysate, (5) cell debris, (6) flow through, (7) wash flow through, (8) pre-SUMO cleavage, (9) post-cleavage and (10) final W105K protein (11) final I98D protein.

Comparing these two methods of protein expression, there are a lot of differences and factors that needed to be changed. *P. aeruginosa* PA1244N3(pPAC46) expresses the pilin protein as an assembly outside the bacterial cell that can be manually sheared off and purified from the supernatant while *E. coli* BL21(DE3) expresses the protein inside the cell and has to be lysed in order to purify the protein. The main difference between the two expressed protein is that the *P. aeruginosa* expressed pilin are mostly in aggregate form while *E. coli* BL21(DE3) mainly expresses pilin in the monomeric form. Despite the different methods used for the expression of native and the truncated pilin mutants, the final protein yields are comparable per L of culture used. We were able to purify ~2-3 mg per L culture of native pilin in *P. aeruginosa*

and in *E. coli* for the pilin $\Delta(1-31)$ for both procedures. Furthermore, the single amino acid mutants yields are low compared to the truncated pilin proteins when expressed in *E. coli*, with 1 mg/ L culture for pilin $\Delta(1-31)$ P111G, 1.5 mg/ L culture for pilin $\Delta(1-31)$ I98D and 0.5 mg/ L culture for pilin $\Delta(1-31)$ W105K.

2.3 Conclusion

We successfully expressed the truncated pilin mutants from *P. aeruginosa* 1244N3(pPAC46) in *E. coli* BL21 (DE3). By ligating the *pilA* gene in the pET-SUMO vector, we were able to generate soluble proteins. Furthermore, we also successfully expressed single amino acid mutants by site direct mutagenesis in the pET-SUMO- pilin $\Delta(1-31)$ plasmid. All the proteins can be overexpressed and purified by using a Nickel affinity column. Our procedure completely eliminates the use of PEG-8000 in the purification process and avoids any possible interference in structural studies. The truncated pilin and single amino acid mutants will be used for futures biological and structural studies to identify potential ligands for pilin protein.

2.4 Experimental Section

2.4.1 Expression and purification of native pilin from *P. aeruginosa* PA1244N3(pPAC46)

Frozen glycerol stock of *P. aeruginosa* PA1244N3(pPAC46)⁸⁵ was streaked and grown overnight on a Luria Bertani (LB) agar plate (1.5 wt% Bacto Agar, 1 wt% NaCl, 1 wt% tryptone, and 0.5 wt% yeast extract) supplemented with 50 ug/mL tetracycline (Tc⁵⁰) and 200 ug/mL carbenicillin (Cb²⁰⁰) at 37 °C. A single colony from the agar plate was grown in 25 mL LB media (Tc⁵⁰, Cb²⁰⁰) overnight at 37°C, with shaking at 250 rpm. The culture was then transferred to 1 L of LB media (Tc⁵⁰, Cb²⁰⁰) followed by adding 1 mM isopropyl β -D-1-

thiogalactopyranoside (IPTG) to induce protein expression overnight at 37 °C with shaking at 250 rpm. The pili on the bacteria cells were sheared off by centrifugation at 20,000 g, 4°C for 30 minutes and the cell pellet was discarded. To the supernatant, 3 % polyethylene glycol 8000 (PEG- 8000) and 0.5 M NaCl was added then incubated on ice for 2 hours to precipitate the pili. Pili was collected from the supernatant by centrifugation at 20,000 g, 4°C for 30 minutes, and the supernatant was discarded. The resulting precipitate was dissolved in 4 mM sodium phosphate buffer, pH = 7.2, with stirring for 1 hour at ambient temperature. The insoluble impurities were collected by centrifugation at 20,000 g, 4°C for 30 minutes and discarded, keeping the supernatant. Precipitation of the pili with PEG-8000 and NaCl followed by solubilization in phosphate buffer was repeated once. Final precipitation by adding 3 wt% PEG 8000/ 0.5 M NaCl to the resulting supernatant then incubation on ice for 30 minutes was done. The resulting pili pellet was collected by centrifugation at 20,000 g, 4°C. The pili precipitate was dissolved in sodium phosphate buffer (50 mM, pH = 7.2) and kept at -80 °C. Purity of pili protein was checked by SDS-PAGE (15 % acrylamide). The concentration of the protein in solution was checked by taking absorbance at 280 nm (A_{280}) using the calculated (ExPASy) extinction coefficient of $17085 \text{ M}^{-1} \text{ cm}^{-1}$.

Table 2.1 Primers used for recombinant expression of pilin in *E.coli*.

Proteins	Mutation	Primers
pilin $\Delta(1-31)$	$\Delta 1-31$	forward: 5'-CAGGTGACCCGTGCCGTGAGTG-3' reverse: 5'-TTAGGATTTTCGGGCAATTAGCCGGAG-3'
pilin $\Delta(1-28)$	$\Delta 1-28$	forward: 5'-ACCGCCTACCCAGG-3' reverse: 5'-TTAGGATTTTCGGGCAATTAGCCGGAG-3'
pilin $\Delta(1-23)$	$\Delta 1-23$	forward: 5'-ACCGCCCGTACCCAGG-3' reverse: 5'-TTAGGATTTTCGGGCAATTAGCCGGAG-3'
truncated W105K	$\Delta 1-31$, W at position 105 is mutated to K	forward: 5'-CTCCTACAGCT <u>AAAAAG</u> CCCAACTACGC-3' reverse: 5'-GCGTAGTTGGGCT <u>TTTTAG</u> CTGTAGGAG-3'
truncated I98D	$\Delta 1-31$, I at position 98 is mutated to D	forward: 5'-CTGGA <u>ACTG</u> CAAAGATACCAAACTCCTAC-3' reverse: 5'-GTAGGAGTTTTGGT <u>ATCT</u> TTGCAGTTCCAG-3'
truncated P111G	$\Delta 1-31$, P at position 111 is mutated to G	forward: 5'-CCA <u>ACTAC</u> GCTGGCGCTAATTGCC-3' reverse: 5'-GGGCAATTAGC <u>GCCAG</u> CGTAGTTGG-3'

2.4.2 Cloning and recombinant expression of truncated pilin proteins.

The pPAC46 plasmid containing the native *pilA* gene was extracted from *P. aeruginosa* strain PA1244N3(pPAC46)⁸⁵ using the PureLink™ Quick Plasmid Miniprep Kit (Thermo Fisher Scientific). Truncated pilin DNA sequences were cloned from the native *pilA* gene, deleting the first 31, 28 and 23 amino acids from the N'-terminus. To pull out the gene, we used IDT primers (Integrated DNA Technologies, IDT) shown in Table 2.1. The truncated native pilin DNA sequences were ligated into the Champion™ pET-SUMO vector (Thermo Fisher Scientific) to yield a plasmid that would express a fusion of truncated pilin proteins with the SUMO protein. The sequence was confirmed by Sanger sequencing (Genewiz). The plasmid containing the truncated pilin proteins were heat-shocked transformed into *E. coli* BL21(DE3). A single colony was grown overnight in LB media (20 mL) supplemented with kanamycin (Kan⁵⁰) at 37 °C with shaking at 250 rpm. This overnight culture was transferred to 1 L of LB media supplemented with kanamycin (Kan⁵⁰) and grown at 37°C to OD₆₀₀ = 0.6. The flask was then chilled on ice for 5 min and protein expression was induced by adding IPTG to a final concentration of 0.5 mM.

The culture was then allowed to grow overnight at 18°C with shaking at 250 rpm. The cells were harvested by centrifugation at 4,000 g, 4°C for 30 minutes. The typical yield of wet cell paste was ~2 g per liter of culture. Cell pellet was flash frozen in liquid nitrogen and stored at -80 °C until needed for purification.

2.4.3 Purification of pilin $\Delta(1-31)$, pilin $\Delta(1-28)$ and pilin $\Delta(1-23)$ from the lysate

Bacterial cells were resuspended in a lysis buffer (25 mM Tris, 100 mM NaCl, 20 mM imidazole, 10% glycerol, 0.1% lauryldimethylamine N-oxide, 0.5 mM PMSF pH =7.5; 5 mL of buffer for 1 g of cell paste) and lysed on ice by sonication for 15 minutes (20 s pulse, 20 s rest). The crude cell lysate was then centrifuged at 20,000 g, 4°C for 30 min, and the supernatant was loaded onto Ni-NTA resin (Clontech, 2 mL). The resin was then washed with 50 mL of the lysis buffer. The protein was eluted with a buffer containing 25 mM Tris, 100 mM NaCl, 250 mM imidazole, pH = 7.5 (elution buffer). Fractions containing protein, detected by Pierce™ BCA Protein Assay Kit (Thermo Fisher Scientific) were collected and concentrated to ~2 mL using an Amicon® Ultra-15 Centrifugal Filter Units 10 kDa MWCO (Millipore Sigma). The concentrated protein was buffer exchanged into SUMO cleavage buffer (50 mM Tris, 50 mM NaCl, pH = 8.0) using an Econo-Pac® 10DG desalting column (Bio-Rad Laboratories). The SUMO tag was cleaved by mixing the fusion protein with EDTA (0.5 mM final concentration), DTT (1 mM) and SUMO protease (the ratio of OD₂₈₀ of protein to OD₂₈₀ of protease is 200:1). The solution was sterilized using a 0.22 µm cellulose acetate filter, followed by incubation of the mixture at 30°C for 3 hours. The protein was then exchanged into storage buffer (25 mM Tris, 100 mM NaCl, pH =7.5) to remove DTT and EDTA. Pure digested protein was collected in the flow through fractions from Ni-NTA column. Fractions containing the protein were collected and concentrated

to the desired volume between 500 μL – 1 mL. The purity (> 95%) of the final samples was checked by SDS-PAGE analysis. The concentration of the protein was determined by measuring A_{280} using the calculated (ExPASy) extinction coefficient of $14105 \text{ M}^{-1} \text{ cm}^{-1}$ for pilin $\Delta(1-31)$, pilin $\Delta(1-28)$ and $17805 \text{ M}^{-1} \text{ cm}^{-1}$ pilin $\Delta(1-23)$.

2.4.4 Purification of pilin $\Delta(1-28)$ from the inclusion bodies

The cell debris from the sonication of the *E. coli* BL21(DE3) cells expressing SUMO-pilin $\Delta(1-28)$ were resuspended in 50 mM Tris, 100 mM NaCl, 4% (v/v) Triton-X and 1 M urea. pH=8.0 (9 mL buffer / g cell pellet) by gently shaking the tube. The suspension incubated at room temperature for 10 minutes followed by centrifugation at 20,000 rcf, 4 °C for 15 minutes. The supernatant was saved for further purification using the standard methods. The inclusion bodies (0.5g) were solubilized in 160 mL of resolubilizing buffer (50 mM Tris, 100 mM NaCl, 8M urea, pH= 7.5) then stirred at room temperature. The next steps were performed in a cold room. The solution of the resolubilized inclusion bodies were added dropwise to 500 mL of refolding buffer (50 mM Tris, 100 mM NaCl and 20% glycerol, pH= 7.5) then allowed to stir for 3 hours. The subsequent purification was done at ambient temperature. ~3.5 mg per L of culture from combining from the lysate, supernatant from resolubilization of the inclusion bodies and refolding from inclusion bodies (Fig. 2.13). The 500 mL solution with the refolded protein was loaded onto Ni-NTA resin (Clontech, 6 mL). The elution and subsequent steps of protein purification was carried out in the same manner as the lysate purification. Fractions containing the protein were collected and concentrated to the desired volume between 500 μL – 1 mL. The purity (> 95%) of the final samples was checked by SDS-PAGE analysis. The concentration of

the protein was determined by measuring A_{280} using the calculated (ExPASy) extinction coefficient of $14105 \text{ M}^{-1} \text{ cm}^{-1}$.

2.4.5 Expression and Purification of Truncated Native Pilin Mutants.

Mutants of the pilin $\Delta(1-31)$ protein were generated using site-directed mutagenesis with the Phusion DNA polymerase (Thermo Fisher Scientific) and primers listed in Table 2.1. The underlined letters are the specific codons that correspond to the mutations introduced in the plasmid. The plasmid containing the DNA expressing the SUMO- pilin $\Delta(1-31)$ was used for site-directed mutagenesis by PCR. PCR products that showed a band at approximately $\sim 6,000$ bp were considered successful mutations of the truncated pilin. The PCR products were subjected to DpnI digestion for 2 hours at 37°C . The plasmid transformed in *E. coli* DH5 α cells and plated on LB agar plates (1.5 w% Bacto-agar). Colonies were grown in 10mL LB media for plasmid miniprep. The plasmids were purified and sent for sequencing. The sequence was confirmed by Sanger sequencing (Genewiz). The transformation, expression and purification of the successfully mutated plasmids followed the same protocol as the pilin $\Delta(1-31)$ (see above). Protein concentration was determined by measuring A_{280} using the calculated (ExPASy) extinction coefficient of $8605 \text{ M}^{-1} \text{ cm}^{-1}$ (truncated W105K) and $14105 \text{ M}^{-1} \text{ cm}^{-1}$ (truncated P111G and truncated I98D).

2.4.6 MALDI-TOF Analysis of Truncated Pilin Molecular Weight.

Truncated pilin proteins were prepared to a final concentration of $\sim 40-50 \mu\text{M}$ with 100 μL volume in 25 mM Tris, 100 mM NaCl, pH=7.5. The protein samples were sent to The Protein Facility of the Iowa State University (Ames, Iowa). The protein samples were prepared with

sinapinic acid as matrix (50% acetonitrile, 0.01% TFA and water) and MALDI-TOF was performed on a Shimadzu AXIMA Confidence MALDI TOF Mass Spectrometer.

Chapter 3. Interactions of Truncated Pilin with Small Molecules Control the Swarming Motility of *P. aeruginosa*.

3.1 Background and Significance

3.1.1 Swarming motility of *P. aeruginosa* is influenced by different factors.

The collective migration of bacterial cells while growing on a hydrated soft gel surface is referred to as bacterial swarming motility.^{22, 23, 28, 53, 59, 60, 97-100} In nature, swarming motility is not exclusive for *P. aeruginosa*, but can also be observed in *E. coli*, *Bacillus subtilis*, *Vibrio parahaemolyticus*, *Proteus mirabilis* and *Myxococcus xanthus*.^{101, 102} The high density of these swarming cells is believed to contribute to the increased resistance to antibiotics – an adaptive mechanism of the bacteria to thrive in harsh environments.^{100, 101} In a laboratory setting, on a hydrated soft agar gel (0.5 wt% agar in a petri dish of 10-cm diameter), swarming motility produces different, complex patterns that have been associated with variable growth conditions.⁵³

Interestingly, for *P. aeruginosa*, different strains exhibit different geometric patterns of bacteria on a 10-cm diameter gel as a result of the swarming motility. Whereas wild type PAO1 swarm to give circular disk pattern with a few cm (<10) in diameter, PA14 (a strain developed from burnt wound and from other patients) produce patterns with protruding tendrils from the center of inoculated colony (Fig. 3.1).¹³ For wild type PAO1 strain, the general assumption is that there is only one phenotype on the plate, and they move in random directions on the gel surfaces when they swarm. As the population increases, the colony area becomes bigger as the result of the swarming movement, forming a circular disc shape of swarming pattern. However, for PA14, overtime, it is recognized that two phenotypes exist on the agar gel. One is a transient swarming strain at the tip of the tendrils; as these bacteria swarm outwardly, they transition into the non-

* The work in this chapter is a collaboration with Felicia Burns in Luk group. She separated the rhamnolipids into monorhamnolipid and dirhamnolipid, performed the swarming motility assay on *rhlA* and collected the ¹H NMR of each rhamnolipid component for the purpose of completing the information.

swarming phenotype and are left behind on the plate. This conclusion is drawn because of the fact that the bacteria in the stems of the tendrils are not swarming, otherwise they will cover the surface between the tendrils. This understanding of PA14 raises the question of whether the wild type PAO1 inside the circular pattern are actually swarming or not. It is also possible that they are not swarming, and only the bacteria on the edge of the disc are swarming, as a transient phenotype. The phenotype bifurcation for the PA14 on the gel, where the swarming branches only from the tendril tips and the stems do not swarm (Fig. 3.1) is a known phenomenon.¹⁰³ The mechanism for this phenotype bifurcation has yet to be elucidated. The bacteria may employ a regulation mechanism as a result of the different phenotypes produced or due to the presence of the secreted rhamnolipids to the environment where the small molecules guide the bacterial motility.

The presence of small molecules in the soft gel also induces different patterns formation by *P. aeruginosa*.^{22, 23, 59} However, the mechanism by which these phenomena occur is still unknown.^{22, 23, 59} *P. aeruginosa* swarming motility requires a nutrient-rich media, semisolid surface (0.4 % to 0.7 % agar), rhamnolipid production, the presence of flagella and pilin protein on the bacteria and cell-to-cell interactions.^{22, 23, 28, 53, 59, 60, 97-100} *P. aeruginosa* produces rhamnolipids, a biosurfactant, is required for swarming motility, believed to lower the surface tension of the gel.^{28, 53, 59, 97} *P. aeruginosa* swarmer cells have been observed to elongate and even produce multiple flagella.^{28, 98} The presence of flagella is important in swarming as this protein powers the motion of the bacteria cells.^{28, 59} Pilin protein expressed by *P. aeruginosa* has also been reported to influence the swarming motility of this bacterium, by which the mechanism is still unknown. Despite having identified these different factors, there is still no clear consensus of whether swarming occurs because of physical conditions or signaling factors.

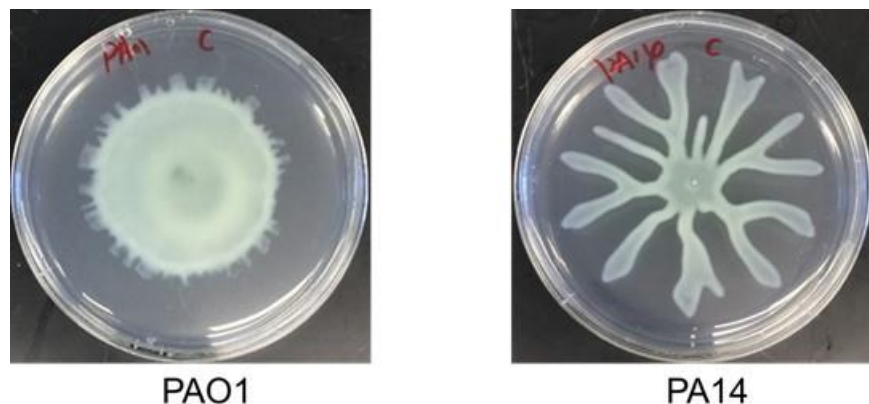


Figure 3.1 Different swarming patterns of two *P. aeruginosa* strains PAO1 (left) and PA14 (right) on M8 soft agar gel (0.5 wt% agar). The swarming assays were performed by Dr. Hewen Zheng (Luk lab).

3.1.2 *Rhamnolipids and synthetic disaccharides control the swarming motility of P. aeruginosa.*

Rhamnolipids are biosurfactants secreted by *P. aeruginosa*, implicated for the virulence of this bacterium, often found in the sputa of patients with cystic fibrosis.¹⁰⁴ Studies on rhamnolipids have shown that this biosurfactant is needed for swarming motility,^{22, 23, 28, 56, 59, 103, 105} the formation of channels in biofilms, as well as for the dispersion of the biofilms.^{18, 106} Rhamnolipids are classified as amphiphilic molecules with a hydrophilic L-rhamnose group and a hydrophobic 3- hydroxy fatty acid chain. *P. aeruginosa* produces two types of rhamnolipids namely mono- and dirhamnolipids. Monorhamnolipid is L-rhamnosyl-3-hydroxydecanoyl-3-hydroxydecanoate and dirhamnolipid is a L-rhamnosyl-L-rhamnosyl-3-hydroxydecanoyl-3-

hydroxydecanoate molecules, these two only vary with the number of the L-rhamnose groups (Fig. 3.2).^{105, 107}

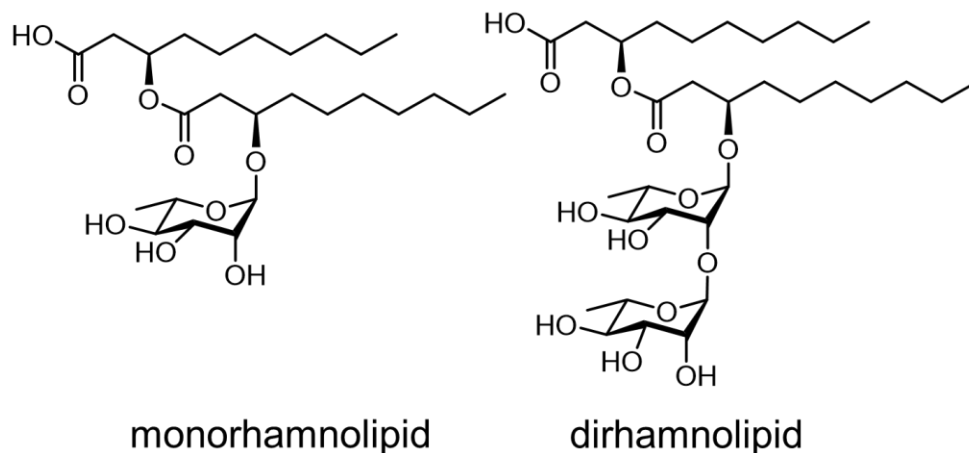


Figure 3.2 Structures of the individual components of rhamnolipids produced by *P. aeruginosa*.

While it has been identified that rhamnolipids are required for the swarming of *P. aeruginosa*,^{22, 23, 28, 56, 59, 103, 105} the function of rhamnolipids remain a controversy. As a biosurfactant, it is believed that rhamnolipids act as surface active agents that facilitate swarming by lowering the surface tension of the hydrated soft gel surface.^{53, 59, 60, 97, 99, 105} However, previous studies have demonstrated that rhamnolipids act as signaling molecules and modulate the swarming of *P. aeruginosa*.^{22, 23, 28, 59, 60} For example, *P. aeruginosa* transposon mutant strain, *rhlA*, is unable to produce rhamnolipids and does not swarm on soft agar gel.^{23, 28, 59, 60} When rhamnolipids are externally added in the swarming gel, *rhlA* swarming is re-activated. Furthermore, a concentration study of adding rhamnolipids into the swarm gel shows that swarming is activated at low concentrations and swarming is inhibited at higher concentration. Moreover, high concentrations of rhamnolipids added to the gel inhibit the swarming of PAO1.²³ General surfactants such as tetra(ethyleneglycol)monododecyl ether (C₁₂EG₄OH) and SDS

exhibited no swarming modulation on *P. aeruginosa* (Fig. 3.3).^{23, 74} These results strongly suggest that rhamnolipids are most likely signaling molecules that control swarming activity of *P. aeruginosa*. As a signaling molecule, there must be a protein receptor that recognizes rhamnolipids resulting in the swarming oscillation of *rhlA*. However, the protein receptor of rhamnolipids is still unknown.

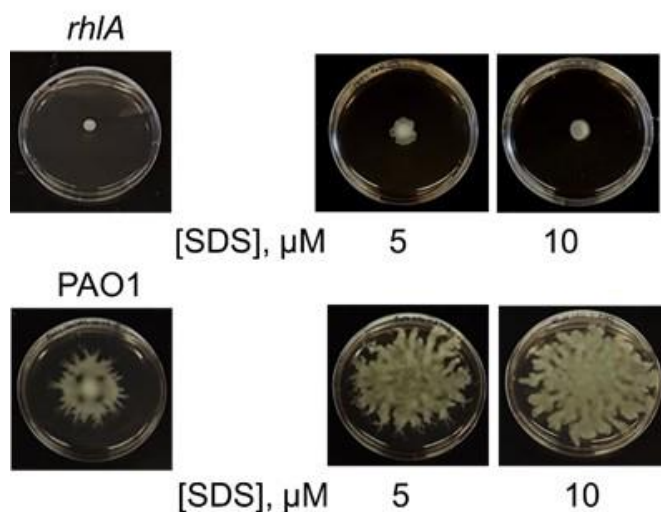


Figure 3.3 The swarming motility of *P. aeruginosa* strain *rhlA* and PAO1 on soft agar plates with SDS.

Pili is implicated for swarming of *P. aeruginosa*, but the nature of its role in swarming is not entirely clear.^{28, 100} Pilin recognizes the D-GalNAc- β -(1 \rightarrow 4)-D-Gal- β disaccharide group of Asialo-GM₁ which primarily leads to cell adhesion then colonization^{8, 9, 51} and bind hydrophobic surfaces.^{16, 17} We explore the possibility that pili are the receptor for rhamnolipids and the swarming motility is directly controlled by the binding between the two. Luk lab synthesized several bulky alkyl-disaccharides that have a general structure resemblance to rhamnolipids, that inhibit swarming motility (Fig. 3.4).^{22, 23} These small molecules may also function as specific

ligands for pilin, and controls the pili assembly, and dynamics of extension and retraction, as well as other pili-related signaling processes.

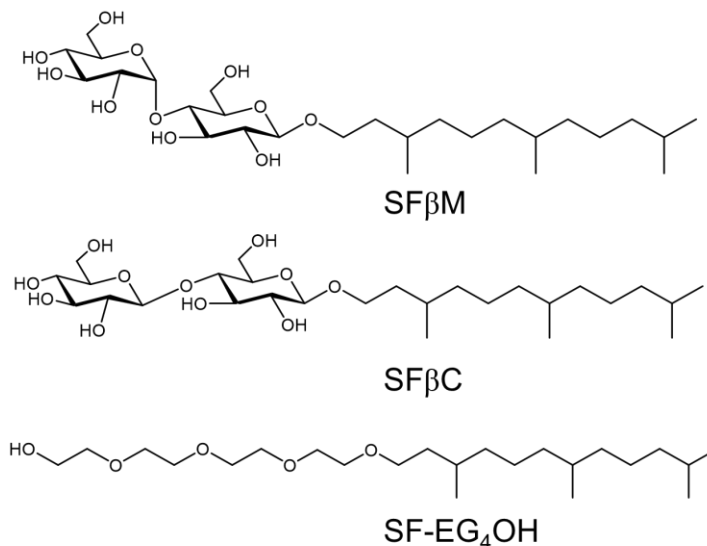


Figure 3.4 Synthetic disaccharides that inhibit swarming of *P. aeruginosa*: SFβM, SFβC and SF-EG₄OH. These molecules are synthesized by Luk lab.

Studies led by Dr. Hewen Zheng (Luk lab) demonstrated that externally adding purified pilin on the gel surface inhibits swarming of *P. aeruginosa* PAO1, leading us to hypothesize that pilin binds to rhamnolipids. This result suggests a mechanism where the externally added pilin competes with the pilin on the bacterium for the rhamnolipids. Because rhamnolipids produced by PAO1 enable the swarming motility of this bacterium, the fact that swarming inhibition is observed suggests that the externally added pilin binds and sequesters the rhamnolipids, leaving none, if not, a deficiency for the pilin on the bacterium to bind and allow swarming to occur. Furthermore, the SFβM-inhibited swarming of PAO1 was reinitiated when externally added pilin was added on the gel, demonstrating that the external pilin is sequestering the SFβM rather than

the rhamnolipids (produced by PAO1) in the gel. However, the combination of native pilin and SF β M can cause the reactivation of swarming motility only at a specific and narrow concentration. Collectively, we hypothesize that pilin is the protein receptor of rhamnolipids and the disaccharide analogs, and that their binding controls the swarming motility of *P. aeruginosa*.

3.1.3 Chapter aim: To test the hypothesis that pilin is the protein receptor of rhamnolipids and synthetic molecules.

In this chapter, we further develop the bacterial motility enabled modified swarming assay to study the direct and specific interactions between pilin and rhamnolipids. We initially determined that monorhamnolipid is more active than dirhamnolipid at controlling the swarming motility of *P. aeruginosa*. Next, we optimize and standardize the parameters of the bacterial motility enabled binding assay for demonstrating the binding between pilin and rhamnolipids. We either applied the protein by spreading or localizing the pilin as a drop on the soft gel surface. The established parameters were carried out in two separate studies- for PAO1 and for *rhlA*. First, we used the wild-type PAO1, for which rhamnolipids are self-secreted by the bacterium into the surrounding environment on the soft gel, needed for the PAO1 to swarm. Second, we used non-swarming *rhlA* mutant, for which rhamnolipids in the gel activates the swarming motility of *rhlA*. We aim to determine if the externally added pilin will revert the rhamnolipids-controlled swarming motilities of these two strains. Moreover, we evaluate the bioactivities of the heterologously expressed pilin proteins and the single amino acid mutants for similar binding activities to rhamnolipids as the native, full-length pilin expressed by *P. aeruginosa* in an effort to determine the binding region as well as the importance of the D-loop to binding rhamnolipids.

3.2 Results and Discussion

3.2.1 The design of the swarming competition assay to identify protein receptors of rhamnolipids: Bacterial motility binding-enabled motility assay

Swarming is performed on a highly hydrated soft agar gel in M8 media supplemented with glucose, casamino acids and salts (~ 97.8 wt% water, 0.5 wt% agar and 2.2 wt% other components) (Table 3.1). We note that this high hydration is essential for *P. aeruginosa* to swarm.^{22, 23, 28, 53, 59, 60, 97-100} Despite the fact that the gel is mostly water (~97.8 wt%), when a drop of water of bacteria culture (3 μ L) is added on the gel surface, the droplet is observed to bead up (Fig. 3.5) showing that the agar gel network creates a physical barrier that limits the accessibility or the motility of the water molecules on the surface of the gel. Previous studies by Luk lab on the effect of small molecule analogs of rhamnolipids on the swarming motility of *P. aeruginosa* were done by dissolving the small molecules in the soft gel solution prior to gelation in a petri dish then allowed to air dry.^{22, 23} To gain understanding of how these surfactants affect the physical properties of the gel surface, we performed the same experiment by dissolving amphiphatic small molecule, dodecyl- β -maltoside (D β M) in the gel solution, then allowed to dry. We observe that the droplets of water or the bacteria culture on the gel collapse on the surface (Fig. 3.5). These results demonstrate that upon gelation the ligand molecules appear to have a preferred partition on the air-gel interface because of their amphiphilic nature, and these molecules can interact with the droplets and cause them to spread on the surface.

Table 3.1 Composition of salts in M8 agar gel.

component	weight (g)	wt%
Na ₂ HPO ₄	6	0.60%
KH ₂ PO ₄	3	0.30%
NaCl	0.5	0.05%
agar	5	0.50%
glucose	2	0.20%
casamino acids	5	0.50%
1 mM MgSO ₄	0.12	0.012%
TOTAL SOLIDS	21.62	2.162%

*Based on 1 L volume of agar solution.

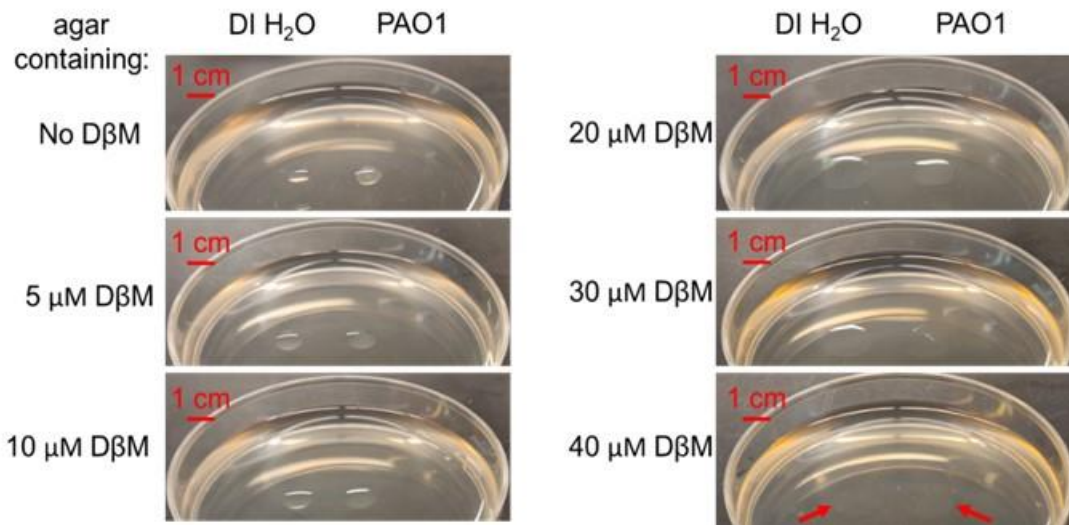


Figure 3.5 Swarm gel prepared by dissolving increasing concentrations of DβM. Droplets (3 μL) of water or PAO1. The droplet assay was performed by Yuchen Jin (Luk lab member).

Swarming motility is a surface-associated motility, suggesting that binding between the pili appendages and the ligand molecules primarily occur on the gel surface despite the small molecules distributed within the gel network. However, we also note that the concentration of the molecules in the bulk of the gel plays an important role in swarming. During 12 to 24-hour course of the swarming assay, the bacteria population increases, and each bacterium continuously expresses pili on its surfaces. Thus, pili sequesters ligands in the monolayer constantly allowing for the swarming motility, indicative of the ligand molecules on the surface monolayer being replenished from the bulk of the gel in a continuous manner.

Based on these concepts, we designed a bacterial motility binding enabled motility assay allowing us to observe direct binding between proteins and rhamnolipids on the gel surface. Pilin proteins are introduced onto the gel surface either by spreading pilin solution on the entire surface of the soft hydrated gel (Fig. 3.6A) or placing microliter-droplets of the protein solution on the gel surface. Followed by brief air-drying, a droplet of *P. aeruginosa* culture is inoculated to for the swarming motility (Fig. 3.6B).

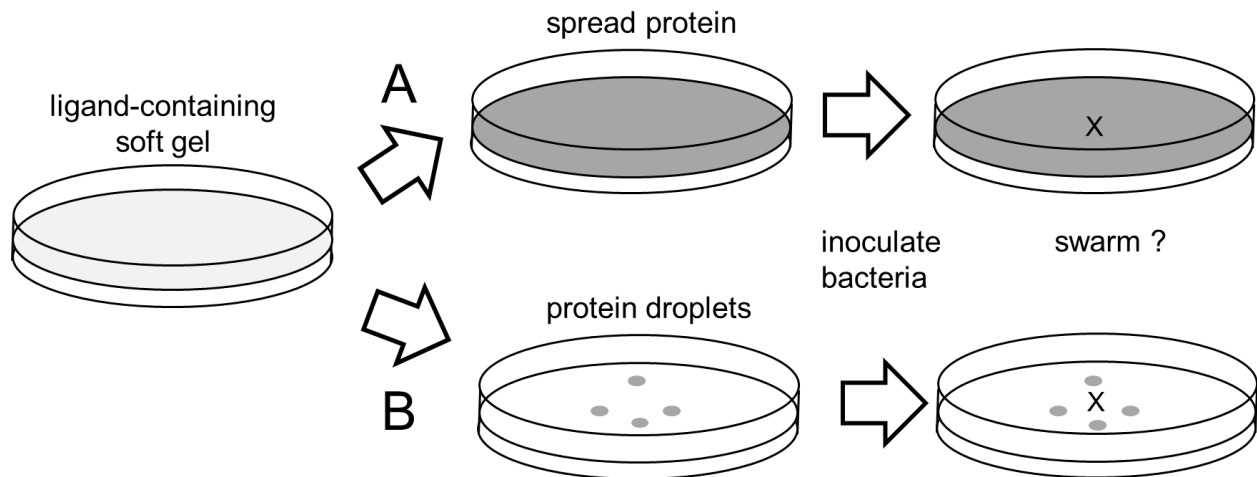
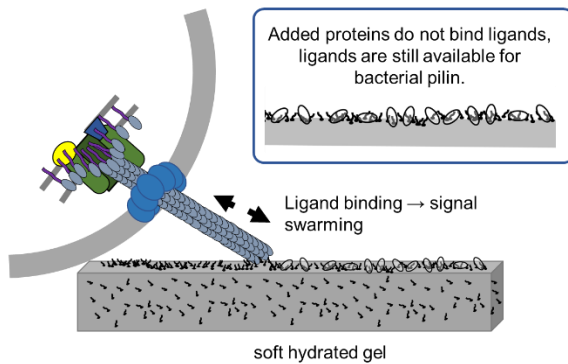


Figure 3.6 Design of the bacterial motility enabled binding assay. The surface of soft gels containing ligand molecules that either inhibit swarming of PAO1 or promote swarming of *rhlA* are introduced with a receptor protein candidate by either (A) spreading a solution of protein (10.5 nmol; 150 μ L of 70 μ M), or (B) placing droplets of protein (250 pmol; 2.5 μ L of 100 μ M). Bacteria (3 μ L, OD₆₀₀ ~ 0.6) is inoculated on the center of gel surface and incubated to monitor the swarming motility.

The premise of the experimental design is that the proteins applied on the surface will come into direct contact with the ligands that settle on the air-gel partition (Fig. 3.7). The externally added pilin will compete with protein receptors, if any, are present on the bacterial surface for binding to the ligands. If the protein added on the gel is a receptor of the ligand, the ligands will not be available for the protein on the bacteria.

Case 1: Bacteria swarms in the presence of spread protein



Case 2: Bacteria does not swarm in the presence of spread protein

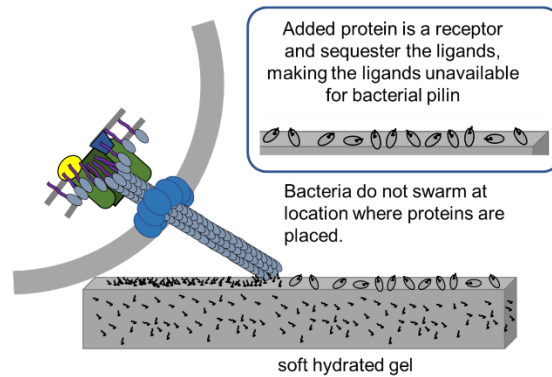


Figure 3.7 Modified swarming binding enabled assay scheme describing case 1: proteins on the gel do not bind ligands and case 2: proteins bind ligands.

We carried out two separate studies for this experimental approach. First, we used non-swarming *rhlA* mutant, for which rhamnolipids in the gel activates the swarming motility of *rhlA*. Adding pilin monomers on the gel surface may bind and sequester the rhamnolipid molecules near the air-gel interface creating a deficiency of available rhamnolipids to the pili appendage on the bacterial surface, rendering the *rhlA* mutant unable to swarm again. Second, we used the wild-type PAO1, for which rhamnolipids are self-secreted by the bacterium into the surrounding environment on the soft gel, needed for the PAO1 to swarm. Adding pilin proteins on the gel may bind and sequester the bacteria-secreted rhamnolipids, making the molecules unavailable for the pilin on PAO1, rendering the PAO1 unable to swarm.

3.2.2 Individual rhamnolipids components control *P. aeruginosa* swarming motility.

Rhamnolipids, present as a mixture of monorhamnolipid and dirhamnolipid, is essential for the swarming motility of *P. aeruginosa*. However, there are limited number of studies on the

individual components of rhamnolipids. O' Toole and co-workers purified rhamnolipids, rhamnolipids precursors and monorhamnolipid excreted by *P. aeruginosa* from the growth media.⁵⁹ They reported that rhamnolipids and monorhamnolipid inhibits the swarming of PA14. However, dirhamnolipid was not isolated and studied. The role of each component still remains unclear.

To test the effects of the individual components of rhamnolipids, Felicia Burns from Luk lab isolated monorhamnolipid and dirhamnolipid from a commercially available mixture of rhamnolipids, extracted from bacterial supernatant (AGAE Technologies) then tested the molecules for swarming activity. The individual monorhamnolipid or dirhamnolipid molecules, with well-defined concentrations, were dissolved in soft agar solution prior to gelation by air-drying. Once the gel has dried, the non-swarming transposon mutant of PAO1, *rhlA*, was then inoculated on the soft gel. When either monorhamnolipid or dirhamnolipid is added into the gel, the swarming motility of *rhlA* is activated (Fig. 3.8). Monorhamnolipid promotes swarming of *rhlA* at 3 μ M, whereas dirhamnolipid promotes at 4 μ M. When the concentrations of both molecules are further increased, we observe that only monorhamnolipid inhibits the *rhlA* swarming at 5 μ M and 20 μ M, but dirhamnolipid still promotes swarming at the same concentrations. These results indicate that both rhamnolipids components are crucial to the swarming motility of *P. aeruginosa*. Interestingly, inhibition of swarming motility at high concentrations of monorhamnolipid suggest that the mechanism of action is not due to the surfactant activity. We note that concentrations of rhamnolipids used do not inhibit growth or kill *P. aeruginosa*. Hence, we believe that rhamnolipids likely act as a signaling molecule in modulating swarming motility. Similar results of promotion and inhibition were previously observed for the rhamnolipids mixture.²³ Interestingly, the “activity reversal” of activating

swarming motility at low concentration, and promoting swarming motility at high concentration is consistent with monorhamnolipid being a signaling molecule that modulates specific bioactivities.⁵⁹ Surprisingly, dirhamnolipid is the major component from the mixture (3:1 dirhamnolipid: monorhamnolipid), but the monorhamnolipid dominates in controlling the swarming. Because rhamnolipids are produced as a mixture by bacteria, the mixture of these two molecules with different activities may help regulate the swarming motility. Furthermore, rhamnolipids have been found to exhibit anti-bacterial properties for other microbial species, and thus may play a role in distinguishing species.

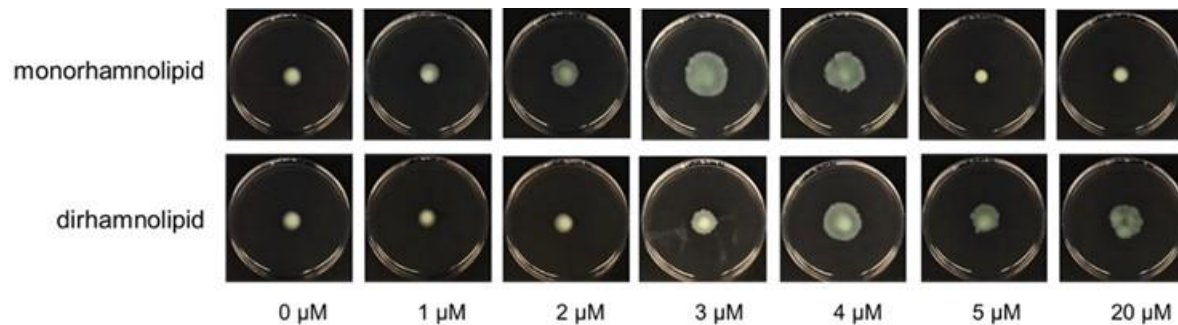


Figure 3.8 Swarming motility of *rhlA* on soft gel mixed with increasing concentrations of monorhamnolipid or dirhamnolipid.

3.2.3 Truncated pilin inhibits the rhamnolipids- induced swarming of *P. aeruginosa*.

We hypothesize that the pilin protein on the *P. aeruginosa* recognize and bind to the rhamnolipids leading to the regulation of the swarming motility of the bacterium. Previous results by Dr. Hewen Zheng⁷⁵ have shown that the native pilin protein purified from *P. aeruginosa* PA1244N3(pPAC46) is able to inhibit the swarming of both *P. aeruginosa* strains

wild-type PAO1 and the clinical isolate strain PA14 using the swarming motility assay. These results show that rhamnolipids are recognized by pilin proteins from different *Pseudomonas aeruginosa* strains.

To further characterize the binding between pilin and rhamnolipids, the three truncated pilin proteins- pilin $\Delta(1-31)$, pilin $\Delta(1-28)$ and pilin $\Delta(1-23)$ were tested to determine if they will bind to rhamnolipids using the bacterial motility binding-enabled motility assay (Fig. 3.9). For ease of reference, will refer to the pilin from PA1244N3(pPAC46) as native pilin in this chapter. We used the conditions that were initially defined, by spreading 1mL of 0.5 mg/mL of purified native pilin (35 nmol), pilin $\Delta(1-31)$ (41 nmol), pilin $\Delta(1-28)$ (40 nmol) and Δ pilin (1-23) (38 nmol) on the air-dried gel surface and allowed to air dry. The *P. aeruginosa* PAO1 was inoculated in the middle of the gel surface and incubated overnight. For the same amount of proteins added on the gel, we observe that only the native pilin and the truncated pilin $\Delta(1-31)$ inhibits the swarming motility of PAO1 while the other truncated pilin proteins did not. This result indicates that removing 31 amino acid residues from the N'-terminus of the pilin protein yields a protein that exhibits the same functionality as the native pilin protein. Furthermore, it is highly likely that either pilin $\Delta(1-31)$ or the binding region of pilin $\Delta(1-31)$ adopts a conformation that is similar to the native pilin, allowing for recognition and binding of rhamnolipids.

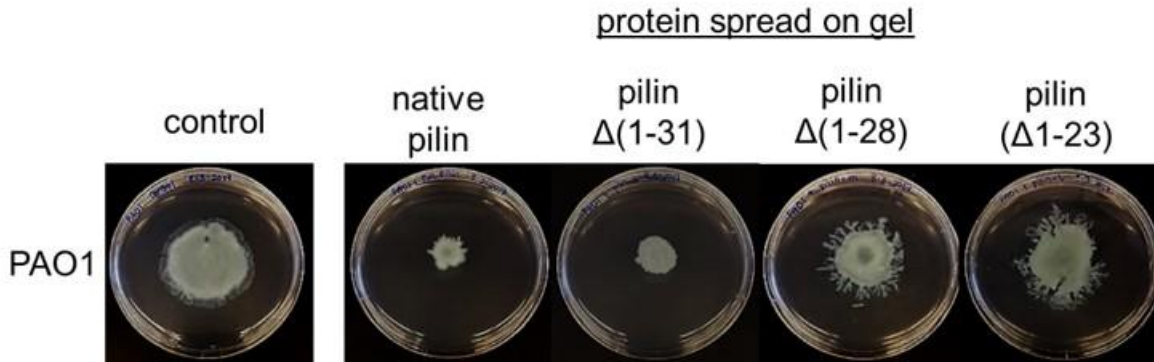


Figure 3.9 Swarming motilities of wild-type PAO1 with and without pilin proteins. Proteins spread on the gel: 1 mL of 0.5 mg/mL native pilin (35 nmol), pilin $\Delta(1-31)$ (41 nmol), pilin $\Delta(1-28)$: (40 nmol) and Δ pilin (1-23) (38 nmol). Protein solutions were prepared in 25 mM Tris, 100 mM NaCl buffer, pH= 7.5, and in 40 mM sodium phosphate buffer, pH= 7.2. Images were taken 24 hours after inoculation.

Next, we tested if localizing the pilin in one spot on the gel will inhibit the swarming of PAO1. Droplets of proteins (2.5 μ L of 250 pmol) - native pilin (1.6 mg/mL) and BSA (6.6 mg/mL) were placed at different areas surrounding the bacterial inoculation, while keeping the inoculation spot in the center. (Fig. 3.5B). PAO1 is observed to swarm on the soft agar gel, but the swarm “avoids” the areas where the pilin droplets were placed on the gel. BSA droplets have no effect on swarming of PAO1 (Fig. 3.10). Here, we demonstrate that the ligand-binding assay both when the proteins are spread on the surface of concentrated as a drop is a selective test for *P. aeruginosa* pilin binding to rhamnolipids.

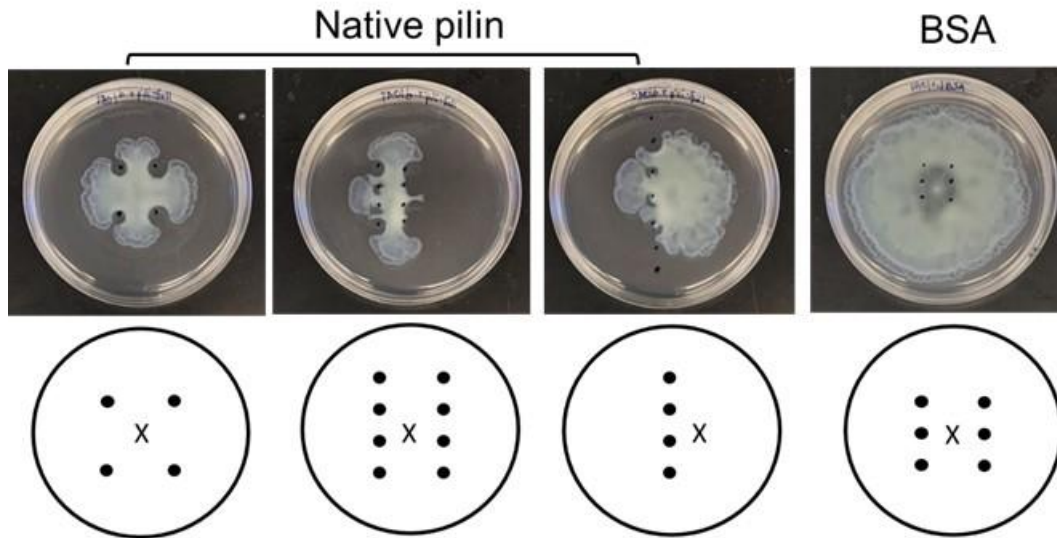


Figure 3.10 Bacterial motility enabled binding assay. The effect of protein droplets on the swarming motility of *P. aeruginosa* PAO1 on soft agar gel (top). Scheme of the swarming motility-based ligand-binding assay (bottom). The amount of protein in each drop on the surface of the gel is 250 pmol (●) 2.5 μ L of native pilin (1.6 mg/mL; 100 μ M) or BSA (6.6 mg/mL; 100 μ M) spot and (x) 3 μ L PAO1 (OD~ 0.7) inoculation spot on soft agar gel. Protein solutions were prepared in 40 mM sodium phosphate buffer, pH= 7.2.

To determine standard conditions for spreading pilin on the gel surface that inhibits the swarming of PAO1, we used a minimum volume of pilin solution (150 μ L instead of 1 mL) that is enough to cover the surface of the gel. We conducted a concentration study by spreading 150 μ L solutions of native pilin with increasing concentrations from .00016 to 21 nmol (0.000016 mg/mL – 2.2 mg/mL) (Fig. 3.11). PAO1 was then inoculated on the gel and incubated overnight. We observed swarming inhibition starting at 10.5 nmol pilin protein (70 μ M, ~1.1 mg/mL) until 21 nmol (140 μ M ~2.2 mg/mL). Therefore, we will use 150 μ L of 10.5 nmol (70 μ M, ~1.1

mg/mL) of native pilin as the standard in the next experiments for the bacterial motility binding enabled assay.

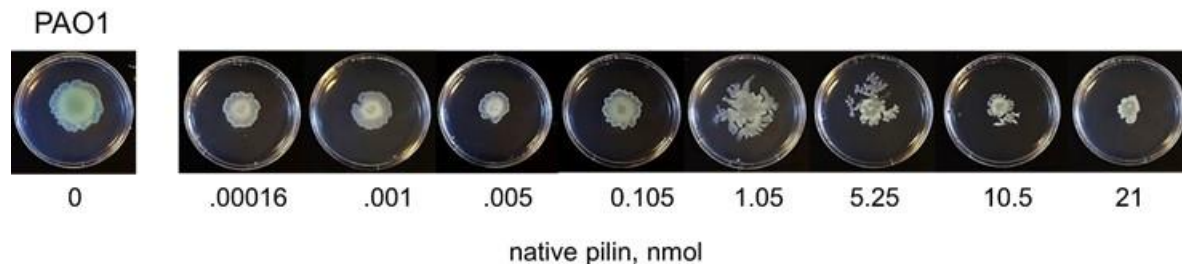


Figure 3.11 Swarming motilities of wild-type PAO1 with increasing amount of native pilin protein spread on the gel; Volume spread: 150 μ L. Protein solutions was prepared in 40 mM sodium phosphate buffer, pH= 7.2 Images were taken 24 hours after inoculation.

Next, we checked if pilin $\Delta(1-31)$ inhibits the swarming of PAO1 at same concentrations as the native pilin using the standard conditions (Fig. 3.12). Pilin $\Delta(1-31)$ solutions (150 μ L) containing 10.5 to 30 nmol (0.84 mg/mL – 2.4 mg/mL) were spread on the gel surface, the same concentration range that the native pilin inhibits swarming of PAO1. For all the concentrations used, pilin $\Delta(1-31)$ was able to inhibit the swarming of PAO1. Consistent with the previous results (Fig. 3.9), pilin $\Delta(1-31)$ exhibits the same activities as the native pilin. We note that BSA does not inhibit swarming of PAO1 at 10.5 nmol spread on the gel. These results would suggest that rhamnolipids are not ligands for BSA. While there is a possibility that nonspecific interactions may exist between the ligands on the interface and the proteins spread on the gel, the fact that PAO1 swarms when BSA is spread on the gel suggest that the selective binding between the ligands and the pili (on the PAO1) is strong and can out-compete and strip the non-specifically absorbed ligands from BSA.

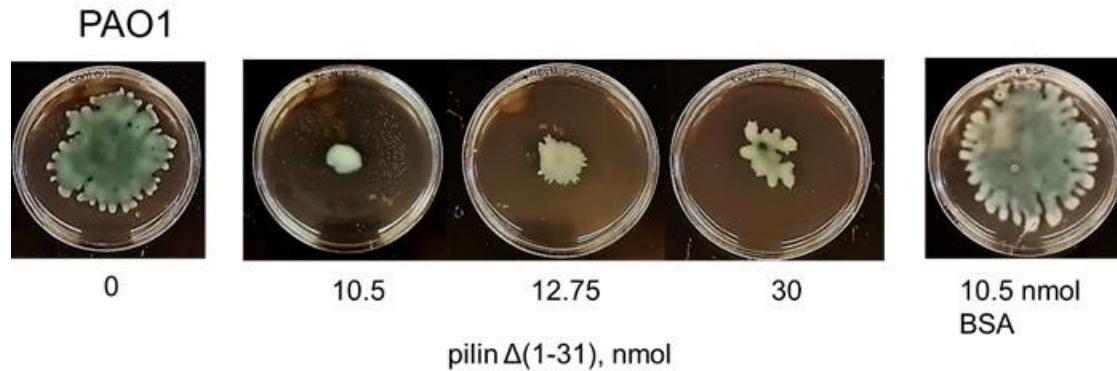


Figure 3.12 Swarming motilities of wild-type PAO1 with increasing amount of pilin $\Delta(1-31)$; Volume spread: 150 μL . Protein solutions were prepared in 25 mM Tris, 100 mM NaCl buffer, pH= 7.5. Images were taken 24 hours after inoculation.

Next, both pilin proteins (native and pilin $\Delta(1-31)$) were tested on the *rhlA* strain. (Fig. 3.13, 3.14). The swarming of *rhlA* oscillates (promotes then inhibits) when increasing concentrations of rhamnolipids are added in the gel; swarming is promoted from 5- 10 μM rhamnolipids and inhibited from 15- 20 μM .²³ First, we tested if the pilin proteins will be able to inhibit the rhamnolipids-induced swarming of *rhlA*. Rhamnolipids (5 μM) was added to the agar gel prior to gelation, the concentration at which enables *rhlA* swarms. Then, 150 μL of pilin with increasing concentrations, 0.1 -21 nmol of native pilin (0.0112 – 2.2 mg/mL) and pilin $\Delta(1-31)$, from 0.1 – 21 nmol (0.009 – 1.7 mg/mL) were spread on gel, allowed to air-dry, followed by the inoculation of *rhlA* (Fig. 3.12) We observe that both proteins inhibit the rhamnolipids-activated swarming of *rhlA*, but at different pilin amounts spread on the gel. Native pilin inhibits swarming at 10.5 nmol and pilin $\Delta(1-31)$ inhibits at 7.5 nmol. These results are consistent with previous findings that pilin bind to the rhamnolipids and control the swarming motility of *P. aeruginosa*. Furthermore, the pilin spread on the surface bind and sequester the rhamnolipid molecules near

the air-gel interface creating a deficiency of available rhamnolipids for the pili appendage on the bacterial surface, rendering the *rhlA* mutant unable to swarm.

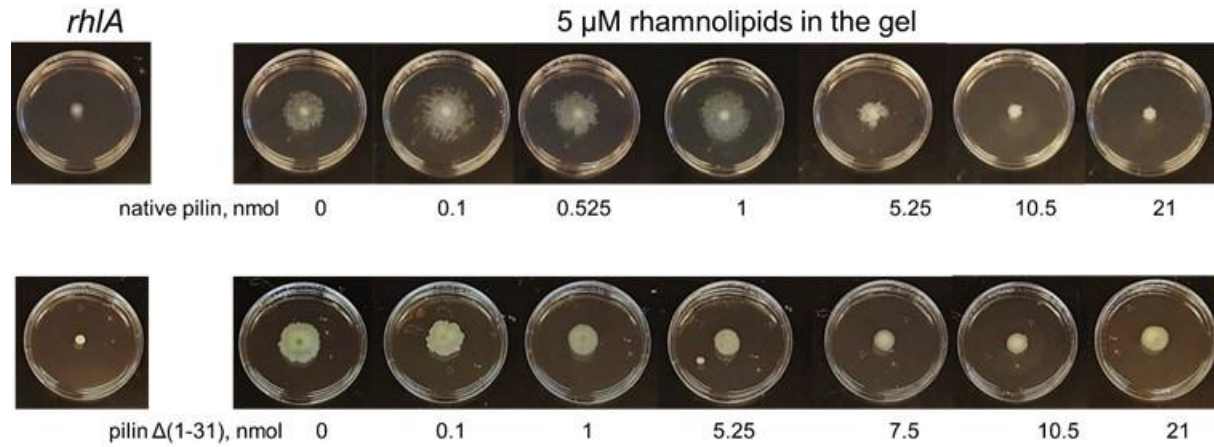


Figure 3.13 Swarming motility of *rhlA* on soft gels with 5 μ M rhamnolipids mixture with increasing amounts of pilin proteins. Proteins spread on the gel: 150 μ L native pilin (top) and pilin $\Delta(1-31)$ (bottom). Native pilin was prepared in 40 mM sodium phosphate buffer, pH= 7.2. Solution of pilin $\Delta(1-31)$ was prepared in 25 mM Tris, 100 mM NaCl buffer, pH= 7.5. Images were taken 24 hours after inoculation.

Next, we tested the binding motility enabled assay at inhibiting concentrations of rhamnolipids (20 μ M) (Fig. 3.14). Here, we checked if added pilin will bind and sequester rhamnolipids, lowering the rhamnolipids concentration to a range that promotes swarming. No significant effect was observed at the native pilin concentrations spread on the gel surface (0.5 – 10.5 nmol; 0.056 – 1.1 mg/mL) (Fig. 3.14). At all concentrations, *rhlA* swarming is inhibited.

Based on these results, swarming modulation by rhamnolipids- pilin binding can be observed at low concentrations added on the gel. At 20 μM , the rhamnolipids concentration might be too high, that the externally added pilin on the surface are all saturated, and because the rhamnolipids at the surface is continuously replenished from the bulk, excess rhamnolipids bind to the pilin on the *rhlA* that still inhibits the swarming.

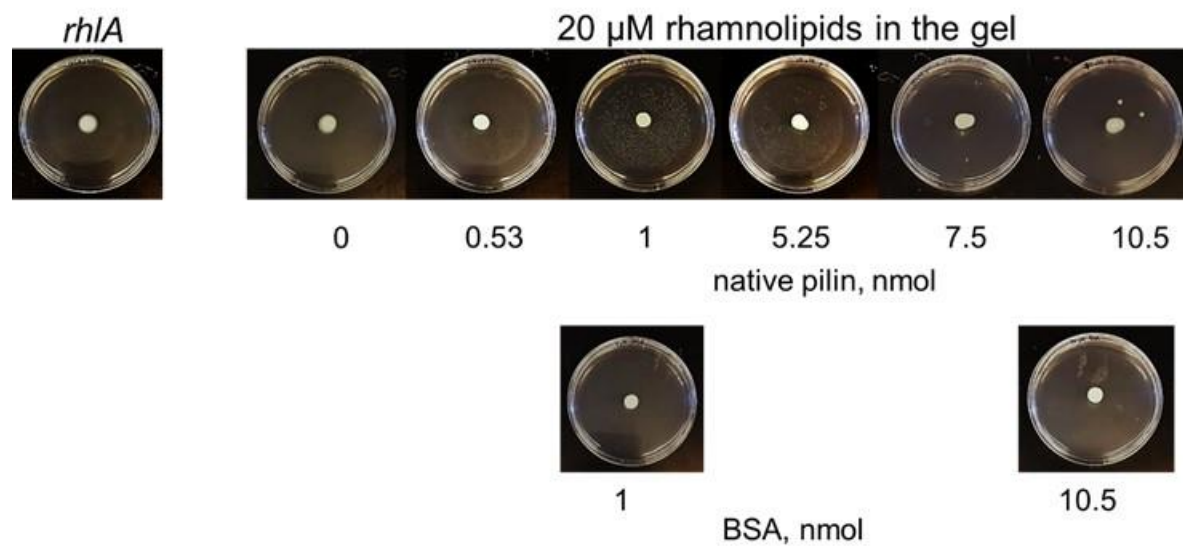


Figure 3.14 Swarming motility of *rhlA* on soft gels with 20 μM rhamnolipids mixture with increasing amounts of pilin proteins. Proteins spread on the gel: 150 μL native pilin (top) and BSA (bottom). Protein solutions were prepared in 25 mM Tris, 100 mM NaCl buffer, pH= 7.5, and in 40 mM sodium phosphate buffer, pH= 7.2. Images were taken 24 hours after inoculation.

3.2.4 *Pilin-rhamnolipids interactions modulate the swarming motility of P. aeruginosa.*

An earlier study reported that pilin-pilin interactions promote cell-to-cell interactions that influence the swarming motility of bacterial cells. When pili sense other pili, the individual cells cluster together rather than swarming on the agar gel.¹⁰⁰ To investigate whether swarming inhibition by pilin occurs as a result of pilin-pilin or pilin-rhamnolipids binding, we spread an inhibiting concentration of pilin (10.5 nmol) on gels containing two concentrations of rhamnolipids- one that promotes (25 μ M) and one that inhibits (30 μ M) PAO1 swarming. (Fig 3.15). If the swarming inhibition is by pilin-pilin interactions, we would expect that pilin-pilin interactions should be able to inhibit swarming at any rhamnolipid concentration added in the gel, even at 25 μ M. We observe that at 25 μ M rhamnolipids in the gel, PAO1 still swarms even in the presence of 10.5 nmol native pilin or pilin Δ (1-31) on the gel surface. In the case where an inhibiting concentration, 30 μ M of rhamnolipids is added in the gel, adding native pilin or pilin Δ (1-31) causes the PAO1 to re-swarm. These results suggest that pilin-rhamnolipids is the main binding interactions that control the swarming of PAO1. As the spread pilin on the surface gets saturated with the rhamnolipids from the gel, the concentration of available rhamnolipids decreases to the promoting concentration range. Furthermore, the unbound rhamnolipids (either from the bulk or produced by PAO1) will be available for the pilin on PAO1 to bind and enable swarming. With these two reasons, we can explain the observed re-swarming of PAO1 on the agar gel when inhibiting concentrations of rhamnolipids (30 μ M) and pilin (10.5 nmol) are on the swarm gel. Collectively, these results suggest that in the inhibition of swarming by externally added pilin protein is unlikely to be caused by pilin-pilin interaction, but added pilin sequesters the secreted rhamnolipids by specific ligand-receptor binding events.

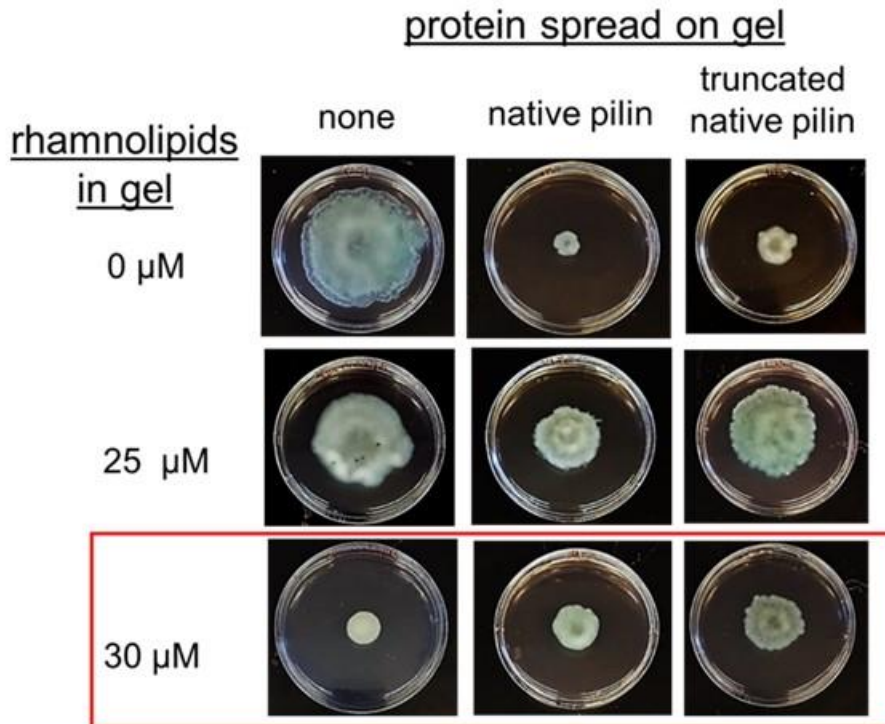


Figure 3.15 The swarming motility of *P. aeruginosa* strain PAO1 on soft gel without and with (25 or 30 μM) rhamnolipids. Proteins spread on the gel surface: 10.5 nmol of native pilin (150 μL of 1.1 mg/ mL) and 10.5 nmol pilin $\Delta(1-31)$ (150 μL of 0.84 mg/ mL). Native pilin was prepared in 4 mM sodium phosphate buffer, pH=7.2 and pilin $\Delta(1-31)$ pilin was prepared in 50 mM Tris, 100 mM NaCl, pH=7.5. Swarm plates were inoculated overnight at 37 $^{\circ}\text{C}$.

The importance of the D-loop in the recognition and binding of rhamnolipids were determined by the modified swarming assay. The single amino acid mutants were spread on the surface of the air-dried gel at concentrations within the inhibiting concentration ranges of both the native pilin and pilin $\Delta(1-31)$ (10.5- 30 nmol). For the mutants, 150 μL of truncated I98D – 17.7 nmol, truncated P111G- 13.8 nmol and W105K – 12 nmol were spread on the gel (Fig. 3.16). We observe that none of the single amino acid mutants inhibited the swarming motility of

PAO1 at these concentrations. These results suggest that changing a single amino acid in the sequence of the D-loop renders the truncated pilin inactive in inhibiting the swarming of PAO1. It is important that the sequence of the D-loop is conserved, confirming that the integrity of this region is important for recognition and binding of pilin to rhamnolipids.

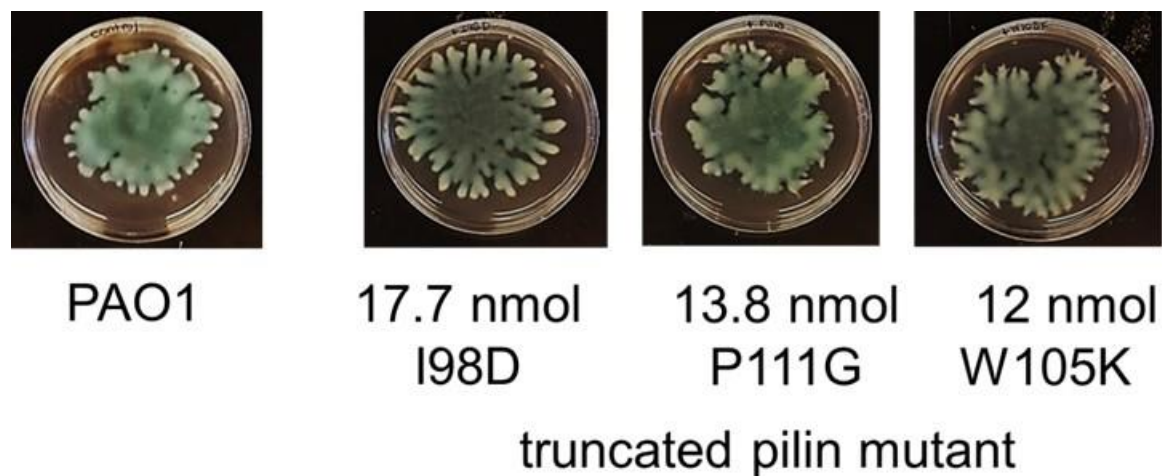


Figure 3.16 The swarming motility of *P. aeruginosa* strain PAO1 on soft gel with pilin $\Delta(1-31)$ mutants- 17.7 nmol (150 μ L of 1.41 mg/mL) I98D, 13.8 nmol (150 μ L of 1.11 mg/mL) P111G, 12 nmol W105K (150 μ L of 0.96 mg/mL) spread on the gel surface. Proteins were prepared in 50 mM Tris, 100 mM NaCl buffer, pH=7.5.

3.3 Conclusion

We show that monorhamnolipid and dirhamnolipid function as signaling molecules in controlling the swarming of *P. aeruginosa*, with monorhamnolipid being more dominant. We have demonstrated, by the “bacterial motility enabled” binding assay that pilin is a receptor for

rhamnolipids and the specific binding between the two, not pilin-pilin interactions, controls the swarming motility of *P. aeruginosa*. For PAO1, the externally added pilin sequesters the rhamnolipids produced by the bacterium and creates a lack of rhamnolipids for the pilin on PAO1, resulting in the inhibition of PAO1 swarming. Parallely, externally added pilin inhibits the rhamnolipids-induced swarming of *rhIA*, indicating that the pilin on the gel surface binds and sequesters the rhamnolipid molecules in the gel, leaving a deficiency of the available rhamnolipids for the pilin on the *rhIA*, rendering the bacterium unable to swarm. Furthermore, we have identified that deletion of 31 amino acids of pilin from the N- terminus retains the binding activity of the truncated pilin and that the integrity of the D-loop's primary sequence plays an important role in the recognition and binding of rhamnolipids and disaccharide analogs.

3.4 Experimental Section

3.4.1 Bacteria strains used in this study

The wild-type strain *P. aeruginosa*, PAO1 were from Dr. Guirong Wang (SUNY Upstate Medical University, Syracuse, NY). The non-swarming mutant of *P. aeruginosa*, *rhIA* (PW6886, *rhIA*-E08::ISphoA/hah) was obtained from PA two-allele library (PAO1 transposon mutant library).¹⁰⁸

3.4.2 Rhamnolipids and Synthetic Ligands Stocks Preparation

Synthetic ligands were either purchased from Agae Technologies or synthesized by Luk lab as previously reported.²³ Stocks were prepared by dissolving solids stocks in Millipore water

to 11.5 mM, then sterilized by passing through a 0.2 μm syringe filter. The stocks were stored in a sealed vial and kept in the $-20\text{ }^{\circ}\text{C}$ refrigerator.

3.4.3 Proteins used in this study.

Both native and pilin $\Delta(1-31)$ expression and purification were both discussed in Chapter 2. The purities of the proteins ($>95\%$) were checked by SDS-PAGE gel. The concentrations were checked by taking A_{280} by UV/Vis spectroscopy with the calculated (ExpASy) extinction coefficient of $171085\text{ M}^{-1}\text{ cm}^{-1}$ for the native pilin, $14105\text{ M}^{-1}\text{ cm}^{-1}$ for pilin $\Delta(1-31)$, $8605\text{ M}^{-1}\text{ cm}^{-1}$ (truncated W105K) and $14105\text{ M}^{-1}\text{ cm}^{-1}$ (truncated P111G and truncated I98D). BSA was purchased from Sigma Aldrich. Proteins were prepared in appropriate buffers, filter sterilized by passing through a $0.22\text{ }\mu\text{m}$ filter and kept in $-80\text{ }^{\circ}\text{C}$ until needed.

3.4.4 General swarming motility assay.

The swarming motility assay was previously described with some modifications.²³ The swarming gels were prepared by autoclaving 0.5 wt% Bacto Agar in M8 medium (0.6 % Na_2HPO_4 , 0.3 % KH_2PO_4 and 0.05 % NaCl) supplemented with 0.2 % glucose, 0.5 % casamino acid and 1 mM MgSO_4 . The gel solution was cooled to $\sim 60\text{ }^{\circ}\text{C}$, and then poured into a Falcon tube for 20 mL, followed by adding aliquots of rhamnolipids in sterile water (11.5 mM) to achieve the desired concentrations. The rhamnolipids-added gel solution was poured into a petri dish (10 cm in diameter) and allowed to cool down and air dry in a Biosafety level II laminar hood for 1 h to solidify the gel. Bacterial culture ($3\text{ }\mu\text{L}$) at $\text{OD}_{600} \sim 0.6$ was inoculated in the middle of the agar gel. The inoculated agar plates were incubated at 37°C for 12 hours, and then

incubated for additional 12 hours at room temperature. Pictures of the swarming plates were taken at desired time points during this 12 hours and 12 hours incubation. For each set of experiments, freshly prepared agar plates were used within the same day.

3.4.5 Binding enabled motility (modified swarming) assay.

The swarming motility assay was previously described with some modifications.²³ The swarming gels were prepared by autoclaving 0.5 wt% Bacto Agar in M8 medium (0.6 % Na₂HPO₄, 0.3 % KH₂PO₄ and 0.05 % NaCl) supplemented with 0.2 % glucose, 0.5 % casamino acid and 1 mM MgSO₄. The gel solution was cooled to ~60 °C, and then poured into a Falcon tube for 20 mL then transferred to a 10-cm diameter petri dish. The gel solution was allowed to cool down and air dry in a Biosafety level II laminar hood for 1 h to solidify the gel. For spreading the protein on the gel surface, solutions (150 µL) of proteins in buffers (native pilin was prepared in 4 mM sodium phosphate buffer, pH=7.2 and truncated pilin, truncated pilin single amino acid mutants and BSA were prepared in 2 mM Tris and 7 mM NaCl, pH= 7.5.) were spread on the solidified agar gel surface with a sterile cell spreader. The protein solution on the gel was air dried in the hood for 45 minutes. For droplets (2.5 µL) of 100 µM proteins (native pilin and BSA) in 40 mM sodium phosphate buffer, pH= 7.2 were placed on the solidified agar gel surface at different areas near the intended bacterial inoculation droplet. The distances were not measured. The protein droplets on the gel were air dried in the hood for ~15 minutes. Bacterial culture (3 µL) at OD₆₀₀~ 0.6 was inoculated in the middle of the agar gel. The inoculated agar plates were incubated at 37°C for 12 hours, and then incubated for additional 12 hours at room temperature. Pictures of the swarming plates were taken at desired time points

during this 12 hours and 12 hours incubation. For each set of experiments, freshly prepared agar plates were used within the same day.

3.4.6 Separation of Rhamnolipids

The mono- and di-rhamnolipids mixture (90% pure) was obtained from AGAE Technologies. Isolation and purification of monorhamnolipid and dirhamnolipid was performed by column chromatography using DCM:MeOH:H₂O (87.5:10:2.5) as the eluent. The crude extract was dissolved in minimal eluent and loaded onto a wet-packed silica gel 60 (40–63 μm mesh, from SiliaFlash®) column. The eluent was kept under stirring conditions and added onto column in aliquots to prevent separation of solvent layers. Separation of the mono- and di-rhamnolipid was confirmed by thin-layer-chromatography (TLC Silica gel 60 F254) developed with DCM:MeOH (4:1) with *rf* values 0.58 and 0.30, respectively. TLCs were visualised using a p-anisaldehyde (PAA) stain (3% PAA in acidified absolute ethanol). The separation of rhamnolipids and collection of ¹H NMR spectra were done by Felicia Burns, Luk lab member.

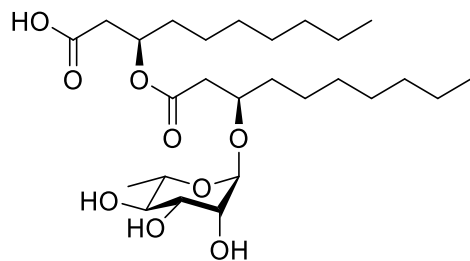
¹H NMR Spectra of monorhamnolipid*



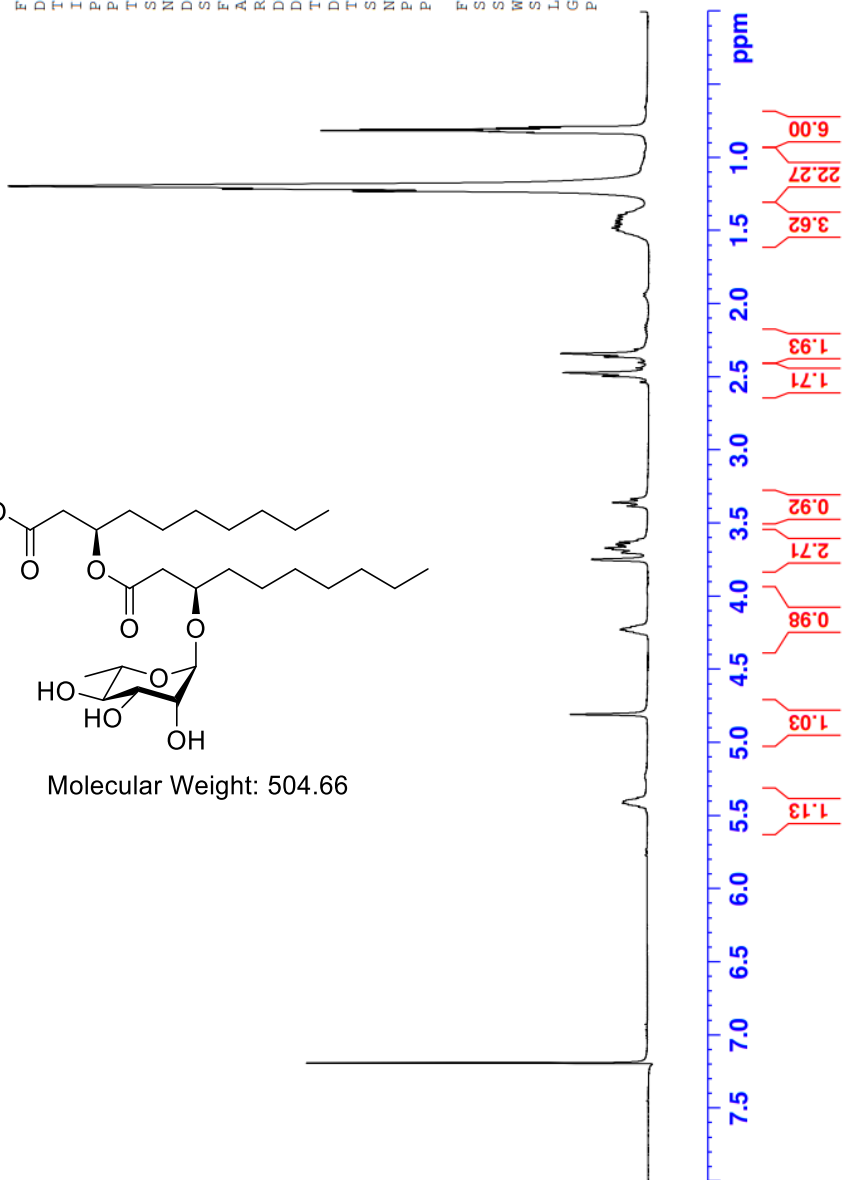
Current Data Parameters
NAME Rhamnolipids
EXPNO 1
PROCNO 1

F2 - Acquisition Parameters
Date_ 20190210
Time_ 11.56 h
INSTRUM spect
PROBHD zg30
PULPROG zg30
TD 65536
SOLVENT CDCl3
NS 16
DS 2
SWH 8012.820 Hz
FIDRES 0.244532 Hz
AQ 4.0894465 sec
RG 74.16
DW 62.400 usec
DE 6.50 usec
TE 298.0 K
D1 1.0000000 sec
TD0 1
SFO1 400.1324708 MHz
NUC1 1H
P1 10.00 usec
PLW1 16.20000076 W

F2 - Processing parameters
SI 65536
SF 400.1300369 MHz
WDW EM
SSB 0
LB 0.30 Hz
GB 0
PC 1.00



Molecular Weight: 504.66



LIMS Container ID 1-25

*This spectrum was taken by Felicia Burns.

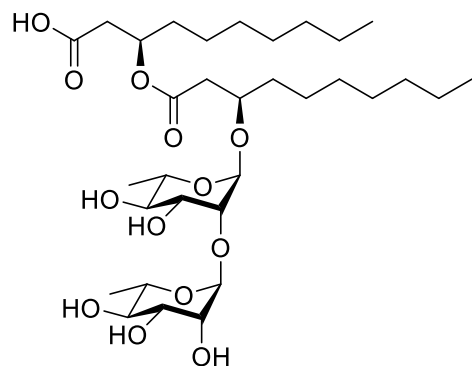
¹H NMR Spectra of dirhamnolipid*



Current Data Parameters
 NAME Rhamnolipids
 EXPNO 2
 PROCNO 1

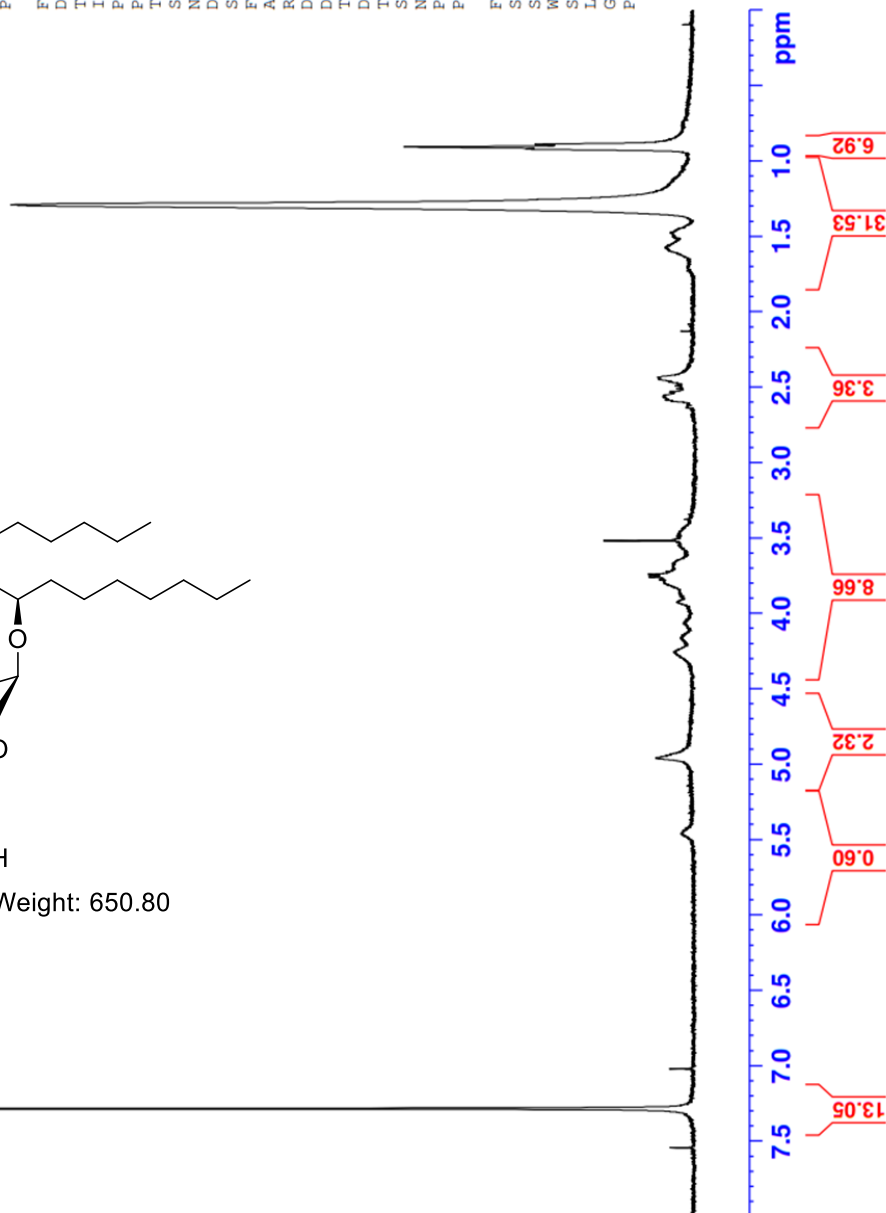
F2 - Acquisition Parameters
 Date_ 20190210
 Time 12.03 h
 INSTRUM spect
 PROBHD Z116098_0203 (z930)
 FULPROG zg30
 TD 65536
 SOLVENT CDCl3
 NS 16
 DS 2
 SWH 8012.820 Hz
 FIDRES 0.244532 Hz
 AQ 4.0894465 sec
 RG 183
 DW 62.400 usec
 DE 6.50 usec
 TE 298.0 K
 D1 1.00000000 sec
 TD0 1
 SFO1 400.1324708 MHz
 NUC1 1H
 P1 10.00 usec
 PLW1 16.20000076 W

F2 - Processing parameters
 SI 65536
 SF 400.1300000 MHz
 WDW EM
 SSB 0
 LB 0.30 Hz
 GB 0
 PC 1.00



Molecular Weight: 650.80

LIMS Container ID 1-74



*This spectrum was taken by Felicia Burns.

Chapter 4. Rhamnolipids and Synthetic Disaccharides Induce Structural Changes in Pilin Upon Ligand-Binding Characterized by Circular Dichroism, Nuclear Magnetic Resonance and Dynamic Light Scattering

4.1 Background and Significance

4.1.1 Tools to characterize protein structures and their interactions with ligands.

A variety of tools are available for structural characterization and ligand-binding of proteins. Different proteins have distinct amino acid sequences that drive the protein's intramolecular and intermolecular interactions to further fold into their native structures. There are four levels by which proteins structures are characterized. The primary structure of a protein is its amino acid sequence. The amino acids are covalently linked, forming the peptide bond between the carbonyl carbon of one amino acid and the nitrogen of another amino acid. Based on Anfinsen's "thermodynamic hypothesis", the amino acid sequence plays an important role in proteins folding into their native conformation to achieve the lowest free energy.¹⁰⁹ The amino acids can further form hydrogen bonds with each other that results in local structures, also known as the secondary structure of the protein. The common secondary structures of proteins are α -helices, β -sheets and random coils, a third classification for structures that are neither helices nor sheets. The tertiary structure is the three-dimensional shape or the native conformation of the protein as the secondary structures and their amino acid side chains form stabilizing salt bridges, hydrogen bonding, disulfide bonds and hydrophobic interactions. The tertiary structure a protein adopts is the most stable or has the lowest free energy system.¹⁰⁹ Lastly, proteins form quaternary structures form when they are comprised of different subunits that associate to form multi-subunit complexes. Furthermore, it is imperative to understand the dynamics of proteins and their structure to also be able to understand the biological activities of these macromolecules.

4.1.1.1 Circular Dichroism gives an insight on the secondary structure of proteins.

Circular dichroism (CD) spectroscopy is commonly used to identify the secondary structure of proteins. Chiral molecules, such as proteins, absorb left- and right- circularly polarized light and the sum of the absorbances from each component results in the peaks of the CD spectrum.^{110, 111} Each secondary protein structures results in a distinct spectrum (Fig. 4.1), providing its value when structurally characterizing recombinant proteins. Absorption in the far-UV region (< 240 nm) primarily arises from two electronic transitions by the peptide bond. The $n \rightarrow \pi^*$ transition results in the signal at 210-220 nm, and the $\pi \rightarrow \pi^*$ transition results in the signals below 210 nm, and absorption signals are unique for each type of protein secondary structure.¹¹⁰ Additionally, CD spectroscopy can also be used for detecting changes in the protein secondary structure resulting from ligand-binding, protein aggregation or denaturation.¹¹⁰⁻¹¹⁵ The addition of small molecules can induce changes the protein secondary and/or tertiary structure or a change in the intensity of the CD signal.^{110, 111} Typically, achiral ligands are used when studying ligand-binding to proteins to avoid any signal interference from the ligand on the CD spectrum. This method provides a rapid way of detecting the secondary structure of proteins; however, CD spectroscopy needs to be coupled with other biophysical methods such as NMR or X-ray crystallography to provide a more detailed structural information of the proteins.

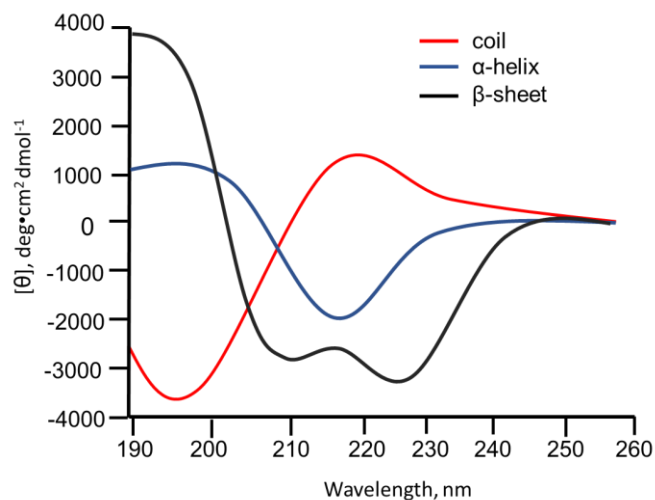


Figure 4.1 Circular dichroism spectra of secondary structures of proteins.

4.1.1.2 Nuclear Magnetic Resonance (NMR) is used to study protein structure and ligand binding.

Nuclear magnetic resonance (NMR) spectroscopy is a widely used tool for the structural characterization of proteins. Different parameters when running NMR spectroscopy can be used to provide a wide variety of information. Generally, a 1D ^1H NMR can be used for preliminary structural evaluation of the protein folding. Typically, a properly folded protein contains a dispersed spectra indicative of the protons exposed to different microenvironments.

Alternatively, two-dimensional (2D) NMR techniques are also of value to efficiently study both scalar coupling and dipole-dipole coupling of macromolecules such as proteins. Nuclear Overhauser Effect (NOE) spectroscopy detects interactions between protons within a 5\AA distance.^{116, 117} Heteronuclear Single Quantum Coherence (HSQC) spectroscopy is a 2D NMR technique that measures the coupling between two connected nuclei such as the hydrogen and the nitrogen or carbon atoms in the protein. HSQC is commonly done on proteins isotopically

labeled during bacterial expression with ^{13}C and/or ^{15}N . The HSQC method will provide a more delineated way of studying proteins by NMR since it reduced the spectral overlap by looking at ^1H alone and providing information of the protein backbone and side chain interactions.¹¹⁶ NMR can be used to determine amino acid residues corresponding to the NMR peaks in the spectra. Furthermore, not only is NMR valued for structural characterization, but also for studying protein-ligand interactions. Monitoring the changes in the chemical shifts in the absence and the presence of ligands can often indicate ligand-binding. NMR is a robust way of doing this study as it is less prone to artifacts. However, this method also has some limitations. NMR is suitable for smaller proteins < 30 kDa.¹¹⁸ The diffusion or tumbling rate of proteins need to be controlled so viscosity of solutions needs to be controlled to ensure that the relaxation time of the proteins give peaks that are measurable. Another interference to the studies of proteins by NMR is the formation of higher-order oligomers in solution. Provided that the right conditions are used for the NMR, this technique will provide meaningful information about the protein and its interactions with ligands.

4.1.1.3 Dynamic Light Scattering (DLS) measures sizes of proteins.

Dynamic light scattering (DLS) is a useful method to study of submicron particles suspended in liquids. Particles in solution exhibit Brownian motion as they collide with the solvent molecules. The resulting random movement of the particles can scatter light when monochromatic light is passed through the solution.^{119, 120} DLS correlates the measured light scattering to provide information such as the diffusion coefficient, hydrodynamic radii and homogeneity of the sample.. The relationship of the light scattering and the size is defined by the Stokes-Einstein equation (Eq. 4.1) where D_T is the diffusion coefficient, k_B is the Boltzmann

constant ($1.380 \times 10^{-23} \text{ kg m}^2 \text{ s}^{-2} \text{ K}^{-1}$), T is the absolute temperature, η is the viscosity of the medium. R_h is the hydrodynamic radius which is the radius of a spherical particle that is assumed to move at the same velocity as the particle. From the experiment, it would be seen that the movement of particles in a solution is affected by factors such as temperature, viscosity of the solution and the size of the particles. DLS can measure particles in the range of 0.3 nm – 100 μm of aggregates in the solution (Malvern Instruments). This method is useful to determine the hydrodynamic radius to estimate the size of proteins in solution.

$$D_T = \frac{k_B T}{6\pi\eta R_h}$$

Equation 4.1. Stokes-Einstein equation

4.1.2 Ligand binding between pilin protein and rhamnolipids and SF-disaccharides

Based on past studies by Luk group, a bulky aliphatic chain of disaccharide derivatives, like SF β M and SF β C, are more potent than rhamnolipids in controlling the swarming motility of *P. aeruginosa*.²³ These molecules, for rhamnolipids and SF β M at least, control swarming motility through binding to pilin of *P. aeruginosa*. Pilin extend and retract upon contact with chemicals or external stimuli, that elicits a biological response. To cause swarming inhibition and activation, these molecules most likely induce a conformational change on the pilin protein that mediates signal transduction from the pili tip, throughout the pili assembly, and into the bacterium. The expressed and isolated pilin proteins from PA1244N3(pPAC46) is active for controlling swarming motility, but it is not clear if its conformation is the same as that in the assembled state on the bacterial surface. Furthermore, the truncated pilin, pilin $\Delta(1-31)$ is also

active for swarming but we do not know the structural details of this protein. Gaining insight on the structure and ligand-induced structural changes for these proteins can help in understanding how rhamnolipids and disaccharide derivatives elicit a biological response upon binding.

4.1.3 Chapter aim: To characterize the secondary structure of recombinant truncated pilin proteins and effects of interactions with small molecules on the pilin structure.

In this chapter, we aim to structurally characterize the expressed pilin $\Delta(1-31)$ protein by different biophysical techniques. Prompted by previous results that rhamnolipids and SF-disaccharide analogs control swarming, we determine the binding between pilin and these small molecules at a molecular level. The bioactive truncated pilin, pilin $\Delta(1-31)$ was used as the model pilin protein to identify ligands of the pilin protein. Circular dichroism was used to determine the secondary structure of the expressed pilin $\Delta(1-31)$ pilin and how it compared to the native, full-length pilin protein. Nuclear magnetic resonance was also used to determine the folding and structure of native pilin. We used all three techniques, circular dichroism, nuclear magnetic resonance, and dynamic light scattering to identify and understand binding between pilin $\Delta(1-31)$ and candidate ligand molecules.

4.2 Results and discussion

4.2.1 The secondary structure of truncated pilin $\Delta(1-31)$ is mainly comprised of coiled structures and β -sheets.

The CD spectra of 25 μ M native, full-length pilin from *Pseudomonas aeruginosa* PA1244N3(pPAC46) and pilin $\Delta(1-31)$ expressed in *E. coli* BL21(DE3) were measured and reported as mean residue ellipticity peaks (MRE) (Fig. 4.2, 4.3). The native pilin showed two

negative peaks at ~208 nm and 220 nm, and a positive peak at ~195 nm, consistent with a protein primarily comprised of an α -helix structure (Fig. 4.2). The resulting spectra of native pilin is consistent with both the PAK and PAO1 pilin proteins for which the native structure is a mixture of α -helix and a β -sheet despite the CD showing a predominantly α -helix signal.¹²¹ The CD spectra from both strains show roughly an α -helical structure, but calculations on the CD signals revealed a secondary structure of a mixture of 47% α -helix and 42% β -sheet.¹²¹ Analysis of circular dichroism signals of proteins containing a mixture of α -helices, β -sheets, such as the pilin proteins, can be tricky. Generally, α -helices have regular structures that give well-defined CD peaks. In contrast, β - sheets are more structurally variable with the possibility of parallel, anti-parallel or turn orientations that result in different and even weak CD peaks.^{122, 123}

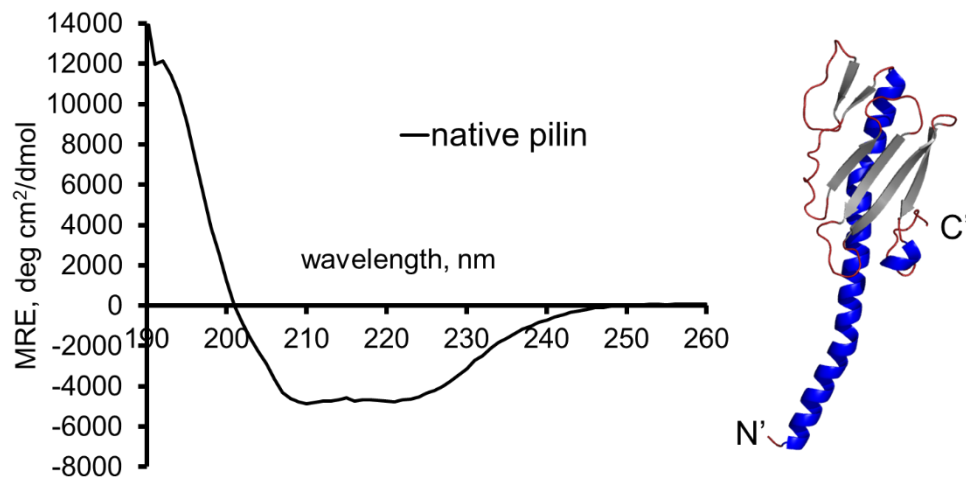


Figure 4.2 Circular dichroism spectrum of 25 μ M native 1244 pilin expressed in *P. aeruginosa* (left). Model of the native pilin generated by Phyre2 (right). Protein was prepared in 4 mM sodium phosphate buffer, pH= 7.2.

The spectrum of the pilin $\Delta(1-31)$ expressed in *E. coli* showed two negative peaks at 202 nm and 218 nm (Fig. 4.3). The negative peak at 202 nm corresponds to the signal for a random coil protein. However, we did not observe a positive peak at ~ 217 nm that is also observed for random coils. Instead, we observed a negative peak at ~ 218 nm that is characteristic of a β -sheet (Figure 4.3).^{111, 112} Interestingly, there is a large change in the CD spectrum of the pilin $\Delta(1-31)$ from the full-length, native pilin. By removing the first 31 amino acids (excluding the leader peptide) that form the α -helix of the native pilin, the CD spectrum of the truncated pilin reveals the remaining structures of the C'-terminal globular domain, which are mainly comprised of β -sheets and coiled structures. This secondary structure of a mixture of coiled structures and β -sheet is consistent with the reported structures of other truncated pilin.^{77, 81, 84} We therefore conclude that removing a part of the N-terminal α -helix of the native pilin retains most of the C'-terminal globular domain of the native pilin.

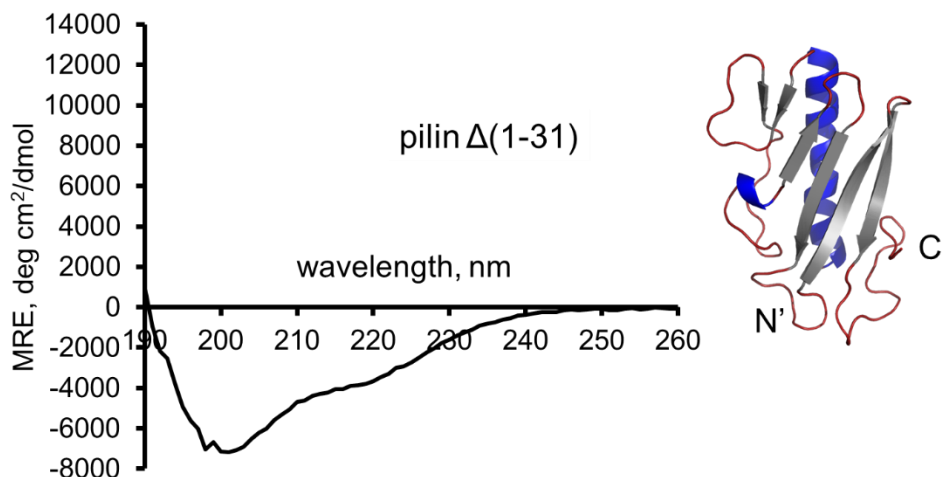


Figure 4.3 Circular dichroism spectrum of 25 μ M pilin $\Delta(1-31)$ heterologously expressed in *E. coli* (left). Model of the native pilin generated by Phyre2 (right). Protein was prepared in 2 mM Tris and 7 mM NaCl, pH= 7.5.

Next, the effect of the single amino acid mutations on the secondary structure of pilin $\Delta(1-31)$ (Fig. 4.4) was checked. CD measurements were done on 25 μM pilin $\Delta(1-31)$, pilin $\Delta(1-31)$ W105K, pilin $\Delta(1-31)$ I98D and 20 μM pilin $\Delta(1-31)$ P111G. Comparing the CD with the unmutated pilin $\Delta(1-31)$, we observe that only W105K has a similar secondary structure with negative peaks at 202 nm and 218 nm. The P111G mutant still has the negative peak at 202 nm and with a reduced signal at 218 nm. The I98D has an intense negative peak at 198 nm and a reduced 218 nm peak suggesting that I98D is predominantly a random coil with a minimal β -sheet character.¹¹⁰ While the spectra shows that the single amino acid mutants signals that are generally considered as coiled structures, we can see that the peaks, especially for ~ 220 nm have different intensities. These results show that changing a single amino acid in the pilin $\Delta(1-31)$ can induce minor changes in the protein that is enough to render the single amino acid mutants inactive for binding to rhamnolipids.

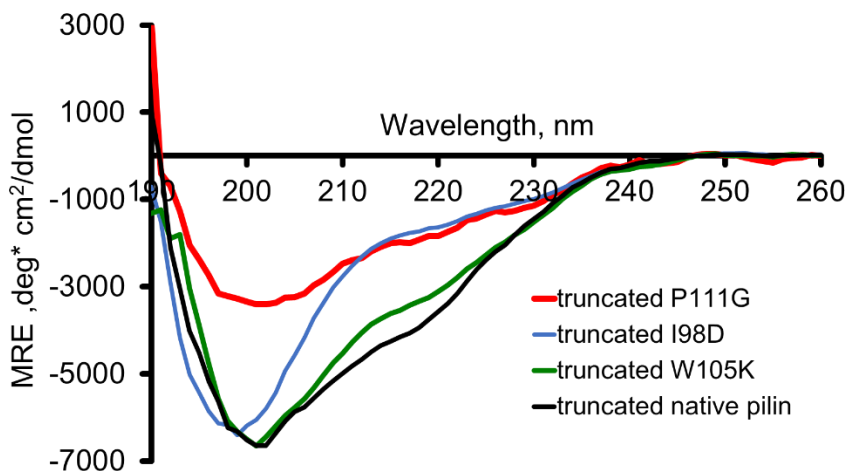


Figure 4.4 Circular dichroism (CD) spectra of 25 μM pilin $\Delta(1-31)$ (black) and single amino acid mutants: 25 μM pilin $\Delta(1-31)$ W105K (green), 25 μM pilin $\Delta(1-31)$ I98D (blue), and 20 μM pilin $\Delta(1-31)$ P111G (red). Proteins were prepared to a final volume of 300 μL in 2 mM Tris and 7 mM NaCl, pH= 7.5.

4.2.2 *Rhamnolipids and synthetic disaccharides induces a change in the secondary structure of pilin $\Delta(1-31)$.*

The binding of pilin $\Delta(1-31)$ to rhamnolipids was determined using CD spectroscopy. First, 200 μM rhamnolipids mixture (3:1 dirhamnolipid: monorhamnolipid) was mixed with 22 μM pilin $\Delta(1-31)$ and allowed to incubate overnight at ambient temperature. The changes in the CD spectrum of pilin $\Delta(1-31)$ before and after adding rhamnolipids were observed. After adding rhamnolipids to pilin $\Delta(1-31)$, the CD spectrum of pilin shows a negative peak at ~ 218 nm, and the disappearance of the signal at ~ 202 nm, indicative of rhamnolipids induced a change in the secondary structure from a coiled structure/ β -sheet to a β -sheet (Fig. 4.1, 4.5) This change in the secondary structure could be indicative of binding between pilin and rhamnolipids (Fig. 4.5).

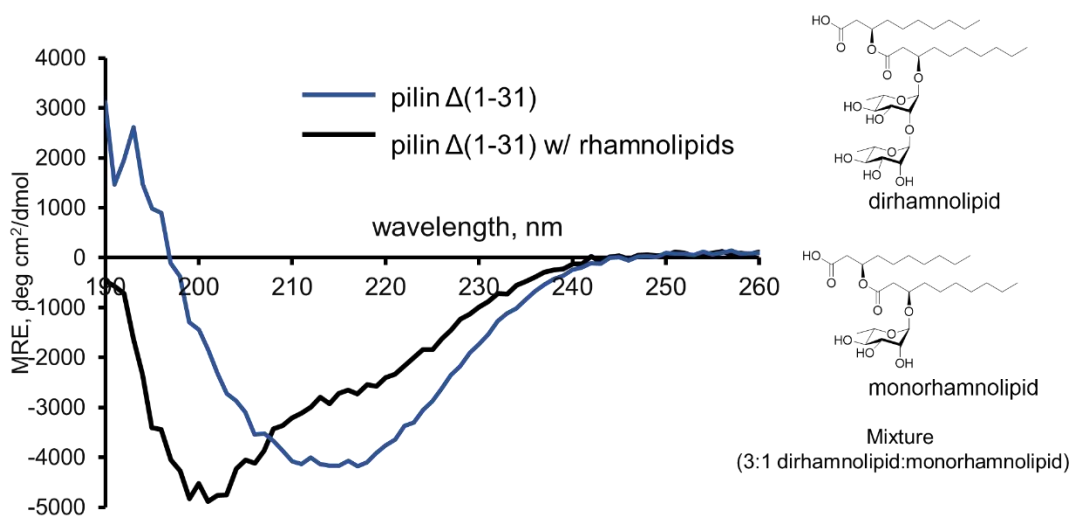


Figure 4.5 CD spectra of 22 μM pilin $\Delta(1-31)$ only (blue) and with 200 μM rhamnolipids mixture (black). Both proteins and ligands are dissolved in 2 mM Tris and 7 mM NaCl, pH= 7.5.

Next, we titrated 25 μM of pilin $\Delta(1-31)$ with increasing amounts of rhamnolipids to a final concentration of 200 μM . When 0-50 μM rhamnolipids are added to pilin $\Delta(1-31)$, we observe signals appearing at 202 nm and 218 nm, and the signal intensity decreases as the concentration of rhamnolipids is increased. When the rhamnolipids concentration is increased to 100 until 200 μM rhamnolipids, the CD spectra changes and one negative signal at 218 nm appears. Based on these results, 100 μM of rhamnolipids changes the secondary structure of pilin $\Delta(1-31)$ from the coiled/ β -sheet to a β -sheet (Fig. 4.6). The change in the secondary structure, together with the decrease in signals observed as the concentration increases, our findings indicate that rhamnolipids bind to pilin $\Delta(1-31)$.

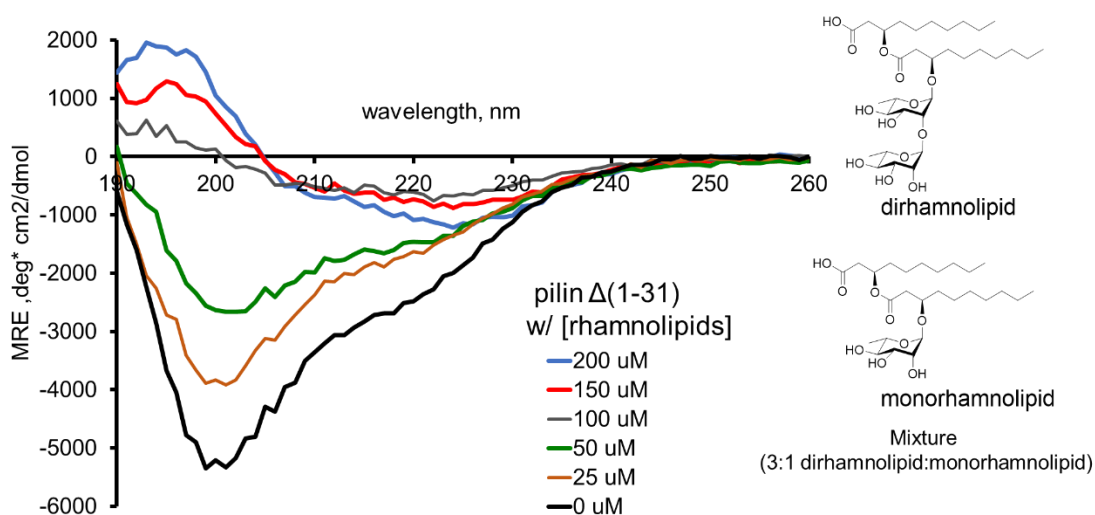


Figure 4.6 CD spectra of 25 μM pilin $\Delta(1-31)$ with increasing amounts of rhamnolipids mixture. Both proteins and ligands are dissolved in 2 mM Tris and 7 mM NaCl, pH= 7.5.

The individual rhamnolipids components, monorhamnolipid and dirhamnolipid, were then tested for binding to pilin $\Delta(1-31)$ (Fig. 4.7). Monorhamnolipid, from 0-100 μM , added to the pilin $\Delta(1-31)$, two negative peaks at 202 nm and 218 nm are observed. When the concentration of monorhamnolipid is increased to 150 – 200 μM , the two negative peaks at 202 nm and 218 nm disappear and a negative peak appears around ~210 nm to 220 nm. Whereas when dirhamnolipid is added, we only observe the CD spectra to have the two negative peaks at 202 nm and 218 nm at all concentrations added. The results demonstrate that monorhamnolipid and dirhamnolipid when mixed with pilin $\Delta(1-31)$ have different effects on the protein. Monorhamnolipid inducing a change in the structure from a random coil to a β -sheet, whereas dirhamnolipid retains the coiled structure and only decreases the intensity of the signal. This result is consistent with previous swarming results that monorhamnolipid is more active at controlling swarming motility than dirhamnolipid.

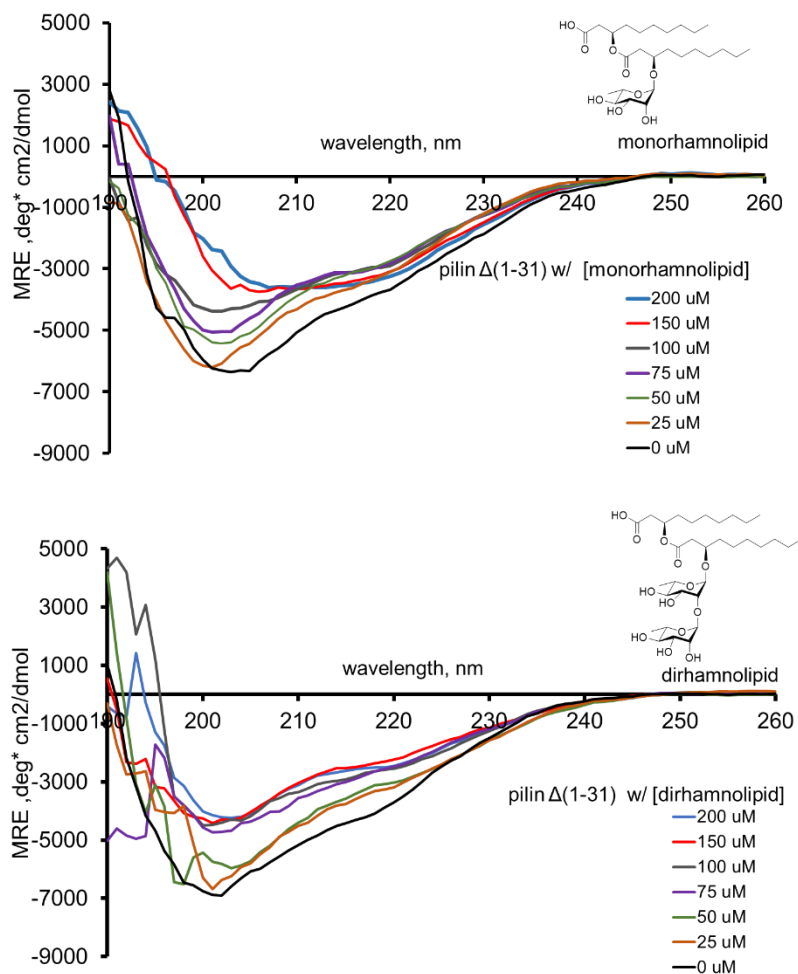


Figure 4.7 CD spectra of 30 μM pilin $\Delta(1-31)$ with increasing amounts of monorhamnolipid (top) and dirhamnolipid (bottom). Both proteins and ligands are dissolved in 2 mM Tris and 7 mM NaCl, pH= 7.5.

We then study binding of rhamnolipids and SF β M to pilin $\Delta(1-31)$. First, rhamnolipids and SF β M to pilin $\Delta(1-31)$ (10:1 ligand: protein) were tested separately. The addition of rhamnolipids to pilin $\Delta(1-31)$ induced a change to the secondary structure of pilin $\Delta(1-31)$ from a coiled structure/ β -sheet to a β -sheet conformation. However, adding SF β M did not change the secondary structure of the pilin $\Delta(1-31)$, with the negative signals appearing at ~ 200 nm and

~220 nm. Next a competitive binding assay was performed by adding the two ligands at the same time to the pilin $\Delta(1-31)$. The CD signal resulted in a curve that is consistent with the pilin $\Delta(1-31)$ binding to SF β M. (Fig. 4.8) Adding the two individual ligands separately resulted in two different CD signals, we believe that binding of pilin $\Delta(1-31)$ to rhamnolipids or SF β M, causes two possible conformations of the protein. Furthermore, the competitive binding assay resulted in a CD signal wherein pilin $\Delta(1-31)$ exists in a conformation bound to SF β M. These results suggest that SF β M may exhibit a higher affinity for binding to pilin than rhamnolipids. These results are consistent with previous findings by Luk lab^{23, 75} where the swarming motility and the binding assays suggest that SF β M binds stronger to pilin than rhamnolipids.

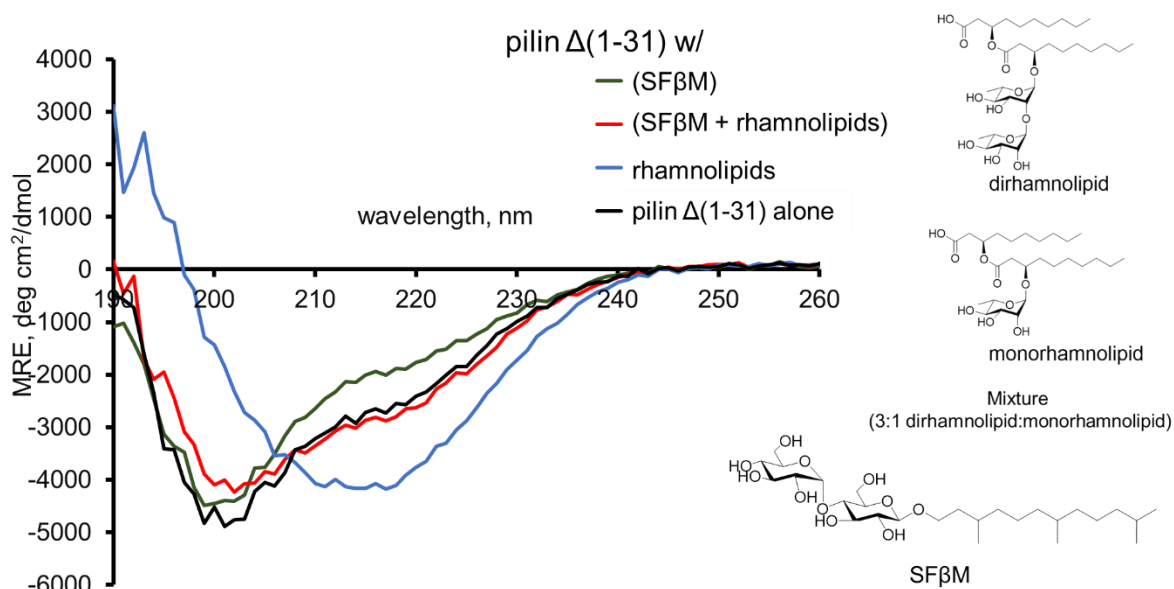


Figure 4.8 CD spectra of 22 μ M pilin $\Delta(1-31)$ with 220 μ M rhamnolipids (blue), SF β M (green), (SF β M & rhamnolipids) (competitive assay) (red). Spectrum of pilin $\Delta(1-31)$ only (black).

Proteins and ligands were dissolved in 2 mM Tris and 7 mM NaCl, pH= 7.5.

Furthermore, we also looked at the native pilin with rhamnolipids and SF β M (Fig. 4.9). In the presence of the ligands, the intensity of the peaks at ~208 nm and ~222 nm change but the secondary structure remains as an α -helix. Because the native pilin retains its assembly structure, the CD signal could arise because of the exposed α -helices from the protein assembly even if there is binding at the C'-terminus, the change could be so small that it could not be detected by CD. By CD, it would be quite challenging to determine binding of the native pilin with rhamnolipids and SF β M because of the lack of changes on the protein structure observed.

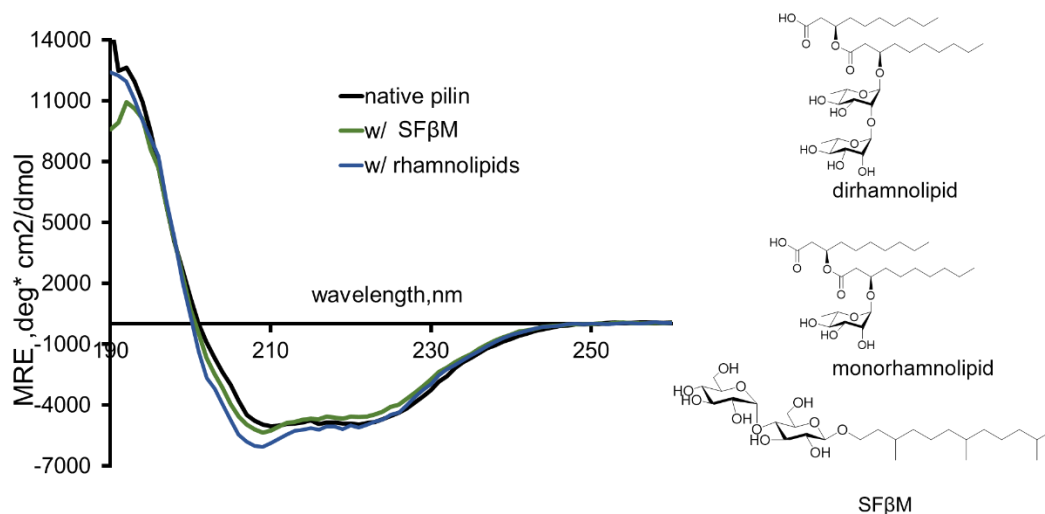


Figure 4.9 CD spectra of 25 μ M native 1244 pilin without (black) and with 250 μ M rhamnolipids (blue), SF β M (green), (SF β M & rhamnolipids) (competitive assay) (red). Spectrum of pilin Δ (1-31) only (black). Proteins and ligands were dissolved in 4 mM sodium phosphate buffer, pH= 7.2.

4.2.3 *¹H NMR of spectrum of native pilin from P. aeruginosa 1244N3 (pPAC46) shows interference of polyethylene glycol 8000 and protein assembly formation.*

Due to the purification process of the native pilin, the final solution of the pilin protein contains polyethylene glycol (PEG) -8000. Therefore, the ¹H NMR of native pilin is dominated by the PEG-8000 signal at approximately 3.7 ppm (Fig. 4.10). Looking into ¹H NMR spectrum, the PEG-8000 peak at ~3.7 ppm interferes in the region where the alpha and aliphatic protons of the protein appear (~3-5 ppm). Furthermore, most of the proton peaks appear to be broadened and not well dispersed due to fact that the pili purified from *P. aeruginosa* are in assembly form and the presence of PEG-8000 increase the viscosity of the solution. In order to dissociate the pili into the monomeric form, it would require the used either strong denaturants such as SDS or high concentrations of octyl-glucoside,¹²¹ which would further complicate the pilin spectra. Also, it has been reported that even when the detergents are removed, the pilin has been found to self-associate.¹²¹

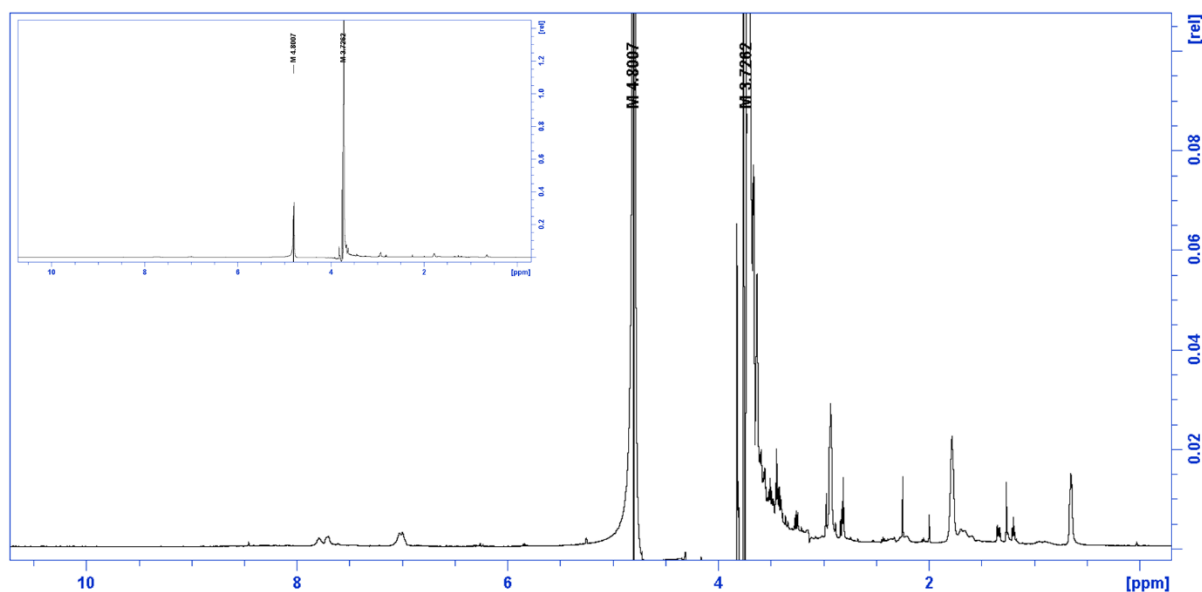


Figure 4.10 ^1H NMR of native 1244 pilin expressed from *P. aeruginosa* PA1244N3(pPAC46). Original spectra (inset). Protein was prepared in 90%/10% $\text{H}_2\text{O}/\text{D}_2\text{O}$ containing 50 mM sodium phosphate buffer, 2.6 mM NaN_3 and 2.6 mM DSS, pH=5.55. The spectrum was taken on a 800 MHz Bruker NMR by Deborah Kerwood (Syracuse University).

4.2.4 Ligand-binding studies by ^{15}N HSQC show additional peaks after adding ligands to pilin $\Delta(1-31)$.

The ^{15}N -labelled native pilin was expressed from *P. aeruginosa* strain 1244N3(pPAC46) for structural studies and investigate ligand binding (Fig. 4.11). Initial HSQC studies of the full pilin spectrum shows peaks mainly in the 8.0 -8.5 ppm which initially would indicate a protein in a random coil. However, in this case, since the CD spectra shows that the pilin has an α -helix secondary structure, the results would suggest that the pilin in solution are mainly in assembly form (Fig. 4.11). In addition, the purification method of the full pilin is the same as the unlabeled full pilin and using PEG-8000 to precipitate the final protein causes the solution to have a high

viscosity. The viscosity of the solution could possibly influence the HSQC by decreasing the molecular mobility of the protein thus resulting in a spectrum that shows a coiled protein structure.^{124, 125} We therefore diluted the sample to decrease the viscosity as well as the potential assembly formation of the pilin in solution. We diluted from 350 μM to 120 μM of pilin for the HSQC experiment. While the spectra show that diluting the protein causes additional peaks to show, the pilin remains in the assembly form as seen by the peaks within 8.0-8.55 ppm.

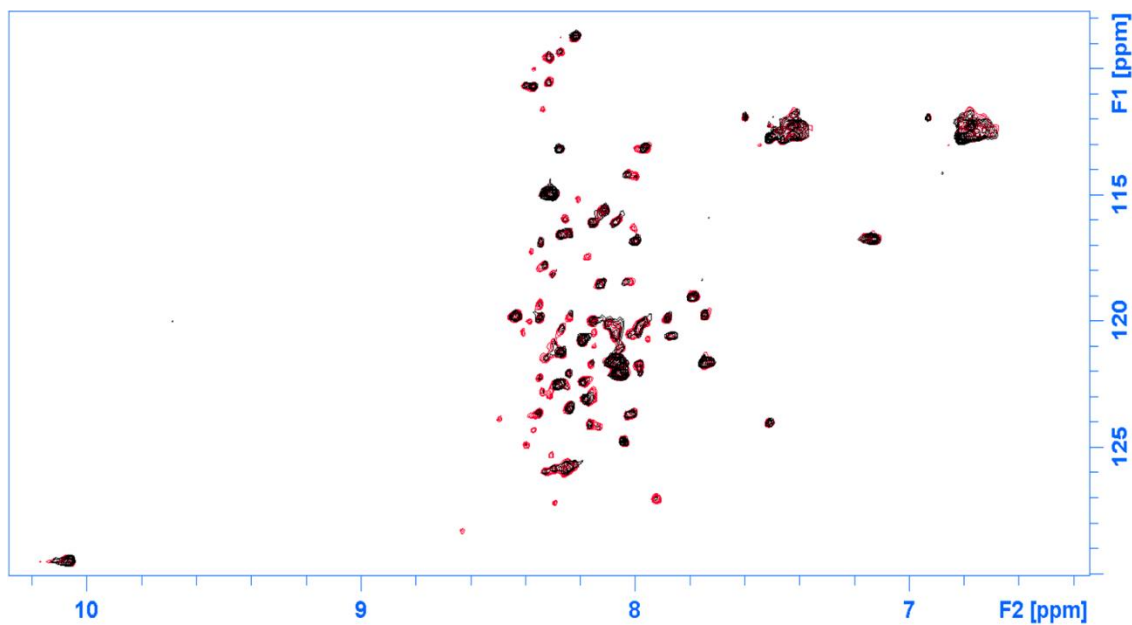


Figure 4.11 ^{15}N HSQC of full pilin from PA1244 overlay spectra. 350 μM native pilin in black, 120 μM native pilin in red. The sample solution was prepared in 90%/10% $\text{H}_2\text{O}/\text{D}_2\text{O}$ containing 50 mM sodium phosphate buffer, 2.6 mM NaN_3 and 2.6 mM DSS, $\text{pH}=5.55$. The spectra were taken on a 800 MHz Bruker NMR by Deborah Kerwood (Syracuse University).

Next, we added the SF-disaccharide, SF βC to the native pilin and performed ^{15}N -HSQC to detect any changes in the protein peaks upon addition of the ligand. Our approach was to add

the SF β C at increasing concentrations one at 50 μ M and then 100 μ M (Fig. 4.12, 4.13). When 50 μ M of SF β C was added, we observe that additional peaks in the spectrum appeared. However, since the peaks are still within the 8-8.5 ppm region, it would be difficult to assign the residues corresponding to the peaks. When the SF β C concentration added to the native pilin was increased to 100 μ M, most of the peaks remain unchanged compared to the 50 μ M SF β C spectrum (Fig. 4.13). These results would indicate that there is binding between native pilin and SF β C, but due to the pilin in the solution mostly in assembly form, the changes might be too subtle for the NMR to detect even when the SF β C is increased.

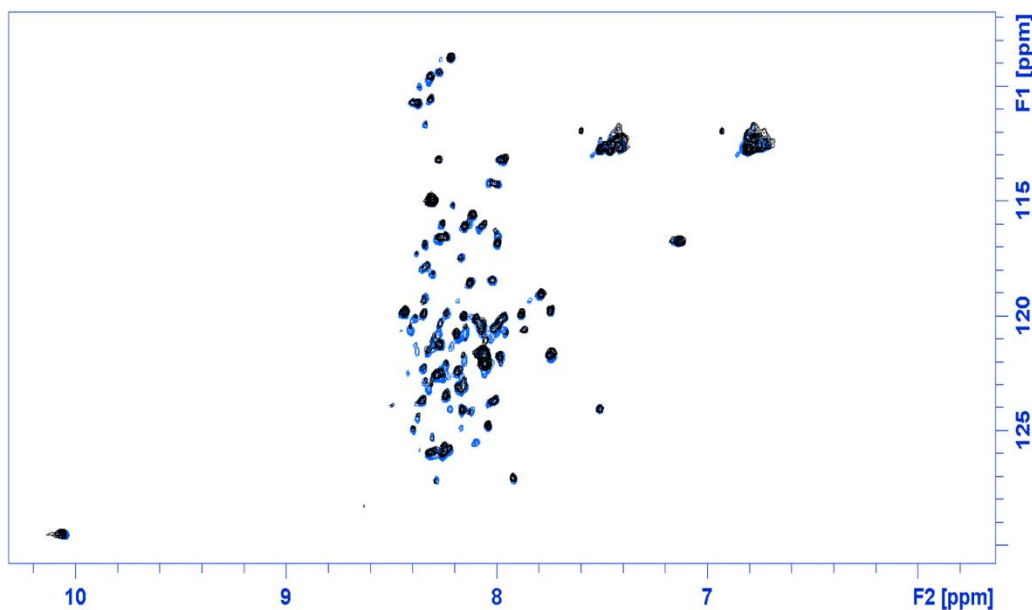


Figure 4.12 15 N HSQC of native pilin from PA1244 overlay spectra. 120 μ M native pilin in black, w/ 50 μ M SF β C in blue. The samples were prepared in 90%/10% H $_2$ O/D $_2$ O containing 50 mM sodium phosphate buffer, 2.6 mM NaN $_3$ and 2.6 mM DSS, pH=5.55. The spectra were taken on a 800 MHz Bruker by Deborah Kerwood (Syracuse University).

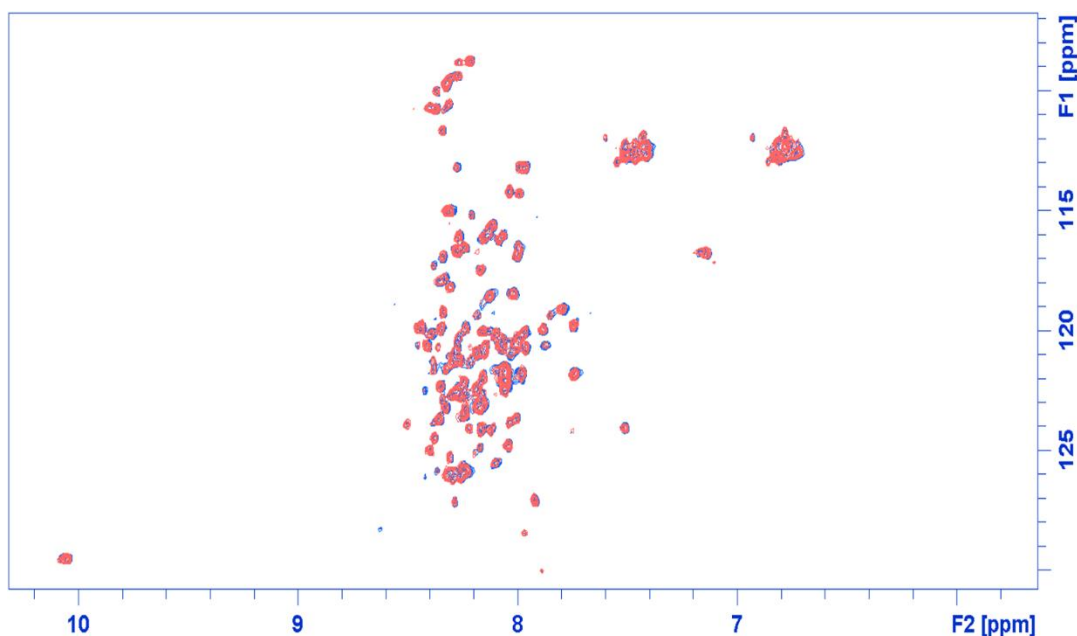


Figure 4.13 ^{15}N HSQC of native pilin from PA1244 overlay spectra with 50 μM SF β C in blue and 120 μM in pink. The samples were prepared in 90%/10% $\text{H}_2\text{O}/\text{D}_2\text{O}$ containing 50 mM sodium phosphate buffer, 2.6 mM NaN_3 and 2.6 mM DSS, pH=5.55. The spectra were taken on a 800 MHz Bruker NMR by Deborah Kerwood (Syracuse University).

4.2.5 Truncated Native Pilin Structure with Coiled and β -sheet Structures.

The truncated pilin, pilin $\Delta(1-31)$, recombinantly expressed in *E. coli* and purified by the Nickel affinity column does not require the use of PEG-8000. No interference of PEG-8000 to the NMR spectrum is expected. Furthermore, since the proteins are expressed in *E. coli*, without the α -helix, the truncated pilin will less likely self-associate and exist as monomers in the solution. The ^1H NMR spectrum of the truncated pilin was taken to determine the folding of the protein (Fig. 4.14). The protein seems to adopt an unfolded conformation, as seen by the spectral overlap of the proton peaks. There is little dispersion in the observed peaks especially along the

side chain to the backbone region (6-10 ppm), where broadened peaks and concentrated peaks around 7.5-8.5 ppm appear. This spectrum indicates that $\Delta(1-31)$ is an unfolded protein with a flexible structure, consistent with the CD results that the protein consists of β -sheets and coiled structures (Fig. 4.3). The presence of coiled structured of the pilin $\Delta(1-31)$ allows for the flexibility of the protein, exposing the amino acids in the same solvent environment, hence, the NMR recognizes an average of the chemical shifts resulting in overlapping of the peaks.¹²⁶

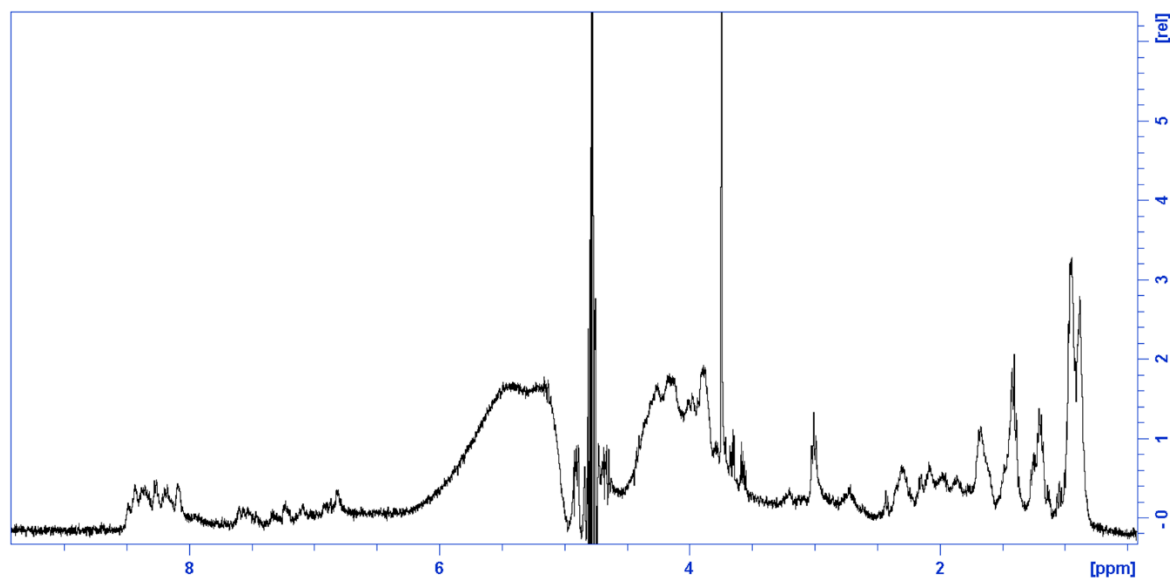


Figure 4.14 ^1H NMR of 120 μM pilin $\Delta(1-31)$. Protein was prepared in 50 mM 90%/10% $\text{H}_2\text{O}/\text{D}_2\text{O}$ containing 50 mM NaPB buffer, pH= 7.5. The spectrum was taken on a 400 MHz Bruker NMR by Deborah Kerwood (Syracuse University).

4.2.6 Ligand-binding studies by ^{15}N HSQC show additional peaks after adding ligands to pilin $\Delta(1-31)$.

^{15}N - HSQC NMR analysis was first performed to detect structural changes caused by ligand-binding to the pilin $\Delta(1-31)$ (Fig. 4.15). The ^{15}N HSQC spectrum is consistent with the ^1H NMR having a flexible structure with most peaks appearing within 8 – 8.5 ppm (Fig. 4.14).

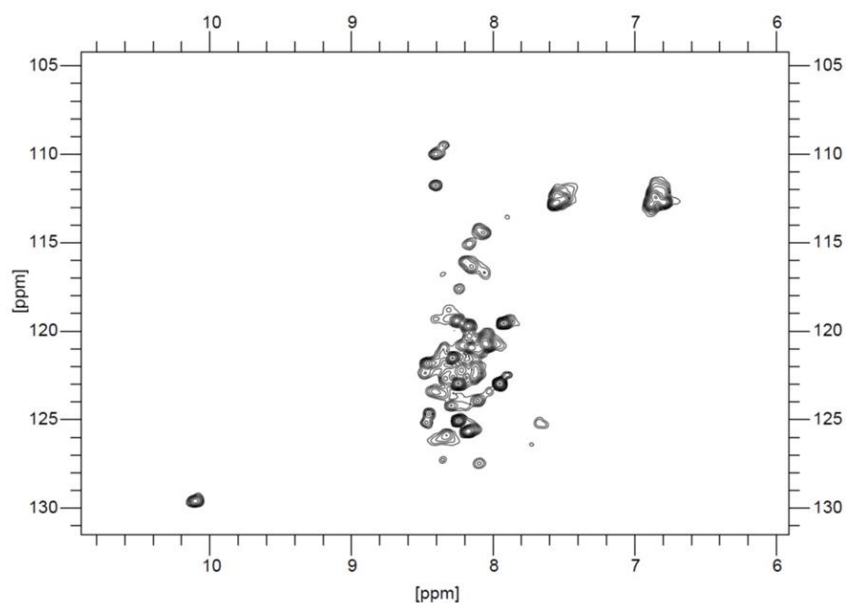


Figure 4.15 ^{15}N - Heteronuclear quantum coherence (HSQC) NMR spectra of pilin $\Delta(1-31)$. Proteins were prepared in 90%/10% $\text{H}_2\text{O}/\text{D}_2\text{O}$, 25 mM Tris, 100 NaCl, 2.6 mM NaN_3 and 2.6 mM DSS, pH=7.5. The spectrum was taken on a 400 MHz Bruker NMR.

Next, 2 mM SF β M and rhamnolipids were then added to 220 μM pilin $\Delta(1-31)$ and the HSQC spectra was taken. For both cases, adding the ligands resulted in additional peaks in the spectra, indicative of changes in the protein upon ligand-binding. The additional peaks are less for SF β M compared to rhamnolipids. (Fig. 4.16). We anticipate that rhamnolipids will induce a

more structured pilin $\Delta(1-31)$ conformation, as previously seen in the CD spectra where the coiled structure/ β -sheet to a β -sheet conformation at the same ligand: protein ratio. (Fig. 4.6)

Although most of the structure exhibits a coiled structure, the fact that additional peaks appeared in the spectra suggest that ligands induced a change in the pilin $\Delta(1-31)$, which could possibly be a result of binding of the ligand to the protein.

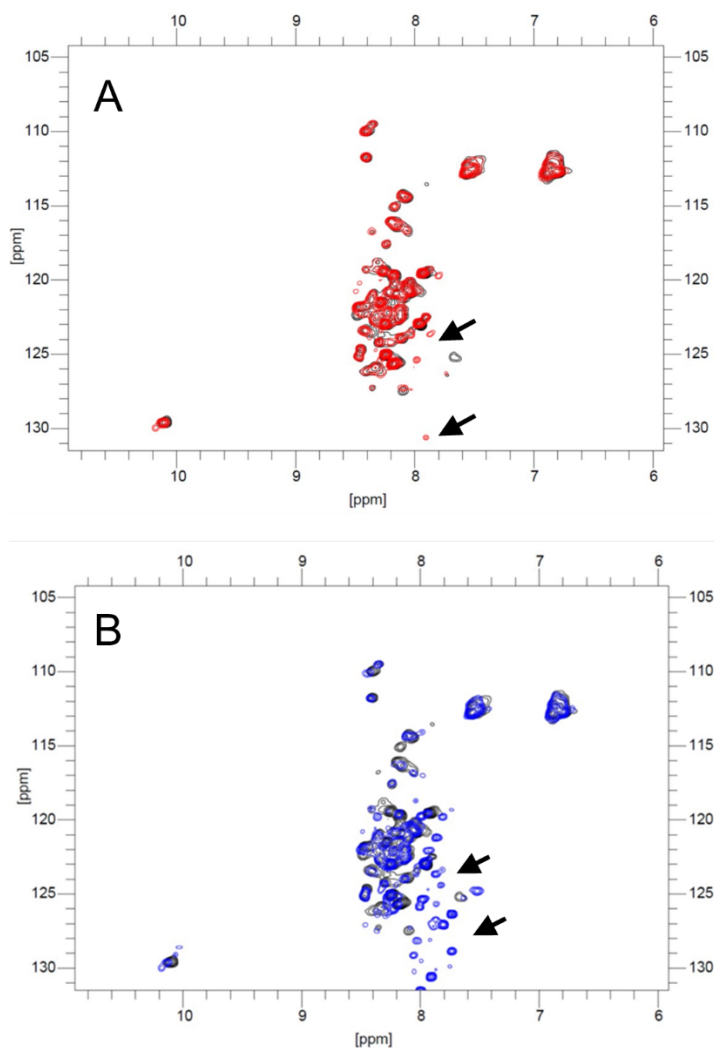


Figure 4.16 ^{15}N - Heteronuclear quantum coherence (HSQC) NMR spectra of pilin $\Delta(1-31)$ with ligands added (A) SF β M overlay spectra: pilin $\Delta(1-31)$ control (black), pilin $\Delta(1-31)$ + SF β M (red), (B) rhamnolipids overlay spectra. pilin $\Delta(1-31)$ control (black), pilin $\Delta(1-31)$ +

rhamnolipids (blue). Proteins were prepared in 90%/10% H₂O/D₂O, 25 mM Tris, 100 NaCl, 2.6 mM NaN₃ and 2.6 mM DSS, pH=7.5. The spectra were taken on a 400 MHz Bruker NMR.

4.2.7 Dynamic light scattering shows an increase in particle size upon addition of ligands.

The dynamic light scattering of 25 μ M pilin $\Delta(1-31)$ was measured before and after adding ligands (Fig. 4.17). For the solution containing 25 μ M pilin $\Delta(1-31)$ alone, aggregates with particle sizes 4.187, 4.849 and 15.69 nm were detected. For solutions of pilin $\Delta(1-31)$ with 200 μ M rhamnolipids, aggregates with particle sizes 50.75 and 37.84 nm are observed and for solutions where SF β M is added, aggregates with particle sizes 91.28 nm and 105.7 nm are observed. From these results, the size of pilin $\Delta(1-31)$ monomers is approximately 4 nm. The observed 15 nm could be nonspecific binding of pilin monomers forming assemblies in solution. As dynamic light scattering requires a large concentration of sample, we used 25 μ M. We note this high concentration of the protein which could then lead to possible protein-protein interactions. With the ligands, we observe significantly larger aggregates than the pilin $\Delta(1-31)$ alone. We observe that rhamnolipids induce aggregates that are 4-10x the size of the monomers while SF β C induces larger aggregates that are 20-26x the monomers.

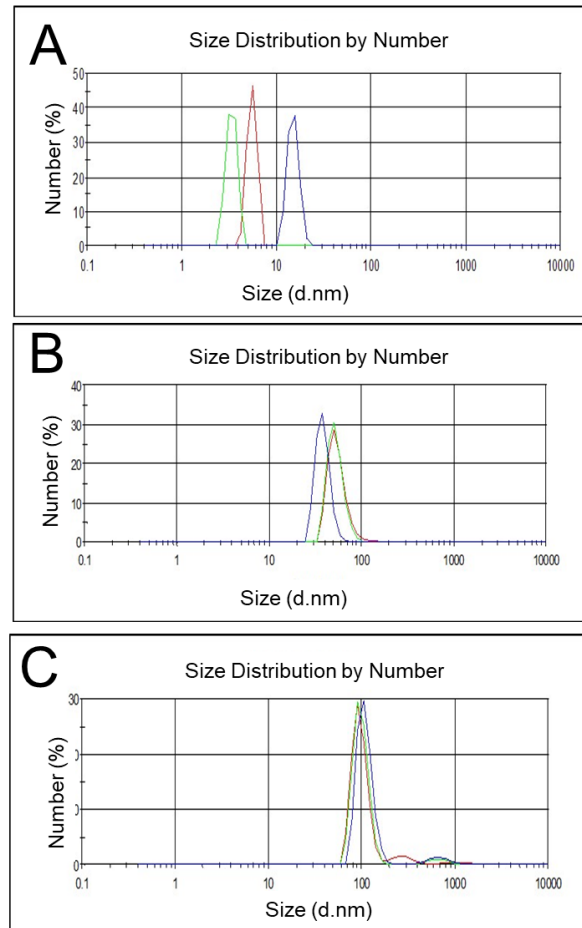


Figure 4.17 The number distribution measured by dynamic light scattering of (A) 25 μM pilin $\Delta(1-31)$, (B) w/ 200 μM rhamnolipids, (C) w/ 200 μM SF β M. Measurements were done on 50 μL solutions in 25 mM Tris and 100 mM NaCl, pH= 7.5.

Because of the high ligand concentration used, there is a possibility that surfactant assemblies interfere with the scattering data. The ligands alone were also measured by dynamic light scattering (Fig. 4.18). The observed sizes of the particles in the ligand solutions at 200 μM are 3-4 nm for SF β C and 15-20 nm for rhamnolipids. These results confirm the detected particles in the mixtures of pilin $\Delta(1-31)$ and ligands are due to proteins and not the ligand.

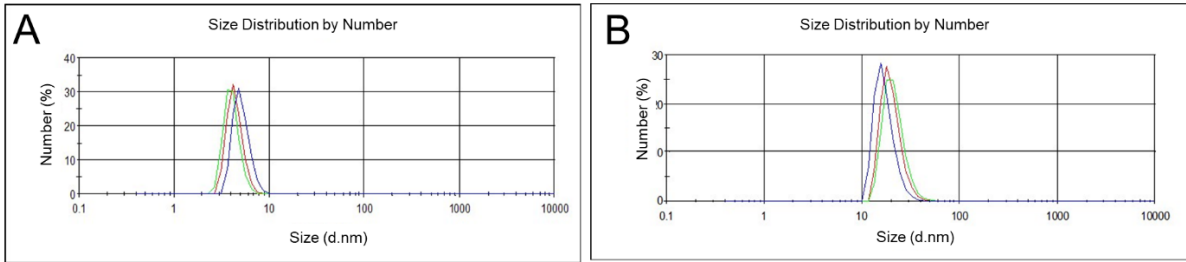


Figure 4.18 The number distribution measured by dynamic light scattering of (A) 200 μM rhamnolipids, (B) 200 μM SF βM . Measurements were done on 50 μL solutions in 25 mM Tris and 100 mM NaCl, pH= 7.5.

To eliminate the possibility of interference by the ligands, dynamic light scattering was done with lower concentrations of the ligand, monorhamnolipid (10 nM and 1 μM), mixed with 25 μM of pilin $\Delta(1-31)$ (Fig 4.19). The measured sizes of the particles in solution increased from $\sim 4-6$ nm (pilin $\Delta(1-31)$ alone) to 5-10 nm (with 10 nM monorhamnolipid) and 10, 15 and 20 nm (with 1 μM monorhamnolipid). These results confirm that the pilin protein form higher order structures in the presence of ligands even at low concentrations. We therefore confirm by DLS the presence of large assemblies of pilin $\Delta(1-31)$ when mixed with ligands.

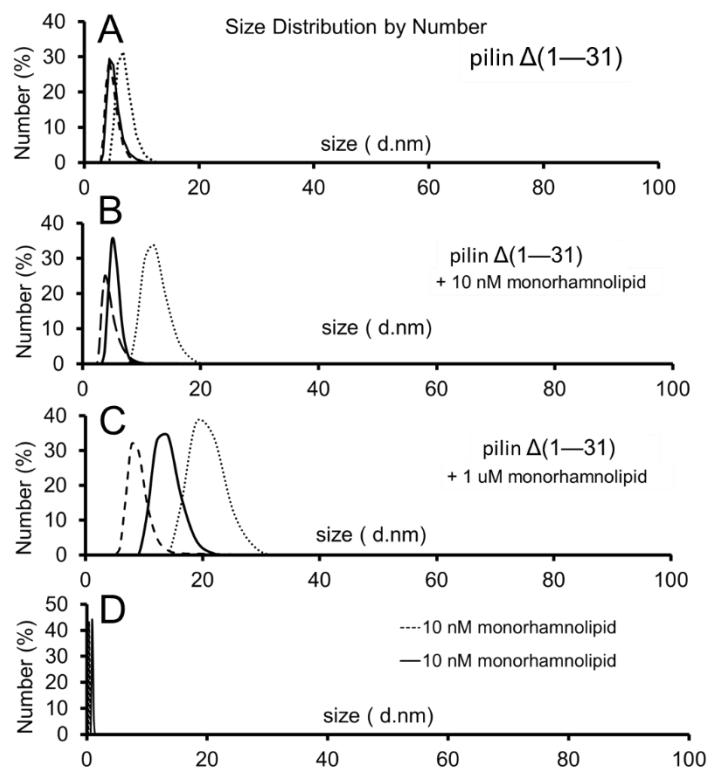


Figure 4.19 The number distribution measured by dynamic light scattering of (A) 25 μ M pilin $\Delta(1-31)$, (B) w/ 10 nM monorhamnolipid, (C) w/ 1 μ M monorhamnolipid and (D) 10 nM monorhamnolipid . Measurements were done on 50 μ L solutions in 25 mM Tris and 100 mM NaCl, pH= 7.5.

4.3 Conclusion

In this chapter, we characterized the pilin proteins and determined ligand-binding using different biophysical techniques such as circular dichroism, NMR and dynamic light scattering. The secondary structure of the native pilin from 1244N3(pPAC46) is mainly comprised of an α -helix. When the native pilin is truncated, pilin $\Delta(1-31)$, removing 31 from the N-terminal α -helix, the secondary structure is comprised of coiled structures and β -sheets. Nuclear magnetic

resonance show that the native pilin is possibly in aggregate form and the structure of pilin $\Delta(1-31)$ reflects a coiled structure. By both circular dichroism and NMR, we were able to detect binding between pilin $\Delta(1-31)$ and rhamnolipids and SF β M. Rhamnolipids and SF β M result in two different secondary structures of pilin $\Delta(1-31)$ when mixed in solution. The ^{15}N -HSQC of native pilin and pilin $\Delta(1-31)$ showed additional peaks when mixed with SF β C and rhamnolipids. Lastly, dynamic light scattering shows that the addition of rhamnolipids or SF β C at both high and low concentrations cause the formation of the larger aggregates of pilin in solution. These results strengthen the hypothesis that pilin is the receptor for rhamnolipids and SF- disaccharide analogs, and that the binding epitope is in the C-terminal globular head of the protein. Further characterization of binding between the pilin $\Delta(1-31)$ and these ligands need to be performed to understand the mechanism of binding.

4.4 Experimental Section

4.4.1 ^{15}N -labelled native pilin expression, purification and SDS-PAGE analysis.

The expression and purification of ^{15}N full pilin was done similarly as the unlabeled full pilin with some exceptions. Briefly, PA1244N3(pPAC46) was streaked on Luria Bertani (LB) agar plates (1.5 wt%) with Tc 50 and Cb 200 then grown overnight at 37°C. The following day a single colony was inoculated in 25 mL Luria Bertani (LB) media treated with Tc 50 and Cb 200 , grown overnight with shaking at 250 rpm, 37°C. The overnight culture was subcultured using a 1:100 ratio in M9 media (0.048 M Na $_2$ HPO $_4$, 0.022 M KH $_2$ PO $_4$, 0.0085 M NaCl, 0.002 M MgSO $_4$, 0.0001 M CaCl $_2$, 0.6 % (w/v) glucose, 0.1 % (w/v) $^{15}\text{NH}_4\text{Cl}$, 0.05 % 1000x metals, 1 % MEM vitamins) treated with Tc 50 and Cb 200 then allowed to grow for 5 hours or until cloudy. The subculture was grown in a larger volume of M9 media treated with Tc 50 and Cb 200 followed by

adding 1mM IPTG to induce pilin protein expression for 14 hours with shaking at 250 rpm, 37°C. The protein expression and purification by nickel affinity column was the same reported procedure for the unlabeled pilin. Pilin protein was stored in storage buffer. Pili protein was checked by SDS-PAGE gel using 15 % separating gel and 4 % stacking gel.

4.4.2 ¹⁵N -labelled truncated pilin expression, purification and SDS-PAGE analysis.

¹⁵N-labelled pilin $\Delta(1-31)$ protein was expressed as previously discussed with modifications. Briefly, the truncated *pilA* gene was cloned from the pPAC46 plasmid of *P. aeruginosa* PA1244N3(pPAC46). The gene was ligated in the pET-SUMO vector and inserted in *E. coli* BL21(DE3) cells. The cells were initially grown in LB media with Kan⁵⁰ for ~4 hours or until cloudy. The culture was transferred in 20 mL of M9 media (0.048 M Na₂HPO₄, 0.022 M KH₂PO₄, 0.0085 M NaCl, 0.002 M MgSO₄, 0.0001 M CaCl₂, 0.6 % (w/v) glucose, 0.1 % (w/v) ¹⁵NH₄Cl, 0.05 % 1000x metals, 1 % MEM vitamins) with Kan⁵⁰, grown for 2 hours with shaking at 250 rpm, 37°C until cloudy. The small M9 culture of BL21 cells were transferred in a larger volume of M9 media treated with kanamycin (50 ug/mL). The protein expression and purification by nickel affinity column was the same reported procedure for the unlabeled pilin $\Delta(1-31)$. Pilin protein was stored in storage buffer. Final protein concentration was check by UV-Vis spectroscopy, measuring absorbance at 280 nm (A₂₈₀). Purity of the protein was checked by SDS-PAGE analysis with a 15% separating gel and 4% stacking gel.

4.4.3 Circular dichroism of pilin proteins.

Solutions of proteins with known concentrations (see above) were diluted to desired concentrations between 20 to 30 μ M. Native pilin was prepared in 4 mM sodium phosphate buffer, pH= 7.2 and

pilin $\Delta(1-31)$ was prepared in 2 mM Tris and 7 mM NaCl, pH= 7.5. Stock solutions of ligands (10 mM; prepared in the same buffers as proteins) were added to the protein solution with the appropriate volumes to achieve the desired final concentrations. For example, 294 μL of 22 μM pilin $\Delta(1-31)$ was mixed with 6 μL of 10 mM rhamnolipids or SF β M to yield final concentrations of 21.6 μM pilin $\Delta(1-31)$ and 200 μM ligands in solution. The solutions were incubated for 24 hours in the shaker at 125 rpm, 25 °C. Circular dichroism (CD) spectra were acquired on a Jasco J-715 CD spectrometer collecting ten scans (4 s averaging time) for each spectrum and using a quartz cuvette with a 1 mm path length. Care was taken that the sample absorbance never exceeded 1.5 at all wavelengths to produce reliable ellipticity values. Mean residue ellipticity (MRE, $\text{deg}\cdot\text{cm}^2\cdot\text{dmol}^{-1}$) values were calculated using the following equation, where θ is ellipticity (mdeg), l is pathlength (cm), C is peptide concentration (M), N is number of residues.

$$\text{MRE} = \frac{\theta}{10 \cdot C \cdot l \cdot N}$$

4.4.4 ^{15}N HSQC studies on pilin protein.

^{15}N -labelled pilin $\Delta(1-31)$ was prepared in 90%/10% $\text{H}_2\text{O}/\text{D}_2\text{O}$ containing 22.5 mM Tris, 2.6 mM NaN_3 and 2.6 mM DSS, pH=7.5 with a final concentration ~ 250 μM . Ligands (SF β M, rhamnolipids) were added (100:1 protein: ligand) and incubated for 24 hours in the shaker at 250 rpm, 25 °C to bind to the pilin. HSQC of both free pilin $\Delta(1-31)$ and ligand + pilin $\Delta(1-31)$ were done in 400 MHz Bruker NMR. ^{15}N full pill pilin was prepared in 90%/10% $\text{H}_2\text{O}/\text{D}_2\text{O}$ containing 50 mM sodium phosphate buffer, 2.6 mM NaN_3 and 2.6 mM DSS, pH=5.55 with a final

concentration $\sim 120 \mu\text{M}$. HSQC of full pilin was done in 800 MHz Bruker NMR. NMR spectra were processed by CcpNmr software or Bruker software.

4.4.5 Dynamic light scattering.

Dynamic Light Scattering (DLS) experiments were measured on Malvern Zetasizer Nanoseries at a scattering angle of 173° at 25°C . The DLS measurement were done on $50 \mu\text{L}$ samples of $25 \mu\text{M}$ native pilin $\Delta(1-31)$ with ligands all dissolved in 25 mM Tris, 100 mM NaCl, $\text{pH}=7.5$. Samples were measured in triplicates.

Chapter 5. Rhamnolipids and Synthetic Disaccharides Bind to Pilin at Low Picomolar Concentrations and Induce Different Assembly Structures

5.1 Background and Significance

5.1.1 Importance of hydrophobic groups to protein-ligand binding

Multiple noncovalent interactions drive the molecular recognition of proteins to their ligands. In biological systems, the multivalent effect is often used to describe molecular interactions between that involve hydrogen bonding between protein and ligands.¹²⁷ However, reports have also shown that hydrophobic interactions also play a role in protein-ligand binding as the major associative force that brings the ligands closer to the protein binding site. In well-known “tight” small molecule-protein binding such as biotin-avidin ($K_d \sim 10^{-15}$ M),¹²⁸ drug-receptor interactions such as WAY 100635- 5HT_{1A} receptor ($K_d \sim 0.087 \times 10^{-9}$ M)¹²⁹, other arylpiperazines with 5HT_{1A} ($K_d \sim$ nM) and Olmesartan- Human angiotensin II AT1 receptor ($K_d \sim 0.087 \times 10^{-9}$ M)¹³⁰, moenomycin and penicillin binding proteins ($K_d \sim$ nM)^{131, 132} and retinol and retinol binding proteins ($K_d \sim$ nM)¹³³⁻¹³⁶, the contribution of hydrophobic interactions have been reported.

Similarly, previous reports have also described hydrophobic interactions influencing the binding between pilin and small molecules.^{9, 24, 75, 137} Irvin and co-workers previously reported that aliphatic chains enhanced the binding of the disaccharide, β -D-GalNAc(1 \rightarrow 4) β -D-Gal, to the pilin protein.⁹ The propylation of the hydroxyl group at the C-4 of the galactose group increased binding by one order of magnitude relative to the unmodified β -D-GalNAc(1 \rightarrow 4) β -D-Gal. To a lesser extent, the methylation of the hydroxyl group at the C-2 of the N-acetylgalactosamine increased the binding twice compared to the unmodified β -D-GalNAc(1 \rightarrow 4) β -D-Gal. Furthermore, Audette and co-workers have reported that hydrophobic

compounds such as 143 mM of 1-undecanethiol and 90 mM 2-methyl-2,4-pentanediol bind to truncated pilin from *P. aeruginosa* K122-4, inducing a conformational change that triggers the self-assembly of the pilin into linear assemblies with 5-6 nm diameter.^{24, 137} Interestingly, studies by Dr. Hewen Zheng from Luk lab demonstrated the direct binding between pilin and the saturated farnesyl (SF) group through covalent ligation of a SF-EG₄-epoxy molecule to pilin, and other proteins do not bind to these molecules.⁷⁵ Collectively, these findings indicated that proteins can have cavities to accommodate large hydrophobic groups (with a less important hydrophilic group) to achieve tight binding.

5.1.2 Fluorescence spectroscopy as a method to determine ligand-binding of pilin and ligands.

Proteins have intrinsic fluorescence properties that arise from the aromatic acids phenylalanine, tryptophan and tyrosine.¹³³⁻¹³⁶ Most commonly, the excitation and emission of tryptophan is used for protein fluorescence studies due to the residue's high quantum yield and extreme sensitivity to the environment.¹³⁴ Tryptophan is typically excited around 280-295 and emits in between 300-400 nm.^{135, 138} The emission profile of tryptophan depends on the protein environment the protein is exposed to.¹³⁹⁻¹⁴⁶ For example, when tryptophan changes its environments and is exposed to a hydrophobic environment, fluorescence maxima is blue-shifted and when exposed to a hydrophilic environment, the fluorescence maxima is red-shifted.^{138, 142} A protein's fluorescence can be utilized to study the protein's structure and dynamics.¹³⁹⁻¹⁴⁶ Hence, the intrinsic fluorescence of protein is valuable in investigating ligand-binding between protein and small molecules as well as any changes in the tryptophan environment caused by folding or denaturation of the protein.^{139, 141, 142, 144-147}

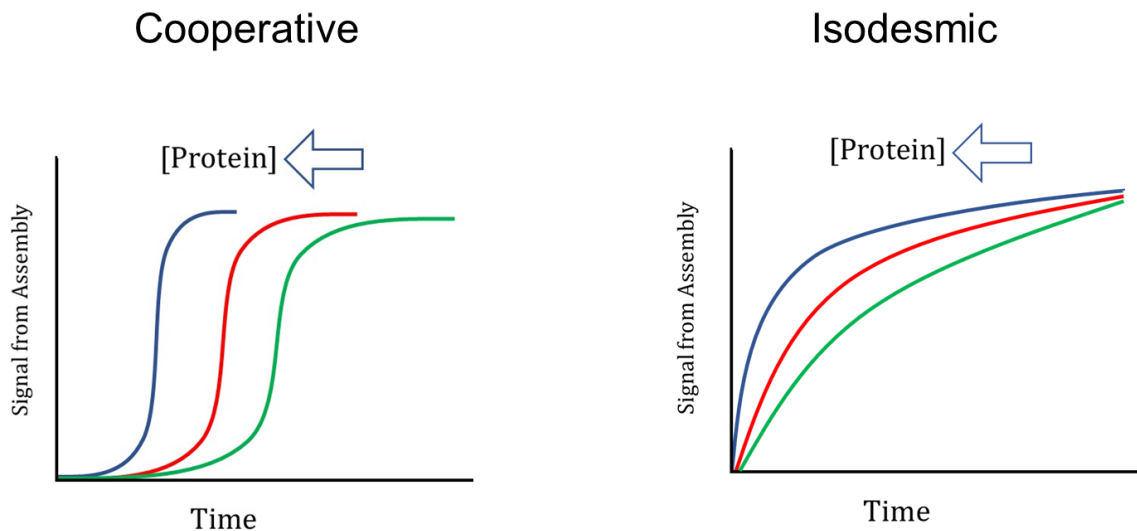
There is little known information on ligands for pilin protein. Our studies on swarming suggest that rhamnolipids and SF-disaccharides are ligands for pilin, however, the ligand-binding has not been studied and characterized. Structurally, our compounds possess surfactant-like properties and could potentially form assemblies when higher concentrations are used. The advantage of using a small amount of protein (nanomolar to micromolar concentrations) for fluorescence spectroscopy would also require minimal amounts of ligands for binding studies. Further, because of the sensitivity of this assay to the environment, it could provide us an idea on whether the environments of the tryptophan residues in pilin are altered by binding to these molecules.

5.1.3 Molecules induce the assembly of truncated pilin protein.

Proteins interact with each other to form higher order structures. Proteins have structural diversity that allows a myriad of noncovalent intermolecular interactions such as H-bonding, electrostatic interactions and hydrophobic interactions that lead to protein assemblies.¹⁴⁸ Biological macromolecules are known to form assemblies in vivo and in vitro given that conditions are suitable.¹⁴⁹ The pili assembly is comprised of circular stacks of 4-6 pilin monomers that form fibers with a diameter of 5-6 nm.^{45, 76, 79, 80, 84} In the assembly, each pilin monomer is associated by the N-terminal α -helix and the β -sheet exposed at the periphery of the fiber.^{45, 76, 79, 80, 84} The exposed α -helix is deemed to be important for the pilin assembly.⁷⁹ However, past studies by Audette and co-workers have shown that even truncated pilin without the exposed α -helix can self-associate to form fibrous assemblies with ~6 nm in diameter.^{24, 137} In that work, the pilin self-assembly is triggered by the presence of hydrophobic compounds,

including 143 mM of 1-undecanethiol and 90 mM 2-methyl-2,4-pentanediol. While the mechanism remains unclear,¹³⁷ the hydrophobic compounds is believed to induce a conformational change in the truncated pilin that facilitates the fiber assemblies.^{24, 137}

To characterize the nature of the protein assembly induced by the ligands, kinetic studies are often used to monitor changes in signals that arise from the assembly formation.^{139, 150, 151} There are two general models of assembly that proteins follow – the cooperative and isodesmic model (Fig. 5.1). In the cooperative model, the formation of the assemblies is concentration-dependent where a certain concentration of proteins must be reached, known as the critical aggregation concentration, before larger assemblies will form. Generally, in a time study, there is an initial lag phase reflecting the formation of small assemblies. The signal will start to increase over time, only when the critical aggregation concentration is reached. The signal will eventually saturate when larger assemblies are formed. Meanwhile, in the isodesmic process, protein assembly follows a “linear” model where there is no requirement of a critical aggregation concentration for protein assembly to occur.^{139, 152-155} In a time study, the expected curve for isodesmic assembly will yield an immediate increase in the signal (no lag time observed) as each monomer adds continuously to the growing assembly and only when the assembly is large enough will the signal saturate.



The lag time in cooperative assembly depends on the protein concentration.

There is no lag time in isodesmic assembly.

Figure 5.1 Scheme of protein assembly models by cooperative (left) and isodesmic (right) assembly.

5.1.4 Chapter aim: To characterize Binding of Truncated Pilin with Rhamnolipids and Synthetic Disaccharides.

In this chapter, we aim to identify the ligands of pilin protein using fluorescence spectroscopy. With previous results showing that rhamnolipids and structural analogs, SF-disaccharides, control the biological activities of *P. aeruginosa* such as swarming, we hypothesize that these molecules are ligands of pilin protein. To conduct binding studies, we used pilin $\Delta(1-31)$ pilin and study its binding to the ligand candidates by measuring the changes in the fluorescence emission of the truncated pilin after adding increasing concentrations of the ligands. We identified rhamnolipids and SF-disaccharides bind to pilin at low picomolar concentrations that lead to further assembly formation of the pilin $\Delta(1-31)$ in solution. Kinetic studies were also performed to determine the process by which the ligand induces the pilin to

form assemblies in solution. Transmission electron microscopy was used to visualize and characterize the pilin assemblies and differentiate the assemblies formed by rhamnolipids and SF-disaccharide molecules.

5.2 Results and Discussion

5.2.1 *Rhamnolipids and synthetic disaccharides bind to pilin protein at low picomolar concentrations.*

To characterize the binding between the ligands and the pilin proteins, we discovered that the intrinsic fluorescence^{138, 139, 141, 142, 156} of pilin protein is highly sensitive to the ligand binding. Here, we used fluorescence spectroscopy to study the *in vitro* binding of the protein with the ligands SF β C, SF-EG₄OH, monorhamnolipid and dirhamnolipid. Pilin protein (100 nM) was excited at 260 nm to minimize the signal distortion from the Raman peak, and emission was collected from 300-400 nm. The fluorescence signals of both native pilin and pilin $\Delta(1-31)$ measured and observed in between 320-340 nm (Fig. 5.2).

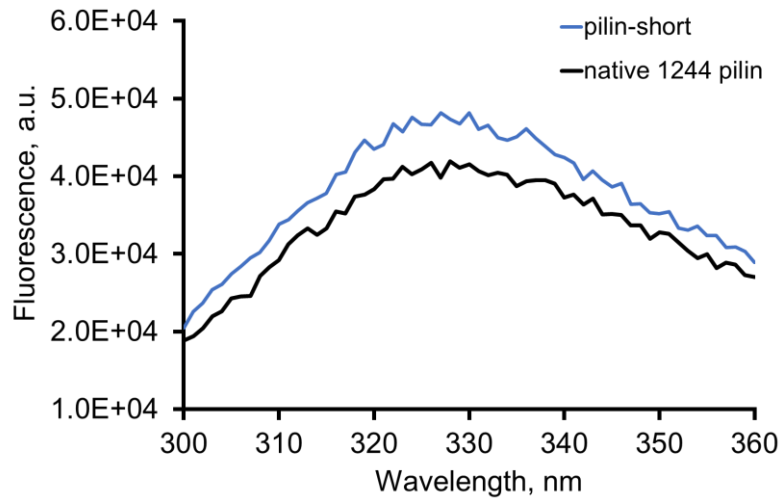


Figure 5.2 Fluorescence emission of native 1244 pilin (black) and $\Delta(1-31)$ (blue) excited at 260 nm. Proteins were prepared as 1 mL solutions of 100 nM proteins in 50 mM Tris, 100 mM NaCl, pH=7.5.

First, selectivity of binding was determined by adding 1 μ M rhamnolipids or SDS to the pilin proteins and measuring the fluorescence emission of the final solution (Fig. 5.3). When rhamnolipids were added to both pilin proteins, an increase in the fluorescence signal were observed for both proteins, whereas SDS had no significant effect on the fluorescence emission of either pilin. The selectivity of binding is consistent with the previous swarming results where rhamnolipids and not SDS were observed to regulate *P. aeruginosa* swarming motilities which we correlate to pilin proteins binding to rhamnolipids but not to SDS. Furthermore, the observed increase in the fluorescence emission and slight blue shift after adding rhamnolipids suggest a change in environment of the tryptophan residues in both pilin proteins, specifically an increase in the hydrophobicity in the environment of the tryptophan residues.^{138, 142} The observed changes in the spectra are likely a result of the rhamnolipids binding to the pilin proteins. However, the mechanism is not clear whether the rhamnolipids causes an indirect change in the

tryptophan environments by binding to the protein and changes the protein conformation or if tryptophan directly interacts with the rhamnolipids that changes the environment. The same fluorescence results for native pilin and pilin $\Delta(1-31)$ suggest that deletion of the N-terminus of native pilin retains the ligand-binding region in the pilin $\Delta(1-31)$ and that the tryptophan residues in both proteins possess the same accessibility to the ligands. Therefore, we could use the fluorescence emission of pilin $\Delta(1-31)$ to study the binding of the pilin protein to different ligands.

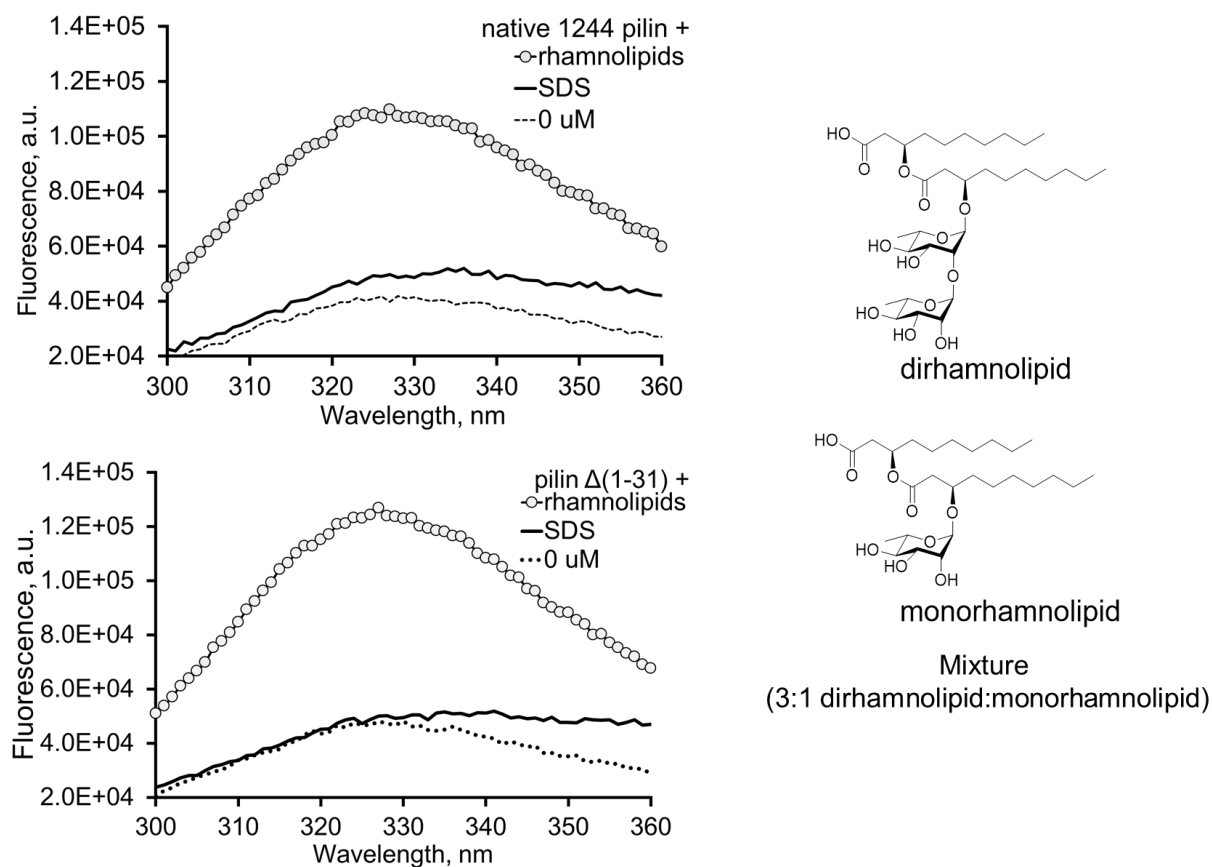


Figure 5.3 Fluorescence emission of native 1244 pilin (top) and pilin $\Delta(1-31)$ (bottom) with ligands 1 μM rhamnolipids and 1 μM SDS. Proteins with and without ligands were prepared in 50 mM Tris, 100 mM NaCl, pH=7.5 with a total final volume of 1 mL.

The fluorescence emission of the single amino acid mutants of truncated pilin after adding rhamnolipids were measured (Fig. 5.4). While truncated I98D did not show any increase in the fluorescence emission, truncated P111G and W105K showed some increase but not as significant as seen with the native and pilin $\Delta(1-31)$ when mixed with rhamnolipids. The small increase in the fluorescence is most likely a partial exposure of one or both of the tryptophan residues to the rhamnolipids as an effect of a change in protein folding resulting from changing the single amino acid in the protein rather than binding because the mutants are inactive in controlling the swarming of *P. aeruginosa*.

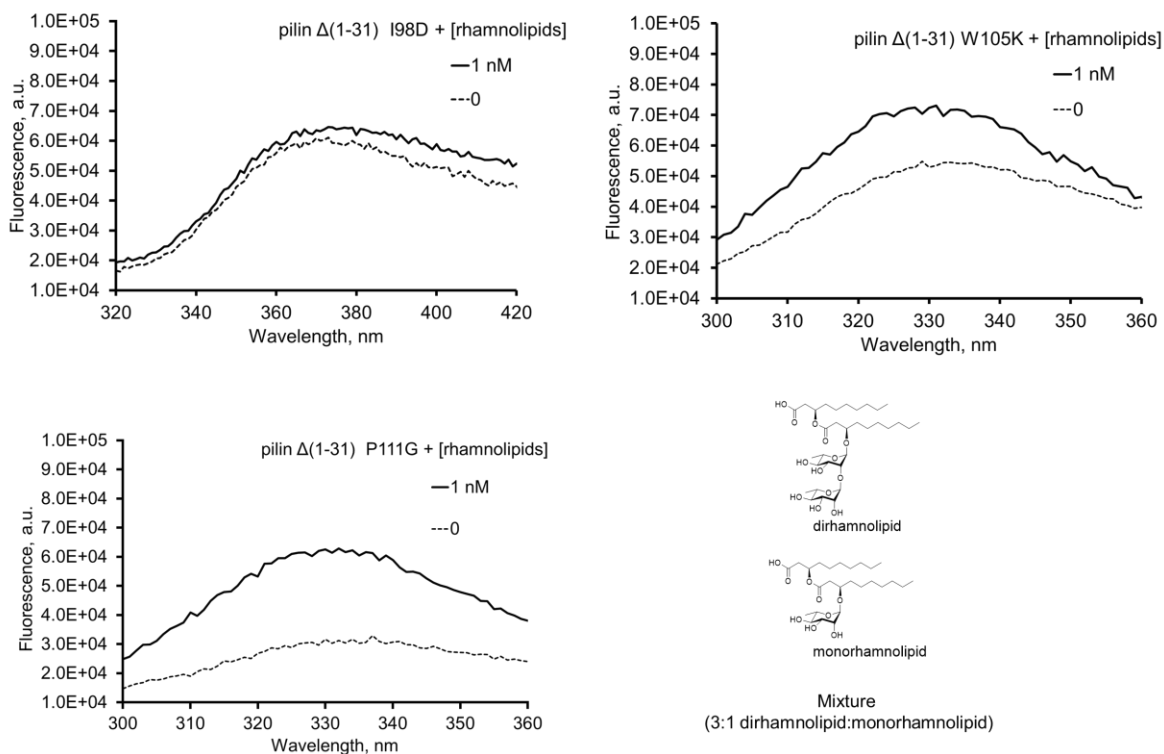


Figure 5.4 Fluorescence emission spectra of 100 nM pilin $\Delta(1-31)$ single amino acid mutants I98D, W105K and P111G (bottom) with ligands 1 μ M rhamnolipids. Proteins with and without ligands were prepared in 50 mM Tris, 100 mM NaCl, pH=7.5 with a total final volume of 1 mL.

Next, pilin $\Delta(1-31)$ (100 nM) was mixed with different ligands SF β C, SF-EG₄OH, monorhamnolipid, dirhamnolipid and SDS to study binding between the protein and ligands. Increasing concentrations of the different ligands were added to individual solutions of 100 nM pilin $\Delta(1-31)$. The fluorescence emission of the truncated pilin solutions after adding the ligands were measured from 300-360 nm (Fig 5.5). We observed that for four ligands, SF β C, SF-EG₄OH, monorhamnolipid, and dirhamnolipid, the fluorescence emission increase with increasing concentrations added in the solution. We note the increase in the fluorescence emission of the pilin $\Delta(1-31)$ occurs at a low concentration of the ligand, at picomolar concentration ranges. Meanwhile, no significant change in the pilin $\Delta(1-31)$ fluorescence signal was observed for SDS.

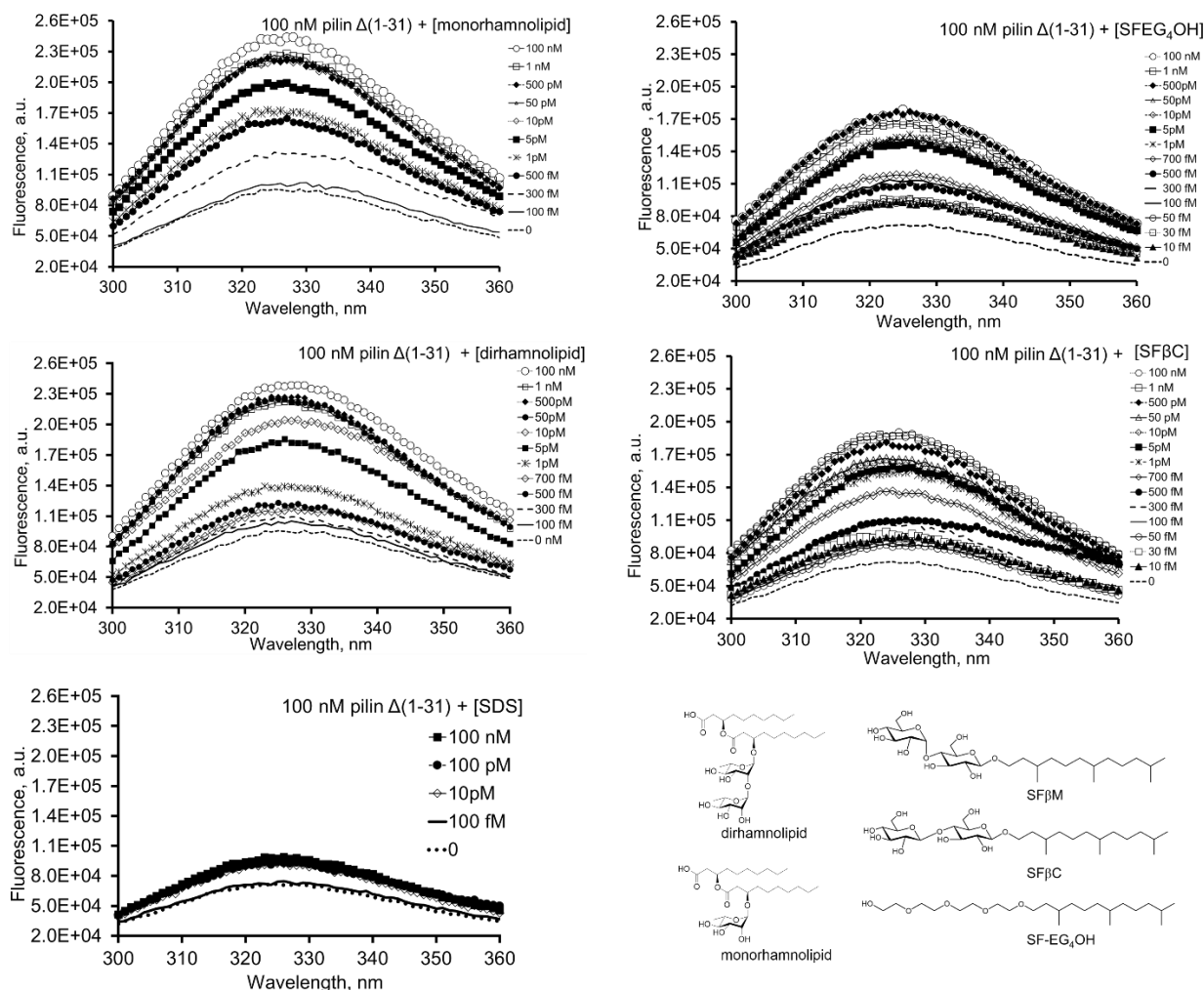


Figure 5.5 Fluorescence emission spectra of 100 nM of pilin $\Delta(1-31)$ with (A)SF-EG₄OH, (B) SF β C, (C) dirhamnolipid, (D) monorhamnolipid and (E) SDS. Proteins and ligands were dissolved in 50 mM Tris and 100 mM NaCl, pH= 7.5. Samples were equilibrated for 16 hours prior to fluorescence measurements.

For each ligand added, the maximum fluorescence for each solution were plotted as a function of ligand concentration. The maximum fluorescence signals were observed in between 320 -340 nm. (Fig. 5.6). At 10 fM, the lowest concentration of ligands added, only SF β C and SF-EG₄OH increased the fluorescence signal of pilin $\Delta(1-31)$ while monorhamnolipid and

dirhamnolipid had no effect on the fluorescence signal. For each of the curves, the half-maximal points were determined at approximately 300 fM SF β C, 500 fM SF-EG₄OH, 700 fM monorhamnolipid and 1 pM dirhamnolipid. The fluorescence signals immediately reach a saturation point at approximately 1 pM SF β C, 1 pM SF-EG₄OH, 10 pM dirhamnolipid and 5 pM monorhamnolipid added to pilin $\Delta(1-31)$. Our results indicate that at low ligand concentrations, 10 fM SF β C, 10 fM SF-EG₄OH, 30 fM dirhamnolipid and 50 fM monorhamnolipid, the ligands interact with the pilin $\Delta(1-31)$ altering the environment of the tryptophan residues causing an increase in intrinsic fluorescence of the protein. We note that the SF-disugar compounds immediately cause an increase in the fluorescence followed by dirhamnolipid then monorhamnolipid. As the fluorescence emission increases with ligand concentration, the half-maximal point in each curve represent the apparent binding constant (K_d) of the ligand to pilin $\Delta(1-31)$ where the lowest to the highest values are for the SF-disugar compounds, followed by monorhamnolipid then dirhamnolipid. For all ligands, saturation of the signals occurs at low picomolar concentrations. Collectively, these results suggest that pilin $\Delta(1-31)$ has a higher affinity for SF-disaccharides over rhamnolipids

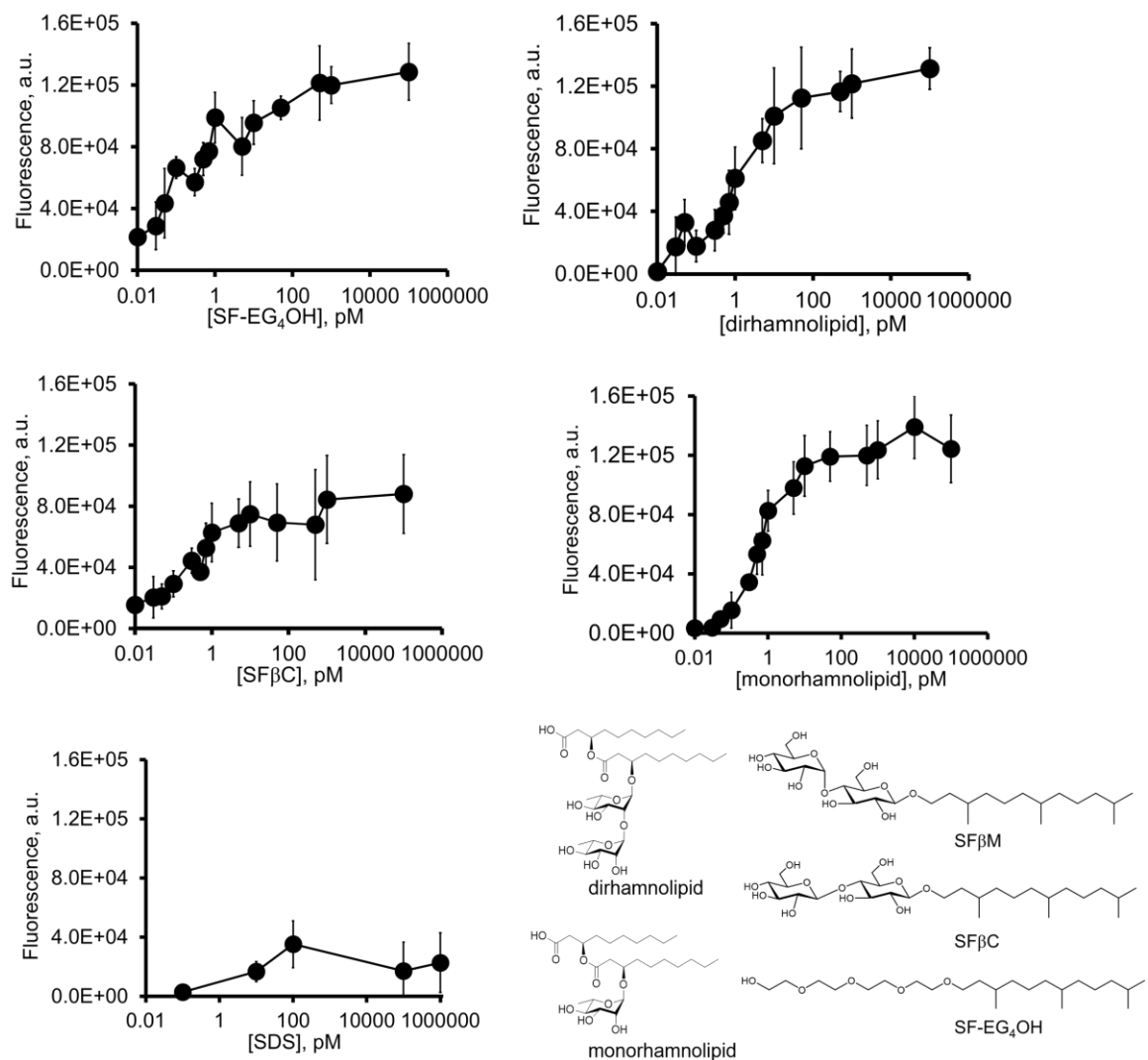


Figure 5.6 Plot of intrinsic fluorescence vs. ligand concentration for individual solutions of 100 nM pilin $\Delta(1-31)$ with different ligands: (A) SF-EG₄OH, (B) SF β C, (C) dirhamnolipid and (D) monorhamnolipid and (E) SDS. Proteins and ligands were dissolved in 50 mM Tris and 100 mM NaCl, pH= 7.5. Fluorescence measurements were taken after 16 h of incubation, n=3.

For most of the ligands tested, the saturation occurs at 1 picomolar of the ligand, which is much lower than the protein concentration (1 pM vs. 100 nM). We note the difference in the binding concentrations for the swarming ($\sim\mu\text{M}$) and the fluorescence measurement ($\sim\text{nM}$) which

could be due to the variation in the number of pilin proteins in the two systems. In swarming, the bacteria number is concentrated in the drop and the ligand surrounding the bacterium is low. Whereas in the fluorescence experiments, the number of pilin and ligands are accurately quantified and mixed in solution. While the observed apparent binding constants (K_d 's) at low ligand concentrations are indicative of binding of the ligand to the pilin $\Delta(1-31)$, the immediate saturation of the fluorescence signal at low ligand concentrations could also reflect some other binding process happening sequentially. First, we believe that this immediate saturation of signals could be due to the presence of some large species in the solution. Second, the formation of protein assemblies could cause a change in the microenvironment of the tryptophan to a more hydrophobic one which results in the increase of the fluorescence of pilin $\Delta(1-31)$.

5.2.2 Tight-binding between ligand binding between pilin and SF-compounds and rhamnolipids induces pilin assembly

The measurements of the intrinsic fluorescence of the assembled proteins indicates that the half-maximal of the signals of pilin assembly reveals the transition of the pilin monomers to larger assemblies. Our results show that around 1 pM of ligands (monorhamnolipid, dirhamnolipid, SF β C and SF-EG₄OH) can cause such transition for 100 nM pilin $\Delta(1-31)$. We note that this picomolar effect does not directly reveal the binding constant between the ligand and the pilin protein, but rather offers two possibilities. First, the ligands indeed bind with high affinity to the pilin proteins at picomolar range, followed by causing the protein to assemble. Second, the ligands bind to the pilin protein with a weaker binding strength, and function as catalysts to induce the assembly of pilin proteins. In the second case, while the pilin proteins

form assembly, the ligand has a significant dissociation rate, and the dissociated ligands induces other free pilin proteins to form assembly.

To distinguish between these two scenarios, we performed a titration experiment, in which a solution of ligand, monorhamnolipid, in excess (100 nM) was added sequentially with pilin $\Delta(1-31)$ to reach the concentrations of 100 pM, 10 nM, 100 nM and 110 nM. The fluorescence signals were measured for each pilin addition (Fig. 5.7). If the ligand binds to the receptor with a high binding constant, close to low picomolar range as observed for inducing pilin assembly, when pilin concentration is titrated to close to 100 nM, the ligands would be largely bound and unavailable to induce nascent pilin assembly. In contrast, if ligand functions as a catalyst with a relatively weak binding constant, the formation of nascent pilin assembly will still be possible for newly added pilin proteins, even when the pilin and ligand concentration comparably close.

The mixture after each addition of pilin was equilibrated for 12 hours prior to measuring the fluorescence (Fig. 5.7). pilin $\Delta(1-31)$ at 100 pM in the presence of an excess of monorhamnolipid (100 nM) exhibited fluorescence signal ($\sim 9 \times 10^4$ units). Further addition of pilin concentration to 10 nM, and 100 nM increased the fluorescence signal from $\sim 11.6 \times 10^4$ to $\sim 12.5 \times 10^4$. But, further addition of pilin to 110 nM did not cause an increase in fluorescence (Fig. 7). This lack of increase in the fluorescent signal indicates that there is no nascent formation of pilin assemblies, and suggests that the ligands are bound, and free ligands are unavailable. This result thus supports a tight binding model, rather than a weak binding catalysis model.

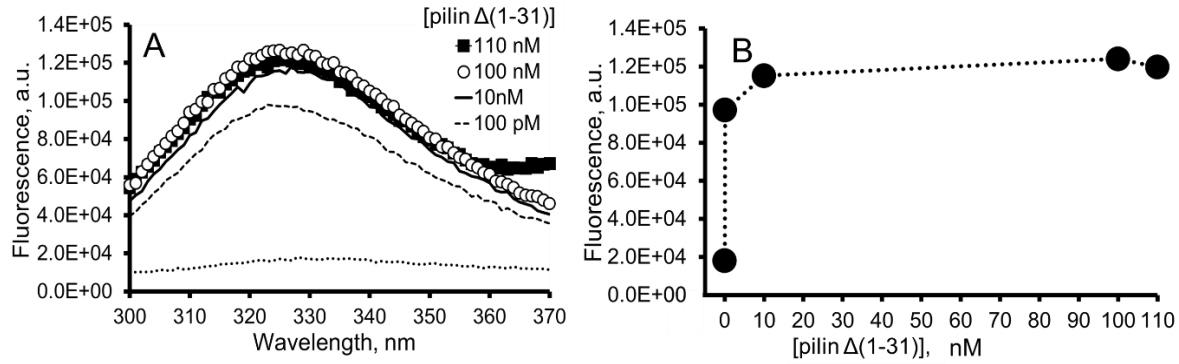


Figure 5.7 (A) Fluorescence emission spectra of 100 nM monorhamnolipid titrated with increasing concentrations of pilin $\Delta(1-31)$. (B) Plot of intrinsic fluorescence vs. pilin conc. titrated into monorhamnolipid solution. Proteins and ligands were dissolved in 50 mM Tris and 100 mM NaCl, pH= 7.5. Measurements were made \sim 12h after adding 10 μ L aliquots of 10 nM, 1 μ M and 9 μ M of truncated pilin into 1 mL of 100 nM of monorhamnolipid.

5.2.3 Ligand-binding to pilin induces pilin assembly formation *in vivo* via the isodesmic process.

Here, we utilized the tryptophan fluorescence of pilin $\Delta(1-31)$ to monitor the signal changes over time after the protein is mixed with ligands. In general, the rate of the protein assembly will depend on the protein concentration for both isodesmic and cooperative assembly. The higher the protein concentration, the faster the protein assembly will occur (Fig 5.8). We studied a range of pilin $\Delta(1-31)$ concentrations (360 nM, 100 nM and 75 nM) with excess ligand (500 nM monorhamnolipid) and the fluorescence signal was measured immediately after mixing to over a course of 24 hours (Fig. 8) The ligand was added in excess in order to ensure all pilin $\Delta(1-31)$ binds to the ligand and prevent any nonspecific binding between the pilin $\Delta(1-31)$ monomers from happening, which can interfere with the fluorescence signal measurements. The

fluorescence emission of the solutions was measured from 0 – 24 hours (Fig. 8) to determine how the protein assembly proceeds. At 360 nM pilin $\Delta(1-31)$ + monorhamnolipid, the initial fluorescence signals decrease from 0 – 30 minutes of incubation, then at 1 hour, the fluorescence signal starts to flatten out then slightly increase at 5 hours. At lower concentrations, 100 and 75 nM pilin $\Delta(1-31)$ + monorhamnolipid, the increase in the fluorescence immediately occurs after 0 hours on mixing ligand to the protein. In general, we observe that for all pilin-short concentrations added, the fluorescence intensity continually increases until the last time point that the fluorescence signal measurement was taken, at 24 hours (Fig. 8). For 360 nM pilin $\Delta(1-31)$, we observe that the fluorescence signal is already high at time 0 and although there is some slight decrease from 0-30 minutes, the signal remains unchanged from 30 minutes to 4 hours, and only slightly increases at 5 hours. This result could be due to the high concentration of pilin-short used, and the rate of the assembly happens too fast, as soon as the ligand is added to the pilin-short. The high fluorescence signal at time zero and the unchanged fluorescence signal from 30 minutes to 4 hours could be due to the immediately population of the solution with protein assemblies. We then used lower pilin concentrations, 100 nM and 75 nM, to slow down the assembly rate and increase the time frame for observing how the protein assembly proceeds. For 100 nM pilin $\Delta(1-31)$, the fluorescence signal immediately increases after time 0 but the significant increase in the fluorescence signal appears at the 2-hour time mark. For 75 nM pilin $\Delta(1-31)$, there is also an immediate increase in the fluorescence signal after time 0, but the large increase takes more time, observed at the 4-hour time mark. These results would confirm that the addition of ligands induce protein assembly of pilin $\Delta(1-31)$. The progression of the fluorescence signals over time shows an immediate increase in the pilin $\Delta(1-31)$ signals, without a lag time, and the fluorescence signal continuously increases over time. The curve resembles an

isodesmic process of assembly where each monomer assembles without the need for nucleation of a critical concentration.^{139, 152-155}

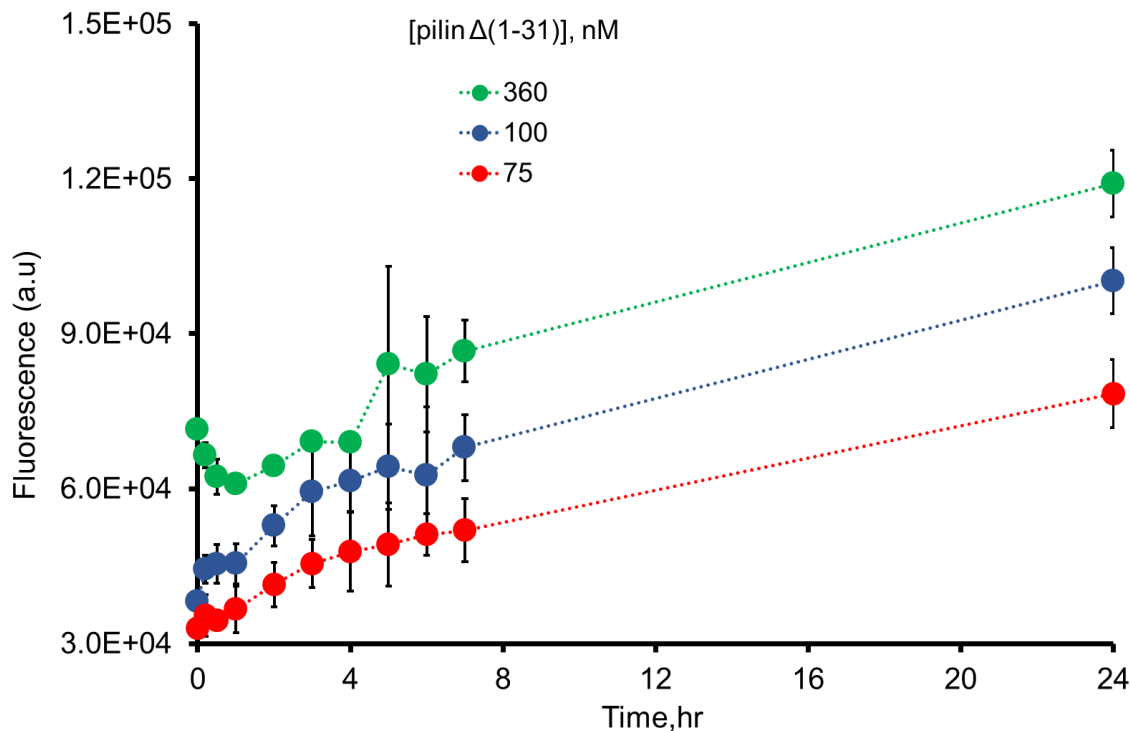


Figure 5.8 Plot of intrinsic fluorescence vs. time (hr) of 500 nM mono-rhamnolipid and varying concentrations of pilin $\Delta(1-31)$ (360, 100 and 75 nM). Proteins and ligands were dissolved in 50 mM Tris and 100 mM NaCl, pH= 7.5.

We also looked at the case when the pilin is in excess compared to the ligand concentration (Fig. 5.9). We tested 1 nM of monorhamnolipid with 100 nM pilin and 50 nM pilin. The observed transition of the fluorescence signal increase occurred at around 1 pM of ligands for 100 nM of pilin $\Delta(1-31)$, a 10^{-5} : 1 ratio. For this experiment, we used 1 nM monorhamnolipid to ensure that the proteins will form assemblies. We also picked low concentrations of the pilin to minimize any nonspecific binding between the proteins that could

interfere with the fluorescence readings. We observe that there is an immediate increase in the fluorescence from 0-3 hours and this increase continues from 20-24 hours. These results also show that the assembly occurs via the isodesmic process.

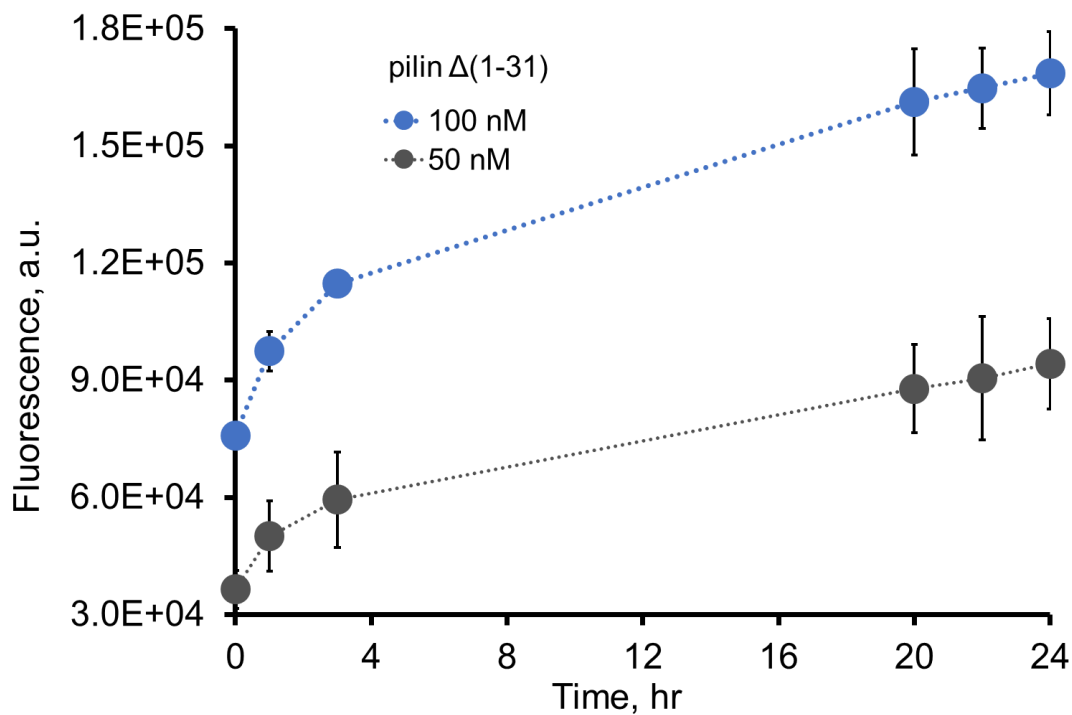
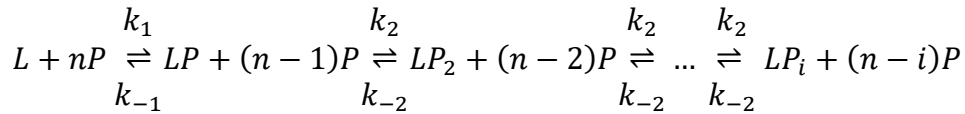


Figure 5.9. Plot of intrinsic fluorescence vs. time (hr) of 1 nM mono-rhamnolipid and varying concentrations of pilin $\Delta(1-31)$ (100 and 50 nM). Proteins and ligands were dissolved in 50 mM Tris and 100 mM NaCl, pH= 7.5.

Here, we have demonstrated that the intrinsic fluorescence of pilin $\Delta(1-31)$ is a useful tool to determine binding of ligands to pilin protein and ligand selectivity. We discovered that ligands bind to the pilin-short at low ligand concentrations and induces the assembly of pilin-short in solution. Furthermore, the kinetic studies confirm that the ligand induced assemblies are of isodesmic in nature.

To describe the pilin assembly induced by ligand-binding, we propose the binding model described by Equation 1. Our model suggests two binding sites at the protein: (1) ligand site and (2) protein site. We hypothesize that the newly assembled proteins also adopt a conformational change similar to the ligand-induced one, and thus leading to further recruitment of proteins and assembly. We assume that the molecular details of protein-protein binding do not change significantly as the linear assembly increases. Thus, we further propose that this ligand induced protein assembly is controlled by two sets of rate constants, one for ligand receptor binding and dissociation (k_1 and k_{-1} , respectively), the other for protein-protein binding and dissociation (k_2 and k_{-2} , respectively).



Equation 5.1 Equation to describe ligand-induced protein binding.

5.2.4 *Transmission electron microscopy shows linear and amorphous assemblies of pilin induced by rhamnolipids and synthetic disaccharides.*

The formation of assemblies by pilin in the presence of ligands were visualized by transmission electron microscopy (TEM). Here, we prepared 80 μM of pilin $\Delta(1-31)$ with 8 nM of monorhamnolipid and SF β C corresponding to a ratio of ligand: pilin corresponding to 10^{-4} :1. The observed transition of the fluorescence signal increase occurred at around 1 pM of ligands for 100 nM of pilin $\Delta(1-31)$, a 10^{-5} : 1 ratio. Passing this concentration of ligands, the fluorescence signal starts to plateau, suggesting that the pilin species in this regime are mainly assemblies. We observe that the TEM images of pilin $\Delta(1-31)$ alone showed scattered small

aggregates with amorphous structures (Fig. 5.10A). Adding 8 nM monorhamnolipid to pilin $\Delta(1-31)$ (80 μM) resulted in the formation of large aggregates with linear assembly structures with a diameter measuring at 5-6 nm. These linear assemblies are aligned to form large assembly with a rough width of 14 nm (Fig. 5. 10, 5.11). Under the same conditions, SF β C induces truncated pilin to form larger aggregates with amorphous details (Fig. 5.10, 5.12).

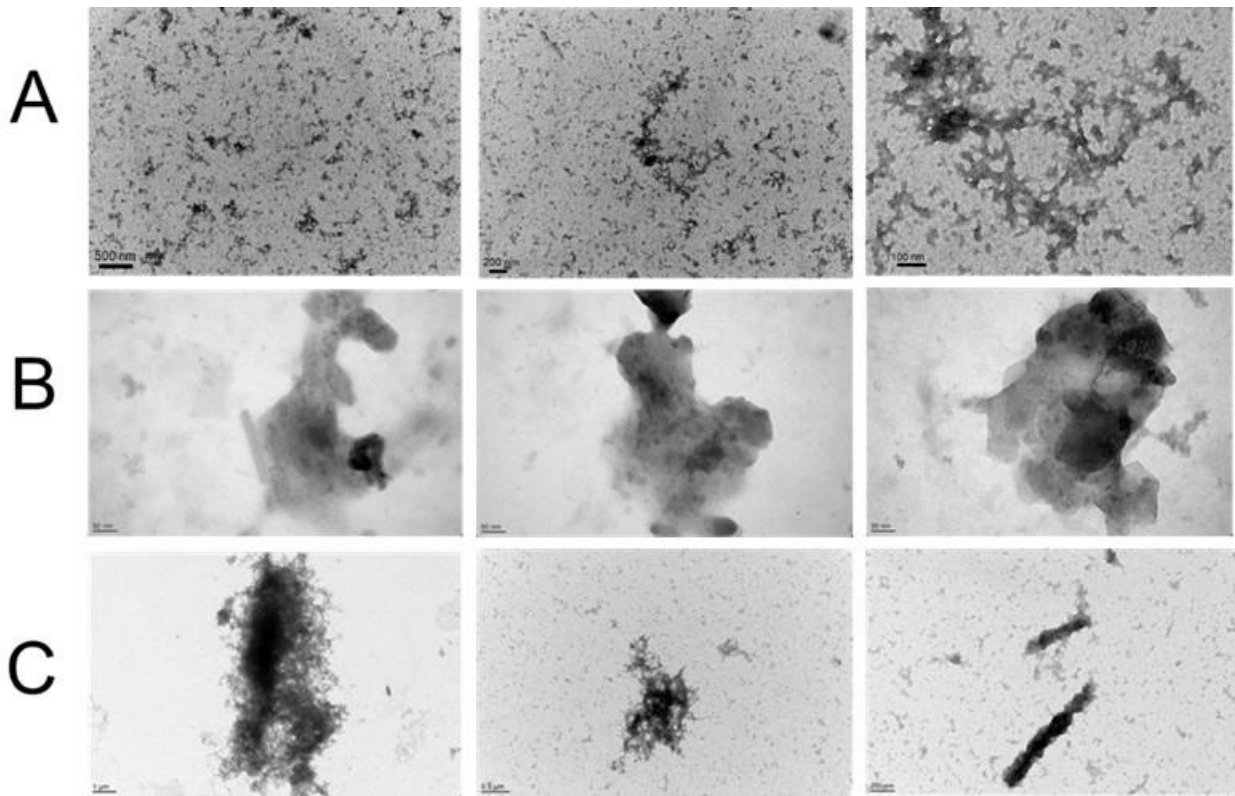


Figure 5.10 TEM images of 80 μM pilin $\Delta(1-31)$ (A), + 8 nM monorhamnolipid (B), and + 8 nM SF β C (C). Micrographs were taken on a FEI Tecnai 12 BioTwin TEM. (Cornell Center for Materials Research, NY, USA) operating at 120 kV.

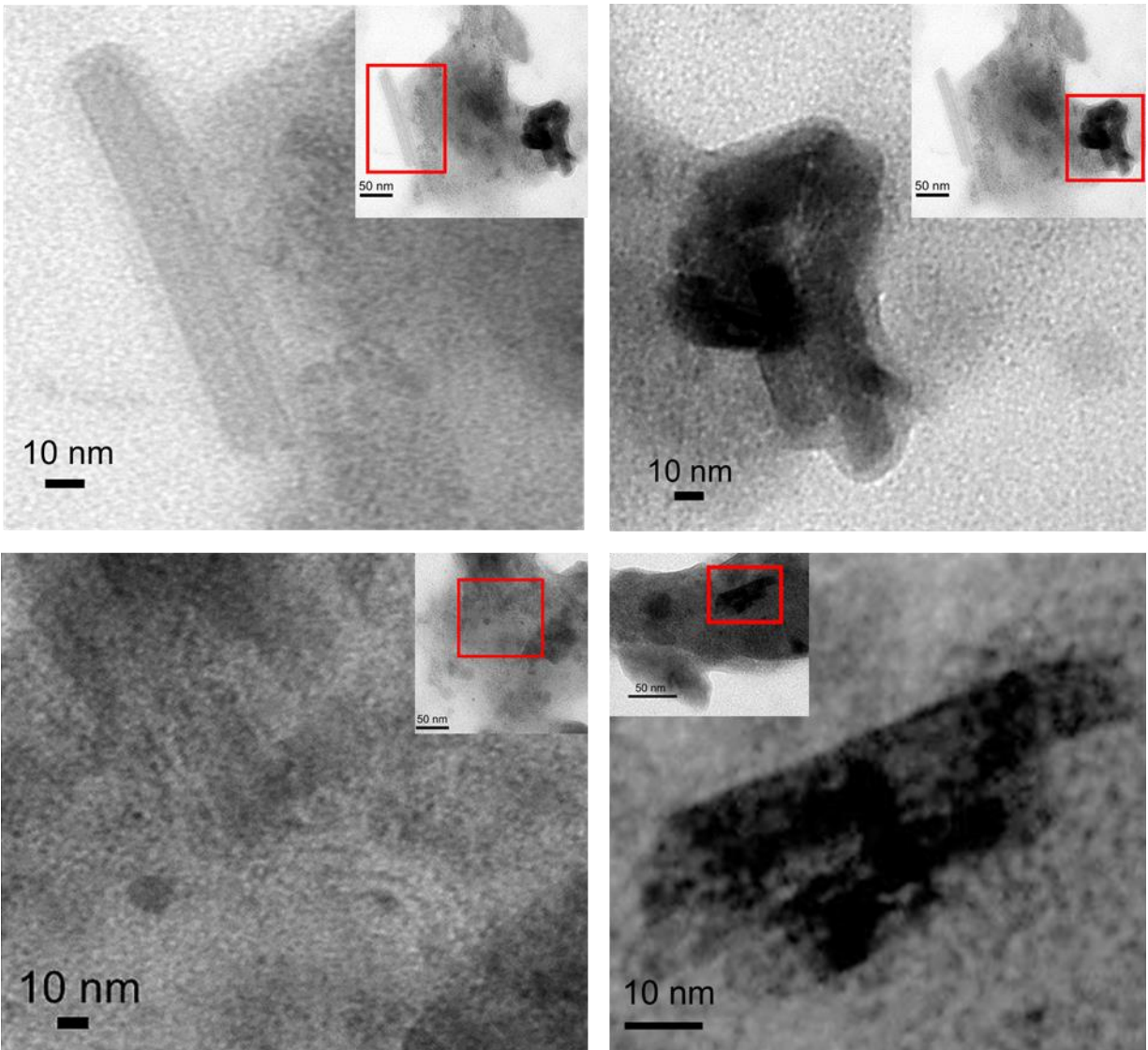


Figure 5.11 Transmission electron micrographs of negatively stained assemblies from a solution of 80 μM pilin $\Delta(1-31)$ with 8 nM monorhamnolipid (A) and 8 nM SF β C (B). Micrographs were taken on a FEI Tecnai 12 BioTwin TEM (Cornell Center for Materials Research, NY, USA) operating at 120 kV.

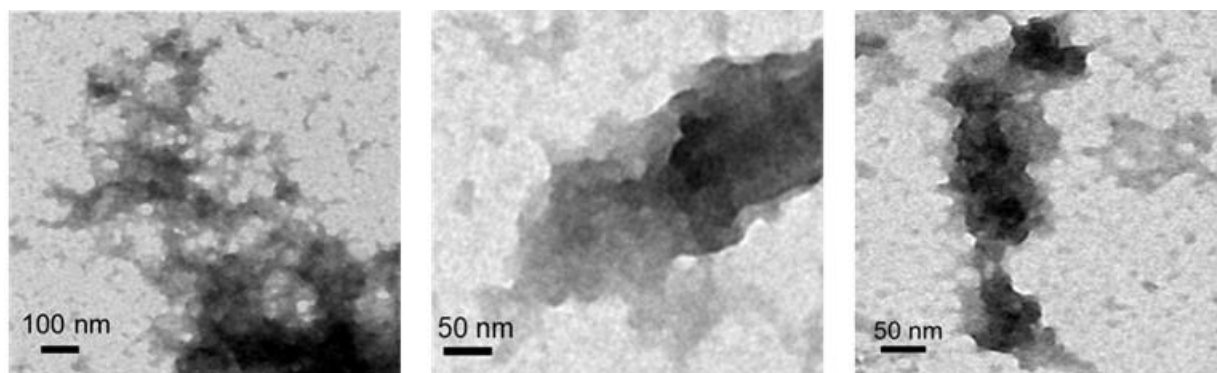


Figure 5.12 TEM images of 80 μM pilin $\Delta(1-31)$ with 8 nM SF β C from three different aggregates on the grid. Micrographs were taken on a FEI Tecnai 12 BioTwin TEM (Cornell Center for Materials Research, NY, USA) operating at 120 kV.

To further examine the assembly structures, we examined pilin $\Delta(1-31)$ assembly at a high concentration, 266 μM with 400 μM monorhamnolipid or SF β C (Fig. 5.13). Here, we study the case when the ligand is in excess of the protein concentration. Under these conditions, we observe similar results as when the protein is in excess of the ligands (Fig. 5.10). The truncated pilin alone forms amorphous aggregates. When ligands monorhamnolipid and SF β C are added, we observe large amount of linear fibrous and amorphous assemblies for the two ligands, respectively. In this case, monorhamnolipid induces the assemblies of linear fibers with 1-5 nm diameter (Fig. 5.14).

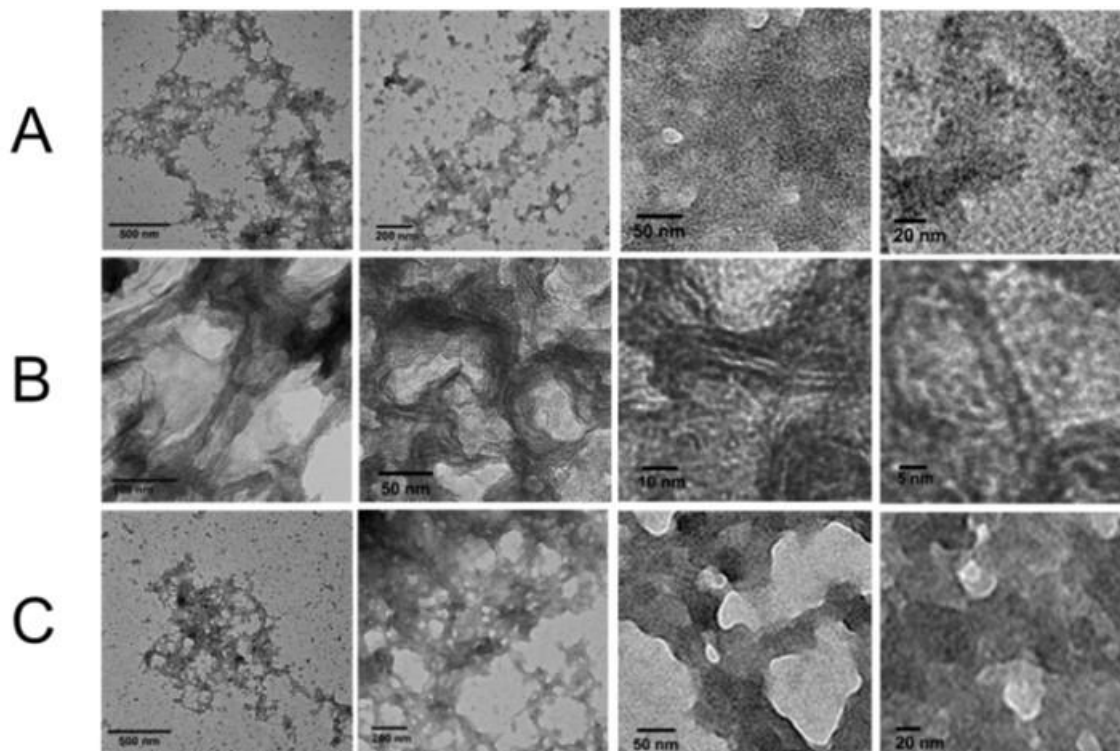


Figure 5.13 TEM images of 266 μM pilin $\Delta(1-31)$ (A), + 400 μM monorhamnolipid (B), and + 400 μM SF β C (C). Images were taken at SUNY-ESF using the JEOL JSM-2000EX microscope.

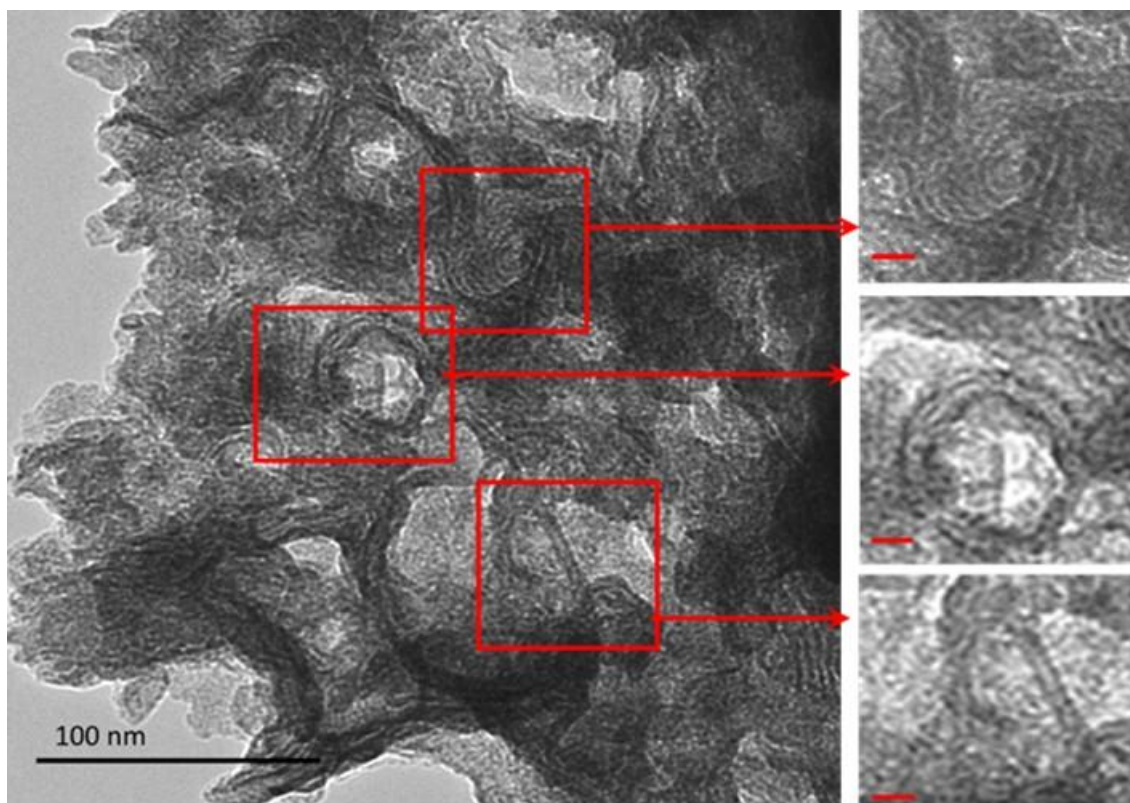


Figure 5.14 Transmission electron micrographs of negatively stained assemblies from a solution of 266 μM pilin $\Delta(1-31)$ and 400 μM monorhamnolipid. Scale bar: 10 nm. Images were taken at SUNY-ESF using the JEOL JSM-2000EX microscope.

At the concentrations of pilin $\Delta(1-31)$ for TEM imaging (80 and 266 μM), which are about 800- to 2000-fold higher than that for the intrinsic fluorescence experiments, we observed some spontaneous self-association of pilin $\Delta(1-31)$ monomers. In contrast, both monorhamnolipid and SF β C at 10^{-4} equivalence induce pilin proteins to form assemblies. While SF β C caused truncated pilin to form amorphous aggregates, monorhamnolipid caused that to form linear fibrous assemblies that can further align to form super-assembly of proteins. We believe for monorhamnolipid, at least, that the mechanism by which the pilin $\Delta(1-31)$ forms assemblies is by

the initially the formation of linear assemblies that further align to form super-assemblies.
(Scheme 5.1).

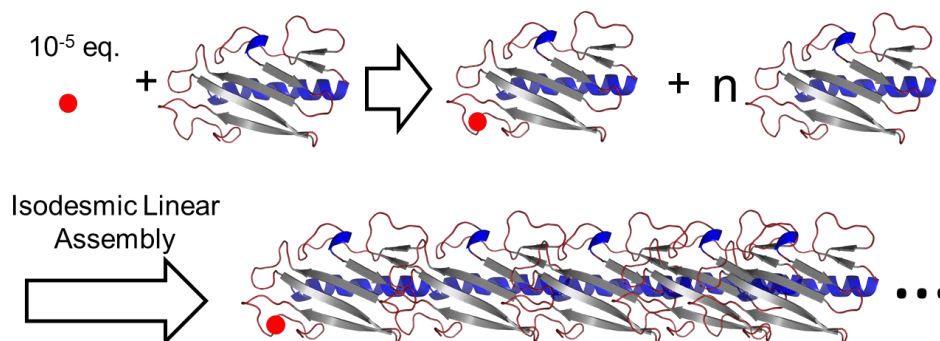


Figure 5.15 Proposed scheme of ligand-induced protein assembly for rhamnolipids.

5.3 Conclusion

Pilin $\Delta(1-31)$ binds to rhamnolipids and SF-disaccharides by measurement of the intrinsic fluorescence of pilin $\Delta(1-31)$. Fluorescence spectroscopy show that 1 picomolar of these ligands is enough to cause 100 nM of truncated pilin to form assemblies in solution by a tight-binding model. The presence of ligand-induced protein assemblies was confirmed by transmission electron microscopy. TEM shows that monorhamnolipid induces the formation of linear filaments, while SF β C induces the formation of amorphous aggregates. Furthermore, the assemblies induced by monorhamnolipid are of 10-20 nm in diameter. Finally, the assembly formation does not require a critical concentration to occur, consistent with the isodesmic process of assembly. The rhamnolipids and synthetic molecules being the ligands for pilin proteins open the opportunity for studying and controlling the bacterial signaling, and related bioactivities, particularly those related to biofilm formation and virulence factors.

5.4 Experimental Section

5.4.1 Cloning, recombinant expression and purification of truncated native pilin protein and mutants.

The cloning, recombinant expression and purification of truncated native pilin protein and mutants were previously reported in Chapter 2.

5.4.2 Fluorescence spectroscopy.

5.4.2.1 General. Solutions of pilin $\Delta(1-31)$ with known concentrations in 50 mM Tris, 100 mM NaCl, pH= 7.5 were diluted with the same buffer to the desired protein concentration for fluorescence spectroscopy. Stock solutions of ligands (rhamnolipids, SF β C and SDS) were prepared in the same buffer. The intrinsic protein fluorescence was measured using the Fluoromax Spectrofluorometer (Horiba Scientific) by exciting the samples at 260 nm, to reduce the peak distortion caused by Raman scattering, and by recording the emission spectra 300 to 400 nm. Slit widths used for both excitation and emission are 5 nm.

5.4.2.2 Binding Studies. Individual solutions (1 mL) of 100 nM pilin $\Delta(1-31)$ with different ligand concentrations ranging from 10 pM to 1 μ M were prepared. For each required final ligand concentration, stock solutions of the ligands were prepared such that 10 μ L of the ligand stock solution is added to each individual solution to ensure the final concentration of protein is consistent in each sample. For example, 990 μ L of 101 nM of pilin $\Delta(1-31)$ is mixed with 10 μ L of 100 μ M of ligand to yield final concentrations of 100 nM pilin $\Delta(1-31)$ and 1 μ M ligand. Each 1 mL solution was aged with shaking at 150 rpm, 25 °C for approximately 16 hours prior to

measuring the fluorescence. The graphs were generated from an average of measurements for three different samples.

5.4.2.3 Protein Assembly Kinetics. Different pilin $\Delta(1-31)$ (75 nM, 100 nM and 360 nM) with 500 nM monorhamnolipid solutions were prepared. The fluorescence of the solution was monitored and measured at different time points from 0 – 24 hours after mixing the proteins and monorhamnolipid in solution. The graphs were generated from an average of measurements for two different samples.

5.4.3 Transmission electron microscopy of pilin assemblies.

The assembly of pilin $\Delta(1-31)$ was induced by mixing equal volumes of pilin $\Delta(1-31)$ solution and ligands (of monorhamnolipid or SF β C) to a final volume of 40 μ L in 50 mM Tris, 100 mM NaCl buffer, pH=7.5. The prepared solutions were then aged overnight for about 16 hours at ambient temperature. The solutions were applied on Transmission Electron Microscopy (TEM) grids for visualization by dispensing a 5 μ L drop of the solution on a 300-mesh Formvar/Carbon coated copper grids. The excess liquid was blotted with a filter paper. The samples on the grids were stained with uranyl acetate (5 μ L of 2 % solution) and allowed to incubate for 2 minutes.

The excess uranyl acetate was removed by dipping the grids in sterile Millipore water approximately 15-20 times, followed by blotting the grids with filter paper. The grids were kept in a dessicator or in a vacuum chamber for at least 24 hours prior to imaging by TEM.

Micrographs were taken on a FEI Tecnai 12 BioTwin TEM. (Cornell Center for Materials Research, NY, USA) operating at 120 kV or on a JEOL JEM 2100F Transmission Electron Microscope (SUNY-ESF, NY, USA) operating at 200 kV.

Chapter 6. Cromoglycate Mesogen Forms Isodesmic Assembly Promoted by Peptides and Induce Aggregation of a Range of Proteins.

6.1 Background and Significance

6.1.1 Disodium Cromoglycate (5'DSCG) is a biocompatible nonamphiphilic mesogen.

Liquid crystals (LC's) have been explored for biological studies and applications.¹⁵⁷⁻¹⁶⁷ Disodium cromoglycate (5'DSCG) belongs to a class of nonamphiphilic molecules that forms nematic chromonic liquid crystals in aqueous solution. As the concentration increases, it is believed that the molecules first form isodesmic assemblies in water, which further align to form liquid crystal phases.¹⁵⁷ Because the chromonic mesogen 5'DSCG does not have a well-separated oily and water-soluble region within its structure (Fig. 6.1), this molecule is benign to protein folding, and appears to be highly compatible for biological applications and studies.^{166, 167} The nematic or liquid crystal phase of this molecule in water has been used for studying surface-oriented movement of bacteria for potential biosensing applications,¹⁵⁸⁻¹⁶³ specific antibody-antigen binding,¹⁶⁶ and protein crystallization.¹⁶⁷ Far from the LC phase concentration, at ~0.14 wt%, 5'DSCG has been demonstrated to promote the crystallization of lysozyme.¹⁶⁷ More surprisingly, this liquid crystal appears to promote the binding between antigens and antibodies,¹⁶⁶ while other conventional surfactant-based liquid crystals do not support the antigen-antibody binding, presumably due to their ability to denature proteins.

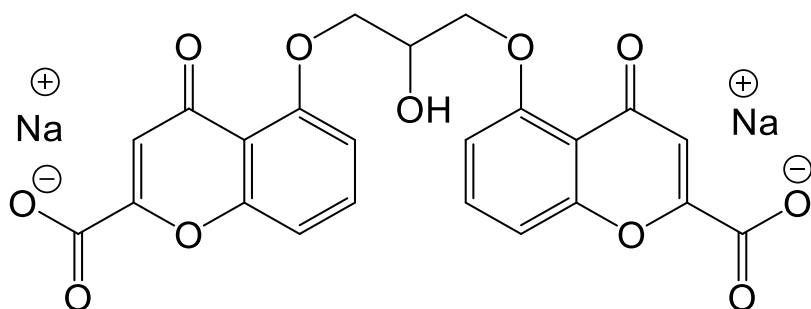


Figure 6.1 Chemical structure of disodium cromoglycate (5'DSCG).

6.1.2 Disodium Cromoglycate (5'DSCG) is a crystallizing agent for proteins.

Among different types of liquid crystals, lyotropic chromonic liquid crystals differ from the conventional surfactant-based lyotropic liquid crystals. Chromonic liquid crystals consist of nonamphiphilic molecules assembled in water, and the assemblies further align to form LC phases.^{157, 168-181} Due to the nonamphiphilic nature of the mesogen, the assembly of the molecules does not proceed with the assembly process of surfactants (conventional lyotropic liquid crystals). Rather, it is believed to proceed with an isodesmic assembly process,^{169-171, 181-183} that is similar to a dynamic noncovalent polymerization without a critical aggregation concentration or a nucleation process. Many novel assembly properties have been observed for this chromonic liquid crystal.^{171, 173, 174, 176} But, it is surprising that the observation and studies for the isodesmic assembly for this class of liquid crystals are scarce,^{169, 170, 178, 180} suggesting that the concentration range for isodesmic assembly may be narrow.

Previous work done by Luk and co-workers crystallized lysozyme using 5'DSCG as a crystallizing agent.¹⁷¹ The ability of 5'DSCG to self-assemble in aqueous solution and form liquid crystals enables protein crystallization. In the liquid crystal phase, the assembly of 5'DSCG is highly hydrated and is able to sequester water molecules in the bulk, leading to favor

proteins to crystallize. This is observed when a solution of lysozyme and 5'DSCG is mixed in water, the liquid crystal phase is achieved at very low concentrations of 5'DSCG (0.14 wt%) compared to 5'DSCG alone in water (11-12 wt%). Consequently, lysozyme crystals also form under these conditions indicating a demixing mechanism between 5'DSCG and lysozyme in aqueous solution. This demixing mechanism between two noncovalent assemblies in aqueous solution can be further characterized and provide a possible general mechanism for crystallizing a wide range of proteins.

6.1.3 Limited available crystal structure of pilin proteins

The pilin assembly is comprised of individual pilin monomers that are collected and assembled as appendages on the surface of the bacteria. Pilin is a general class of protein consisting of an α -helix and a β -sheet domain. The appendage consists of circular assemblies of 4-5 pilin monomers that linearly stack on top of each assembly. These pili appendages can extend and retract in response to chemical signals or environmental stimuli, and are responsible for a wide range biological function of bacteria including swarming motility, twitching motility, recognizing the sugar moieties (asialo-GM₁) on mammalian cells, and the hydrophobic surface of abiotic surfaces.^{37, 68, 77, 78, 81, 84, 184-187} Because of the importance of this class of proteins, vaccine development has been explored for these proteins and several crystal structures of pilin exist,^{68, 77, 78, 81, 84, 187} most of which are of the truncated versions of pilin.^{77, 81, 84} Because of the nature of the pilin structure, with a long, protruding hydrophobic N'-terminal α -helix, the protein is partially insoluble and difficult to crystallize. It would be difficult to achieve a saturated solution of the protein without the risk of the protein aggregating in aqueous solution. Hence, most of the successful pilin proteins crystallized are of the truncated pilin proteins, removing the

first 28 amino acids of the α -helix, which results in a more soluble protein for crystallization studies.^{77, 81, 84} Meanwhile, the crystal structures of ligand-bound pilin complexes are still lacking.

6.1.4 Chapter Aim: Crystallization of pilin protein from *P. aeruginosa* by utilizing the isodesmic assemblies of 5'DSCG.

In this chapter, we aim to demonstrate that the presence of peptides promotes the isodesmic assembly of 5'DSCG over a broad range of concentrations before reaching the liquid crystal phase. We will also study the effect of non-ionic polymers in promoting the isodesmic assembly of 5'DSCG in aqueous solution. These assemblies were detected by measuring absorbance at 600 nm (OD₆₀₀) and corroborated by nuclear magnetic resonance (NMR). We further explored this demixing mechanism to precipitate a wide range of proteins, including lectin A, esterase, lipase, bovine serum albumin, trypsin, native pilin protein from bacterium *Pseudomonas aeruginosa* PA1244N3(pPAC46), and the truncated pilin, pilin Δ (1-31) recombinantly expressed in *E. coli*.

6.2 Results and discussion

6.2.1 Components of Luria Bertani media promote isodesmic assembly of 5'DSCG

Additives such as ions and water-soluble organic molecules can have an impact on the transition concentration of 5'DSCG from isotropic solutions to nematic liquid crystal phases.^{169, 173, 179, 188-190} The isodesmic assembly formation is predicted to be a step towards the formation of the LC phase as these isodesmic assemblies align in solution.^{169, 170, 183} However, the extensive

studies and characterization of these isodesmic assemblies are lacking. Some studies showed the assembly of 5'DSCG molecules form small noncovalent oligomers that is consistent of isodesmic assemblies.^{174, 191} Here, we discover a simple system containing chemical additives that promote the formation of large and readily detectable isodesmic assembly 5'DSCG (Fig. 6.2).

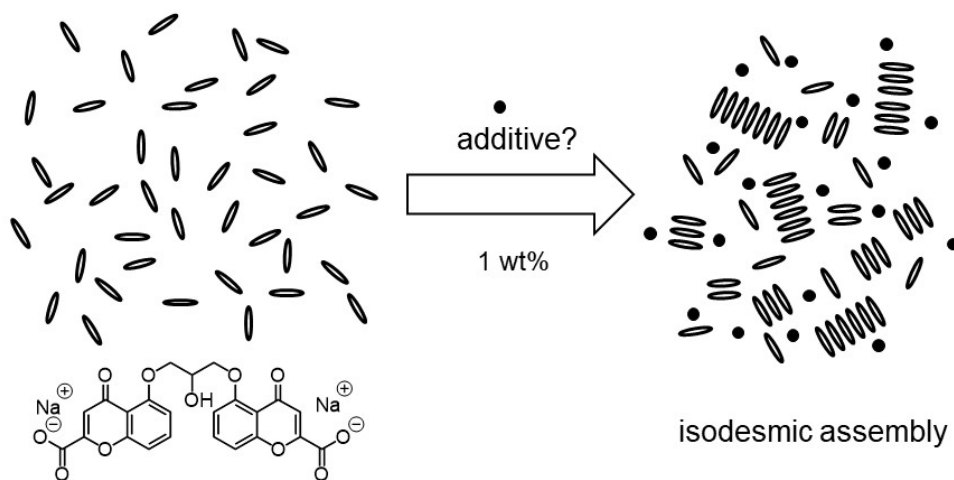


Figure 6.2 Schematic representation of formation of isodesmic assembly of 5'DSCG induced by chemical additives.

To explore the potential biological applications using 5'DSCG phases, we first conducted a study on the effect of Luria Bertani (LB) media for culturing bacteria (1 wt% tryptone, 1 wt% sodium chloride, 0.5 wt% yeast extract) on the assembly and phase property of 5'DSCG. Initial studies show that LB media caused 5'DSCG to form nematic phases at a lower concentration than in deionized water (8 wt% rather than 11 wt%) (Fig. 6.3), suggesting that the components of LB media induced the assembly of 5'DSCG. These results led to the discovery that isodesmic

assemblies of 5'DSCG can be readily measured by the light scattering of the solution via the absorbance at 600nm (OD_{600}). Measuring OD_{600} is commonly used for measuring bacteria densities by light scattering of the bacterial cells. Isodesmic assemblies, if existing, are comprised of different oligomers and polymers in equilibria.^{169-171, 181, 183} Light scattering of the solution provides a readily accessible method to detect the presence of these isodesmic assemblies in solution.

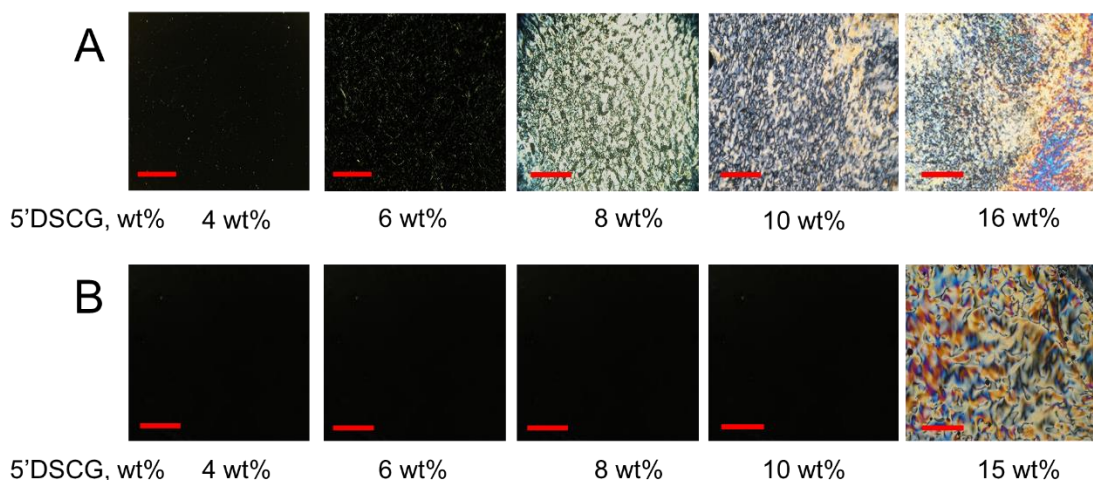


Figure 6.3 Images of 5'DSCG solutions at different concentrations in (A) Millipore water (B) Luria Bertani (LB) media (1 wt% sodium chloride, 1 wt% tryptone and 0.5 wt% yeast extract) viewed under cross polars. Scale bar = 760 μ m.

Measurement of the optical density (OD_{600}) revealed the formation of assemblies of 5'DSCG. The OD_{600} of 5'DSCG in deionized water did not change significantly until the concentration reached the transition to form the liquid crystal phase (11-12 wt%); whereas in LB media, the OD_{600} readings increase rapidly with concentration starting around 1.5 wt % of

5'DSCG, then reaching a plateau at around ~3.5 wt% (Fig. 6.4). These low concentrations are of a large contrast to the nematic concentrations of 5'DSCG in water (11-14 wt%). Between the saturation of the OD₆₀₀ reading at around 3.5 wt% and the appearance of liquid crystals at around 8 wt%, we believe that this concentration range is saturated with isodesmic assemblies of increasing sizes and not with increasing number of assemblies.

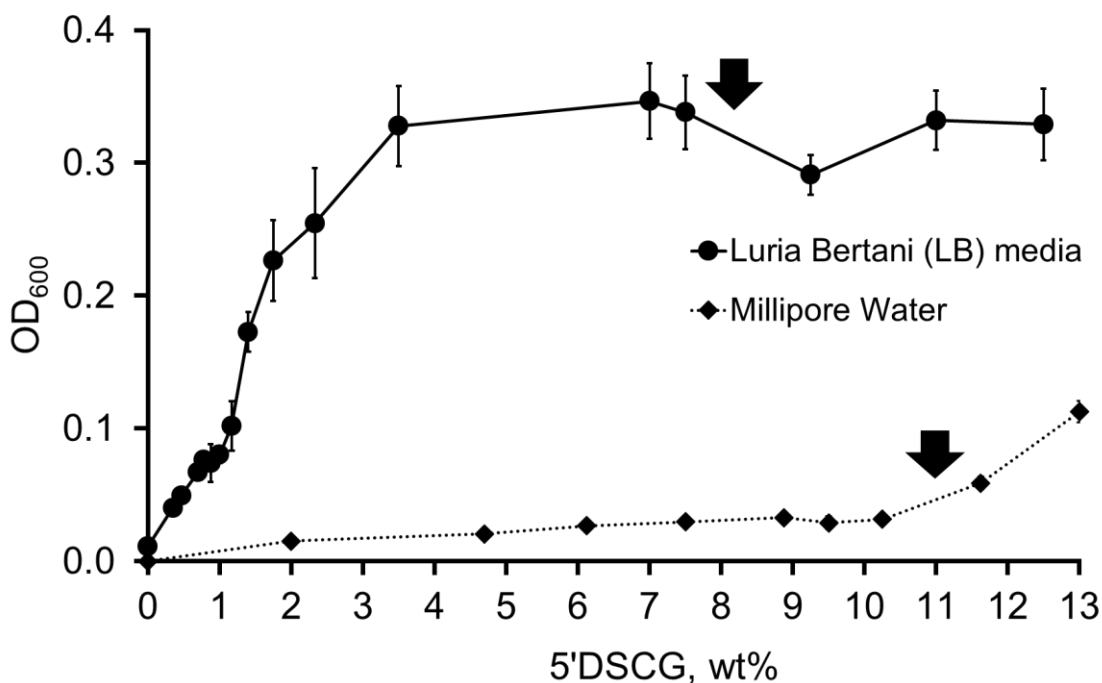


Figure 6.4 Optical density (OD₆₀₀) measurements versus the concentrations 5'DSCG in deionized water and in LB medium. Arrows indicate the concentrations at which the liquid crystal (LC) phase forms.

To confirm that the rise of the (OD₆₀₀) readings is due to the assembly of 5'DSCG in LB media rather than the aggregation of LB components, we studied the proton NMR spectra of the

5'DSCG in D₂O and in LB media (Fig. 6.5). Proton (¹H) NMR has been used to study 5'DSCG assembly in solution.¹⁹¹ The self-assembly of 5'DSCG results in the slow diffusion of the molecules and causes the proton peaks to broaden in the ¹H NMR spectra. Furthermore, an upfield shift is usually observed due to the protons being shielded, resulting from the intramolecular assembly.^{171, 174, 191} These results enable a direct correlation between assembly characteristics and the identity of molecules that assemble in isotropic solutions. We prepared samples of 1.5 wt% of 5'DSCG and 2.5 wt% of 5'DSCG with and without LB components in D₂O (see Experimental section), as well as only LB components in D₂O. The presence of LB components (1 wt% tryptone, 1 wt% sodium chloride, 0.5 wt% yeast extract) caused the proton signals of 5'DSCG to broaden and shift upfield. When LB components were present in 1.5 wt% 5'DSCG, the isopropyl linkage protons H_e and H_f at 4.38 and 4.49 ppm were shifted upfield to 4.30 and 4.47 ppm, respectively. The aromatic protons H_d, H_a, H_c and H_b, at 6.52, 6.90, 6.99 and 7.57 ppm, were shifted upfield to 6.49, 6.85, 6.92 and 7.52 ppm, respectively. At this concentration (1.5 wt% of 5'DSCG), there was no significant broadening of the peaks observed due to the presence of LB components, but a new splitting fine structure of H_e was observed, suggesting a change in the molecular conformation. In contrast, for 2.5 wt% 5'DSCG with LB components, we observe significant broadening and upfield shifting of the peaks as compared to that without LB components. The isopropyl linkage protons H_e and H_f shifted upfield from 4.33 and 4.47 ppm to 4.24 and 4.45 ppm respectively; and the aromatic protons H_d, H_a, H_c and H_b, at 6.50, 6.87, 6.94 and 7.54, shifted upfield to 6.43, 6.80, 6.85 and 7.47 ppm, respectively. These results are consistent with the molecular aggregation of 5'DSCG,¹⁹¹ and that presence of LB components has caused assembly of 5'DSCG at concentration as low as 1.5 wt%. There was no noticeable peak broadening of the LB components with or without the presence of 5'DSCG.

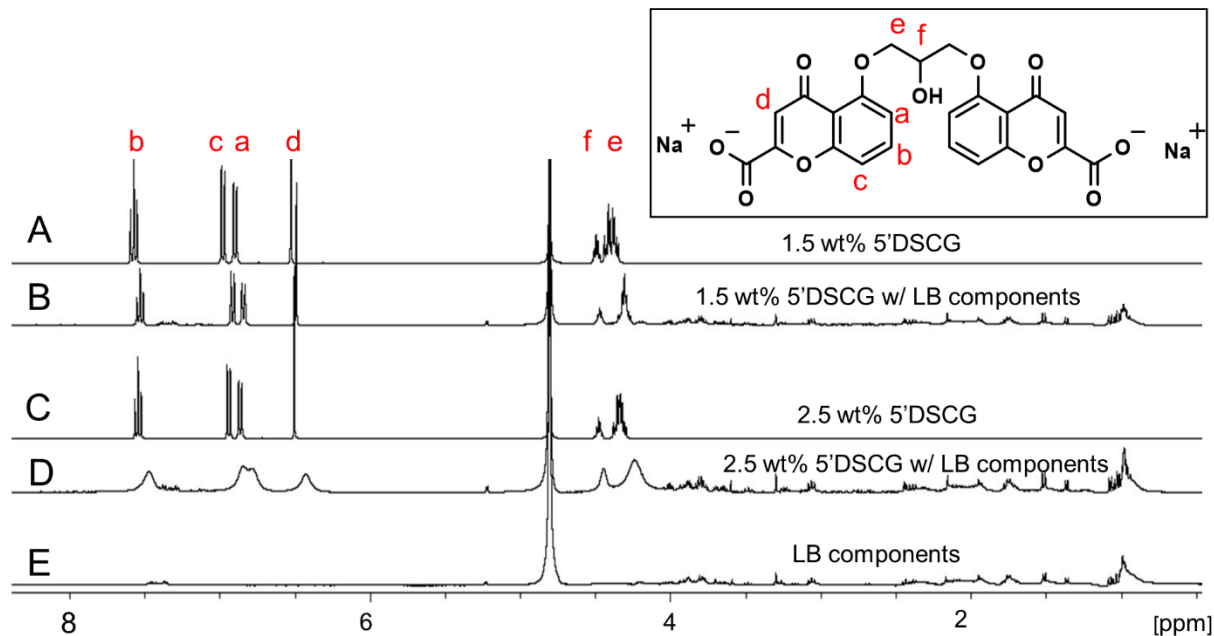


Figure 6.5 ^1H NMR spectra of 1.5 wt% of 5'DSCG without (A) and with (B) LB components, 2.5 wt% 5'DSCG without (C) and with (D) LB components, and (E) LB components in D_2O . The protons of 5'DSCG and peak assignments are labelled in red.

The observed peak broadening and shifts are consistent with the formation of slow tumbling assemblies of 5'DSCG in the solution. The past study by Robinson and co-workers showed that the proton NMR signals of 5'DSCG broaden and shift upfield rapidly from 1 wt% to about 6 wt%.¹⁹¹ Beyond 6 wt%, the peak broadening starts to plateau; however, the peaks continue to shift upfield. They suggested that the rapid peak broadening was caused by the formation of 5'DSCG oligomers that are not micelles, and that the slow tumbling at concentrations above 6 wt% were due to large micelle-like aggregates. Our results using light scattering revealed that in just water, no significant optical density reading was observed until the concentration of 5'DSCG reached 12 wt%. We believe that the light scattering measurement

is sensitive to large molecular assemblies, whereas NMR is sensitive to small molecular assemblies that lead to reduced molecular dynamics. Interestingly, we observed that the presence of LB components caused the optical density reading to increase when the concentration of 5'DSCG was as low as 1.5 wt% (Fig. 6.4). This result suggests the presence of certain components in the LB media promotes readily detectable and large isodesmic assemblies, whereas without the presence of additives, 5'DSCG may only progressively form small oligomers. Together, these results indicated that LB components have a significant impact on promoting 5'DSCG to form large aggregates in water, and these aggregates did not form liquid crystal phase until about 8 wt%. We note that the fine structure (splitting pattern) of ^1H NMR signal of the methylene unit of the isopropyl linkage (H_c) is more collapsed with the presence of LB components (Fig. 6.5B) than without LB (Fig. 6.5A). When the concentration of 5'DSCG is increased in water without LB components, we also observed similar collapse of the fine structure (Fig. 6.6). These results suggest that there is a change in the average conformation of the molecule when they are in the assembly in compared to when they are individually solvated in solution. However, the presence of LB components only lowers the concentration of assembly formation, without causing a significant difference to the assembly structure formed in just water without LB components.

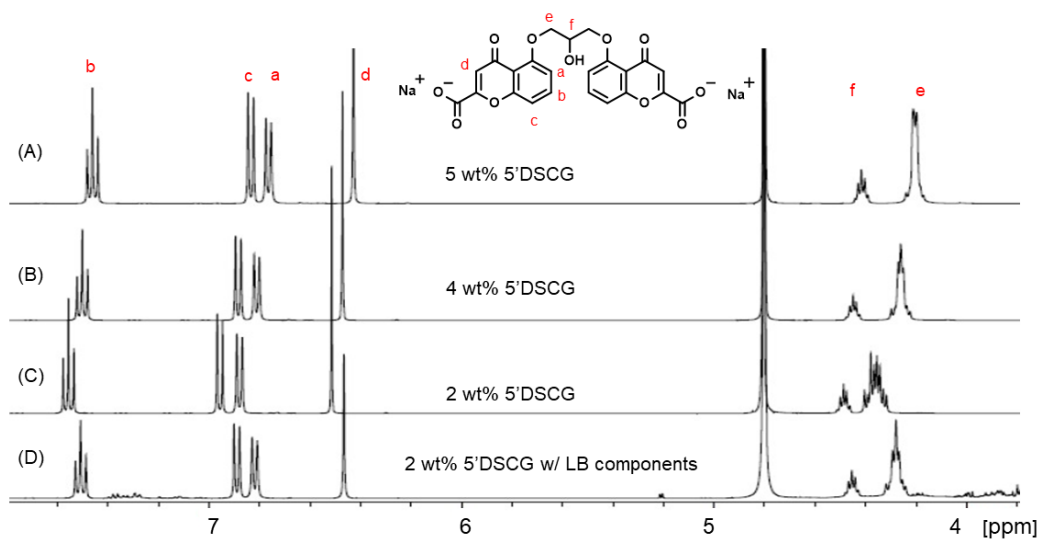


Figure 6.6 ^1H NMR spectra of 5 wt% 5'DSCG (A), 4 wt% 5'DSCG (B), 2 wt% 5'DSCG without (C) and with LB components (D) in D_2O . The protons of 5'DSCG and peak assignments are labelled in red.

To explore the assembly structure of 5'DSCG, we studied the Nuclear Overhauser Effect (NOE) of the sample with and without LB components. Examining the NOESY spectra of 5'DSCG (2 wt%) with LB components, we did not observe any NOE signals between the LB components and the 5'DSCG molecules (Fig. 6.7). This result suggests that there is no direct molecular interaction (within 5 Å) between 5'DSCG and LB components.

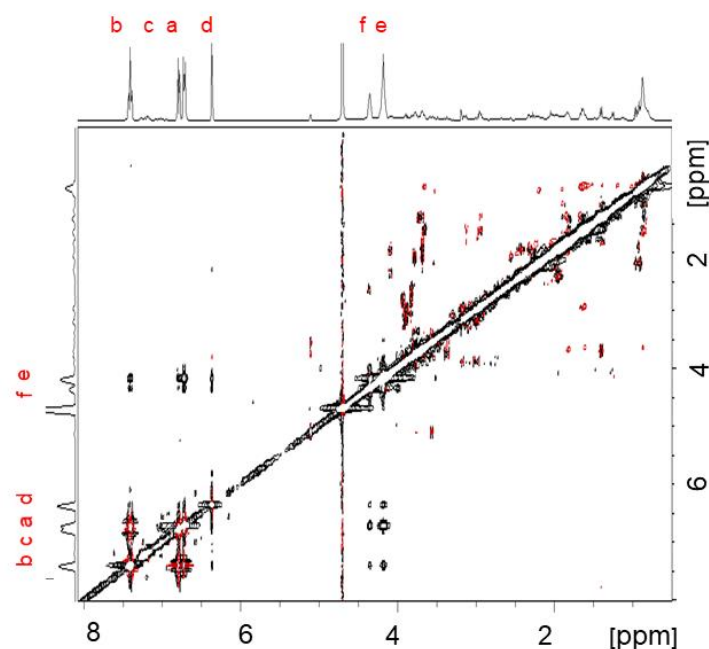


Figure 6.7 NOESY spectra of 2 wt% 5'DSCG with LB components (1 wt% sodium chloride, 1 wt% tryptone and 0.5 wt% yeast extract).

Comparing the NOESY spectra of 2 wt% 5'DSCG with and without LB components, we observed extra NOE signals for 5'DSCG when LB components were present (Fig. 6.7, 6.8) between the isopropyl linkage protons (H_e and H_f) and the aromatic protons (H_d , H_a , H_c , and H_b), which were not present in the sample without LB components. Furthermore, although an NOE between H_e and H_a is observed for both samples, this NOE signal is positive for the sample with LB components, and is negative for the sample without LB. The negative NOE signals suggest a fast dynamic of the conformational changes. Together, these results indicate that, without LB components, the negative NOE's are due to the intramolecular interaction between protons H_e and H_a within a 5'DSCG molecule. With LB components, cross peak 1 of protons H_f and H_d ; cross peak 2 of protons H_e and H_d ; and cross peak 5 of H_e and H_b are intermolecular NOE

transfers between stacked 5'DSCG molecules, whereas cross peak 3 of protons H_f and H_a/H_c, and cross peak 4 of protons H_e and H_a/H_c are the results of a mixture of intermolecular and intramolecular NOE signals.

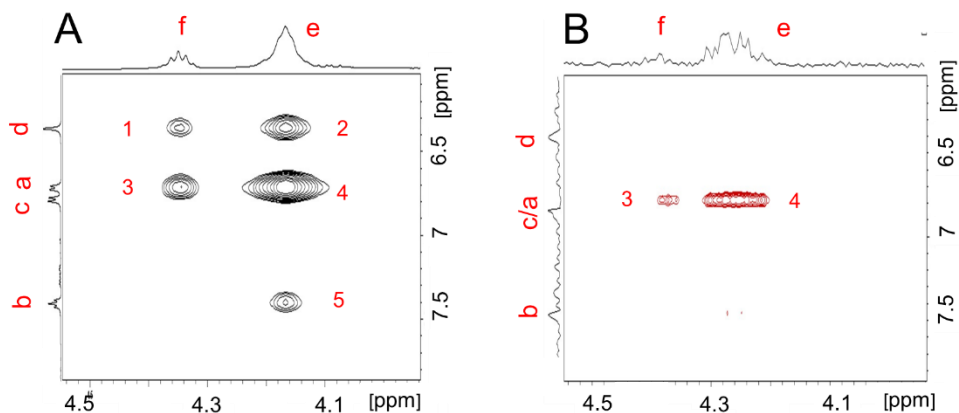


Figure 6.8 NOESY spectra of 2 wt% 5'DSCG with (A) and without (B) LB components in D₂O. With LB, cross peaks 1, 2, 5 are intermolecular NOEs; 3 and 4 are a mixture of inter- and intramolecular NOEs. Without LB, cross peaks 3 and 4 are intramolecular NOEs.

To confirm the nature of isodesmic assembly, we studied NOESY as a function of temperature. We first established that the assemblies “melted” at relative low temperature, at ~ 31-33°C. We then followed the NOEs of the protons of 5'DSCG (Fig. 6.8A-E) as a function of temperature between ambient condition (21 °C) to complete melting of the assembly. In general, we observed that as the temperature was decreased from 33 °C (when there was no intermolecular NOE observed), the intermolecular NOEs emerged and their intensities increased. Because cross peak 2 represents solely the NOE between the stacked molecules, this signal is an

indication of the assembly progression. Plotting the intensity of cross peak 2 versus temperature (Fig. 6.8F) reveals a curve of concave shape, rather than convex.

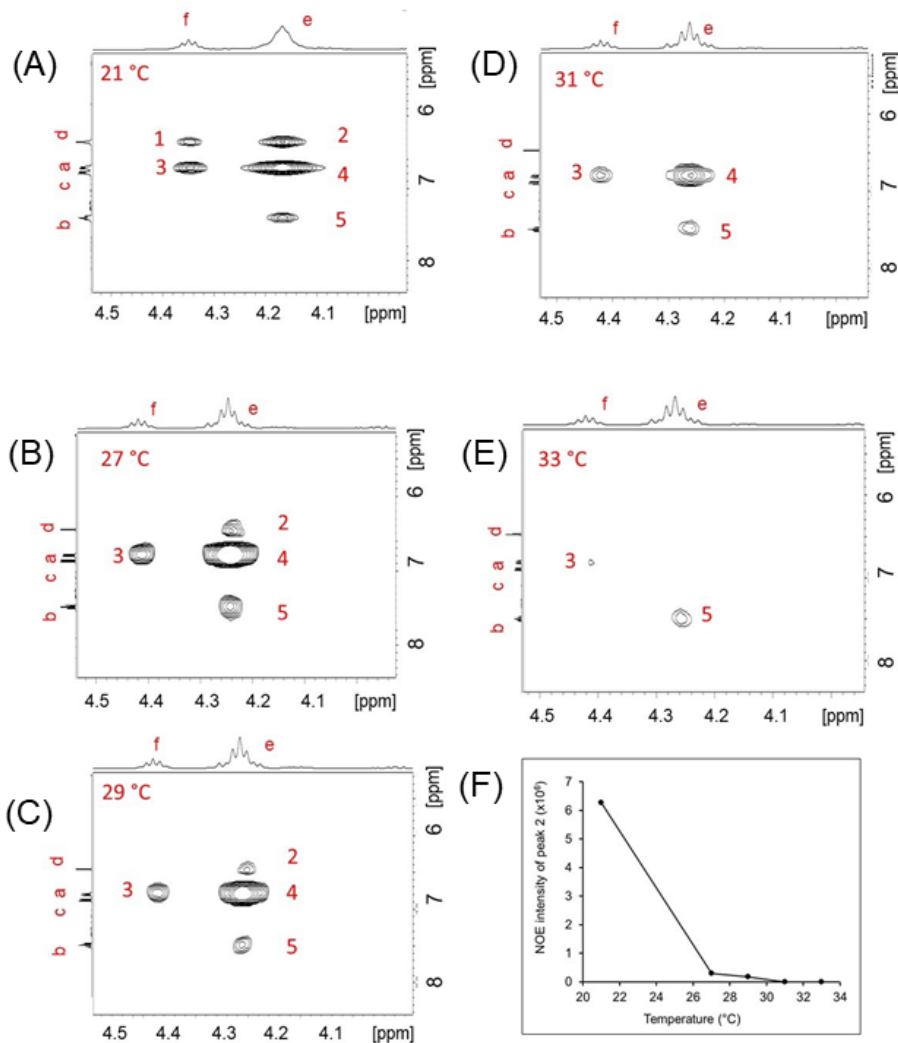


Figure 6.9 NOESY spectra of 2 wt% 5'DSCG with LB components at different temperatures: 221°C (A), 27°C (B), 29°C (C), 31°C (D) , and 33°C (E). Plot of NOE intensity of peak 2 vs. temperature (F).

We note that plots of intensity versus temperature for the all observed NOE signals from 5'DSCG exhibited a concave shape (Fig. 6.10). This concave relation supports that the

disassembly process are gradual, rather than cooperative, and is consistent with an isodesmic assembly or disassembly process.

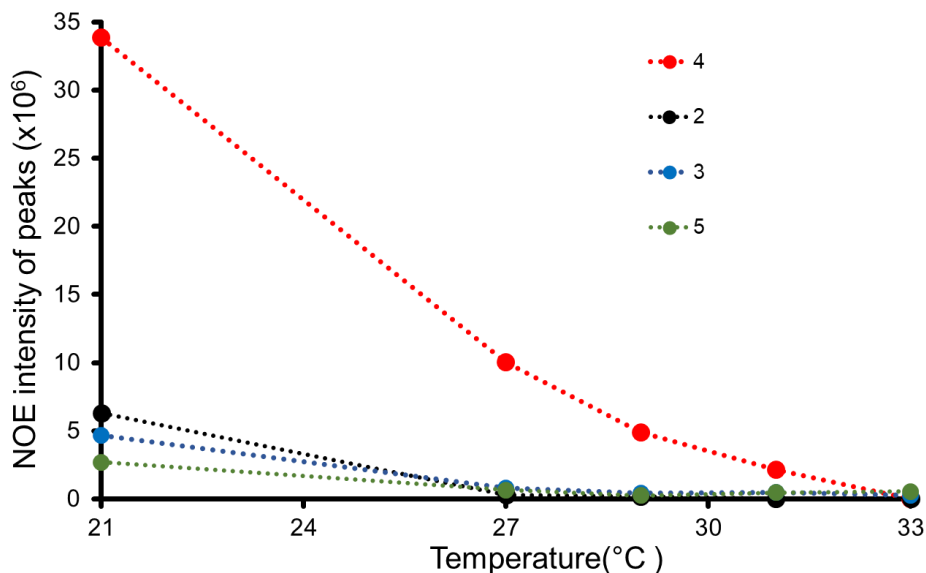


Figure 6.10 Plot of intensity of NOE cross peaks vs. temperature for 2 wt% 5'DSCG with LB components.

6.2.2 Peptides promote the isodesmic assembly of 5'DSCG.

LB media consists of 1 wt% tryptone, 1 wt% sodium chloride, 0.5 wt% yeast extract. The tryptone and yeast extract are mixtures of mainly peptides. We examined each of these three components individually to determine which component promoted the isodesmic assembly of 5'DSCG. At 7 wt% in water, 5'DSCG alone does not give a significant OD₆₀₀ reading. Adding each LB component at this 5'DSCG concentration can potentially induce the formation of 5'DSCG isodesmic assemblies leading to measurable optical densities (absorbance at 600 nm). We found that mixing 7 wt% 5'DSCG with tryptone or with yeast extract caused an increase in OD₆₀₀ readings, but at higher concentrations than they are in LB media. LB media contains 1

wt% of tryptone and 0.5 wt% of yeast extract. For tryptone alone, we observed increase in OD₆₀₀ only when the tryptone concentration reached 3 wt%. For yeast extract alone, we observed OD₆₀₀ increase only when the concentration reached 2 wt% (Fig. 6.11). Sodium chloride did not cause an increase in the OD₆₀₀ readings. These results led us to believe that peptides cause a demixing with 5'DSCG, which further promote 5'DSCG to form isodesmic assembly, while other ions only play a secondary role in assisting the demixing between peptides and 5'DSCG.

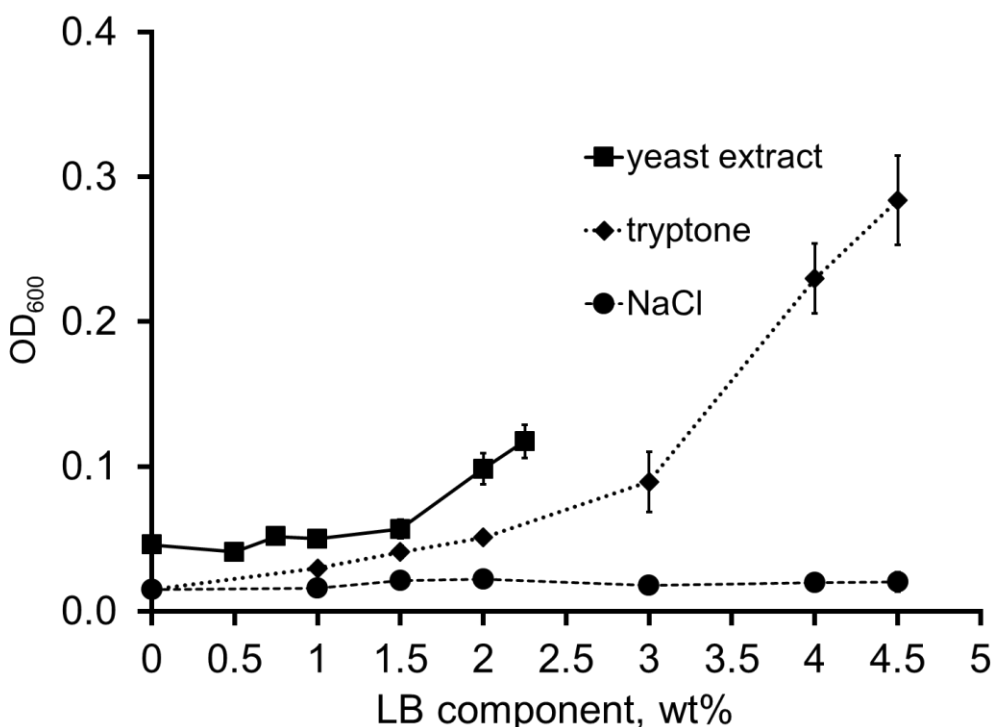


Figure 6.11 Optical density (OD₆₀₀) measurements of solutions containing 7 wt% 5'DSCG mixed with individual LB media components: yeast extract, tryptone and sodium chloride at different concentrations. (7 wt% 5'DSCG with yeast extract at concentration higher than 2.5 wt% caused precipitation).

We also tested peptone and casitone, which are similar peptide mixtures to tryptone used for culturing bacteria. Adding these peptide mixtures at similar concentrations as tryptone in LB media (~1 wt%) to a range of 5'DSCG concentrations revealed that these peptides also promoted the isodesmic assembly of 5'DSCG (Fig. 6.12). We observe a similar light scattering trend between the LB components (Fig. 6.4) and other peptides when added to a range of 5'DSCG concentrations. The addition of tryptone caused the OD₆₀₀ readings to increase at 2 wt% 5'DSCG and remained at a similar OD₆₀₀ (~0.2) for the rest of the high concentrations we studied. For peptone and casitone, the OD₆₀₀ readings started to increase at 2 wt% of 5'DSCG until reaching a plateau at around 6 wt% of 5'DSCG. Overall, these results show that among the LB media components, peptides are the primary cause for promoting assemblies of 5'DSCG in water that are detectable by light scattering.

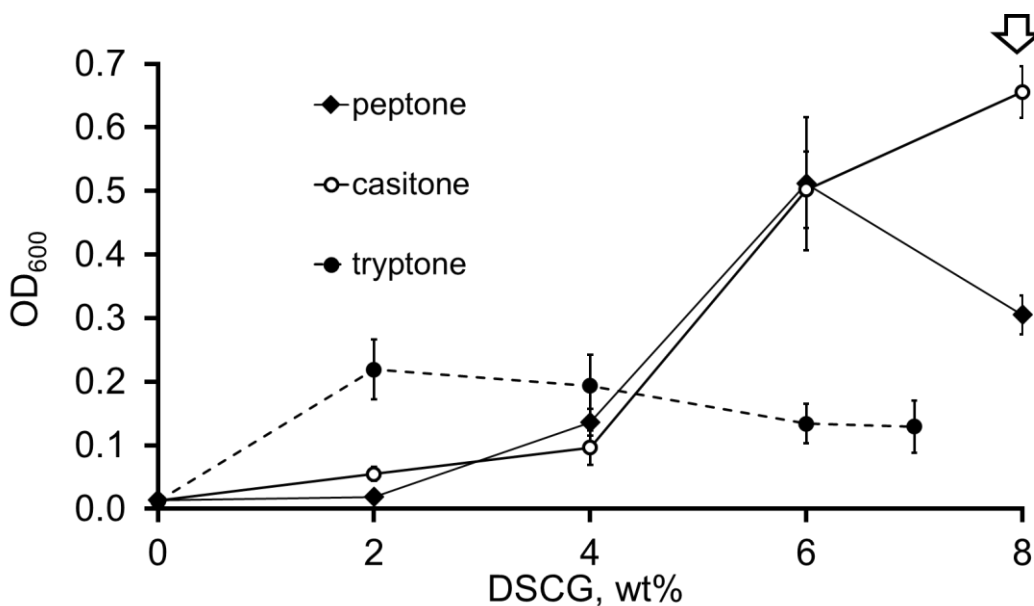


Figure 6.12 Optical density (OD₆₀₀) measurements of the solutions containing 1 wt% peptide mixtures (peptone, casitone, and tryptone) mixed with different concentrations of 5'DSCG. The arrow indicates 5'DSCG concentration at which the liquid crystal (LC) droplets appear.

While 1 wt% of these peptide mixtures promoted the aggregation signal of 5'DSCG differently, we explored the effect of different concentrations of peptide mixtures on a fixed amount of 5'DSCG (Fig. 6.13). We observed that the addition of increasing concentrations of peptides (peptone, tryptone, or casitone) to 3 wt% 5'DSCG caused the formation of isodesmic assemblies detectable by OD_{600} measurements. The amount of peptide needed ranges between 2 wt% to 4 wt% (peptone at ~2 wt%, casitone at ~3 wt%, and tryptone at ~4 wt%). The results suggest that effect of peptide on 5'DSCG is quite general.

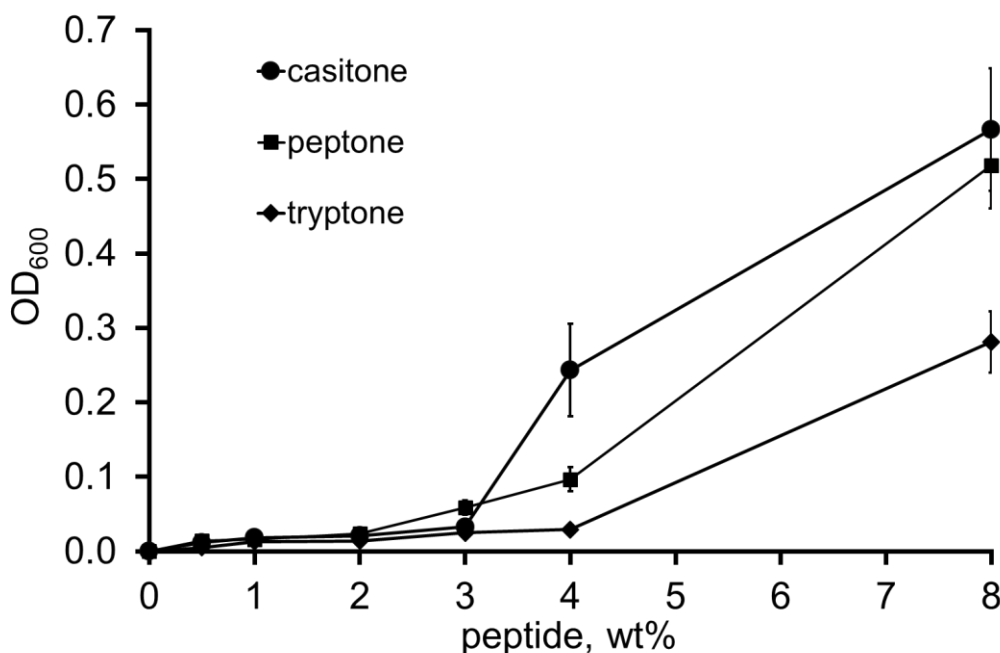


Figure 6.13 Optical density (OD_{600}) measurements of solutions containing 3 wt% 5'DSCG mixed with different concentrations of peptides: casitone, peptone, and tryptone.

Together, we believe that these results indicate a demixing process between the peptides and 5'DSCG molecules in solution. As the assemblies of 5'DSCG stay in solution rather than forming precipitates, we believe that water molecules are sequestered and bound to the

assemblies for solvation of the assemblies in water. Thus, the presence of peptides (~1 wt%) causes the transition of 5'DSCG (individual) → 5'DSCG (isodesmic assembly) in aqueous solution. To further confirm that peptides are the primary component that enabled the assembly of 5'DSCG, we tested components, including individual amino acids, salts, and urea, and found that none of these small molecules promoted the isodesmic assembly of 5'DSCG in solution (Fig. 6.14).

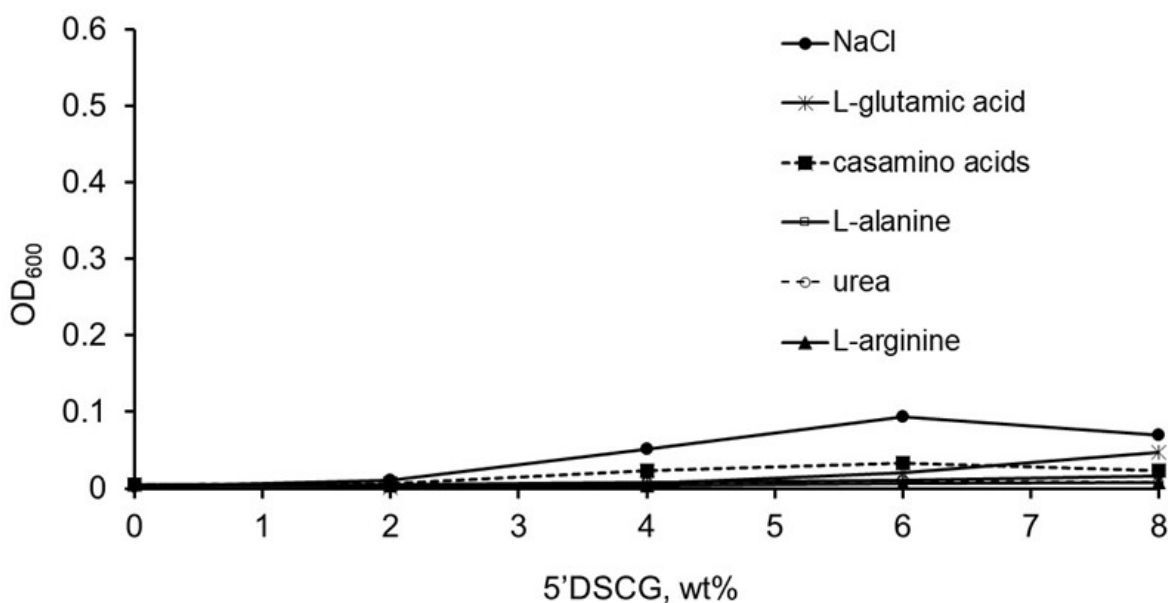


Figure 6.14 Optical density (OD_{600}) measurements of solutions containing additives: 4.6 wt% NaCl, 1 wt% casamino acids, 31.5 wt% urea, 8.53 wt% L- glutamic acid, 2.35 wt% L-alanine and 2.94 wt% L-arginine mixed with different concentrations of 5'DSCG.

6.2.3 Non-ionic polymers do not promote 5'DSCG to form isolated isodesmic assemblies

We have previously shown that certain non-ionic water-soluble polymers, poly-vinylpyrrolidone (PVP), poly-vinylalcohol (PVA), and poly-acrylamide (PAAm), when mixed with 5'DSCG, can cause a water-in-water emulsion, for which 5'DSCG assemblies align to form

water-based LC droplets in an aqueous solution.^{171, 173} Here, we study the effect of the three non-ionic polymers (PVP, PVA and PAAm) on the isodesmic assembly formation of 5'DSCG. The non-ionic polymers were mixed with isotropic solutions of 5'DSCG (7 wt%) and the optical density (OD_{600}) was measured as a function of the polymer concentration (Fig. 6.15). At 7 wt% 5'DSCG, we recorded the OD_{600} of the 5'DSCG/polymer mixtures when the PVP concentration reached 8 wt% and PVA concentration reached 4 wt%. LC droplet phases were also observed around these concentrations, indicating that the promotion of isodesmic assemblies is likely accompanied with formation of LC phases, and that there is a narrow range of concentration over which only isodesmic assembly forms. Interestingly, over a broad range of concentrations studied (0-12 wt%), PAAm did not cause any significant increase in OD_{600} readings when mixed with 7 wt% of 5'DSCG (Fig. 6.15).

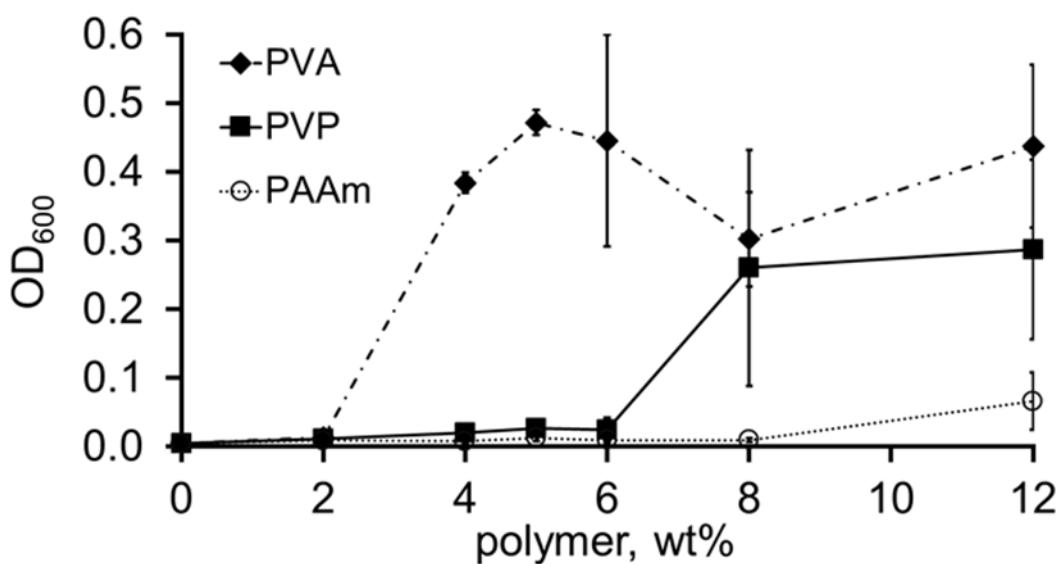


Figure 6.15 Optical density (OD_{600}) measurements of solutions containing 7 wt% 5'DSCG mixed with different concentrations of non-ionic polymers: poly-vinylalcohol (PVA, mw ~ 9,000-10,000), poly-vinylpyrrolidone (PVP, mw ~40,000), and poly-acrylamide (PAAm, mw~

9,000-10,000). Arrows indicate the polymer concentration mixed with 7 wt% 5'DSCG at which the the liquid crystal (LC) droplets appear.

Meanwhile, we also tested the effect of non-ionic polymers on 3 wt% 5'DSCG and no measurable isodesmic assembly was detected (Fig. 6.16). We note the liquid crystal phases mixed with isotropic solution was observed at 4 wt% and 5 wt% of PVA and PVP, respectively, which contributed to the large errors of the scattering at higher concentrations.

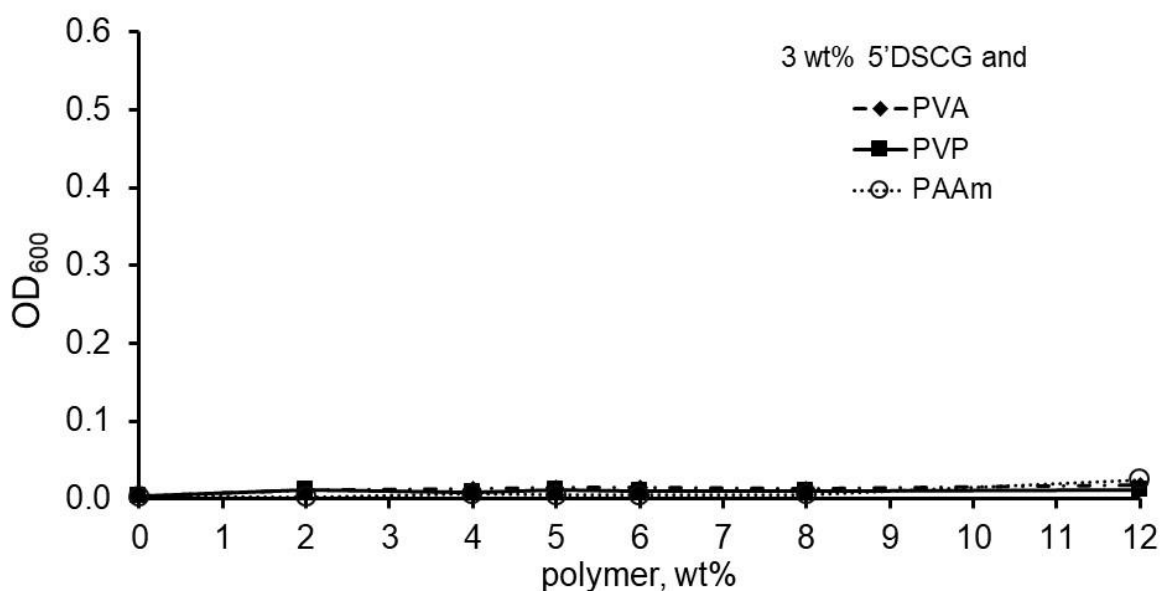


Figure 6.16 Optical density (OD_{600}) measurements of solutions containing 3 wt% 5'DSCG mixed with different concentrations of non-ionic polymers: poly-vinylalcohol (PVA, mw ~ 9,000-10,000), poly-vinylpyrrolidone (PVP, mw ~40,000), and poly-acrylamide (PAAm, mw~ 9,000-10,000)

Furthermore, we note that there is a correlation between the ability of a polymer to promote isodesmic assembly and the type of liquid crystal droplet that forms. Polymers, PVP and PVA, promoted isodesmic assemblies of 5'DSCG (along with liquid crystal droplets) at

relatively low concentrations, whereas PAAm did not promote isodesmic assembly. PVP and PVA cause spherical liquid crystal droplets with the 5'DSCG assemblies that align perpendicular to the droplet surfaces, whereas PAAm causes ellipsoidal droplets with the assemblies align parallel to the droplet surfaces (Table 6.1).

Table 6.1 Correlation between the effect of polymers on 5'DSCG assembly and the types of liquid crystal droplets promoted by the polymers.

	Isodesmic assembly ^a	Droplet shape ^b	Assembly orientation in droplets ^{c, d}
PVP	Yes ^e	Spherical ^c	Perpendicular ^f
PVA	Yes ^e	Spherical ^d	Perpendicular ^f
PAAm	No	Ellipsoidal ^d	Parallel ^f

^a By optical density measurement.

^b Shape of the water-based liquid crystal droplets in a polymer aqueous solution.

^c see ref. 23.

^d see ref. 13.

^e Mixed with liquid crystal droplets.

^f To the surface of the droplets

6.2.4 Protein aggregation is induced by 5'DSCG.

We examined the effect of presence of proteins on the assembly behaviour of 5'DSCG. The proteins have a lower solubility than peptides, and readily cause foaming when concentration increases. At the usual operable concentrations of proteins (0.5 to 5 mg/mL, or 0.05 to 0.5 wt%), we did not observe any promotion of isodesmic assemblies that is detectable by scattering. However, the formation of isodesmic assemblies of 5'DSCG in the presence of peptides does suggest a demixing process between the two components. In a previous work,¹⁶⁷ we have shown that 5'DSCG at a low concentration (~0.14 wt% or ~2.74 mM) caused the crystallization of lysozyme. Furthermore, 5'DSCG appears to be non-disruptive to protein folding by being able to facilitate the specific recognition and binding between proteins and their

antibody.¹⁶⁶ Based on these observations, we explore the use of 5'DSCG to precipitate or crystallize a range of different proteins in solution.

Chemical agents that can precipitate or aggregate proteins are critical for protein crystallization,¹⁹²⁻²⁰⁰ and yet, there is no theoretical or empirical set of rules to guide the choice of precipitants to crystallize a specific protein. For this reason, chemical screening kits have been developed to screen for the large sets of reagents and conditions for protein crystallization.¹⁹²⁻¹⁹⁶ Rather surprisingly, poly(ethylene glycol) (PEG) is often one of the major component for these kits and research.¹⁹²⁻¹⁹⁵ PEG does not denature proteins and presumably excludes proteins in the solution.¹⁹⁷⁻¹⁹⁹ Other non-denaturing chemicals such as cyclodextrins have also been used as nucleants for seeding of protein aggregates and crystals.²⁰⁰ For this consideration, we note that 5'DSCG also does not denature protein folding.¹⁶⁶ Furthermore, it appears that using PEG as a precipitant for protein crystallization requires a higher concentration range (~5-45 wt%)¹⁹³⁻¹⁹⁷ compared to 5'DSCG shown in this study (See below). Based on these observations, we explore the use of 5'DSCG to precipitate or crystallize a range of different proteins in solution. Here, we examined the effect of 5'DSCG on the aggregation or crystallization of a range of proteins, including lectin A, esterase, lipase, bovine serum albumin, trypsin and a pilin monomer from *Pseudomonas aeruginosa*, as well as the truncated version of the pilin protein monomer. Using hanging droplet setups and over the course of 5-15 days, we observed that the presence of 5'DSCG causes all proteins, except trypsin, to form aggregates (Fig. 6.17). In parallel, we also studied the effect of using sodium chloride in place of 5'DSCG at different concentrations. We found that sodium chloride is less capable of aggregating proteins; truncated pilin, trypsin and BSA did not form aggregate at the conditions we studied. A general feature of using 5'DSCG to

aggregate or precipitate proteins is that only relatively low concentrations of 5'DSCG are required.

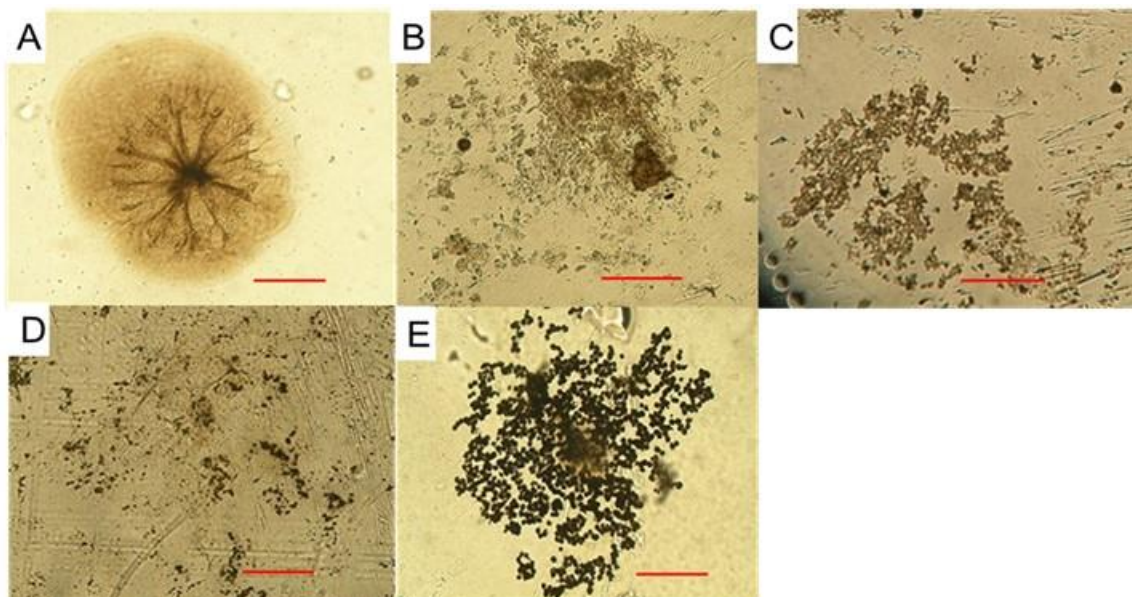


Figure 6.17 Different protein aggregates induced by 5'DSCG in hanging droplets. The droplets (5 μ L) contained (A) 0.625 wt% 5'DSCG and 25 mg/mL pilin, (B) 0.625 wt% 5'DSCG and 1 mg/mL lectin A, (C) 0.625 wt% 5'DSCG and 20.5 mg/mL esterase, (D) 0.625 wt% 5'DSCG and 20.5 mg/mL bovine serum albumin, and (E) 0.14 wt% 5'DSCG + 37.5 mg/mL lipase. The reservoir solution contained 350 μ L of (A, B, C, D) 1.25 wt% 5'DSCG, and (E) 0.28 wt% 5'DSCG. Hanging drops kept at ambient temperature were observed over 5-15 days. All solutions were prepared using 25 mM Tris buffer, pH = 7.5; except for (D) where pH = 6.5. Scale bar = 380 μ m.

Particularly, various concentrations of less than 1 wt% of 5'DSCG induced aggregation of the native pilin protein (Fig. 6.18, Table 6.2). These native pilin aggregates differ from other protein aggregates in two characters (Fig. 6.17, 6.18). First, there are branches extending from the center of the aggregation; and second, there is a dark circular region surrounding the

aggregate. We observe the same aggregate morphology for pilin when varying concentrations of 5'DSCG or sodium chloride was used (Fig. 6.18D). We believe that the dark region represents a concentrated solution of pilin protein.

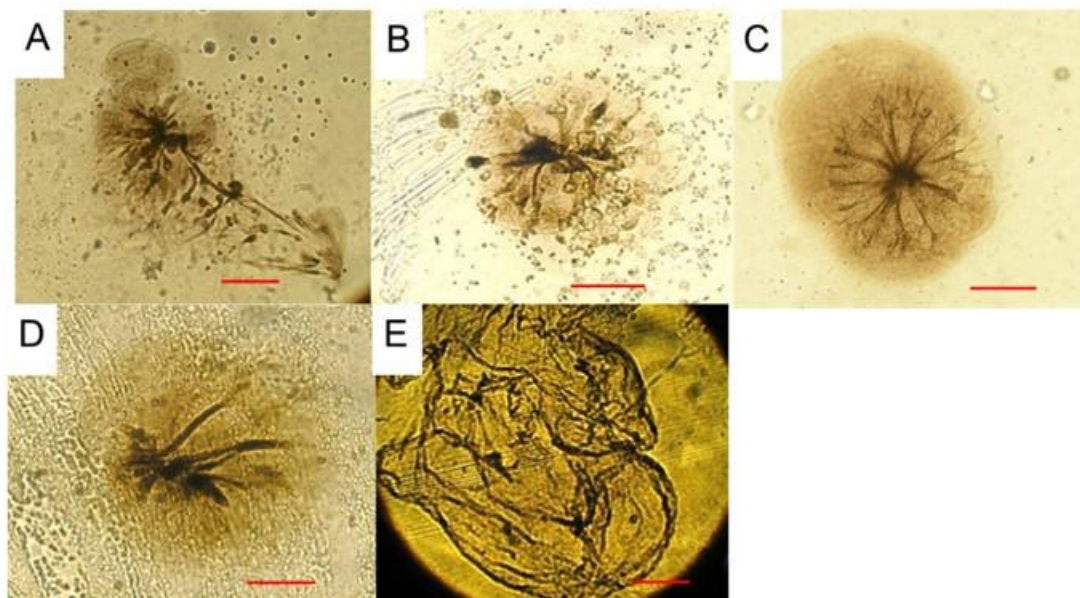


Figure 6.18 Native pilin aggregates induced by different precipitants in hanging droplets. The droplets (5 μ L) contained (A) 0.15 wt% 5'DSCG and 50 mg/mL pilin, (B) 0.375 wt% 5'DSCG and 5 mg/mL pilin, (C) 0.625 wt% 5'DSCG and 25 mg/mL pilin, (D) 0.5 wt% NaCl and 10 mg/mL pilin, and (E) 1.5 wt% PEG8000 and 5 mg/mL pilin. The reservoir solution contained 350 μ L of (A) 0.30 wt% 5'DSCG, (B) 0.75 wt% 5'DSCG, (C) 1.25 wt% 5'DSCG, (D) 1 wt% NaCl, and (E) 3 wt% PEG8000. Hanging drops kept at ambient temperature were observed over 5-15 days. All solutions were prepared using 25 mM Tris buffer, pH = 7.5. Scale bar = 380 μ m.

Table 6.2 Native pilin protein precipitation with NaCl and 5'DSCG as precipitants.

	Reservoir Solution			
	2.8 wt% NaCl	0.25 wt% 5'DSCG	0.5 wt% 5'DSCG	1 wt% 5'DSCG
5 mg/mL powder	no precipitate	with precipitate ¹	with precipitate ²	no precipitate
10 mg/mL powder	no precipitate	with precipitate ¹	with precipitate ²	no precipitate
20 mg/mL powder	no precipitate	with precipitate ¹	with precipitate ²	no precipitate

Precipitate observed after 3 days¹ and 5 days²

For the truncated pilin, pilin $\Delta(1-31)$, we observed birefringent crystalline aggregates induced by 5'DSCG (Fig. 6.19). Notably, the crystalline aggregates are smaller when a higher 5'DSCG concentration is used as a precipitant (Fig 6.19C, D vs. 6.19E, F). No aggregates were observed when sodium chloride was used to aggregate the truncated pilin. However, when sodium chloride was added with 5'DSCG together, the aggregates had smaller domains of birefringence and appeared to be more compact and polycrystalline (Fig. 6.19G, H). In contrast, although PEG also induced formation of aggregates for pilin and truncated pilin, the aggregate morphology is grossly different than those induced by 5'DSCG. The aggregates induced PEG are thread-like and spread out with aqueous solution in between the threads (Fig. 6.18E, 6.19I). These results, together with past studies,^{166, 167} suggest that 5'DSCG is a potent agent for inducing protein aggregation and when combining with other chemicals, has the potential to induce protein crystallization.

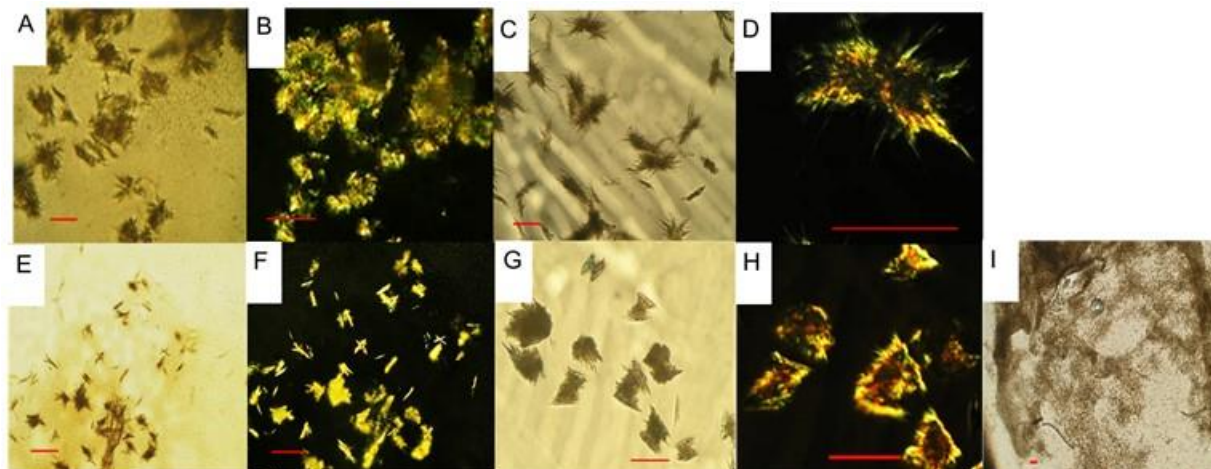


Figure 6.19 Truncated pilin (pilin $\Delta(1-31)$), aggregates induced by different precipitants in hanging droplet. The droplets (5 μL) contained 0.375 wt% 5'DSCG & 5 mg/mL truncated pilin, without polarizer (A), and under cross polars (B); 0.625 wt% 5'DSCG & 1 mg/mL truncated pilin, without polarizer (C), and under cross polars (D); 1.25 wt% 5'DSCG & 5 mg/mL truncated pilin, without polarizer (E), and under cross polars (F); 0.15 wt% 5'DSCG & 0.375 wt% NaCl & 2.5 mg/mL truncated pilin without polarizer (G) and under cross polars (H) and 25 wt% PEG4000 & 1 mg/mL truncated pilin without polarizer (I). The reservoir solution contained 350 μL of (A, B) 0.75 wt% 5'DSCG, (C, D) 1.25 wt% 5'DSCG, (E, F) 2.5 wt% 5'DSCG and (G,H) 0.3 wt% 5'DSCG & 0.75 wt% NaCl, and (I) 50 wt% PEG4000. Hanging drops kept at ambient temperature were observed over 5-15 days. All solutions were prepared using 25 mM Tris buffer, pH = 7.5. Scale bar = 76 μm .

6.3 Conclusion

We have demonstrated that measuring the light scattering (OD_{600}) of a solution is highly effective for detecting isodesmic assemblies of chromonic mesogens. We found that the presence

of peptides can promote the formation of isodesmic assemblies at low concentrations of 5'DSCG, as low as 1.5 wt% indicating a demixing between 5'DSCG and peptides in solution. The isodesmic assembly of 5'DSCG in solution is corroborated by the chemical shift changes and peak broadening of proton NMR signals of 5'DSCG. Water-soluble non-ionic polymers, PVP, PVA and PAAm, demix with 5'DSCG and promote 5'DSCG to form LC droplet phases, but do not promote isolated isodesmic assemblies. With this general demixing observation between 5'DSCG and other water-soluble molecules, we demonstrated that 5'DSCG also caused the aggregation of a wide range of proteins and have the potential to be a potent protein precipitant for enabling protein crystallization.

6.4 Experimental Section

6.4.1 Chemicals

Disodium cromoglycate (5'DSCG), 98% purity, was obtained from TCI Chemicals (Philadelphia, PA). Tryptone, yeast extract, sodium chloride, Tris base, urea, lauryldimethylamine N-oxide and poly(ethylene) glycol (PEG8000) were purchased from Fisher Scientific (Fair Lawn, NJ), and were used to make Luria Bertani media and buffers. All aqueous solutions were dissolved in deionized water with resistivity greater than 18.2 M Ω ·cm. or deuterium oxide (D₂O, 99.9%) (Cambridge Isotope Laboratories, Inc., Andover, MA). Casamino acids (Amresco, Solon, OH), peptone (Bio Basic, Amherst, NY) and casitone (BD Biosciences, MD). L-amino acids (L-glutamic acid, L- alanine, L- arginine), poly-vinylpyrrolidone (PVP, MW ~40,000), poly-vinylalcohol (PVA, MW ~ 9,000-10,000), poly-acrylamide (PAAm, MW~ 9,000-10,000), poly(ethylene) glycol (PEG4000), and proteins (lectin A, esterase, lipase, bovine serum albumin

and trypsin) were purchased from Sigma Aldrich (St. Louis, MO). *Pseudomonas aeruginosa* strain PA1244N3 (pPAC46) was from Dr. Castric and Dr. Horzempa.^{85, 88}

6.4.2 Preparation of Isodesmic assemblies of disodium cromoglycate (5'DSCG).

Deionized water was used to prepare all solutions. 5'DSCG were prepared in Luria Bertani (LB) media (1 wt% tryptone, 1 wt% sodium chloride, 0.5 wt% yeast extract), or mixed with additives including, peptides (peptone, casein, casein acids), amino acids (L-glutamic acid, L-alanine, L-arginine), urea; and non-ionic polymers, poly-vinylpyrrolidone (PVP, MW ~40,000), poly-vinylalcohol (PVA, MW ~ 9,000-10,000), and poly-acrylamide (PAAm, MW ~9,000-10,000). The optical density at 600 nm (OD₆₀₀) of each solution was measured in triplicates using Biotek ELx800 Microplate Reader.

6.4.3 ¹H NMR Spectroscopy Measurements

Stock solutions of 5'DSCG were prepared and dissolved in either deionized water or LB media (1 wt% tryptone, 1 wt% sodium chloride, 0.5 wt% yeast extract). The stock solutions were diluted with the same solvent (deionized water or LB media) to prepare 1 mL solutions with the final concentrations of 1.5 and 2.5 wt% 5'DSCG. The 1mL solutions were lyophilized overnight to remove H₂O. The resulting powder was dissolved in 1 mL D₂O to maintain the same 5'DSCG concentration of 5'DSCG. ¹H NMR spectroscopy measurements were done on 400-MHz Bruker spectrometer.

6.4.4 Pilin Expression

Both native and truncated native pilin expression were described in Chapter 2.

6.4.5 Hanging drops precipitation of proteins

Proteins (lectin A, esterase, lipase, bovine serum albumin, trypsin, whole and truncated pilin proteins from *P. aeruginosa*) were prepared in 25 mM Tris, pH=7.5 at varying concentrations. Reservoir solutions were prepared individually with different concentrations of NaCl or 5'DSCG in the same buffer, 25 mM Tris, pH= 7.5. Both protein and reservoir solutions were passed through a 0.2 μm syringe filter to remove any impurities. Hanging drops were prepared by mixing equal volumes (2.5 μL each) of the filtered protein- and reservoir-solution and suspending as an inverted drop on a coverslip over a well with 350 μL reservoir solution. Aggregation in the drops were observed within 5-15 days of incubation at ambient temperature.

Chapter 7. Exploring Filamentous Bacteria as Hosts for Protein Expression

7.1 Background and Significance

7.1.1 Antibiotics induce surface-mediated bacterial growth.

Previous studies led by Yuchen Jin from Luk lab have demonstrated that antibiotics, particularly β -lactams such as carbenicillin, colistin, aztreonam and penicillin induce the filamentous bacterial growth.¹⁷ These antibiotics are known to bind penicillin binding proteins and to alter the cell-wall of bacteria resulting in filament growth.²⁰¹ Filaments form as cells grow by elongation but does not undergo cell division.²⁰² In the same study, different conditions that result in filaments formation were identified.¹⁷ More filaments grow for bacteria in the lag phase than in the log phase, suggesting that antibiotic selection occurs to allow filament growth of the younger bacterial cells and kill the older ones. The process of filament formation is rapid, observed over a course of 2 hours then followed by detachment on the surface. Surface proteins also play a crucial role in the formation of filaments allowing for protein adsorption on surface to mediate the filaments to form. However, it is unclear if filament formation is exclusive for cells that express surface proteins. Filament formation is favored when bacteria are grown under stationary conditions compared to shaking conditions. It has been previously reported that filaments enhance bacterial adhesion on surfaces.²⁰³ Further confirmation that the surface chemistry affects the filament formation where APS-coated and plastic surfaces form more filaments than glass surfaces. Interestingly, in an effort to optimize the geometry of the container of filament for increasing the surface area and thus the amount of filaments produced, Felicia Burns from Luk lab showed that both increasing the surface area for filament attachment and maintaining oxygen gas accessibility are important. These efforts are

currently (Fall 2020) being pursued to engineer container for maximal filaments culture and production. Collectively, Luk lab has proposed a mechanism for filamentous growth, which starts with adhesion of bacteria on a surface, followed by the selection of the young bacteria at the lag phase followed by the elongation of the cells to form filaments then surface detachment. With the reported lifestyle of filaments, we believe that they can be candidates as hosts for protein expression by controlling their growth on surfaces and a rapid turnover of cell expressing proteins.

7.1.2 Chapter Aim: Explore filamentous bacteria for potential as protein expression hosts

We aim to use optimal conditions determined by Luk lab members to grow filamentous bacteria and explore these filaments as hosts for recombinant protein expression. It is unknown if cell lines such as *E.coli* BL21(DE3), specifically engineered protein expression and do not express fimbriae, are susceptible to antibiotic-induced filament formation.²⁰⁴ Using *E. coli* BL21 (DE3) carrying the pET-26b plasmid expressing proteorhodopsin, we explore the filament formation and protein expression of the filaments of this strain. Because filament growth is rapid, we would like to explore if protein expression can be maximized over a short time scale. Furthermore, attempts to identify, purify and quantify of proteorhodopsin from filamentous bacteria will also be discussed in this chapter.

7.2 Results and Discussion

7.2.1 Carbenicillin induces filament formation of *E. coli* BL21(DE3).

Filament formation of *E. coli* BL21 (DE3) containing plasmid expressing proteorhodopsin was performed under shaking conditions. The formation of filaments can be induced anywhere between 9 -100 µg/mL carbenicillin, as previously reported by Luk lab.¹⁷ We used 50 µg/mL carbenicillin to induce the filaments of *E. coli* BL21(DE3). Conditions similar to previously used by Luk lab were used to induce filament formation. Filaments were induced by adding carbenicillin at $A_{600} \sim 0.2$ with Carbenicillin and allowed to growth for 4 hours with shaking. After growing, we observe that the tube without antibiotics are cloudier than the tube without the antibiotics (Fig. 1). These results were consistent with previous findings where the filaments form a less turbid solution than the non-filaments. Measuring the absorbance at 600 nm (OD_{600}) cannot be used to detect the growth of filaments¹⁷ because the morphology between filamentous and regular bacteria are different. Aliquots (5 µL) of the cultures were sandwiched under two microscope slides and observed under the microscope (Fig. 7.1). The tube is turbid shows more spherical cells while the tube that is less turbid shows more elongated filamentous species. The images confirm that carbenicillin induces the formation of filamentous bacteria of *E. coli* BL21 (DE3).

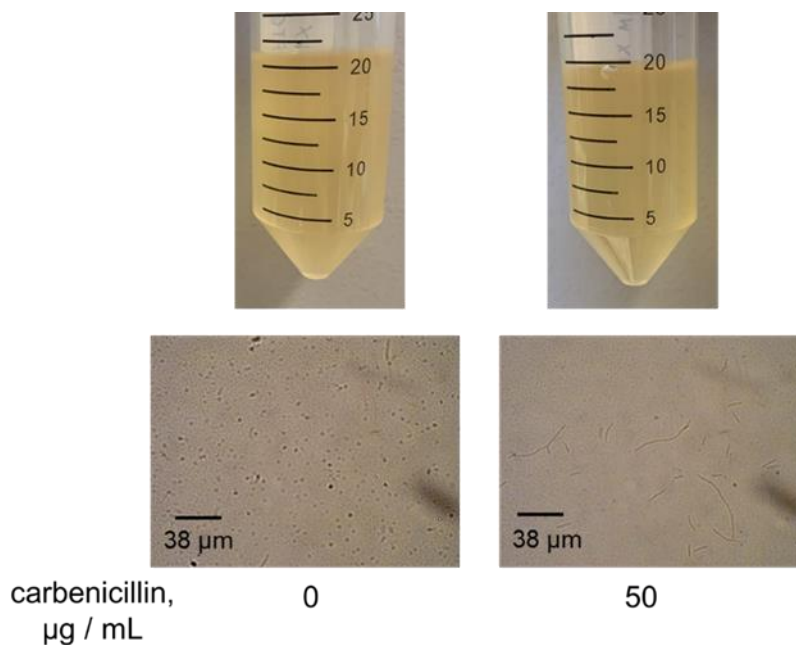


Figure 7.1 Cell cultures of *E. coli* BL21(DE3) with pET-26b plasmid expressing proteorhodopsin grown with shaking at 250 rpm, 37 °C (top) and microscope images of the cell culture (bottom).

7.2.2 Filament growth of E. coli BL21(DE3) is promoted by stationary growth and containers with a large surface area.

Carbenicillin filaments are believed to be mediated by surface attachment and stationary growth promotes more filaments to form.¹⁷ In addition, it was discovered by Felicia Burns from Luk lab that filaments grow on containers that have a larger surface area. We then grew the filaments under stationary conditions. Similar to previous experiments, the subcultures were grown to $A_{600} \sim 0.2$, then carbenicillin was added to a final concentration of 50 $\mu\text{g}/\text{mL}$ then poured on a plastic petri dish with 10-cm diameter and incubated at 37 °C for 4 hours without shaking. The appearance of the cultures in the petri dish without and with carbenicillin are distinct (Fig 7.2). The culture without carbenicillin looks homogenous while the culture of the

induced filaments shows the appearance of clumped white particles consistent with reports that filaments form aggregates.¹⁷ We then looked at both cultures under the microscope by taking 5 μL aliquots sandwich between glass slides (Fig. 7.2). We observe similar results as the shaking conditions. The culture without carbenicillin shows round cells, while the culture with carbenicillin shows filaments formed. These results indicate that stationary growth forms more filaments than under shaking conditions with the same carbenicillin concentration used (Fig 7.1 vs. 7.2). We also believe the increased surface area of the petri dish compared to the Falcon tube contributed to the increased filament formation.

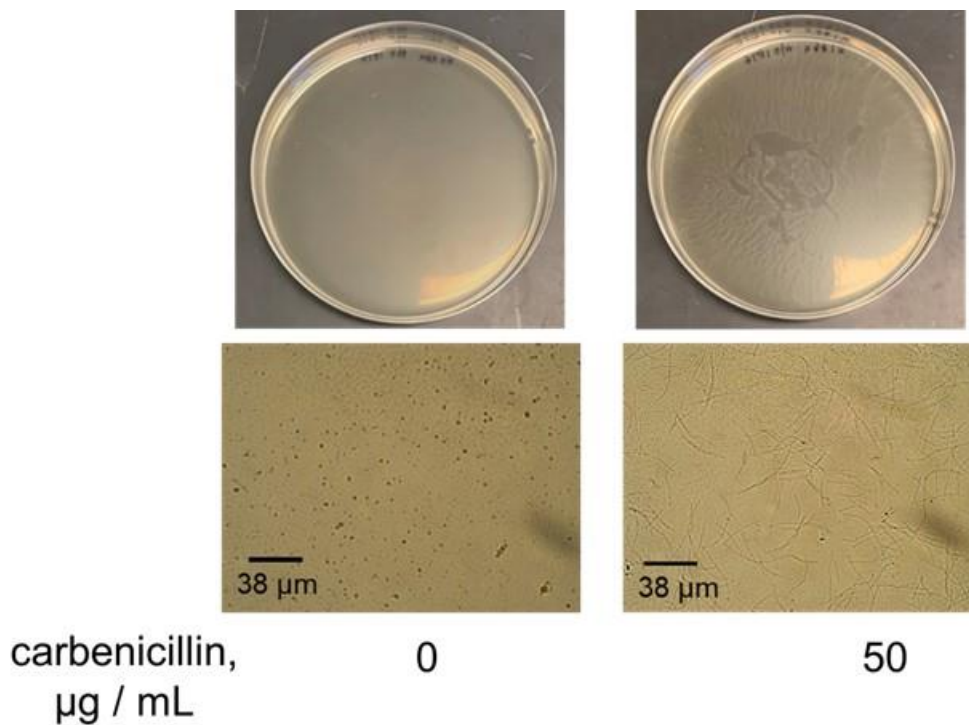


Figure 7.2 Cell culture of *E. coli* BL21(DE3) with pET-26b plasmid expressing proteorhodopsin grown under stationary conditions (top) and microscope images of the cell culture (bottom).

The concentration dependency of filament formation by *E. coli* BL21 (DE3) to the carbenicillin concentration was studied. Two carbenicillin concentrations were compared- 20 and 100 $\mu\text{g}/\text{mL}$ for stationary growth of filaments (Fig. 7.3). Our results show that more filaments are induced at 100 $\mu\text{g}/\text{mL}$ than 20 $\mu\text{g}/\text{mL}$. The higher carbenicillin concentration must provide a higher antibiotic stress to the lag phase bacteria, thus forming more filaments compared to the lower carbenicillin concentration.

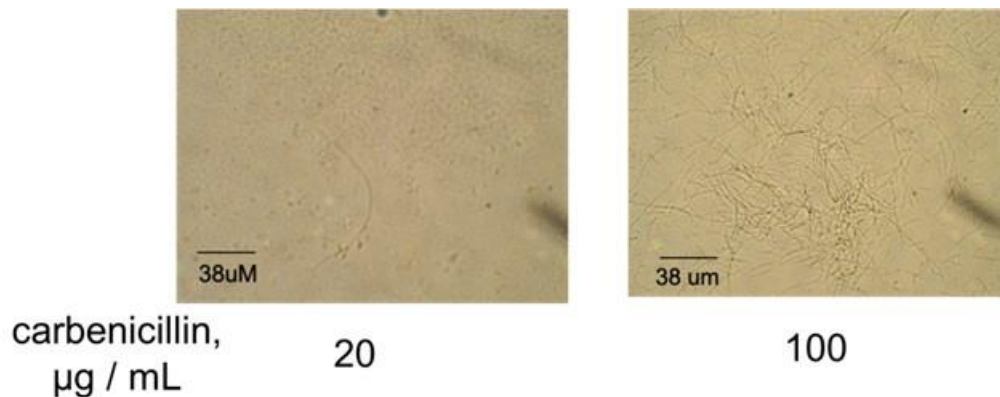


Figure 7.3 Images of *E. coli* BL21(DE3) with pET-26b plasmid expressing proteorhodopsin grown under stationary conditions at two different carbenicillin concentrations: 20 and 100 $\mu\text{g}/\text{mL}$.

7.2.3 Filament formation of *E. coli* BL21(DE3) favors plastic vs. glass substrates.

The effect of different surface to the growth of the *E. coli* BL21(DE3) filaments were then observed. Stationary growth of the filaments was performed on two different surfaces, on a 10-cm diameter plastic and glass petri dish (Fig. 7.4). Filaments were induced with 100 $\mu\text{g}/\text{mL}$ carbenicillin. More filaments are observed to grow on a plastic petri dish compared to a glass

petri dish, consistent with previous findings.¹⁷ These results would suggest that there could be some adhesion mechanism by *E. coli* BL21 (DE3) that interacts with the hydrophobic plastic surface of the plastic and promotes the formation of filaments. However, this mechanism still needs to be further characterized.

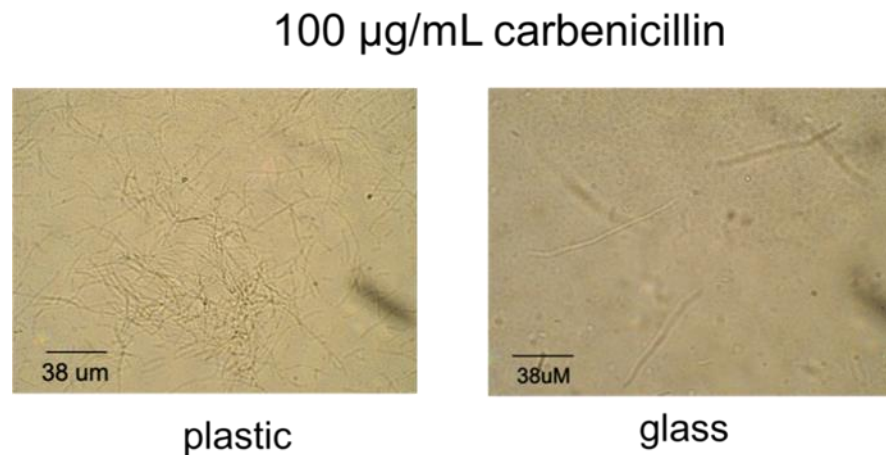


Figure 7.4 Images of *E. coli* BL21(DE3) with pET-26b plasmid expressing proteorhodopsin grown under stationary conditions with 100 µg/mL.

7.2.4 *Filamentous bacteria produce red cell pellets when proteorhodopsin expression is induced.*

The protein expression of filamentous bacteria was explored. Two controls were prepared. First, the filaments of *E. coli* BL21 without inducing the proteorhodopsin expression. Second, nonfilament *E. coli* BL21 induced to express proteorhodopsin. For filamentous bacterial protein expression, the proteorhodopsin expression was induced at the same time that the

filaments were formed, $A_{600} \sim 0.2$, then grown with shaking at 37 °C for four hours. The cell pellets for each culture were collected by centrifugation (Fig 7.5). The filaments without protein expression yielded a yellowish white cell pellet (85 mg/ 30 mL culture). The nonfilament with protein expression yielded a pinkish pellet (141 mg/ 30 mL culture). While the filament with protein expression yielded a dark red pellet (28 mg/ 30 mL culture). The resulting pink or red color indicates the presence of proteorhodopsin expressed indicating the formation of a Schiff base between all-trans retinal and proteorhodopsin.²⁰⁵ In addition, we also observe that the nonfilaments result in a heavier cell pellet than the filaments, and filaments that express proteins have lower cell pellet yield than filaments without proteins expressed. These results are consistent with the nonfilaments being able to divide while growing, while filaments can only elongate so the number of the cells would not increase. Furthermore, the process of protein expression could also add to the stress of the cells while they form filaments, hence the less cell pellet weight of the filament without and with induction (85 vs. 28 mg).

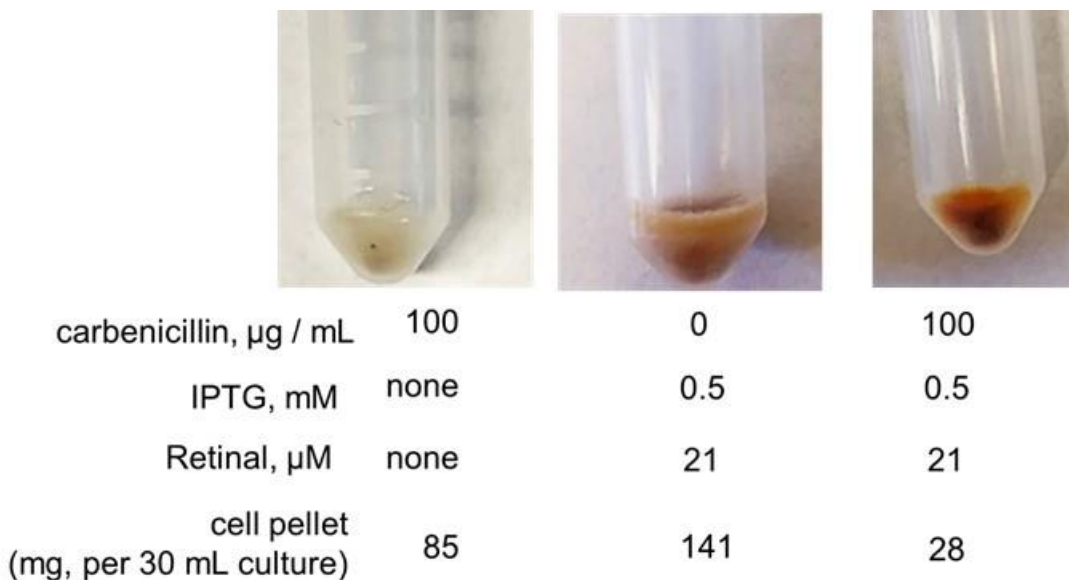


Figure 7.5 Cell pellets of *E. coli* BL21(DE3) with pET-26b plasmid expressing proteorhodopsin grown under shaking conditions. The growth conditions are indicated for each tube, chemicals were added at $A_{600} \sim 0.2$ for all tubes.

Next, the proteorhodopsin expression was checked by UV-Vis spectroscopy. Proteorhodopsin can be detected at $\lambda_{\text{max}} = 520 \text{ nm}$.²⁰⁵ The cell pellets were re-suspended in 0.9 wt% saline and the absorbance of the solution was measured (Fig. 7.6). We observe a slight peak at $\sim 520 \text{ nm}$ for the filaments with induced protein expression, but we do not observe this peak for the uninduced filaments. We also would like to note that the filaments are slimy and difficult to resuspend in saline. Only some cells would re-suspend and most of the pellet settles at the bottom even when more saline was added which poses a challenge for the detection of proteorhodopsin by UV-Vis spectroscopy. For absorbance measurements, only the liquid was measured leaving the undissolved cells in the tube.

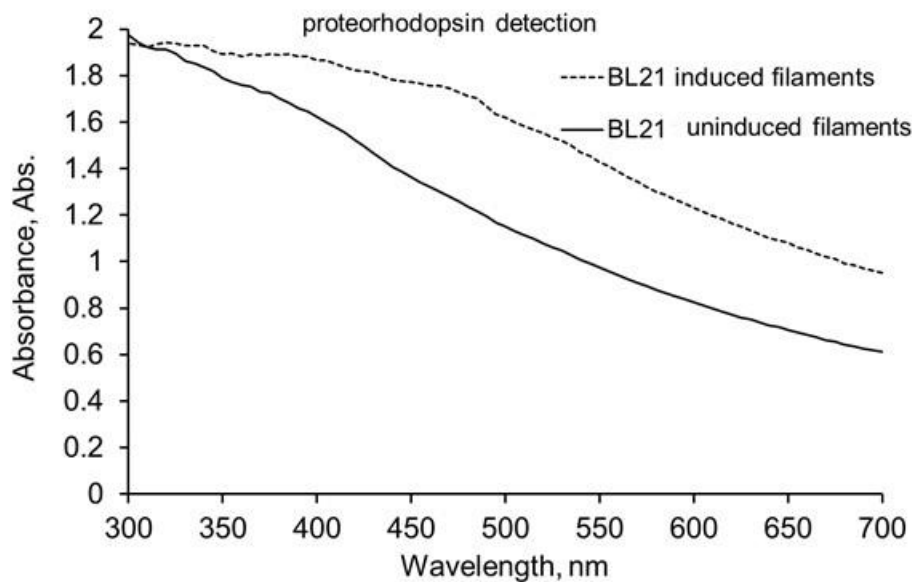


Figure 7.6 Absorbance spectra of resuspended filaments *E. coli* BL21(DE3) with pET-26b plasmid expressing proteorhodopsin in 0.9 % NaCl solution.

The effect of adding different carbenicillin concentrations to the protein expression was studied (Fig. 7.7). Carbenicillin was added at 6, 13, 33 and 66 $\mu\text{g}/\text{mL}$ to the cells and were induced to express protein at the same time. We observe that the higher the carbenicillin culture, the less cell pellet mass is produced, but the redder the cell pellet is. These results would indicate that the higher carbenicillin concentration produces more filaments and more proteorhodopsin. The resulting cell pellets were also slimy and difficult to re-suspended in saline. The resulting solution of re-suspended pellets and the absorbance was measured (Fig 7.7). We observe an inverse relationship between the carbenicillin added and the intensity of the absorbance peaks. There are two possible explanations for the results. First, this could possibly be because of the weight of the resulting cell pellets where the lowest carbenicillin concentration produces more pellets than the higher concentrations of carbenicillin, hence the absorbance at 6 $\mu\text{g}/\text{mL}$ is higher

than 13 $\mu\text{g}/\text{mL}$, 33 $\mu\text{g}/\text{mL}$ and 66 $\mu\text{g}/\text{mL}$. Second, since the filaments are difficult to resuspend, most the filaments that settle at the bottom of the tube still contain the proteorhodopsin and this undetected by the UV-Vis.

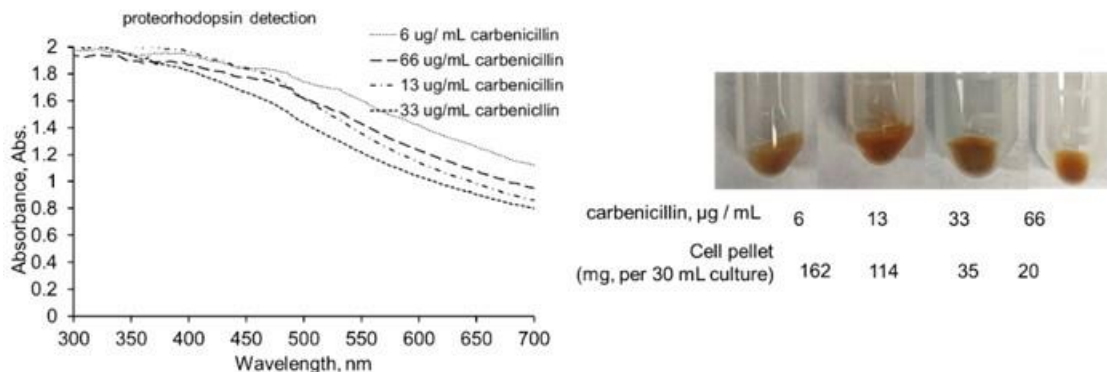


Figure 7.7 Absorbance measurements of the resuspended filaments from 300 -700 nm (left). Cell pellets of induced filaments of *E. coli* BL21(DE3) with pET-26b plasmid expressing proteorhodopsin grown under shaking conditions with different carbenicillin concentrations. The growth conditions are indicated for each tube. All tubes have 0.5 mM IPTG and 21 μM retinal (right).

To solve the difficulty in resuspending the filaments, we tried to resuspend induced filaments in buffer sonicate using a tip sonicator to completely break down the cells (Fig 7.8). The resulting solution was shown to have an intense yellow color which could indicate that the proteorhodopsin has denatured and free retinal is released in the solution, also confirmed by the UV-Vis measurements (Fig. 7.9). The peak observed in between 300-400 nm indicate the free retinal in the solution.²⁰⁶

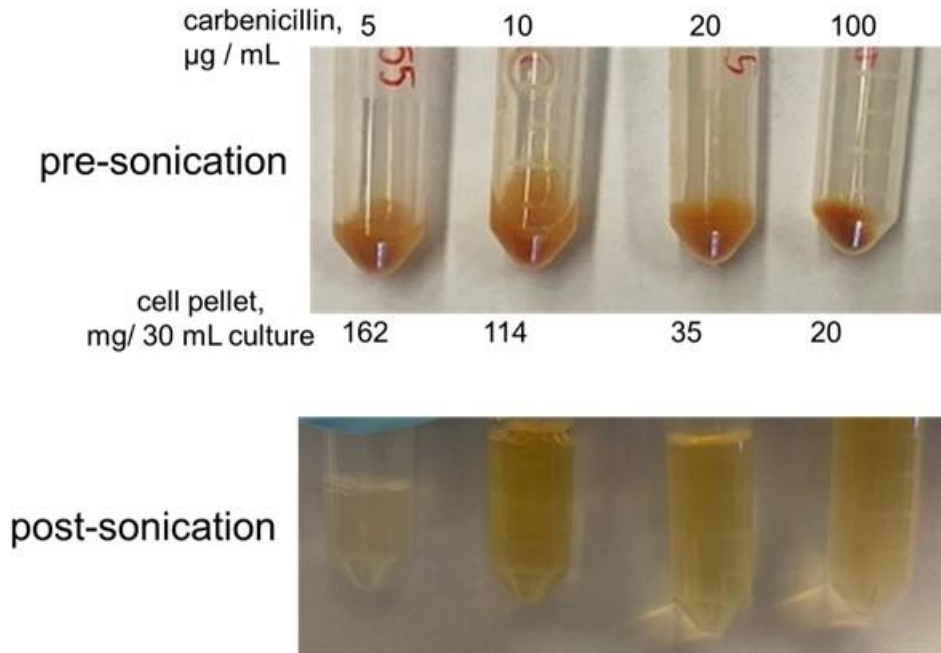


Figure 7.8 Cell pellets of induced filaments of *E. coli* BL21(DE3) with pET-26b plasmid expressing proteorhodopsin grown under shaking conditions with different carbenicillin concentrations (top). Post-sonication solutions (bottom). Filaments were resuspended in 50 mM HEPES, 150 mM KCl, 2% D β M and 0.5 mM PMSF, pH = 7. All tubes have 0.5 mM IPTG and 21 μ M retinal.

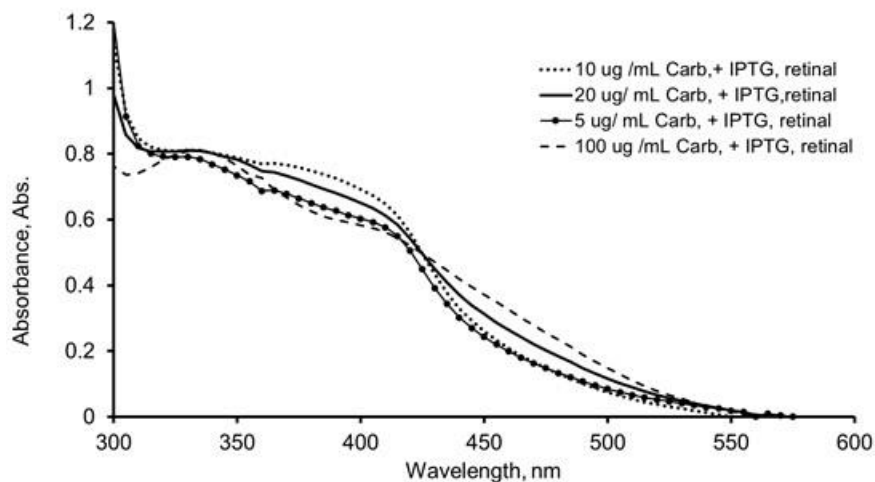


Figure 7.9 Absorbance measurements of the sonicated *E. coli* BL21(DE3) with pET-26b plasmid expressing proteorhodopsin grown under shaking conditions filaments from 300-600 nm.

Proteorhodopsin expression by filaments, induced with 50 $\mu\text{g}/\text{mL}$ carbenicillin, grown stationary on different surfaces (plastic vs. glass petri dish) (Fig. 7.10). Consistent with previous results, more filaments formed on the plastic rather than the glass petri dish. While the resulting cell pellets had color, the color is yellow. An attempt to measure the absorbance of the filaments were performed, but the resulting pellets were too small, and the absorbance spectra showed no significant peaks.

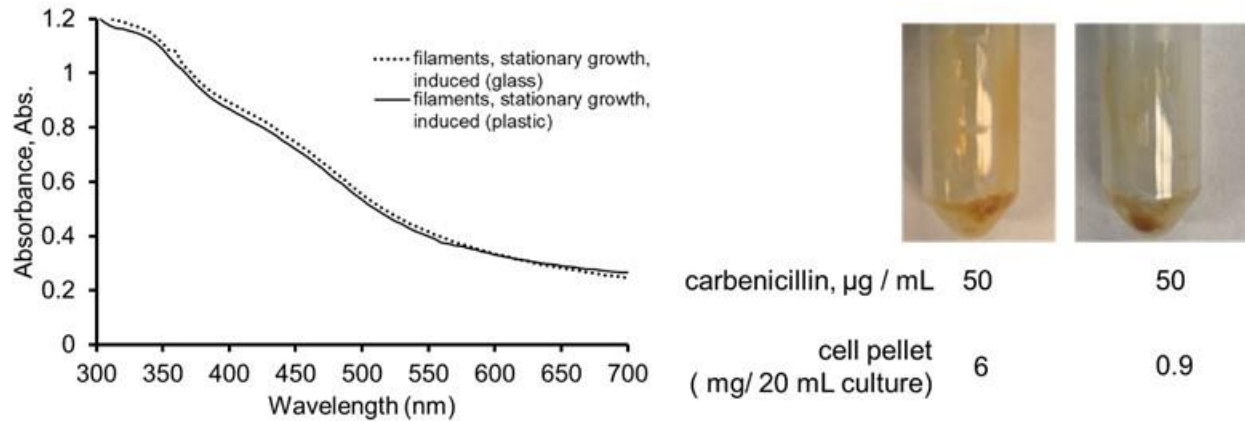


Figure 7.10 Absorbance measurements of the resuspended filaments from 300 -700 nm (left). Cell pellets of induced filaments of *E. coli* BL21(DE3) with pET-26b plasmid expressing proteorhodopsin grown under stationary conditions with different carbenicillin concentrations. The growth conditions are indicated for each tube. All tubes have 0.5 mM IPTG and 21 μM retinal (right).

7.3 Conclusion

We have demonstrated that previously determined optimal conditions for filament growth of fimbriated bacteria can also induce the filament growth of *E. coli* BL21 (DE3) with the plasmid expressing proteorhodopsin. These conditions include inducing filament formation with carbenicillin concentrations from 6-100 $\mu\text{g}/\text{mL}$, more favorable filament growth in plastic compare to glass substrates, and more filaments observed in a container with a larger surface area. As this strain is reported to have no fimbriae, the mechanism of filament formation is still unclear and yet to be determined. Inducing the filaments to express proteorhodopsin results in a colored pellet with a reddish color characteristic of a successful proteorhodopsin expression by cells. The filaments are quite slimy posing a challenge to handle for further studies. Attempts to

quantify and purify the proteorhodopsin were made, however, these were unsuccessful. This is an avenue that need to be explored in the future. Overall, this chapter has provided insight that filaments can potentially be used as a protein expression host given the short time needed to express proteins.

7.4 Experimental Section

7.4.1 Aerobic filament growth and protein expression.

Grow the frozen stock of bacteria (*E. coli* BL21(DE3) with pET28b expressing proteorhodopsin (a gift from Dr. John Franck) in LB, shaking at 250 rpm, 37 °C, overnight. The next day, subculture the bacteria by pipetting 150 µL of the overnight culture into 15 mL of LB media. Two 15 mL of LB treated with 3 µg/mL, 6 µg/mL, 13 µg/mL and 66 µg/mL of carbenicillin each were prepared. The subcultures were grown for ~2 hours to reach OD₆₀₀~ 0.2, shaking at 250 rpm, 37 °C. After 2 hours, the corresponding Carbenicillin concentrations (3 µg/mL, 6 µg/mL, 13 µg/mL and 66 µg/mL) were added to each set (2 x 15 mL) of the subcultures, followed by adding 15 µL of 21 mM retinal to achieve 21 µM retinal and 7.5 µL of 1 M IPTG to achieve 0.5 mM IPTG in each 15 mL subculture. The Falcon tubes were covered with foil and allowed to shake at 250 rpm, 37 °C for 4 hours to induce the filament formation. After 4 hours, the cultures were spun down for 20 minutes at 6000 rpm, RT. Discard the supernatant. To lyse the cells, resuspend the pellet in 1 mL buffer (50 mM HEPES, 150 mM KCl, 2% DβM and 0.5 mM PMSF, pH = 7) and sonicate 3 seconds sonicate, 3 seconds break for 2 minutes. The supernatant was subjected to UV-Vis measurements to check a peak at 520-580 nm.

7.4.2 Stationary filament growth and protein expression.

Grow the frozen stock of bacteria (*E. coli* BL21DE3) overnight in LB, shaking at 250 rpm, 37 °C. The next day, subculture the bacteria by pipetting 200 µL of the overnight culture into 20 mL of LB media. The subcultures were grown for ~2 hours to reach OD₆₀₀~ 0.2, shaking at 250 rpm, 37 °C. After 2 hours, the carbenicillin was added to achieve 20 ug/mL and 100 ug/mL in the subculture, followed by adding 21 µM retinal and 0.5 mM IPTG to both subcultures. The IPTG-induced subcultures were poured in separate petri dishes (glass and plastic), then covered with the lid. The petri dishes were placed in the incubator for 4 hours at 37 °C. After 4 hours, the cultures were pipetted from the petri dish into a Falcon tube then spun down for 20 minutes at 6000 rpm, RT. Discard the supernatant. To lyse the cells, resuspend the pellet in 1 mL buffer (50 mM HEPES, 150 mM KCl, 2% DβM and 0.5 mM PMSF, pH = 7) and sonicate 3 seconds sonicate, 3 seconds break for 2 minutes. The supernatant was subjected to UV-Vis measurements to check a peak at 520-580 nm.

Chapter 8. Conclusions and Future Directions

8.1 Conclusions from this thesis

8.1.1 Clarification of the effect of individual components of rhamnolipids. The pili of *P. aeruginosa* control multiple bioactivities such as swarming motility. Rhamnolipids are biosurfactants produced by *P. aeruginosa* that are also important for the swarming motility of this bacterium. However, the role of each individual component -monorhamnolipid and dirhamnolipid to control swarming motility is not clear. In this thesis, we show that monorhamnolipid is more potent at controlling swarming compared to dirhamnolipid supported by the observed oscillation (promotion at low concentrations and inhibition at high concentrations) of the swarming motility of *P. aeruginosa* as a function of the monorhamnolipid concentration but not for dirhamnolipid.

8.1.2 Identification of pili as the receptor for rhamnolipids and synthetic ligands. Luk lab previously demonstrated the same specific control of rhamnolipids on the swarming of *P. aeruginosa*, but evidence of a ligand-receptor binding event that connects this swarming control to pili is lacking. The work in this dissertation provides a direct evidence that pili is the receptor for rhamnolipids (natural) and synthetic ligands primarily by fluorescence spectroscopy and transmission electron microscopy (TEM). Supporting evidence on the binding was also obtained by other characterization methods such as circular dichroism (CD), nuclear magnetic resonance (NMR) and dynamic light scattering (DLS), however, these are less compelling because of the small changes in the pilin conformation upon binding, and the high ligand concentration requirement.

8.1.3 Picomolar binding induces pilin protein assembly. Fluorescence spectroscopy results show that about 1 pM of ligands- monorhamnolipid, dirhamnolipid, SF β C and SF-EG₄OH is enough to saturate the fluorescence signal of 100 nM of truncated pilin. Furthermore, fluorescence spectroscopy also reveals that the ligand-binding induces pilin assemblies *in vitro*. Kinetic studies show that pilin assembly induced by monorhamnolipid occurs via the isodesmic process. Transmission electron microscopy (TEM) was used to visualize the assemblies, showing that rhamnolipids and SF β C induce two different pilin assemblies, linear and amorphous, respectively.

8.1.4 Bacterial Motility Enabled binDing assay (BMED). Most importantly, we obtained direct binding evidence of pilin to ligands from a new design of ligand receptor binding assay by utilizing bacterial swarming motility. In this assay, we added microliter droplets of pilin on the surface of solidified soft hydrated gel followed by the inoculation of the *P. aeruginosa*. The bacterium does not swarm where the droplet is placed but swarms around the vicinity of the droplet. The result of this assay demonstrates that the added pili on the surface of the gel inhibits the swarming of the wild type *P. aeruginosa* by binding and sequestering the rhamnolipids secreted by the bacterium. Spreading the pilin on the surface of the soft hydrated gel also inhibits the swarming of the wild type strain by sequestering rhamnolipids and also binds to synthetic inhibitors added in the soft gel to reactivate the swarming motility of *P. aeruginosa*.

8.1.5. Mutant study is consistent with D-loop being the binding pocket. This work involves the expression of truncated pilin mutants in *E. coli* BL21(DE3) using recombinant

techniques and evaluated their binding to rhamnolipids using BMED. Our results show that deleting 31 amino acids is the minimum structure that inhibits swarming and thus, binds to rhamnolipids. Three single amino acid mutants in the D-loop of the truncated pilin $\Delta(1-31)$ were also expressed and tested by BMED, showing that these mutants were inactive for swarming inhibition, thus do not bind to rhamnolipids. Collectively, these results confirmed that the D-loop in the C'-terminal globular head of pilin is an important region for recognizing and binding rhamnolipids and the synthetic ligands.

8.2 Future work and thoughts:

8.2.1 Hypothesis of Chemo mechanics: alpha-helix and beta-sheet sequence shift to transmit signals and control extension and retraction, and motilities. It is widely recognized that the filamentous pili assembly is driven by the hydrophobic interactions and subsequent insertion of the α -helices in the core of the circular, helical assembly with 4-6 monomers per turn and the C'-terminal globular heads are exposed at the surface of the pili assembly (Fig 8A, B).^{24, 84, 207} However, the exact role that the C'-terminal globular head plays in the assembly is poorly understood. In particular, the chemo mechanics of the pili assembly and how the tip-binding of pili transmits signals through the pili assembly and cause the depolymerization of the pilin monomers (retraction) and assembly (extension) resulting in different bioactivities remains a big question. We hypothesize that stacking of each circular assembly of the pili is also aided by the C'-terminal globular head, in particular, the D-loop. We propose that ligand binding and surface attachment of the D-loop causes a conformational change in the pilin monomer that alter the β -

sheet and α -helix content, resulting in the D-loop to adopting a distinct conformation from the unbound state. While the bound state and change in the D-loop conformation may not affect the global structure of the pilin monomer, the binding to D-loop possibly cause an amino acid shift and change the α -helix and β -sheets contents of pilin. This bound conformation of the D-loop structure will transmit a signal through the linear pili structure resulting in different biological responses such as retraction and extension leading swarming motility or irreversible retraction leading to swarming inhibition. We propose this hypothesis because first, the proximity of the C'-terminal globular heads in the ring stacking of the pili assembly makes it probable to transmit signals to the adjacent loops in the pili assembly (Fig. 8C). Second, the modelling of the full 1244 pilin and the truncated pilin $\Delta(1-31)$ show that the pilin secondary structure is sensitive to changes in the amino acid sequence. These calculated structures using Phyre2 show that the truncation of the pilin results in the disappearance of the helix in the C'-terminal loop shown in the full 1244 pilin structure (Fig 8D). While these structures are only calculated and the actual structure still needs to be confirmed, the fact that we see structural sensitivity may suggest that pili could also experience a similar structural sensitivity when binding to ligands that transmit signals through the pili assembly and cause extension and retraction.

Furthermore, twitching motility of *P. aeruginosa* occurs as a result of cycles of pili extension, attachment to surfaces, and retraction.^{29, 54, 55} These steps generate a force that is strong enough to translocate bacterial cells on surfaces.^{47, 48} Factors such as surface viscosity and chemical signals have been reported to influence the twitching motility.²⁹ However, the molecular understanding of how these factors induce the twitching is still under tremendous research. The attachment and recognition of surfaces by pili is primarily mediated by the D-loop but how this attachment causes the pili assembly to retract and start the cycle of the pili to cause

twitching is unknown. By the same reasoning as our hypothesis, we believe that the D-loop adopts a conformational change that transmit a signal through the pili assembly that will induce the depolymerization of the pili assembly that will cause retraction and the subsequent cycle of extension, attachment will occur.

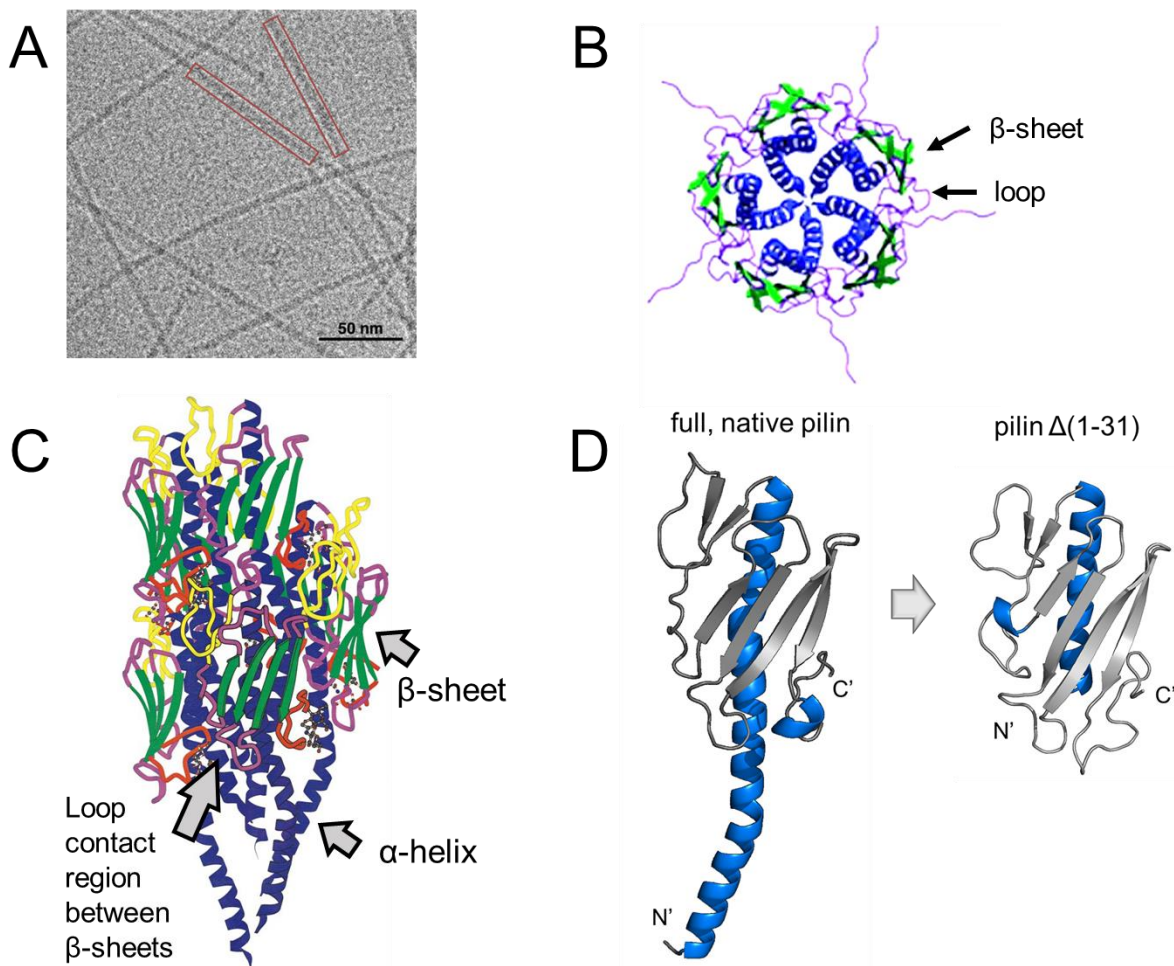


Figure 8.1 (A) Cryoelectron micrograph of *P. aeruginosa* pilin. Red rectangles indicate boxed pilus filaments. Reprinted with permission from reference 207. Copyright © 2017 Elsevier Ltd.

(B) Axial view of a single turn of the type IV pilus. The α -helix in blue, β -sheet in green, and loops in purple are shown. Reprinted with permission from reference 29. Copyright © 2004,

American Chemical Society . (C) *P. aeruginosa* PAK pilin fiber model based on the assembly parameters described by Parge *et al.* (1995). The α -helix (blue) and major β -sheet (green) are shown. The minor β -sheet region (yellow coils), the C-terminal disulphide-bonded loop (red coils) and the remainder of the residues (purple coils) are also shown. The graphical elements of the second monomer from the bottom are enclosed in bold lines to highlight the boundary of a pilin monomer. The receptor analogue β -d-GalNAc(1 \rightarrow 4)- β -d-Gal, represented as a ball-and-stick model, is shown in a position suggested by molecular docking studies. It has been included to illustrate the location of the binding site and the size of the disaccharide relative to the pilus. However, the depicted binding mode is not expected to be correct in its details. Adopted from reference 84. Copyright © 2000 Academic Press. All rights reserved. (D) Predicted full *P. aeruginosa* 1244 pilin (left) and truncated pilin Δ (1-31) using Phyre2 and visualized by PyMOL.

Further studies to understand how ligand binding controls the chemomechanics is an area that will be explored in the future. The pili structure is widely studied, but there is limited knowledge on how the assembly structure and conformational changes are induced by surface sensing or by chemical binding. Furthermore, it is unclear how the dynamic control correlates to the extension and retraction of the pili assembly. It is also unknown whether only pili tip, or the stem of pili, or both are important for the sensing and mechanics. The specific ligand binding results in this thesis form the basis for future study in this area. The exact experimental design is the task for future scientists.

8.2.2 *Structure optimization.* Luk lab conducting ongoing research on the structural optimization of the synthetic molecules that functions as ligands of pilin to inhibit pili-mediated activities. While Luk lab has a number of ligands that control pili-mediated activities, research is still underway to identify the best structure of synthetic ligands for this function. Together with the structural optimization of the synthetic ligand molecules, a number of other applications for these molecules are also being studied. First, the use of the synthetic molecules in combination with existing antibiotics to reduce drug tolerance, persistence and resistance by *P. aeruginosa*. Our synthetic molecules have the potential to reduce drug tolerance and persistence by biofilm reduction and lowering levels of cyclic di-GMP in the bacterium; while drug resistance is reduced by of inhibiting horizontal gene transfer mediated by pili. Second, exploring the integration of bacterial killing activity while maintaining the pili inhibition activities. Swarming and other motilities are major mechanisms for infections. The effectiveness of our molecules in the of swarming inhibition coupled with bacterial killing is also one avenue to be explored for our molecules.

8.2.3 *New principles of antibiotics.* The antibiotic resistance in *P. aeruginosa* remains a big problem in the medical field. Thus, the development of novel approaches to eliminate infections by drug-resistant bacteria strains are continuously being pursued. The molecules developed by Luk lab bind to pilin and inhibit biological activities such as swarming motility and biofilm formation, but do not kill bacteria. Preliminary studies on eradicating drug-resistant biofilms have shown that our molecules enhance the killing of biofilms when mixed with existing antibiotics in the market such as Tobramycin (aminoglycoside) and Aztreonam (β -lactam). We believe that our molecules bind to protein receptors such as pili and lectin A to

control the drug-tolerance and persistence. While for the observed increased resistance to Aztreonam is possibly mediated by the inhibition of β -lactamase production. Efforts to understand how the combination of our molecules and antibiotics are still underway. This observed synergistic effect open new opportunities to study our molecules in combination with existing antibiotics in market to provide greater efficiency to eliminate drug-tolerant and persister cells of *P. aeruginosa*.

8.2.4 Expansion to other microbes. The class of synthetic molecules our lab developed binds to the pili protein which exhibits dual functionality in recognizing the polar sialic acid groups on human cells and binds to nonpolar abiotic surfaces. Other microbes and viruses, such as envelope viruses, have surface protein appendages on their membrane envelope that could also bind to both human cell receptors and abiotic nonpolar surfaces.^{208, 209} These microbes could thrive for days on these surfaces and could lead to infections. As the binding of our molecules to pilin is in the picomolar range, and both pili and surface proteins exhibit dual functions, these molecules can provide an novel approaches to develop potential treatments to inhibit biological activities. The use of the BMED, can also be used to evaluate the binding between the synthetic molecules and other surface proteins exhibiting dual binding functionality and determine strong ligand candidates. Further direct binding approaches can be used to validate the approach and later develop a new therapeutic approach that could inhibit microbial activities.

References

1. Bodey, G. P.; Bolivar, R.; Fainstein, V.; Jadeja, L., Infections caused by *Pseudomonas aeruginosa*. *Reviews of infectious diseases* **1983**, *5* (2), 279-313.
2. Pachori, P.; Gothwal, R.; Gandhi, P., Emergence of antibiotic resistance *Pseudomonas aeruginosa* in intensive care unit; a critical review. *Genes Dis* **2019**, *6* (2), 109-119.
3. Marcus, H.; Austria, A.; Baker, N. R., Adherence of *Pseudomonas aeruginosa* to tracheal epithelium. *Infect Immun* **1989**, *57* (4), 1050-1053.
4. Ramphal, R.; Sadoff, J. C.; Pyle, M.; Silipigni, J. D., Role of pili in the adherence of *Pseudomonas aeruginosa* to injured tracheal epithelium. *Infect Immun* **1984**, *44* (1), 38-40.
5. Krivan, H. C.; Ginsburg, V.; Roberts, D. D., *Pseudomonas aeruginosa* and *Pseudomonas cepacia* isolated from cystic fibrosis patients bind specifically to gangliotetraosylceramide (asialo GM1) and gangliotriaosylceramide (asialo GM2). *Archives of Biochemistry and Biophysics* **1988**, *260* (1), 493-496.
6. Ramphal, R.; Pyle, M., Evidence for mucins and sialic acid as receptors for *Pseudomonas aeruginosa* in the lower respiratory tract. *Infect Immun* **1983**, *41* (1), 339-344.
7. Woods, D. E.; Straus, D. C.; W. G. Johanson, J.; Berry, V. K.; Bass, J. A., Role of pili in adherence of *Pseudomonas aeruginosa* to mammalian buccal epithelial cells. *Infect Immun* **1980**, *29* (3), 1146-1151.
8. Sheth, H.; Lee, K.; Wong, W.; Srivastava, G.; Hindsgaul, O.; Hodges, R.; Paranchych, W.; Irvin, R., The pili of *Pseudomonas aeruginosa* strains PAK and PAO bind specifically to the carbohydrate sequence β GalNAc (1-4) β Gal found in glycosphingolipids asialo-GM1 and asialo-GM2. *Molecular microbiology* **1994**, *11* (4), 715-723.

9. Schweizer, F.; Jiao, H.; Hindsgaul, O.; Wong, W. Y.; Irvin, R. T., Interaction between the pili of *Pseudomonas aeruginosa* PAK and its carbohydrate receptor β -D-GalNAc (1- \rightarrow 4) β -D-Gal analogs. *Canadian journal of microbiology* **1998**, *44* (3), 307-311.
10. Irvin, R.; Doig, P.; Lee, K.; Sastry, P.; Paranchych, W.; Todd, T.; Hodges, R., Characterization of the *Pseudomonas aeruginosa* pilus adhesin: confirmation that the pilin structural protein subunit contains a human epithelial cell-binding domain. *Infect Immun* **1989**, *57* (12), 3720-3726.
11. Chi, E.; Mehl, T.; Nunn, D.; Lory, S., Interaction of *Pseudomonas aeruginosa* with A549 pneumocyte cells. *Infect Immun* **1991**, *59* (3), 822-828.
12. Lee, K.; Sheth, H.; Wong, W.; Sherburne, R.; Paranchych, W.; Hodges, R.; Lingwood, C.; Krivan, H.; Irvin, R., The binding of *Pseudomonas aeruginosa* pili to glycosphingolipids is a tip-associated event involving the C-terminal region of the structural pilin subunit. *Molecular microbiology* **1994**, *11* (4), 705-713.
13. Doig, P.; Todd, T.; Sastry, P. A.; Lee, K. K.; Hodges, R. S.; Paranchych, W.; Irvin, R. T., Role of pili in adhesion of *Pseudomonas aeruginosa* to human respiratory epithelial cells. *Infect Immun* **1988**, *56* (6), 1641-1646.
14. Climo, M. W.; Pastor, A.; Wong, E. S., An Outbreak of *Pseudomonas aeruginosa* Related to Contaminated Urodynamic Equipment. *Infection Control and Hospital Epidemiology* **1997**, *18* (7), 509-510.
15. Curtis Nickel, J.; Downey, J.; Costerton, J. W., Movement of *pseudomonas aeruginosa* along catheter surfaces A mechanism in pathogenesis of catheter-associated infection. *Urology* **1992**, *39* (1), 93-98.

16. Giltner, C. L.; Van Schaik, E. J.; Audette, G. F.; Kao, D.; Hodges, R. S.; Hassett, D. J.; Irvin, R. T., The *Pseudomonas aeruginosa* type IV pilin receptor binding domain functions as an adhesin for both biotic and abiotic surfaces. *Molecular microbiology* **2006**, *59* (4), 1083-1096.
17. Jin, Y.; Zheng, H.; Ibanez, A. C. S.; Patil, P. D.; Lv, S.; Luo, M.; Duncan, T. M.; Luk, Y. Y., Cell-Wall-Targeting Antibiotics Cause Lag-Phase Bacteria to Form Surface-Mediated Filaments Promoting the Formation of Biofilms and Aggregates. *Chembiochem : a European journal of chemical biology* **2019**, *21* (6), 825-835.
18. Davey, M. E.; Caiazza, N. C.; O'Toole, G. A., Rhamnolipid surfactant production affects biofilm architecture in *Pseudomonas aeruginosa* PAO1. *Journal of bacteriology* **2003**, *185* (3), 1027-1036.
19. Boles, B. R.; Thoendel, M.; Singh, P. K., Rhamnolipids mediate detachment of *Pseudomonas aeruginosa* from biofilms. *Molecular microbiology* **2005**, *57* (5), 1210-1223.
20. Pamp, S. J.; Tolker-Nielsen, T., Multiple roles of biosurfactants in structural biofilm development by *Pseudomonas aeruginosa*. *Journal of bacteriology* **2007**, *189* (6), 2531-2539.
21. Zheng, H.; Singh, N.; Shetye, G. S.; Jin, Y.; Li, D.; Luk, Y.-Y., Synthetic analogs of rhamnolipids modulate structured biofilms formed by rhamnolipid-nonproducing mutant of *Pseudomonas aeruginosa*. *Bioorganic & medicinal chemistry* **2017**, *25* (6), 1830-1838.
22. Shetye, G. S.; Singh, N.; Jia, C.; Nguyen, C. D.; Wang, G.; Luk, Y. Y., Specific maltose derivatives modulate the swarming motility of nonswarming mutant and inhibit bacterial adhesion and biofilm formation by *Pseudomonas aeruginosa*. *ChemBioChem* **2014**, *15* (10), 1514-1523.

23. Singh, N.; Shetye, G. S.; Zheng, H.; Sun, J.; Luk, Y. Y., Chemical Signals of Synthetic Disaccharide Derivatives Dominate Rhamnolipids at Controlling Multiple Bacterial Activities. *ChemBioChem* **2016**, *17* (1), 102-111.
24. Audette, G. F.; van Schaik, E. J.; Hazes, B.; Irvin, R. T., DNA-binding protein nanotubes: Learning from nature's nanotech examples. *Nano Letters* **2004**, *4* (10), 1897-1902.
25. Bradley, D. E., Shortening of *Pseudomonas aeruginosa* pili after RNA-phage adsorption. *Microbiology* **1972**, *72* (2), 303-319.
26. Van Schaik, E. J.; Giltner, C. L.; Audette, G. F.; Keizer, D. W.; Bautista, D. L.; Slupsky, C. M.; Sykes, B. D.; Irvin, R. T., DNA binding: a novel function of *Pseudomonas aeruginosa* type IV pili. *Journal of bacteriology* **2005**, *187* (4), 1455-1464.
27. Anyan, M. E.; Amiri, A.; Harvey, C. W.; Tierra, G.; Morales-Soto, N.; Driscoll, C. M.; Alber, M. S.; Shrout, J. D., Type IV pili interactions promote intercellular association and moderate swarming of *Pseudomonas aeruginosa*. *Proceedings of the National Academy of Sciences of the United States of America* **2014**, *111* (50), 18013-18018.
28. Köhler, T.; Curty, L. K.; Barja, F.; Delden, C. v.; Pechère, J.-C., Swarming of *Pseudomonas aeruginosa* Is Dependent on Cell-to-Cell Signaling and Requires Flagella and Pili. *Journal of Bacteriology* **2000**, *182* (21), 5990-5996.
29. Burrows, L. L., *Pseudomonas aeruginosa* Twitching Motility: Type IV Pili in Action. *Annual Review of Microbiology* **2012**, *66* (1), 493-520.
30. Chiang, P.; Burrows, L. L., Biofilm formation by hyperpiliated mutants of *Pseudomonas aeruginosa*. *Journal of bacteriology* **2003**, *185* (7), 2374-2378.
31. O'Toole, G. A.; Kolter, R., Flagellar and twitching motility are necessary for *Pseudomonas aeruginosa* biofilm development. *Molecular microbiology* **1998**, *30* (2), 295-304.

32. Zolfaghar, I.; Evans, D. J.; Fleiszig, S. M. J., Twitching motility contributes to the role of pili in corneal infection caused by *Pseudomonas aeruginosa*. *Infect Immun* **2003**, *71* (9), 5389-5393.
33. Persat, A.; Inclan, Y. F.; Engel, J. N.; Stone, H. A.; Gitai, Z., Type IV pili mechanochemically regulate virulence factors in *Pseudomonas aeruginosa*. *Proceedings of the National Academy of Sciences* **2015**, *112* (24), 7563-7568.
34. Laventie, B.-J.; Sangermani, M.; Estermann, F.; Manfredi, P.; Planes, R.; Hug, I.; Jaeger, T.; Meunier, E.; Broz, P.; Jenal, U., A surface-induced asymmetric program promotes tissue colonization by *Pseudomonas aeruginosa*. *Cell host & microbe* **2019**, *25* (1), 140-152. e6.
35. Jain, R.; Behrens, A.-J.; Kaever, V.; Kazmierczak, B. I., Type IV pilus assembly in *Pseudomonas aeruginosa* over a broad range of cyclic di-GMP concentrations. *Journal of bacteriology* **2012**, *194* (16), 4285-4294.
36. Chua, S. L.; Liu, Y.; Yam, J. K. H.; Chen, Y.; Vejborg, R. M.; Tan, B. G. C.; Kjelleberg, S.; Tolker-Nielsen, T.; Givskov, M.; Yang, L., Dispersed cells represent a distinct stage in the transition from bacterial biofilm to planktonic lifestyles. *Nature communications* **2014**, *5* (1), 1-12.
37. Burrows, L. L., *Pseudomonas aeruginosa* twitching motility: type IV pili in action. *Annual review of microbiology* **2012**, *66*, 493-520.
38. Nunn, D.; Bergman, S.; Lory, S., Products of three accessory genes, pilB, pilC, and pilD, are required for biogenesis of *Pseudomonas aeruginosa* pili. *Journal of bacteriology* **1990**, *172* (6), 2911-2919.
39. Strom, M. S.; Lory, S., Mapping of export signals of *Pseudomonas aeruginosa* pilin with alkaline phosphatase fusions. *Journal of bacteriology* **1987**, *169* (7), 3181-3188.

40. Strom, M. S.; Nunn, D. N.; Lory, S., A single bifunctional enzyme, PilD, catalyzes cleavage and N-methylation of proteins belonging to the type IV pilin family. *Proceedings of the National Academy of Sciences* **1993**, *90* (6), 2404-2408.
41. Pasloske, B. L.; Finlay, B. B.; Paranchych, W., Cloning and sequencing of the *Pseudomonas aeruginosa* PAK pilin gene. *FEBS letters* **1985**, *183* (2), 413-416.
42. Johnson, K.; Parker, M.; Lory, S., Nucleotide sequence and transcriptional initiation site of two *Pseudomonas aeruginosa* pilin genes. *Journal of Biological Chemistry* **1986**, *261* (33), 15703-15708.
43. Ishimoto, K. S.; Lory, S., Formation of pilin in *Pseudomonas aeruginosa* requires the alternative sigma factor (RpoN) of RNA polymerase. *Proceedings of the National Academy of Sciences* **1989**, *86* (6), 1954-1957.
44. Watts, T. H.; Kay, C. M.; Paranchych, W., Spectral properties of three quaternary arrangements of *Pseudomonas* pilin. *Biochemistry* **1983**, *22* (15), 3640-3646.
45. Folkhard, W.; Marvin, D.; Watts, T.; Paranchych, W., Structure of polar pili from *Pseudomonas aeruginosa* strains K and O. *Journal of molecular biology* **1981**, *149* (1), 79-93.
46. Paranchych, W.; Sastry, P.; Frost, L.; Carpenter, M.; Armstrong, G.; Watts, T., Biochemical studies on pili isolated from *Pseudomonas aeruginosa* strain PAO. *Canadian journal of microbiology* **1979**, *25* (10), 1175-1181.
47. Maier, B.; Potter, L.; So, M.; Seifert, H. S.; Sheetz, M. P., Single Pilus Motor Forces Exceed 100 pN. *Proceedings of the National Academy of Sciences of the United States of America* **2002**, *99* (25), 16012-16017.
48. Merz, A. J.; Sheetz, M. P.; So, M., Pilus retraction powers bacterial twitching motility. *Nature* **2000**, *407* (6800), 98-102.

49. Skerker, J. M.; Berg, H. C., Direct Observation of Extension and Retraction of Type IV Pili. *Proceedings of the National Academy of Sciences of the United States of America* **2001**, *98* (12), 6901-6904.
50. Beachey, E. H., Bacterial adherence: adhesin-receptor interactions mediating the attachment of bacteria to mucosal surfaces. *Journal of Infectious Diseases* **1981**, *143* (3), 325-345.
51. Comolli, J. C.; Waite, L. L.; Mostov, K. E.; Engel, J. N., Pili binding to asialo-GM1 on epithelial cells can mediate cytotoxicity or bacterial internalization by *Pseudomonas aeruginosa*. *Infect Immun* **1999**, *67* (7), 3207-3214.
52. Gordon, V. D.; Wang, L., Bacterial mechanosensing: the force will be with you, always. *Journal of Cell Science* **2019**, *132* (7), jcs227694.
53. Kearns, D. B., A field guide to bacterial swarming motility. *Nature reviews. Microbiology* **2010**, *8* (9), 634-644.
54. Bradley, D. E., A function of *Pseudomonas aeruginosa* PAO polar pili: twitching motility. *Canadian journal of microbiology* **1980**, *26* (2), 146-154.
55. Kaiser, D., Bacterial motility: how do pili pull? *Current Biology* **2000**, *10* (21), R777-R780.
56. Overhage, J.; Lewenza, S.; Marr, A. K.; Robert, E. W. H., Identification of Genes Involved in Swarming Motility Using a *Pseudomonas aeruginosa* PAO1 Mini-Tn5-lux Mutant Library. *Journal of Bacteriology* **2007**, *189* (5), 2164-2169.
57. Amy, T. Y. Y.; Ellen, C. W. T.; Jamshidi, F.; Bains, M.; Wiegand, I.; Robert, E. W. H.; Overhage, J., Swarming of *Pseudomonas aeruginosa* Is Controlled by a Broad Spectrum of Transcriptional Regulators, Including MetR. *Journal of Bacteriology* **2009**, *191* (18), 5592-5602.

58. Overhage, J.; Bains, M.; Brazas, M. D.; Robert, E. W. H., Swarming of *Pseudomonas aeruginosa* Is a Complex Adaptation Leading to Increased Production of Virulence Factors and Antibiotic Resistance. *Journal of Bacteriology* **2008**, *190* (8), 2671-2679.
59. Caiazza, N. C.; Shanks, R. M.; O'toole, G., Rhamnolipids modulate swarming motility patterns of *Pseudomonas aeruginosa*. *Journal of bacteriology* **2005**, *187* (21), 7351-7361.
60. Tremblay, J.; Richardson, A. P.; Lépine, F.; Déziel, E., Self-produced extracellular stimuli modulate the *Pseudomonas aeruginosa* swarming motility behaviour. *Environmental microbiology* **2007**, *9* (10), 2622-2630.
61. Eberhard, A.; Burlingame, A. L.; Eberhard, C.; Kenyon, G. L.; Nealson, K. H.; Oppenheimer, N. J., Structural identification of autoinducer of *Photobacterium fischeri* luciferase. *Biochemistry* **1981**, *20* (9), 2444-2449.
62. Johnsborg, O.; Eldholm, V.; Håvarstein, L. S., Natural genetic transformation: prevalence, mechanisms and function. *Research in Microbiology* **2007**, *158* (10), 767-778.
63. Nolan, L. M.; Turnbull, L.; Katrib, M.; Osvath, S. R.; Losa, D.; Lazenby, J. J.; Whitchurch, C. B., *Pseudomonas aeruginosa* is capable of natural transformation in biofilms. *Microbiology* **2020**.
64. Ellison, C. K.; Dalia, T. N.; Ceballos, A. V.; Wang, J. C.-Y.; Biais, N.; Brun, Y. V.; Dalia, A. B., Retraction of DNA-bound type IV competence pili initiates DNA uptake during natural transformation in *Vibrio cholerae*. *Nature microbiology* **2018**, *3* (7), 773-780.
65. Laurenceau, R.; Péhau-Arnaudet, G.; Baconnais, S.; Gault, J.; Malosse, C.; Dujancourt, A.; Campo, N.; Chamot-Rooke, J.; Le Cam, E.; Claverys, J.-P.; Fronzes, R., A type IV pilus mediates DNA binding during natural transformation in *Streptococcus pneumoniae*. *PLoS pathogens* **2013**, *9* (6), e1003473.

66. Seifert, H.; Ajioka, R.; Paruchuri, D.; Heffron, F.; So, M., Shuttle mutagenesis of *Neisseria gonorrhoeae*: pilin null mutations lower DNA transformation competence. *Journal of bacteriology* **1990**, *172* (1), 40-46.
67. Friedrich, A.; Prust, C.; Hartsch, T.; Henne, A.; Averhoff, B., Molecular analyses of the natural transformation machinery and identification of pilus structures in the extremely thermophilic bacterium *Thermus thermophilus* strain HB27. *Applied and Environmental Microbiology* **2002**, *68* (2), 745-755.
68. Campbell, A. P.; Wong, W. Y.; Houston, M.; Schweizer, F.; Cachia, P. J.; Irvin, R. T.; Hindsgaul, O.; Hodges, R. S.; Sykes, B. D., Interaction of the receptor binding domains of *Pseudomonas aeruginosa* pili strains PAK, PAO, KB7 and P1 to a cross-reactive antibody and receptor analog: implications for synthetic vaccine design. *Journal of molecular biology* **1997**, *267* (2), 382-402.
69. Lee, K.; Doig, P.; Irvin, R.; Paranchych, W.; Hodges, R., Mapping the surface regions of *Pseudomonas aeruginosa* PAK pilin: the importance of the C-terminal region for adherence to human buccal epithelial cells. *Molecular microbiology* **1989**, *3* (11), 1493-1499.
70. Doig, P.; Sastry, P. A.; Hodges, R. S.; Lee, K. K.; Paranchych, W.; Irvin, R. T., Inhibition of pilus-mediated adhesion of *Pseudomonas aeruginosa* to human buccal epithelial cells by monoclonal antibodies directed against pili. *Infect Immun* **1990**, *58* (1), 124-130.
71. Blumenstein, M.; Matsueda, G. R.; Timmons, S.; Hawiger, J., A beta.-turn is present in the 392-411 segment of the human fibrinogen. gamma.-chain. Effects of structural changes in this segment on affinity to antibody 4A5. *Biochemistry* **1992**, *31* (44), 10692-10698.
72. Rini, J. M.; Schulze-Gahmen, U.; Wilson, I. A., Structural evidence for induced fit as a mechanism for antibody-antigen recognition. *Science* **1992**, *255* (5047), 959-965.

73. Stanfield, R. L.; Fieser, T. M.; Lerner, R. A.; Wilson, I. A., Crystal structures of an antibody to a peptide and its complex with peptide antigen at 2.8 Å. *Science* **1990**, *248* (4956), 712-719.
74. Shetye, G. S. Discovering the Biological Activities of Maltose Derivatives for Controlling Bacterial Multicellular Behaviors. ProQuest Dissertations Publishing, 2015.
75. Zheng, H. Chimera Ligand for Pili and Lectin A Protein Controls Antibiotic-Promoted Biofilm Formation, Swarming Motility, Tolerance and Persister Formation by *Pseudomonas aeruginosa*. ProQuest Dissertations Publishing, 2018.
76. Parge, H. E.; Forest, K. T.; Hickey, M. J.; Christensen, D. A., Structure of the fibre-forming protein pilin at 2.6 angstroms resolution. *Nature* **1995**, *378* (6552), 32.
77. Audette, G. F.; Irvin, R. T.; Hazes, B., Crystallographic analysis of the *Pseudomonas aeruginosa* strain K122-4 monomeric pilin reveals a conserved receptor-binding architecture. *Biochemistry* **2004**, *43* (36), 11427-11435.
78. Craig, L.; Taylor, R. K.; Pique, M. E.; Adair, B. D.; Arvai, A. S.; Singh, M.; Lloyd, S. J.; Shin, D. S.; Getzoff, E. D.; Yeager, M.; Forest, K. T.; Tainer, J. A., Type IV Pilin Structure and Assembly: X-Ray and EM Analyses of *Vibrio cholerae* Toxin-Coregulated Pilus and *Pseudomonas aeruginosa* PAK Pilin. *Molecular Cell* **2003**, *11* (5), 1139-1150.
79. Craig, L.; Volkmann, N.; Arvai, A. S.; Pique, M. E.; Yeager, M.; Egelman, Edward H.; Tainer, J. A., Type IV Pilus Structure by Cryo-Electron Microscopy and Crystallography: Implications for Pilus Assembly and Functions. *Molecular Cell* **2006**, *23* (5), 651-662.
80. Keizer, D. W.; Slupsky, C. M.; Kalisiak, M.; Campbell, A. P.; Crump, M. P.; Sastry, P. A.; Hazes, B.; Irvin, R. T.; Sykes, B. D., Structure of a pilin monomer from *Pseudomonas*

aeruginosa: Implications for the assembly of pili. *Journal of Biological Chemistry* **2001**, 276 (26), 24186-24193.

81. Nguyen, Y.; Jackson, S. G.; Aidoo, F.; Junop, M.; Burrows, L. L., Structural Characterization of Novel *Pseudomonas aeruginosa* Type IV Pilins. *Journal of Molecular Biology* **2010**, 395 (3), 491-503.

82. Kus, J. V.; Tullis, E.; Cvitkovitch, D. G.; Burrows, L. L., Significant differences in type IV pilin allele distribution among *Pseudomonas aeruginosa* isolates from cystic fibrosis (CF) versus non-CF patients. *Microbiology* **2004**, 150 (5), 1315-1326.

83. Asikyan, M. L.; Kus, J. V.; Burrows, L. L., Novel proteins that modulate type IV pilus retraction dynamics in *Pseudomonas aeruginosa*. *Journal of bacteriology* **2008**, 190 (21), 7022-7034.

84. Hazes, B.; Sastry, P. A.; Hayakawa, K.; Read, R. J.; Irvin, R. T., Crystal structure of *Pseudomonas aeruginosa* PAK pilin suggests a main-chain-dominated mode of receptor binding¹. *Journal of molecular biology* **2000**, 299 (4), 1005-1017.

85. Castric, P., pilO, a gene required for glycosylation of *Pseudomonas aeruginosa* 1244 pilin. *Microbiology* **1995**, 141 (5), 1247-1254.

86. Ramphal, R.; Koo, L.; Ishimoto, K. S.; Totten, P. A.; Lara, J. C.; Lory, S., Adhesion of *Pseudomonas aeruginosa* pilin-deficient mutants to mucin. *Infect Immun* **1991**, 59 (4), 1307-1311.

87. Comer, J. E.; Marshall, M. A.; Blanch, V. J.; Deal, C. D.; Castric, P., Identification of the *Pseudomonas aeruginosa* 1244 pilin glycosylation site. *Infect Immun* **2002**, 70 (6), 2837-2845.

88. Horzempa, J.; Held, T. K.; Cross, A. S.; Furst, D.; Qutyan, M.; Neely, A. N.; Castric, P., Immunization with a *Pseudomonas aeruginosa* 1244 Pilin Provides O-Antigen-Specific Protection. *Clinical and Vaccine Immunology* **2008**, *15* (4), 590-597.
89. Horzempa, J.; Comer, J. E.; Davis, S. A.; Castric, P., Glycosylation Substrate Specificity of *Pseudomonas aeruginosa* 1244 Pilin. *Journal of Biological Chemistry* **2006**, *281* (2), 1128.
90. Smedley, J. G.; Jewell, E.; Roguskie, J.; Horzempa, J.; Syboldt, A.; Stolz, D. B.; Castric, P., Influence of Pilin Glycosylation on *Pseudomonas aeruginosa* 1244 Pilus Function. *Infect Immun* **2005**, *73* (12), 7922-7931.
91. Farinha, M. A.; Conway, B. D.; Glasier, L. M.; Ellert, N. W.; Irvin, R. T.; Sherburne, R.; Paranchych, W., Alteration of the pilin adhesin of *Pseudomonas aeruginosa* PAO results in normal pilus biogenesis but a loss of adherence to human pneumocyte cells and decreased virulence in mice. *Infect Immun* **1994**, *62* (10), 4118-4123.
92. Wong, W. Y.; McInnes, C.; Sykes, B. D.; Paranchych, W.; Irvin, R. T.; Hodges, R. S., Structure-function analysis of the adherence-binding domain on the pilin of *Pseudomonas aeruginosa* strains PAK and KB7. *Biochemistry* **1995**, *34* (40), 12963-12972.
93. Campbell, A. P.; McInnes, C.; Hodges, R. S.; Sykes, B. D., Comparison of NMR solution structures of the receptor binding domains of *Pseudomonas aeruginosa* pili strains PAO, KB7, and PAK: implications for receptor binding and synthetic vaccine design. *Biochemistry* **1995**, *34* (50), 16255-16268.
94. Castric, P.; Cassels, F. J.; Carlson, R. W., Structural characterization of the *Pseudomonas aeruginosa* 1244 pilin glycan. *The Journal of biological chemistry* **2001**, *276* (28), 26479-85.

95. Campbell, A. P.; Sheth, H.; Hodges, R. S.; Sykes, B. D., NMR solution structure of the receptor binding domain of *Pseudomonas aeruginosa* pilin strain P1. Identification of a β -turn. *International journal of peptide and protein research* **1996**, *48* (6), 539-552.
96. McInnes, C.; Sonnichsen, F. D.; Kay, C. M.; Hodges, R. S.; Sykes, B. D., NMR solution structure and flexibility of a peptide antigen representing the receptor binding domain of *Pseudomonas aeruginosa*. *Biochemistry* **1993**, *32* (49), 13432-13440.
97. Yang, A.; Tang, W. S.; Si, T.; Tang, J. X., Influence of Physical Effects on the Swarming Motility of *Pseudomonas aeruginosa*. *Biophys J* **2017**, *112* (7), 1462-1471.
98. Rashid, M. H.; Kornberg, A., Inorganic polyphosphate is needed for swimming, swarming, and twitching motilities of *Pseudomonas aeruginosa*. *Proceedings of the National Academy of Sciences* **2000**, *97* (9), 4885-4890.
99. Du, H.; Xu, Z.; Anyan, M.; Kim, O.; Leevy, W. M.; Shrout, J. D.; Alber, M., High density waves of the bacterium *Pseudomonas aeruginosa* in propagating swarms result in efficient colonization of surfaces. *Biophys J* **2012**, *103* (3), 601-609.
100. Anyan, M. E.; Amiri, A.; Harvey, C. W.; Tierra, G.; Morales-Soto, N.; Driscoll, C. M.; Alber, M. S.; Shrout, J. D., Type IV pili interactions promote intercellular association and moderate swarming of *Pseudomonas aeruginosa*. *Proceedings of the National Academy of Sciences* **2014**, *111* (50), 18013-18018.
101. Butler, M. T.; Wang, Q.; Harshey, R. M., Cell density and mobility protect swarming bacteria against antibiotics. *Proceedings of the National Academy of Sciences* **2010**, *107* (8), 3776-3781.
102. Kaiser, D.; Warrick, H., *Myxococcus xanthus* swarms are driven by growth and regulated by a pacemaker. *Journal of bacteriology* **2011**, *193* (21), 5898-5904.

103. Tremblay, J.; Déziel, E., Gene expression in *Pseudomonas aeruginosa* swarming motility. *BMC genomics* **2010**, *11* (1), 587.
104. Kownatzki, R.; Tümmler, B.; Döring, G., Rhamnolipid of *Pseudomonas aeruginosa* in sputum of cystic fibrosis patients. *Lancet (London, England)* **1987**, *1* (8540), 1026-1027.
105. Deziel, E.; Lepine, F.; Milot, S.; Villemur, R., rhlA is required for the production of a novel biosurfactant promoting swarming motility in *Pseudomonas aeruginosa*: 3-(3-hydroxyalkanoyloxy)alkanoic acids (HAAs), the precursors of rhamnolipids. *Microbiology* **2003**, *149* (8), 2005-2013.
106. Lequette, Y.; Greenberg, E., Timing and localization of rhamnolipid synthesis gene expression in *Pseudomonas aeruginosa* biofilms. *Journal of bacteriology* **2005**, *187* (1), 37-44.
107. Maier, R. M.; Soberon-Chavez, G., *Pseudomonas aeruginosa* rhamnolipids: biosynthesis and potential applications. *Applied Microbiology and Biotechnology* **2000**, *54* (5), 625-633.
108. Jacobs, M. A.; Alwood, A.; Thaipisuttikul, I.; Spencer, D.; Haugen, E.; Ernst, S.; Will, O.; Kaul, R.; Raymond, C.; Levy, R.; Chun-Rong, L.; Guenther, D.; Bovee, D.; Olson, M. V.; Manoil, C., Comprehensive Transposon Mutant Library of *Pseudomonas aeruginosa*. *Proceedings of the National Academy of Sciences of the United States of America* **2003**, *100* (24), 14339-14344.
109. Anfinsen, C. B., Principles that govern the folding of protein chains. *Science* **1973**, *181* (4096), 223-230.
110. Kelly, S. M.; Price, N. C., The use of circular dichroism in the investigation of protein structure and function. *Current protein and peptide science* **2000**, *1* (4), 349-384.
111. Greenfield, N. J., Applications of circular dichroism in protein and peptide analysis. *TrAC Trends in Analytical Chemistry* **1999**, *18* (4), 236-244.

112. Juárez, J.; Alatorre-Meda, M.; Cambón, A.; Topete, A.; Barbosa, S.; Taboada, P.; Mosquera, V., Hydration effects on the fibrillation process of a globular protein: the case of human serum albumin. *Soft Matter* **2012**, *8* (13), 3608-3619.
113. Drzewiecki, K. E.; Grisham, D. R.; Parmar, A. S.; Nanda, V.; Shreiber, D. I., Circular Dichroism Spectroscopy of Collagen Fibrillogenesis: A New Use for an Old Technique. *Biophys J* **2016**, *111* (11), 2377-2386.
114. Siddiqi, M. K.; Alam, P.; Iqbal, T.; Majid, N.; Malik, S.; Nusrat, S.; Alam, A.; Ajmal, M. R.; Uversky, V. N.; Khan, R. H., Elucidating the Inhibitory Potential of Designed Peptides Against Amyloid Fibrillation and Amyloid Associated Cytotoxicity. *Frontiers in Chemistry* **2018**, *6* (311).
115. Siligardi, G.; Hussain, R., Biomolecules interactions and competitions by non-immobilised ligand interaction assay by circular dichroism. *Enantiomer* **1998**, *3* (2), 77-87.
116. Becker, W.; Bhattiprolu, K. C.; Gubensäk, N.; Zangger, K., Investigating Protein-Ligand Interactions by Solution Nuclear Magnetic Resonance Spectroscopy. *Chemphyschem* **2018**, *19* (8), 895-906.
117. Wüthrich, K., NMR with proteins and nucleic acids. *Europhysics News* **1986**, *17* (1), 11-13.
118. Barile, E.; Pellecchia, M., NMR-based approaches for the identification and optimization of inhibitors of protein–protein interactions. *Chemical reviews* **2014**, *114* (9), 4749-4763.
119. Stetefeld, J.; McKenna, S. A.; Patel, T. R., Dynamic light scattering: a practical guide and applications in biomedical sciences. *Biophys Rev* **2016**, *8* (4), 409-427.
120. Pecora, R., Dynamic Light Scattering Measurement of Nanometer Particles in Liquids. *Journal of Nanoparticle Research* **2000**, *2* (2), 123-131.

121. Watts, T. H.; Kay, C. M.; Paranchych, W., Dissociation and characterization of pilin isolated from *Pseudomonas aeruginosa* strains PAK and PAO. *Canadian journal of biochemistry* **1982**, *60* (9), 867-872.
122. Micsonai, A.; Wien, F.; Kernya, L.; Lee, Y.-H.; Goto, Y.; Réfrégiers, M.; Kardos, J., Accurate secondary structure prediction and fold recognition for circular dichroism spectroscopy. *Proceedings of the National Academy of Sciences* **2015**, *112* (24), E3095-E3103.
123. Whitmore, L.; Wallace, B. A., Protein secondary structure analyses from circular dichroism spectroscopy: methods and reference databases. *Biopolymers: Original Research on Biomolecules* **2008**, *89* (5), 392-400.
124. Nanny, M. A.; Minear, R. A.; Leenheer, J. A., *Nuclear magnetic resonance spectroscopy in environmental chemistry*. Oxford University Press: New York, 1997.
125. Simpson, A. J.; Woods, G.; Mehrzad, O., Spectral Editing of Organic Mixtures into Pure Components Using NMR Spectroscopy and Ultraviscous Solvents. *Analytical Chemistry* **2008**, *80* (1), 186-194.
126. Wüthrich, K., *NMR of proteins and nucleic acids*. Wiley: New York, 1986.
127. Mammen, M.; Choi, S. K.; Whitesides, G. M., Polyvalent interactions in biological systems: implications for design and use of multivalent ligands and inhibitors. *Angewandte Chemie International Edition* **1998**, *37* (20), 2754-2794.
128. Green, N. M., Avidin. 1. The Use Of (14-C)Biotin For Kinetic Studies and For Assay. *Biochem J* **1963**, *89* (3), 585-591.
129. Parkel, S.; Rinken, A., Characteristics of binding of [3 H] WAY100635 to rat hippocampal membranes. *Neurochemical research* **2006**, *31* (9), 1135-1140.

130. Le, M.; Pugsley, M.; Vauquelin, G.; Van Liefde, I., Molecular characterisation of the interactions between olmesartan and telmisartan and the human angiotensin II AT1 receptor. *British journal of pharmacology* **2007**, *151* (7), 952-962.
131. Cheng, T.-J. R.; Sung, M.-T.; Liao, H.-Y.; Chang, Y.-F.; Chen, C.-W.; Huang, C.-Y.; Chou, L.-Y.; Wu, Y.-D.; Chen, Y.-H.; Cheng, Y.-S. E.; Wong, C.-H.; Ma, C.; Cheng, W.-C., Domain requirement of moenomycin binding to bifunctional transglycosylases and development of high-throughput discovery of antibiotics. *Proceedings of the National Academy of Sciences of the United States of America* **2008**, *105* (2), 431-436.
132. King, D. T.; Wasney, G. A.; Nosella, M.; Fong, A.; Strynadka, N. C. J., Structural Insights into Inhibition of Escherichia coli Penicillin-binding Protein 1B. *The Journal of biological chemistry* **2017**, *292* (3), 979-993.
133. Cowgill, R. W., Fluorescence and the structure of proteins II. Fluorescence of peptides containing tryptophan or tyrosine. *Biochimica et Biophysica Acta* **1963**, *75*, 272-273.
134. Shore, V. G.; Pardee, A. B., Fluorescence of some proteins, nucleic acids and related compounds. *Archives of Biochemistry and Biophysics* **1956**, *60* (1), 100-107.
135. Teale, F., The ultraviolet fluorescence of proteins in neutral solution. *Biochemical journal* **1960**, *76* (2), 381.
136. Teale, F.; Weber, G., Ultraviolet fluorescence of the aromatic amino acids. *Biochemical Journal* **1957**, *65* (3), 476.
137. Petrov, A.; Lombardo, S.; Audette, G. F., Fibril-mediated oligomerization of pilin-derived protein nanotubes. *Journal of nanobiotechnology* **2013**, *11* (1), 24.
138. Lakowicz, J. R., *Principles of fluorescence spectroscopy*. Springer Science & Business Media: 2013.

139. Chen, Y.; Bjornson, K.; Redick, S. D.; Erickson, H. P., A Rapid Fluorescence Assay for FtsZ Assembly Indicates Cooperative Assembly with a Dimer Nucleus. *Biophys J* **2005**, *88* (1), 505-514.
140. Constantinescu, I.; Lafleur, M., Influence of the lipid composition on the kinetics of concerted insertion and folding of melittin in bilayers. *Biochimica et Biophysica Acta (BBA)-Biomembranes* **2004**, *1667* (1), 26-37.
141. Huang, Y.; Zhou, Y.; Castiblanco, A.; Yang, W.; Brown, E. M.; Yang, J. J., Multiple Ca²⁺-Binding Sites in the Extracellular Domain of the Ca²⁺-Sensing Receptor Corresponding to Cooperative Ca²⁺ Response. *Biochemistry* **2009**, *48* (2), 388-398.
142. Kenoth, R.; Simanshu, D. K.; Kamlekar, R. K.; Pike, H. M.; Molotkovsky, J. G.; Benson, L. M.; Bergen, H. R.; Prendergast, F. G.; Malinina, L.; Venyaminov, S. Y., Structural determination and tryptophan fluorescence of heterokaryon incompatibility C2 protein (HET-C2), a fungal glycolipid transfer protein (GLTP), provide novel insights into glycolipid specificity and membrane interaction by the GLTP fold. *Journal of Biological Chemistry* **2010**, *285* (17), 13066-13078.
143. Kozachkov, L.; Padan, E., Site-directed tryptophan fluorescence reveals two essential conformational changes in the Na⁺/H⁺ antiporter NhaA. *Proceedings of the National Academy of Sciences* **2011**, *108* (38), 15769-15774.
144. Kraft, C. A.; Garrido, J. L.; Fluharty, E.; Leiva-Vega, L.; Romero, G., Role of phosphatidic acid in the coupling of the ERK cascade. *Journal of Biological Chemistry* **2008**, *283* (52), 36636-36645.
145. Ward, L. D., [22] Measurement of ligand binding to proteins by fluorescence spectroscopy. In *Methods in Enzymology*, Academic Press: 1985; Vol. 117, pp 400-414.

146. Liu, X.; Obianyo, O.; Chan, C. B.; Huang, J.; Xue, S.; Yang, J. J.; Zeng, F.; Goodman, M.; Ye, K., Biochemical and biophysical investigation of the brain-derived neurotrophic factor mimetic 7, 8-dihydroxyflavone in the binding and activation of the TrkB receptor. *Journal of Biological Chemistry* **2014**, *289* (40), 27571-27584.
147. Tovar, J. D.; Claussen, R. C.; Stupp, S. I., Probing the Interior of Peptide Amphiphile Supramolecular Aggregates. *Journal of the American Chemical Society* **2005**, *127* (20), 7337-7345.
148. Jones, S.; Thornton, J. M., Principles of protein-protein interactions. *Proceedings of the National Academy of Sciences* **1996**, *93* (1), 13-20.
149. Pieters, B. J. G. E.; van Eldijk, M. B.; Nolte, R. J. M.; Mecinović, J., Natural supramolecular protein assemblies. *Chemical Society Reviews* **2016**, *45* (1), 24-39.
150. Oosawa, F.; Kasai, M., A theory of linear and helical aggregations of macromolecules. *Journal of Molecular Biology* **1962**, *4* (1), 10-21.
151. Sahoo, N.; Beatty, W.; Heuser, J.; Sept, D.; Sibley, L. D., Unusual kinetic and structural properties control rapid assembly and turnover of actin in the parasite *Toxoplasma gondii*. *Mol Biol Cell* **2006**, *17* (2), 895-906.
152. Dogra, P.; Bhattacharya, M.; Mukhopadhyay, S., pH-Responsive mechanistic switch regulates the formation of dendritic and fibrillar nanostructures of a functional amyloid. *The Journal of Physical Chemistry B* **2017**, *121* (2), 412-419.
153. Miraldi, E. R.; Thomas, P. J.; Romberg, L., Allosteric models for cooperative polymerization of linear polymers. *Biophys J* **2008**, *95* (5), 2470-2486.

154. Skillman, K. M.; Ma, C. I.; Fremont, D. H.; Diraviyam, K.; Cooper, J. A.; Sept, D.; Sibley, L. D., The unusual dynamics of parasite actin result from isodesmic polymerization. *Nature communications* **2013**, *4*, 2285.
155. Ibanez, A. C. S.; Marji, E.; Luk, Y.-Y., Cromoglycate mesogen forms isodesmic assemblies promoted by peptides and induces aggregation of a range of proteins. *RSC Advances* **2018**, *8* (52), 29598-29606.
156. Vivian, J. T.; Callis, P. R., Mechanisms of Tryptophan Fluorescence Shifts in Proteins. *Biophys J* **2001**, *80* (5), 2093-2109.
157. Lydon, J., Chromonic liquid crystalline phases. *Liquid Crystals* **2011**, *38* (11-12), 1663-1681.
158. Zhou, S.; Sokolov, A.; Lavrentovich, O. D.; Aranson, I. S., Living liquid crystals. *Proceedings of the National Academy of Sciences of the United States of America* **2014**, *111* (4), 1265-1270.
159. Mushenheim, P. C.; Trivedi, R. R.; Tuson, H. H.; Weibel, D. B.; Abbott, N. L., Dynamic self-assembly of motile bacteria in liquid crystals. *Soft Matter* **2014**, *10* (1), 88-95.
160. Mushenheim, Peter C.; Trivedi, Rishi R.; Weibel, Douglas B.; Abbott, Nicholas L., Using Liquid Crystals to Reveal How Mechanical Anisotropy Changes Interfacial Behaviors of Motile Bacteria. *Biophys J* **2014**, *107* (1), 255-265.
161. Genkin, M. M.; Sokolov, A.; Lavrentovich, O. D.; Aranson, I. S., Topological Defects in a Living Nematic Ensnare Swimming Bacteria. *Physical Review X* **2017**, *7* (1), 011029.
162. Sokolov, A.; Zhou, S.; Lavrentovich, O. D.; Aranson, I. S., Individual behavior and pairwise interactions between microswimmers in anisotropic liquid. *Physical Review E* **2015**, *91* (1), 013009.

163. Trivedi, R. R.; Maeda, R.; Abbott, N. L.; Spagnolie, S. E.; Weibel, D. B., Bacterial transport of colloids in liquid crystalline environments. *Soft Matter* **2015**, *11* (43), 8404-8408.
164. Peng, C.; Lavrentovich, O. D., Chirality amplification and detection by tactoids of lyotropic chromonic liquid crystals. *Soft Matter* **2015**, *11* (37), 7257-7263.
165. Tam-Chang, S.-W.; Huang, L., Chromonic liquid crystals: properties and applications as functional materials. *Chemical Communications* **2008**, (17), 1957-1967.
166. Luk, Y.-Y.; Jang, C.-H.; Cheng, L.-L.; Israel, B. A.; Abbott, N. L., Influence of Lyotropic Liquid Crystals on the Ability of Antibodies To Bind to Surface-Immobilized Antigens. *Chemistry of Materials* **2005**, *17* (19), 4774-4782.
167. Simon, K. A.; Shetye, G. S.; English, U.; Wu, L.; Luk, Y.-Y., Noncovalent Polymerization of Mesogens Crystallizes Lysozyme: Correlation between Nonamphiphilic Lyotropic Liquid Crystal Phase and Protein Crystal Formation. *Langmuir* **2011**, *27* (17), 10901-10906.
168. Collings, P. J.; Dickinson, A. J.; Smith, E. C., Molecular aggregation and chromonic liquid crystals. *Liquid Crystals* **2010**, *37* (6-7), 701-710.
169. Collings, P. J.; Goldstein, J. N.; Hamilton, E. J.; Mercado, B. R.; Nieser, K. J.; Regan, M. H., The nature of the assembly process in chromonic liquid crystals. *Liquid Crystals Reviews* **2015**, *3* (1), 1-27.
170. Maiti, P. K.; Lansac, Y.; Glaser, M. A.; Clark, N. A., Isodesmic self-assembly in lyotropic chromonic systems. *Liquid Crystals* **2002**, *29* (5), 619-626.
171. Simon, K. A.; Sejwal, P.; Falcone, E. R.; Burton, E. A.; Yang, S.; Prashar, D.; Bandyopadhyay, D.; Narasimhan, S. K.; Varghese, N.; Gobalasingham, N. S.; Reese, J. B.;

- Luk, Y.-Y., Noncovalent polymerization and assembly in water promoted by thermodynamic incompatibility. *Journal of Physical Chemistry B* **2010**, *114* (32), 10357-10367.
172. Cox, J. S. G.; Woodard, G. D.; McCrone, W. C., Solid-state chemistry of cromolyn sodium (disodium cromoglycate). *Journal of Pharmaceutical Sciences* **1971**, *60* (10), 1458-1465.
173. Simon, K. A.; Sejwal, P.; Gerecht, R. B.; Luk, Y.-Y., Water-in-water emulsions stabilized by non-amphiphilic interactions: Polymer-dispersed lyotropic liquid crystals. *Langmuir* **2007**, *23* (3), 1453-1458.
174. Wu, L.; Lal, J.; Simon, K. A.; Burton, E. A.; Luk, Y.-Y., Nonamphiphilic Assembly in Water: Polymorphic Nature, Thread Structure, and Thermodynamic Incompatibility. *Journal of the American Chemical Society* **2009**, *131* (21), 7430-7443.
175. Ostapenko, T.; Nastishin, Y. A.; Collings, P. J.; Sprunt, S. N.; Lavrentovich, O. D.; Gleeson, J. T., Aggregation, pretransitional behavior, and optical properties in the isotropic phase of lyotropic chromonic liquid crystals studied in high magnetic fields. *Soft Matter* **2013**, *9* (39), 9487-9498.
176. Tortora, L.; Park, H.-S.; Kang, S.-W.; Savaryn, V.; Hong, S.-H.; Kaznatcheev, K.; Finotello, D.; Sprunt, S.; Kumar, S.; Lavrentovich, O. D., Self-assembly, condensation, and order in aqueous lyotropic chromonic liquid crystals crowded with additives. *Soft Matter* **2010**, *6* (17), 4157-4167.
177. Zhou, S.; Neupane, K.; Nastishin, Y. A.; Baldwin, A. R.; Shiyanovskii, S. V.; Lavrentovich, O. D.; Sprunt, S., Elasticity, viscosity, and orientational fluctuations of a lyotropic chromonic nematic liquid crystal disodium cromoglycate. *Soft Matter* **2014**, *10* (34), 6571-6581.

178. Van Hecke, G. R.; Karukstis, K. K.; Rayermann, S., Deriving binary phase diagrams for chromonic materials in water mixtures via fluorescence spectroscopy: cromolyn and water. *Physical Chemistry Chemical Physics* **2015**, *17* (2), 1047-1052.
179. Kostko, A. F.; Cipriano, B. H.; Pinchuk, O. A.; Ziserman, L.; Anisimov, M. A.; Danino, D.; Raghavan, S. R., Salt Effects on the Phase Behavior, Structure, and Rheology of Chromonic Liquid Crystals. *The Journal of Physical Chemistry B* **2005**, *109* (41), 19126-19133.
180. Nastishin, Y. A.; Liu, H.; Shiyanovskii, S. V.; Lavrentovich, O. D.; Kostko, A. F.; Anisimov, M. A., Pretransitional fluctuations in the isotropic phase of a lyotropic chromonic liquid crystal. *Physical Review E - Statistical, Nonlinear, and Soft Matter Physics* **2004**, *70* (5), 1-51706.
181. Horowitz, V. R.; Janowitz, L. A.; Modic, A. L.; Heiney, P. A.; Collings, P. J., Aggregation behavior and chromonic liquid crystal properties of an anionic monoazo dye. *Physical Review E* **2005**, *72* (4), 041710.
182. Smulders, M. M. J. M.; Nieuwenhuizen, M. M. L. M.; Greef, d. T. F. A. T.; Schoot, v. d. P. P.; Schenning, A. A.; Meijer, E. W. B., How to distinguish isodesmic from cooperative supramolecular polymerisation. *Chemistry - A European Journal* **2010**, *16* (1), 362-367.
183. Henderson, J., Discotic amphiphiles. *The Journal of Chemical Physics* **2000**, *113* (14), 5965-5970.
184. Giltner, C. L.; Nguyen, Y.; Burrows, L. L., Type IV pilin proteins: versatile molecular modules. *Microbiology and Molecular Biology Reviews* **2012**, *76* (4), 740-772.
185. Hahn, H. P., The type-4 pilus is the major virulence-associated adhesin of *Pseudomonas aeruginosa*—a review. *Gene* **1997**, *192* (1), 99-108.

186. Craig, L.; Li, J., Type IV pili: paradoxes in form and function. *Current Opinion in Structural Biology* **2008**, *18* (2), 267-277.
187. Cachia, P. J.; Glasier, L. M. G.; Hodgins, R. R. W.; Wong, W. Y.; Irvin, R. T.; Hodges, R. S., The use of synthetic peptides in the design of a consensus sequence vaccine for *Pseudomonas aeruginosa*. *Journal of Peptide Research* **1998**, *52* (4), 289-299.
188. Berride, F.; Troche-Pesqueira, E.; Feio, G.; Cabrita, E. J.; Sierra, T.; Navarro-Vazquez, A.; Cid, M. M., Chiral amplification of disodium cromoglycate chromonics induced by a codeine derivative. *Soft Matter* **2017**, *13* (38), 6810-6815.
189. Ruiz-Fernandez, A. R.; Lopez-Cascales, J. J.; Giner-Casares, J. J.; Araya-Maturana, R.; Diaz-Banos, F. G.; Weiss-Lopez, B. E., Composition effect on the aggregate/solution interface of a nematic lyotropic liquid crystal. *RSC Advances* **2016**, *6* (88), 85411-85419.
190. Shirai, T.; Shuai, M.; Nakamura, K.; Yamaguchi, A.; Naka, Y.; Sasaki, T.; Clark, N. A.; Le, K. V., Chiral lyotropic chromonic liquid crystals composed of disodium cromoglycate doped with water-soluble chiral additives. *SOFT MATTER* **2018**, *14* (9), 1511-1516.
191. Ding, X.; Stringfellow, T. C.; Robinson, J. R., Self-association of cromolyn sodium in aqueous solution characterized by nuclear magnetic resonance spectroscopy. *Journal of Pharmaceutical Sciences* **2004**, *93* (5), 1351-1358.
192. Jancarik, J.; Kim, S.-H., Sparse matrix sampling: a screening method for crystallization of proteins. *Journal of Applied Crystallography* **1991**, *24* (4), 409-411.
193. Liu, Y.; Zhang, X.-F.; Zhang, C.-Y.; Guo, Y.-Z.; Xie, S.-X.; Zhou, R.-B.; Cheng, Q.-D.; Yan, E.-K.; Liu, Y.-L.; Lu, X.-L.; Lu, Q.-Q.; Lu, H.-M.; Ye, Y.-J.; Yin, D.-C., A protein crystallisation screening kit designed using polyethylene glycol as major precipitant. *CrystEngComm* **2015**, *17* (29), 5488-5495.

194. McPherson, A.; Cudney, B., Optimization of crystallization conditions for biological macromolecules. *Acta Crystallographica Section F* **2014**, *70* (11), 1445-1467.
195. Parker, J. L.; Newstead, S., Current trends in α -helical membrane protein crystallization: An update. *Protein Science* **2012**, *21* (9), 1358-1365.
196. Cudney, B.; Patel, S.; Weisgraber, K.; Newhouse, Y., Screening and optimization strategies for macromolecular crystal-growth. *Acta Crystallographica Section-D Biological Crystallography* **1994**, *50* (Pt 4), 414-4123.
197. Patel, S.; Cudney, B.; McPherson, A., Polymeric Precipitants for the Crystallization of Macromolecules. *Biochemical and Biophysical Research Communications* **1995**, *207* (2), 819-828.
198. A McPherson, Jr., Crystallization of proteins from polyethylene glycol. *Journal of Biological Chemistry* **1976**, *251* (20), 6300-6303.
199. Ingham, K. C., [23] Precipitation of proteins with polyethylene glycol. In *Methods in Enzymology*, Deutscher, M. P., Ed. Academic Press: 1990; Vol. 182, pp 301-306.
200. Yang, X. Z.; Zhang, C. Y.; Wang, Q. J.; Guo, Y. Z.; Dong, C.; Yan, E. K.; Liu, W. J.; Zheng, X. W.; Yin, D. C., Utilization of Cyclodextrins and Its Derivative Particles as Nucleants for Protein Crystallization. *Crystal Growth & Design* **2017**, *17* (12), 6189-6200.
201. Spratt, B. G., Distinct penicillin binding proteins involved in the division, elongation, and shape of Escherichia coli K12. *Proceedings of the National Academy of Sciences* **1975**, *72* (8), 2999-3003.
202. Fredborg, M.; Rosenvinge, F. S.; Spillum, E.; Kroghsbo, S.; Wang, M.; Sondergaard, T. E., Automated image analysis for quantification of filamentous bacteria. *BMC microbiology* **2015**, *15* (1), 255.

203. Möller, J.; Emge, P.; Vizcarra, I. A.; Kollmannsberger, P.; Vogel, V., Bacterial filamentation accelerates colonization of adhesive spots embedded in biopassive surfaces. *New Journal of Physics* **2013**, *15* (12), 125016.
204. Studier, F. W.; Daegelen, P.; Lenski, R. E.; Maslov, S.; Kim, J. F., Understanding the Differences between Genome Sequences of Escherichia coli B Strains REL606 and BL21(DE3) and Comparison of the E. coli B and K-12 Genomes. *Journal of Molecular Biology* **2009**, *394* (4), 653-680.
205. Syed, F. F. B. Citrate binding to the membrane protein proteorhodopsin. ProQuest Dissertations Publishing, 2011.
206. Han, Y.; Cheng, K.; Simon, K. A.; Lan, Y.; Sejwal, P.; Luk, Y.-Y., A Biocompatible Surfactant with Folded Hydrophilic Head Group: Enhancing the Stability of Self-Inclusion Complexes of Ferrocenyl in a β -Cyclodextrin Unit by Bond Rigidity. *Journal of the American Chemical Society* **2006**, *128* (42), 13913-13920.
207. Wang, F.; Coureuil, M.; Osinski, T.; Orlova, A.; Altindal, T.; Gesbert, G.; Nassif, X.; Egelman, E. H.; Craig, L., Cryoelectron Microscopy Reconstructions of the Pseudomonas aeruginosa and Neisseria gonorrhoeae Type IV Pili at Sub-nanometer Resolution. *Structure* **2017**, *25* (9), 1423-1435.e4.
208. Van Doremalen, N.; Bushmaker, T.; Morris, D. H.; Holbrook, M. G.; Gamble, A.; Williamson, B. N.; Tamin, A.; Harcourt, J. L.; Thornburg, N. J.; Gerber, S. I., Aerosol and surface stability of SARS-CoV-2 as compared with SARS-CoV-1. *New England Journal of Medicine* **2020**, *382* (16), 1564-1567.

209. Lan, J.; Ge, J.; Yu, J.; Shan, S.; Zhou, H.; Fan, S.; Zhang, Q.; Shi, X.; Wang, Q.; Zhang, L., Structure of the SARS-CoV-2 spike receptor-binding domain bound to the ACE2 receptor. *Nature* **2020**, *581* (7807), 215-220.



RightsLink®



Home



Help



Email Support



Arizza Ibanez ▾



Interaction of the receptor binding domains of *Pseudomonas aeruginosa* pili strains PAK, PAO, KB7 and P1 to a cross-reactive antibody and receptor analog: implications for synthetic vaccine design 1 1 Edited by P. E. Wright

Author:

A.Patricia Campbell,Wah Y Wong, Mike Houston, Frank Schweizer, Paul J Cachia, Randall T Irvin, Ole Hindsgaul, Robert S Hodges, Brian D Sykes

Publication: Journal of Molecular Biology

Publisher: Elsevier

Date: 28 March 1997

Copyright © 1997 Academic Press. All rights reserved.

Order Completed

Thank you for your order.

This Agreement between Ms. Arizza Ibanez ("You") and Elsevier ("Elsevier") consists of your license details and the terms and conditions provided by Elsevier and Copyright Clearance Center.

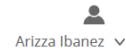
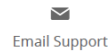
Your confirmation email will contain your order number for future reference.

License Number 4933400671578

[Printable Details](#)

License date Oct 20, 2020

📄 Licensed Content		📄 Order Details	
Licensed Content Publisher	Elsevier	Type of Use	reuse in a thesis/dissertation
Licensed Content Publication	Journal of Molecular Biology	Portion	figures/tables/illustrations
Licensed Content Title	Interaction of the receptor binding domains of Pseudomonas aeruginosa pili strains PAK, PAO, KB7 and P1 to a cross-reactive antibody and receptor analog: implications for synthetic vaccine design 1 1 Edited by P. E. Wright	Number of figures/tables/illustrations	1
Licensed Content Author	A,Patricia Campbell,Wah Y Wong,Mike Houston,Frank Schweizer,Paul J Cachia,Randall T Irvin,Ole Hinds Gaul,Robert S Hodges,Brian D Sykes	Format	both print and electronic
Licensed Content Date	Mar 28, 1997	Are you the author of this Elsevier article?	No
Licensed Content Volume	267	Will you be translating?	No
Licensed Content Issue	2		
Licensed Content Pages	21		
Journal Type	S&T		
📄 About Your Work		📄 Additional Data	
Title	Natural and Synthetic Ligand-Binding Induces Different Pilin Assemblies in vitro and Controls P. aeruginosa Bioactivities in vivo, and development of Bacterial-Motility Enabled Binding Assays	Portions	Fig. 1
Institution name	Syracuse University		
Expected presentation date	Nov 2020		
📍 Requestor Location		📄 Tax Details	
Requestor Location	Ms. Arizza Ibanez 121 Remington Ave. SYRACUSE, NY 13210 United States Attn: Ms. Arizza Ibanez	Publisher Tax ID	98-0397604
💰 Price			
Total	0.00 USD		
			Total: 0.00 USD
CLOSE WINDOW		ORDER MORE	



Structural Characterization of Novel Pseudomonas aeruginosa Type IV Pilins

Author: Ylan Nguyen, Sean G. Jackson, Francisca Aidoo, Murray Junop, Lori L. Burrows

Publication: Journal of Molecular Biology

Publisher: Elsevier

Date: 22 January 2010

Copyright © 2009 Elsevier Ltd. All rights reserved.

Order Completed

Thank you for your order.

This Agreement between Ms. Arizza Ibanez ("You") and Elsevier ("Elsevier") consists of your license details and the terms and conditions provided by Elsevier and Copyright Clearance Center.

Your confirmation email will contain your order number for future reference.

License Number 4933891126721

[Printable Details](#)

License date Oct 21, 2020

Licensed Content		Order Details	
Licensed Content Publisher	Elsevier	Type of Use	reuse in a thesis/dissertation
Licensed Content Publication	Journal of Molecular Biology	Portion	figures/tables/illustrations
Licensed Content Title	Structural Characterization of Novel Pseudomonas aeruginosa Type IV Pilins	Number of figures/tables/illustrations	1
Licensed Content Author	Ylan Nguyen,Sean G. Jackson,Francisca Aldoo,Murray Junop,Lori L. Burrows	Format	both print and electronic
Licensed Content Date	Jan 22, 2010	Are you the author of this Elsevier article?	No
Licensed Content Volume	395	Will you be translating?	No
Licensed Content Issue	3		
Licensed Content Pages	13		
Journal Type	S&T		
About Your Work		Additional Data	
Title	Natural and Synthetic Ligand-Binding Induces Different Pilin Assemblies in vitro and Controls P. aeruginosa Bioactivities in vivo, and development of Bacterial-Motility Enabled Binding Assays	Portions	Fig. 1
Institution name	Syracuse University		
Expected presentation date	Nov 2020		
Requestor Location		Tax Details	
	Ms. Arizza Ibanez 121 Remington Ave.	Publisher Tax ID	98-0397604
Requestor Location	SYRACUSE, NY 13210 United States Attn: Ms. Arizza Ibanez		
\$ Price			
Total	0.00 USD		
			Total: 0.00 USD
CLOSE WINDOW		ORDER MORE	



Home

Help

Email Support

Arizza Ibanez

Structure



Cryoelectron Microscopy Reconstructions of the Pseudomonas aeruginosa and Neisseria gonorrhoeae Type IV Pili at Sub-nanometer Resolution

Author:

Fengbin Wang, Mathieu Coureuil, Tomasz Osinski, Albina Orlova, Tuba Altindal, Gaël Gesbert, Xavier Nassif, Edward H. Egelman, Lisa Craig

Publication: Structure

Publisher: Elsevier

Date: 5 September 2017

© 2017 Elsevier Ltd.

Order Completed

Thank you for your order.

This Agreement between Ms. Arizza Ibanez ("You") and Elsevier ("Elsevier") consists of your license details and the terms and conditions provided by Elsevier and Copyright Clearance Center.

Your confirmation email will contain your order number for future reference.

License Number 4952760205183

[Printable Details](#)

License date Nov 19, 2020

📄 Licensed Content		📁 Order Details	
Licensed Content Publisher	Elsevier	Type of Use	reuse in a thesis/dissertation
Licensed Content Publication	Structure	Portion	figures/tables/illustrations
Licensed Content Title	Cryoelectron Microscopy Reconstructions of the Pseudomonas aeruginosa and Neisseria gonorrhoeae Type IV Pili at Sub-nanometer Resolution	Number of figures/tables/illustrations	1
Licensed Content Author	Fengbin Wang, Mathieu Coureuil, Tomasz Osinski, Albina Orlova, Tuba Altında, Gaël Gesbert, Xavier Nassif, Edward H. Egelman, Lisa Craig	Format	both print and electronic
Licensed Content Date	Sep 5, 2017	Are you the author of this Elsevier article?	No
Licensed Content Volume	25	Will you be translating?	No
Licensed Content Issue	9		
Licensed Content Pages	17		
Journal Type	S&T		
📄 About Your Work		📁 Additional Data	
Title	Natural and Synthetic Ligand-Binding Induces Different Pilin Assemblies in vitro and Controls P. aeruginosa Bioactivities in vivo, and development of Bacterial-Motility Enabled Binding Assays	Portions	Figure 1
Institution name	Syracuse University		
Expected presentation date	Nov 2020		
📍 Requestor Location		📄 Tax Details	
	Ms. Arizza Ibanez 121 Remington Ave.	Publisher Tax ID	98-0397604
Requestor Location	SYRACUSE, NY 13210 United States Attn: Ms. Arizza Ibanez		
💰 Price			
Total	0.00 USD		
			Total: 0.00 USD
CLOSE WINDOW		ORDER MORE	



RightsLink®



Home



Help



Email Support



Arizza Ibanez ▾

DNA-Binding Protein Nanotubes: Learning from Nature's Nanotech Examples



Author: Gerald F. Audette, Erin J. van Schaik, Bart Hazes, et al

Publication: Nano Letters

Publisher: American Chemical Society

Date: Oct 1, 2004

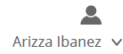
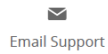
Copyright © 2004, American Chemical Society

PERMISSION/LICENSE IS GRANTED FOR YOUR ORDER AT NO CHARGE

This type of permission/license, instead of the standard Terms & Conditions, is sent to you because no fee is being charged for your order. Please note the following:

- Permission is granted for your request in both print and electronic formats, and translations.
 - If figures and/or tables were requested, they may be adapted or used in part.
 - Please print this page for your records and send a copy of it to your publisher/graduate school.
 - Appropriate credit for the requested material should be given as follows: "Reprinted (adapted) with permission from (COMPLETE REFERENCE CITATION). Copyright (YEAR) American Chemical Society." Insert appropriate information in place of the capitalized words.
 - One-time permission is granted only for the use specified in your request. No additional uses are granted (such as derivative works or other editions). For any other uses, please submit a new request.
- If credit is given to another source for the material you requested, permission must be obtained from that source.

[BACK](#)[CLOSE WINDOW](#)



Crystal structure of Pseudomonas aeruginosa PAK pilin suggests a main-chain-dominated mode of receptor binding 1 1 Edited by R. Huber

Author: Bart Hazes, Parimi A Sastry, Koto Hayakawa, Randy J Read, Randall T Irvin

Publication: Journal of Molecular Biology

Publisher: Elsevier

Date: 16 June 2000

Copyright © 2000 Academic Press. All rights reserved.

Order Completed

Thank you for your order.

This Agreement between Ms. Arizza Ibanez ("You") and Elsevier ("Elsevier") consists of your license details and the terms and conditions provided by Elsevier and Copyright Clearance Center.

Your confirmation email will contain your order number for future reference.

License Number 4952760550999

[Printable Details](#)

License date Nov 19, 2020

Licensed Content		Order Details	
Licensed Content Publisher	Elsevier	Type of Use	reuse in a thesis/dissertation
Licensed Content Publication	Journal of Molecular Biology	Portion	figures/tables/illustrations
Licensed Content Title	Crystal structure of Pseudomonas aeruginosa PAK pilin suggests a main-chain-dominated mode of receptor binding 1 1 Edited by R. Huber	Number of figures/tables/illustrations	1
Licensed Content Author	Bart Hazes,Parimi A Sastry,Koto Hayakawa,Randy J Read,Randall T Irvin	Format	both print and electronic
Licensed Content Date	Jun 16, 2000	Are you the author of this Elsevier article?	No
Licensed Content Volume	299	Will you be translating?	No
Licensed Content Issue	4		
Licensed Content Pages	13		
Licensed Content Journal Type	S&T		
About Your Work		Additional Data	
Title	Natural and Synthetic Ligand-Binding Induces Different Pilin Assemblies in vitro and Controls P. aeruginosa Bioactivities in vivo, and development of Bacterial-Motility Enabled Binding Assays	Portions	Figure 5
Institution name	Syracuse University		
Expected presentation date	Nov 2020		
Requestor Location		Tax Details	
Requestor Location	Ms. Arizza Ibanez 121 Remington Ave.	Publisher Tax ID	98-0397604
	SYRACUSE, NY 13210 United States Attn: Ms. Arizza Ibanez		
Price			
Total	0.00 USD		
		Total: 0.00 USD	
CLOSE WINDOW		ORDER MORE	

Arizza Chiara S. Ibañez

Syracuse, New York • 315-883-9817 • arizza.ibanez@gmail.com • linkedin.com/in/arizzaibanez

Professional Profile

- Adept in cloning (PCR) and cell culturing techniques for vector production and protein overexpression.
- Experience in conventional molecular and macromolecular analytical techniques spectroscopic (UV-Vis, IR, NMR, Fluorescence), chromatographic (LC-MS), electrophoretic (SDS-PAGE, Native) methodologies, biophysical characterization of physical interactions (CD, ITC, DLS) and antibody-based assays (ELISA).
- Provides strategic solutions to complex problems in a timely manner to meet the organization's needs.
- A team player who is able to work in collaboration with cross-functional teams both technical and non-technical personnel.

Research Experience

2015-present

Syracuse University- *Research Assistant*, (Advisor: Dr. Yan-Yeung Luk)

- Designed primers, cloned DNA by PCR and expressed recombinant proteins for mechanism-of-action studies on bacterial anti-pilin therapeutics.
- Optimized protein expression by using filamentous bacteria as expression hosts.
- Identified protein-ligand interactions by developing, screening and optimizing a novel swarming bioassay.
- Characterized ligand-induced structural changes and assembly formation of proteins by fluorescence spectroscopy, circular dichroism, NMR, dynamic light scattering and transmission electron microscopy.
- Discovered peptide-induced molecular assemblies of nonamphiphilic mesogens and utilized this system for preliminary protein crystallization studies.

Professional Experience

LifeUnit Inc.

2019/2020 (Internship)

-Commercial and biological research laboratory focused on antimicrobial therapeutics.

- Evaluated the potency of small molecule inhibitors of spike protein (SARS-CoV2) by independently designing and conducting direct key cellular and molecular biology studies then confirming by ELISA.
- Identified small molecule biofilm inhibitors for *P. aeruginosa* by performing biofilm formation and dispersion assays.

Omya Chemical Merchants Inc.

2010-2015

- A specialty chemicals distribution company serving a variety of industrial companies

Product Sales Manager -Paints and Coatings (2013 -2015)

- Increased distribution business by at least 35% per year while managing a technical sales representative.

Syracuse University (Syracuse, New York, USA)

- **Master of Philosophy in Chemistry** **2017**

Syracuse University (Syracuse, New York, USA)

- **Bachelor of Science in Chemistry** **2009**

University of the Philippines-Diliman (Quezon City, Philippines)

Languages

- English (fluent), Tagalog (native), Mandarin (intermediate)